Title Investigation of the effects of different cryopreservation parameters on the genome of 51/4 hpf zebrafish (Danio rerio) embryos

Name Raju Ahmed

INVESTIGATION OF THE EFFECTS OF DIFFERENT CRYOPRESERVATION PARAMETERS ON THE GENOME OF 5¼ hpf ZEBRAFISH (*Danio rerio*) EMBRYOS

RAJU AHMED

PhD

UNIVERSITY OF BEDFORDSHIRE

2013

INVESTIGATION OF THE EFFECTS OF DIFFERENT CRYOPRESERVATION PARAMETERS ON THE GENOME OF 5¼ hpf ZEBRAFISH (*Danio rerio*) EMBRYOS

By

RAJU AHMED

A thesis is submitted to the University of Bedfordshire in accordance with the requirements for the degree of Doctor of Philosophy

Institute of Biomedical and Environmental Science and Technology
University of Bedfordshire
250 Butterfield
Great Marlings
LU2 8DL

June 2013

INVESTIGATION OF THE EFFECTS OF DIFFERENT CRYOPRESERVATION PARAMETERS ON THE GENOME OF 5¼ hpf ZEBRAFISH (*Danio rerio*) EMBRYOS

Raju Ahmed

Abstract

In recent years, numerous studies have linked cryopreservation with increased occurrence of mutations, DNA fragmentation and the event of apoptosis in biological objects. However, the evidence emerged from such studies is somewhat inconclusive. The current study, therefore, aimed to analyse the DNA damage response (DDR) from the cryopreserved cells in order to characterise the nature of the putative DNA damage.

The study set out to investigate the effects of different cryopreservation parameters on the genome in terms of double strand breaks (DSBs), single strand breaks (SSBs), and various forms of sequence alteration using 5¼ hour post fertilisation (hpf) zebrafish (*Danio rerio*) embryos. The experimental conditions under which the investigation was carried out were short term chilling at 0˚C, treatment with two cryoprotective agents (CPA), namely, MeOH and Me_2SO, and cooling to -35˚C. Assays for detecting DSB-activated DDR proteins and SSB-activated DDR proteins in 5¼ hpf zebrafish (*Danio rerio*) were developed and then utilised to investigate the occurrence of DSBs and SSBs in the genome of the embryos treated with the experimental conditions. The study then analysed the expression profiles of a set of genes unique to the base excision repair (BER), nucleotide excision repair (NER) and mismatch repair (MMR) pathways as indicators of the occurrence of various forms of sequence alterations in the genome of the embryos treated with the experimental conditions. It was found that chilling and CPA treatment did not induce DSBs or SSBs but up-regulated the MMR and BER, respectively. CPA treatment also down-regulated the NER and the MMR mechanisms. Cooling, on the contrary, did not induce DSBs but induced SSBs in the genome, which were repaired when the embryos were provided with a recovery time. Cooling also up-regulated the NER and the BER mechanisms in the embryos. The overall finding of the study indicated that the experimental conditions increased the occurrence of various single stranded DNA lesions in the genome of the embryos.

The present study provided important insights into how eukaryotic cells respond to different cryopreservation parameters, which will significantly enhance the current knowledge of the effects of cryopreservation on the genome of biological objects.

ACKNOWLEDGEMENT

I would like to acknowledge a number of outstanding people for their help and support throughout my research work.

I would like to thank my director studies, Professor Tiantian Zhang, for her supervision, perseverance and valuable advice during the course of this work. Without her support and guidance this work would not have been possible.

I would like convey my gratitude to my supervisor, Dr. Emma Spikings, for being exceptionally supportive helpful throughout the course of the research work. I can not thank her enough for her encouraging words which motivated me throughout the research work.

I would like to thank my second supervisor, Dr Shaobo Zhao, for his help and support during the research work.

I would also like to thank my external supervisor, Dr Andrew Thompsett, for his support throughout the course of the research work.

I would like to acknowledge DR. Barry Haggett and Gowri Dep for providing guidance and instructions for safe working in the laboratory.

I would like to thank Professor S. Sreenivasaprasad for his valuable advice during my research work

I would like to thank my fellow colleagues Kunjan Desai, Krishan Vishnollia, Siji Anil, Deborah Patrocini, and Jahabeen Jahangir and many others in IBEST for their kindness, help and friendship.

Finally, I would like to thank my parents and family for supporting me throughout the course the research work. Without their support and love, this work would not have been completed.

DECLARATION

I declare that this is my own unaided work. It is being submitted for the degree of Doctor of Philosophy at the University of Bedfordshire.

It has not been submitted before any degree or examination in any other University.

Name of the candidate Raju Ahmed Signature

Date:

CONTENTS

CHAPTER 2: MATERIALS AND METHODS

CHAPTER 3: OPTIMISATION, DEVELOPMENT AND VALIDATION OF TECHNIQUES AND METHODS USED IN THE INVESTIGATION OF THE EFFECTS OF DIFFERENT CRYOPRESERVATION PARAMETERS ON THE GENOME OF 5¼ hpf ZEBRAFISH (*Danio rerio*) EMBRYOS

CHAPTER 4: EFFECTS OF CHILLING ON THE GENOME OF 5¼ hpf ZEBRAFISH (*Danio rerio*) EMBRYOS

CHAPTER 5: INVESTIGATION OF THE EFFECTS OF CPA TREATMENT ON THE GENOME OF 5 ¼ hpf ZEBRAFISH (*Danio rerio*) EMBRYOS

CHAPTER 6: INVESTIGATION ON THE EFFECTS OF COOLING AND WARMING ON THE GENOME OF 5¼ hpf ZEBRAFISH (*Danio rerio*) EMBRYOS

CHAPTER 7: CONCLUSIONS

LIST OF TABLES

CHAPTER 1: INTRODUCTION

CHAPTER 2: MATERIALS AND METHODS

LIST OF FIGURES

CHAPTER 1: INTRODUCTION

CHAPTER 2: MATERIALS AND METHODS

CHAPTER 3: OPTIMISATION, DEVELOPMENT AND VALIDATION OF TECHNIQUES AND METHODS USED IN THE INVESTIGATION OF THE EFFECTS OF DIFFERENT CRYOPRESERVATION PARAMETERS ON THE GENOME OF ZEBRAFISH (*Danio rerio*)

Example of melting curve profile for *ACTB* and *EF1 alpha*. Standard (brown), negative control (light blue) and samples (other colours. All samples produced a single melting peak indicating that the samples had no contamination, mispriming and primer-dimers.

Expression of *ACTB* and *EF1 alpha* was not affected by chilling. Graphical presentation of the expression profiles of *ACTB* (A) and *EF1 alpha* (B) in the embryos chilled for different periods. 5¼ hpf zebrafish (*Danio rerio*) embryos were chilled at 0˚C for 30, 60 and 120 min. Total RNAs were extracted from each treated group and a group of fresh embryos and converted to cDNA from which *ACTB* and *EF1 alpha* were amplified and quantified using qRT-PCR. Values shown are mean-/+ SEM of the expression level relative to that in the fresh embryos. Different letter indicates statistically significant ($p<0.05$) difference among the groups being compared.

Expression of *ACTB* and *EF1 alpha* was not affected by MeOH incubation. Graphical presentation of the expression profiles of *ACTB* (A) and *EF1 alpha* (B) in the embryos treated with MeOH. 5¼ hpf zebrafish (*Danio rerio*) embryos were incubated with 1M , 2M and 3M MeOH for 30 min. Total RNAs were extracted from each treated group and a group of fresh embryos and converted to cDNA from which *ACTB* and *EF1 alpha* were amplified and quantified using qRT-PCR. Values shown are mean-/+ SEM of the expression levels relative to that in the fresh embryos. Different letters indicate statistically significant ($p<0.05$) difference among the groups being compared.

Expression of *ACTB* and *EF1 alpha* was not affected by Me_2SO incubation. Graphical presentation of the expression profiles of *ACTB* (A) and *EF1 alpha* (B) in the embryos treated with different concentrations of Me_2SO. 5¼ hpf zebrafish (*Danio rerio*) embryos were incubated in 1M, 1.5M and 2M Me_2SO for 30 min. Total RNAs were extracted from each treated group and a group of fresh embryos and converted to cDNA from which *ACTB* and *EF1 alpha* were amplified and quantified using qRT-PCR. Values shown are mean-/+ SEM of the expression levels relative to that in the fresh embryos. different letters indicate statistically significant ($p<0.05$) difference among the groups being compared.

Expression of *ACTB* and *EF1 alpha* was not affected by cooling to -35°C. Graphical presentation of the expression profiles of *ACTB* (A) and *EF1 alpha* (B) in the embryos cooled to **-35°C.** 5¼ hpf zebrafish (*Danio rerio*) embryos were cooled to **-35°C** using MeOH and Me_2SO as CPAs. Total RNAs were extracted from each treated group and a group of fresh embryos and converted to cDNA from which *ACTB* and *EF1 alpha* were amplified and quantified using qRT-PCR. Values shown are mean-/+ SEM of the

expression levels relative to that in the fresh embryos. different letters indicate statistically significant ($p<0.05$) difference among the groups being compared.

CHAPTER 4: EFFECTS OF CHILLING ON THE GENOME OF 5¼ hpf ZEBRAFISH (*Danio rerio*) EMBRYOS

CHAPTER 5: INVESTIGATION OF THE EFFECTS OF CPA TREATMENT ON THE GENOME OF 5 ¼ hpf ZEBRAFISH (*Danio rerio*) EMBRYOS

MeOH and Me_2SO did not affect the hatching of the $5^1/_4$ hpf zebrafish (*Danio rerio*) embryos. (A) Graphical presentation of the hatching rates of 5¼ hpf embryos incubated for 30 minutes in 0, 1, 2, and 3M MeOH. **(B)** Graphical presentation of the hatching rates of 5¼ hpf embryos incubated for 30 minutes in 0, 1.5 and 2 M Me_2SO. Values shown are mean +/- SEM of the hatching rates obtained from three independent experiments. Different letters, where appropriate, indicate statistically significant ($p<0.05$) difference among the groups being compared.

DSB-affected and SSB-affected DDR proteins were not affected in 5¼ hpf zebrafish (*Danio rerio*) embryos treated with MeOH. (A) Representative blot of three independent experiments. 5¼ hpf embryos were incubated for 30 minutes in 0, 1, 2, and 3M MeOH. Total proteins were extracted from each treated group and probed alongside DSB^- and DSB^+ embryo lysates with anti-S*/T*Q, and anti-β-*actin* simultaneously. *β actin* served as a control for variations in protein loading. **(B)** Graphical presentation of the intensity of phosphorylation of the proteins detected in the $DSB^-$and DSB^+ embryos. Values shown are mean +/- SEM of β-*actin* normalised band intensities obtained from three replicates and presented as relative to those in the DSB^-embryos **(C)** Graphical presentation of the intensity of phosphorylation of the proteins affected in the $SSB^-$and SSB^+ embryos. Values shown are mean +/- SEM of β-*actin* normalised band intensities obtained from three replicates and presented as relative to those in the SSB^- embryos. **(D)** Graphical presentation of the intensity of phosphorylation of the proteins detected in the lysates prepared from the embryos treated with different concentrations of MeOH. Values shown are mean +/- SEM of β-*actin* normalised band intensities obtained from three replicates and presented as relative to those in the lysate prepared from the non-treated embryos (0M). Different letters, where appropriate, indicate statistically significant ($p<0.05$) difference among the groups being compared. MW represents MagicMark™ XP Western protein standards (Invitrogen, LC5602).

DSB-affected DDR proteins were not affected in 5¼ hpf zebrafish (*Danio rerio*) embryos treated with Me_2SO. (A) Representative blot of three independent experiments. 5¼ hpf embryos were incubated for 30 minutes in 0, 1, 1.5 and 2M Me_2SO. Total proteins were extracted from each treated group and probed alongside DSB^- and DSB^+ embryo lysates with anti-S*/T*Q, and anti-β-*actin* simultaneously. *β actin* served as a control for variations in protein loading. **(B)** Graphical presentation of the intensity of phosphorylation of the proteins detected in the $DSB^-$and DSB^+ embryos. Values shown are mean +/- SEM of β-*actin* normalised band intensities obtained from three replicates and presented as relative to those in the DSB^- embryos. **(C)** Graphical presentation of the intensity of phosphorylation of the proteins detected in the $SSB^-$and SSB^+ embryos. Values shown are mean +/- SEM of β-*actin* normalised band intensities obtained from three replicates and presented as relative to those in the SSB^- embryos. **(D)** Graphical presentation of the intensity of phosphorylation of the proteins detected in the lysates

CHAPTER 6: INVESTIGATION ON THE EFFECTS OF COOLING AND WARMING ON THE GENOME OF 5¼ hpf ZEBRAFISH (*Danio rerio*) EMBRYOS

were extracted from the non-treated embryos (NT) and the cooled embryos (-35°C), and probed alongside SSB^- and SSB^+ embryo lysates with anti-S*/T*Q, and anti-β-*actin* simultaneously. *β actin* served as a control for variations in protein loading. **(B)** Graphical presentation of the intensity of phosphorylation of the proteins detected in the $SSB^-$and SSB^+ embryo lysates. **(C)** Graphical presentation of the intensity of phosphorylation of the proteins detected in the lysates prepared from the embryos cooled using MeOH and warmed subsequently. Values shown are mean +/- SEM of β-*actin* normalised band intensities obtained from three replicates and presented as relative to those in the lysate prepared from non-treated embryos. Different letters, where appropriate, indicate statistically significant ($p<0.05$) difference among the groups being compared.

DSB affected DDR proteins were not affected in 5¼ hpf zebrafish (*Danio rerio*) embryos cooled with Me_2SO. (A) Representative blot of three independent experiments. 5¼ hpf embryos were cooled to -35°C using Me_2SO as CPA. Total proteins were extracted from the non-treated (NT) and cooled (-35°C) embryos and probed alongside DSB^- and DSB^+ embryo lysates with anti-S*/T*Q, and anti-β-*actin* simultaneously. *β actin* served as a control for variations in protein loading. **(B)** Graphical presentation of the intensity of phosphorylation of the proteins detected in the $DSB^-$and DSB^+ embryos. Values shown are mean +/- SEM of β-*actin* normalised band intensities obtained from three replicates and presented as relative to those in the DSB^- embryos. **(C)** Graphical presentation of the intensity of phosphorylation of the proteins detected in the $SSB^-$and SSB^+ embryos**.** Values shown are mean +/- SEM of β-*actin* normalised band intensities obtained from three replicates and presented as relative to those in the SSB^- embryos. **(D)** Graphical presentation of the intensity of phosphorylation of the proteins detected in the embryos cooled with Me_2SO. Values shown are mean +/- SEM of β-*actin* normalised band intensities obtained from three replicates and presented as relative to those in the non-treated embryos. Different letters, where appropriate, indicate statistically significant ($p<0.05$) difference among the groups being compared. MW represents MagicMark™ XP Western protein standards (Invitrogen, LC5602).

Expression levels of the genes selected from the ERMs were affected by cooling and warming. **(A)** Graphical presentation of the expression profiles of the genes of the ERMs in MeOH-cooled embryos (B) Graphical presentation of the expression profiles of the genes of the ERMs in Me_2SO-cooled embryos. Values shown are mean +/- SEM of *ACTB* and *EF1 alpha*-normalised expression levels of the genes obtained from three independent experiments and presented as relative to those in the corresponding non-treated embryos. Different letter indicates statistically significant ($p>0.05$) difference among the groups being compared.

LIST OF ABBREVIATIONS

ACTB	Actin beta
ANOVA	Analysis of variance
ATM	Ataxia Telangiectasia Mutated
ATP	Adenosine triphosphate
ATR	Ataxia Telangiectasia Mutated, related
BER	Base excision repair
CPAs	Cryoprotective agents
cDNA	Complementary deoxyribonucleic acid
DDR	DNA damage response
DNA	Deoxyribonucleic acid
dNTP	Deoxyribonucleotide triphosphate
DSB	Double strand break
ERM	Excision repair mechanism
E2	Embryo medium 2
ERCC1	Excision Repair Cross-Complementing Rodent Repair Deficiency, Complementation Group 1
HKGs	Housekeeping genes
HPF	Hours post fertilisation
IIF	Intracellular ice formation
MBT	Mid-blastula transition
MMR	Mismatch repair
mRNA	Messenger RNA
MSH2	MutS homologue 2
NER	Nucleotide excision repair
RNA	Ribonucleic acid
PCR	Polymerase chain reaction
qRT-PCR	Quantitative real time PCR
ROS	Reactive oxygen species
SDS-PAGE	Sodium dodecyl sulphate polyacrylamide gel electrophoresis
SEM	Standard error of mean
SSB	Single strand break
tRNA	Transfer RNA
TDG	Thymine DNA glycosylase
UDG	Uracil DNA glycosylase

CHAPTER I: INTRODUCTION

1.1 Background

Cryopreservation is a method of preserving biological objects at subzero temperature in liquid nitrogen for an indefinite period of time. It has found its fullest development in the fields of biomedicine, animal reproduction and conservation biology. Cryopreservation offers the flexibility to preserve the genetic information of a species and therefore it is routinely used to preserve biological objects such as gametes for *in vitro* fertilisation (IVF) and artificial insemination (AI), embryos for *in vitro* maturation (IVM), and stem cells for research and transplantation purposes (Massip et al, 2004).

The most commonly used method of cryopreservation is the controlled slow cooling. In controlled slow cooling, biological objects are cooled to below freezing point, usually -196°C, at controlled rates, hence the name. Evidently, cryopreservation is a stressful process and unquestionably it would have some harmful effects on the biological objects. In the past few decades, efforts have been made to identify and characterise the harmful effects that cryopreservation may have on biological objects. Some of the well established harmful effects of cryopreservation are chilling injury, cryoprotective agent (CPA) toxicity, freezing injury, and thawing injury.

1.2 Chilling injury

The term chilling injury refers to the damaging effects sustained by a biological object when it is introduced to chilling temperature which ranges from physiological temperature to 0˚+/-5˚C (Balasubramanian and Rho, 2006). Injuries exerted by chilling temperature are usually classified into two types, direct chilling injury (also known as cold shock) and indirect chilling injury. Direct chilling injury is the damaging effects sustained by biological objects from simple exposure to chilling temperature. It is dependant on cooling rate, with a rapid cooling rate being more damaging. Indirect chilling injury, on the other hand, is the damaging effects sustained by biological objects when they are held at chilling temperature. It is cooling rate independent. However, the

effects of direct chilling injury and indirect chilling injury are somewhat overlapping, especially in terms of the effects on cell membrane. It has been shown that direct chilling injury causes thermotropic phase transition in the cell membrane, in which the lipid phase transforms from being liquid crystals to gel phase (Drobnis et al., 1993). This phase transition transiently permeabilises the cell membrane resulting in an efflux of K^+ ions and an influx of Na^+ and H^+ ions. The movement of ions across the membrane decreases the cellular pH, which modifies the biological structure and functions of proteins (Fujita, 1999). Exposure to chilling temperature for extended period of time results in permanent gel phase separation (Figure 1.1), which disrupts membrane structure leading to cell death.

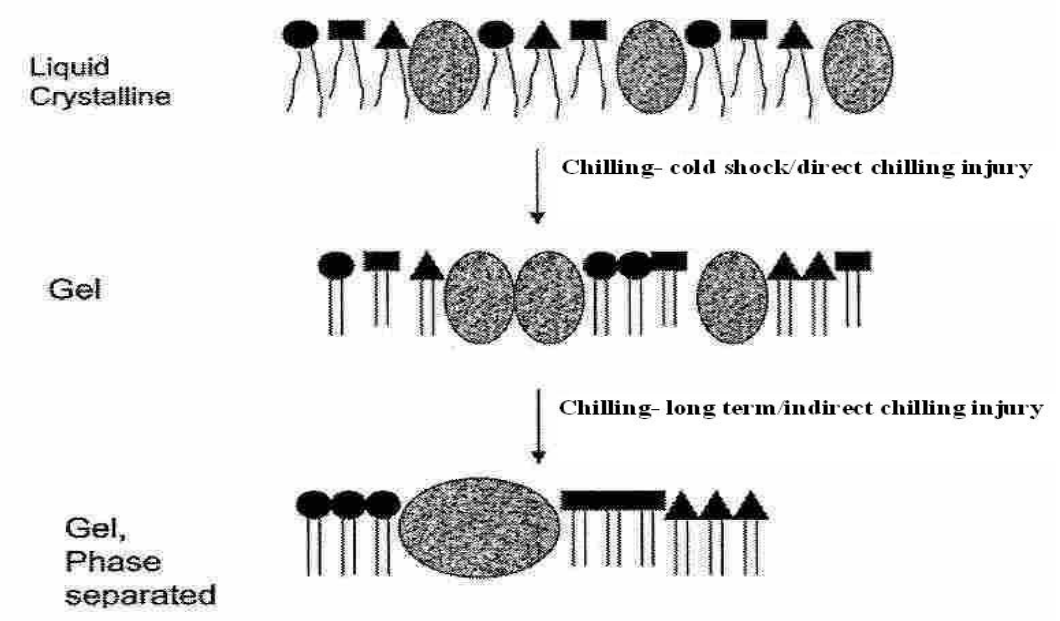

Figure 2.1: Schematic diagram showing the effects of chilling temperature on cell membrane. Cold shock causes liquid crystalline lipid in the membrane to transform into gel phase. Extended exposure to chilling temperature results in permanent gel phase separation. (Best, 2013)

Studies have shown that chilling temperature have numerous other damaging effects on biological objects. It has been shown that chilling temperature suppresses metabolic processes such as replication, transcription and translation as manifested in the relatively slower growth rate of cells cultured at temperatures below their physiological temperature (Fujita, 1999). It has also been shown that chilling temperature destabilises the three dimensional structure of proteins by breaking the hydrophobic bonds (Lattman, 1994), which modifies the biological function of proteins. During controlled slow cooling cryopreservation, biological objects endure the chilling temperature as they are cooled

towards the freezing point and, therefore, are likely to sustain the damaging effects of chilling temperature as discussed above.

1.3 Freezing injury

Freezing injury is mainly caused by intracellular ice formation (IIF), which is lethal for biological objects. During cooling, at around -5°C, the intracellular and extracellular water remains unfrozen due to a phenomenon called supercooling (Mazur 1984). As the temperature is decreased, spontaneous ice formation takes place between -5˚C and -15˚C, which grows rapidly in every direction resulting in IIF. To prevent IIF, therefore, ice formation in the external medium is manually induced in a process called ice nucleation. On ice nucleation, the extracellular water starts freezing but the intracellular water remains supercooled because the cell membrane interferes with ice formation in the cytoplasm (Ozkavukcu, 2002). Growing ice in the extracellular water results in continuously increasing solute concentration in the unfrozen fraction; and to reach equilibrium with the extracellular water, cells lose free intracellular water via exosmosis. In the case of rapid cooling, cells cannot loose water quickly enough to reach equilibrium with the extracellular water and IIF takes place, which leads to cell death. In the case of slow cooling, on the other hand, cells are able to dehydrate by losing free intracellular water and avoid IIF (Mazur, 2004) (Figure 1.1).

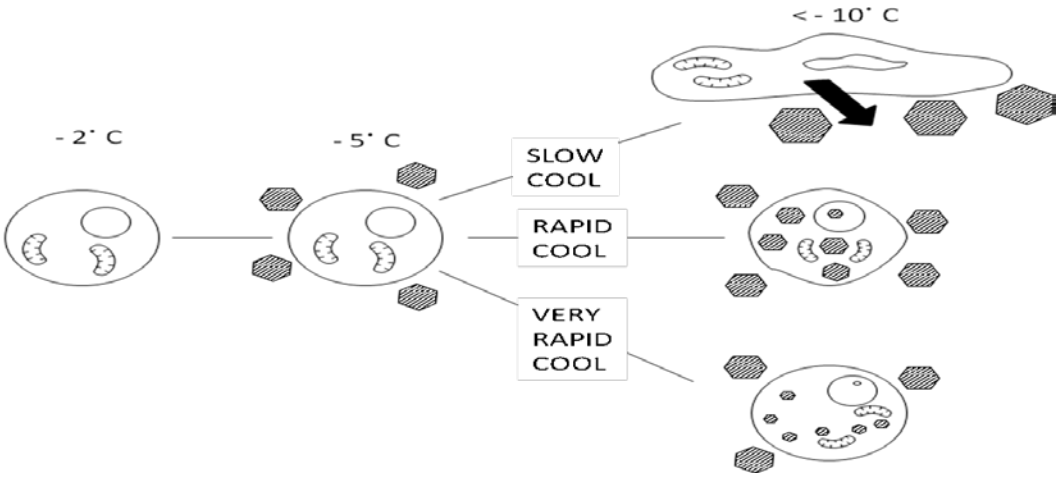

Figure 1.2: Schematic diagram showing the events taking place during cooling of biological objects. In rapid cooling cells can not lose intracellular water fast enough to avoid IIF. In slow cooling cells are able to lose intracellular water via exosmosis and thereby avoid IIF (Mazur, 1977**)**

However, damage can still occur even when the osmotic equilibrium is achieved and IIF is avoided by way of a slow cooling rate. It is thought that high solute concentration, both intracellular and extracellular, and excessive dehydration are the cause of such damage (Muldrew et al, 2004). It has been put forward that during slow cooling cells are exposed to high solute concentration for extended period. It has also been put forward that efflux of free intracellular water during freezing results in a decrease of cell volume by fifty percent leading to structural deformation of the cellular organelles (Muldrew et al, 2004). An efficient protocol for controlled slow cooling cryopreservation, therefore, is the one that employs an intermediate cooling rate that allows cells enough time to lose intracellular water as well as minimise the exposure time to high solute concentrations as exemplified in Figure 1.2, which shows an intermediate cooling rate to be optimum for a number of biological objects.

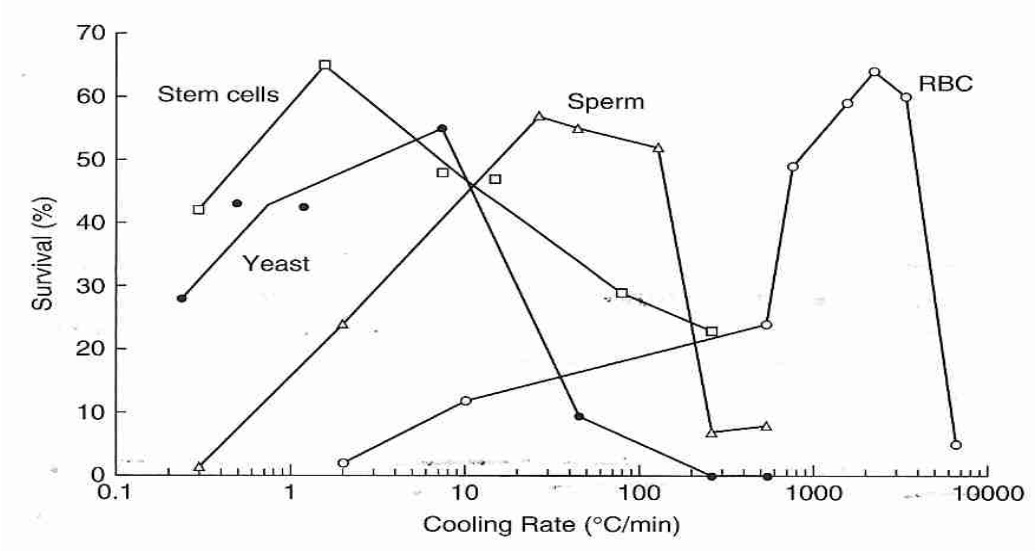

Figure 1.3: Showing the cooling rate for stem cells, yeast, mouse sperm, and human red blood cells (RBC). Fewer cells survive when the cooling rate is too slow or too high. Maximum survival occurs at an intermediate cooling rate (Mazur 2004).

1.4 Thawing injury

Cryopreserved biological objects need to be thawed before they can be utilised subsequently; and damage can occur during the thawing process, too. During thawing, the events that take place throughout the course of the freezing process are reversed. As ice starts melting, the solute concentration in the extracellular water is decreased and to maintain osmotic equilibrium across the membrane, extracellular water enters into the

cells. This influx of water may lead to swelling and rupture of the cells (Mazur, 2004). It is also thought that during thawing cells can sustain injuries from re-crystallisation of the ultramicroscopic ice into relatively larger ice crystals (Mazur, 1984). Ultramicroscopic ice can form either during freezing from the residual cellular water or during thawing from the de-vitrification of glassy water (Mazur, 2004).

1.5 CPA toxicity

To ward off the cellular damage resulting from freezing and thawing, CPAs are added to the preservative solution. Based on the mode of action, CPAs are classified into two groups, permeable CPAs and non-permeable CPAs. Permeable CPAs are low molecular weight, water soluble compounds such as methanol (MeOH), which can penetrate the cell membrane, whereas, non-permeable CPAs are long-chain polymers such as polyethylene glycol, which are soluble in water but cannot penetrate the cell membrane. Permeable CPAs exert their protective effect by lowering the concentration of physiological salts in the unfrozen fraction at a given temperature (Muldrew et al, 2004). Permeable CPAs also depress the freezing point, preventing spontaneous IIF. Non-permeable CPAs, on the contrary, achieve their protective effect by dehydrating the cells before freezing process begins. During, freezing, therefore, cells need not loose as much water to remain in osmotic equilibrium with the extracellular water. However, CPAs are also known to have damaging effects on cells. For example, MeOH, a neurotoxin, has been shown to affect the retina and optic nerve in rat (Eells et al, 2000). It has also been shown that MeOH and ethanol disorientate the bilayer membrane by binding to the phospholipids (Hotelmans, 2001, Lindhi 2001). CPAs can also exert osmotic stress on cells during their addition and removal. When cells are exposed to high concentration of CPAs, they initially shrink by dehydrating and then swell by re-hydrating. Excessive shrinkage or swelling may cause permanent damage to various organelles resulting in cell death (Sceider and Mazur, 1984).

1.6 Effects of cryopreservation on genetic integrity

Most of the damaging effects of cryopreservation described in the foregoing sections can be avoided or reduced by using carefully and empirically devised cryopreservation

protocols. However, evidence, accumulated over the years, from research around the globe indicates that cryopreservation can damage the genetic material of biological objects, too. Before describing the evidence as regards to the impact of cryopreservation on genetic material, an overview of the structure of the eukaryotic genetic material and the maintenance of its integrity is presented.

1.6.1 Structure of genetic material

In all eukaryotes, the hereditary information is carried by deoxyribonucleic acid (DNA). Genetic information in DNA is stored in the form of a sequence of nucleotides, the subunits of nucleic acid molecule. A nucleotide is composed of a pentose sugar, a five-carbon carbohydrate molecule, called ribose, a nitrogenous base, and a phosphate group. The phosphate group is linked to the ribose molecule by a phosphor-ester bond, and ribose, in turn, is linked to the nitrogenous base (figure 1.4).

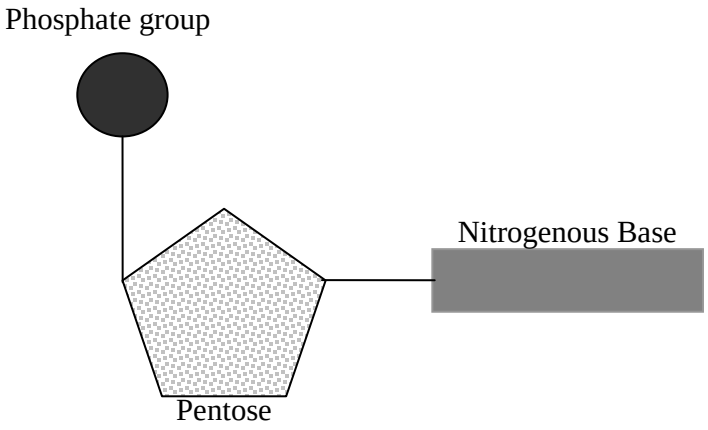

Figure 1.4: Structure of a nucleotide showing a pentose sugar linked to a nitrogenous base and a phosphate group

In DNA, ribose occurs in its deoxygenated form, hence called deoxyribonucleic acid. There are only four different types of bases found in DNA, adenine (A), cytosine (C), guanine (G), and thymine (T). In ribonucleic acid (RNA), the only other type of nucleic acid with critical functions in relaying the genetic information, a T is replaced by a Uracil (U). Among the bases found in DNA, A and G are derived from purine, a five membered

imidazole ring fused to a six-member ring, and C and T are derived from pyrimidine, a six member heterocyclic, conjugated ring (Cooper and Hausman, 2009).

Eukaryotic native DNA consists of two complimentary strands of polynucleotides twisted around each other to form a double helix (Cox et al., 2012). The backbone of each strand is composed of repeating nucleotides linked by phosphodiester bonds (Figure 1.5). From this backbone, purine and pyrimidne bases protrude inwards as side groups.

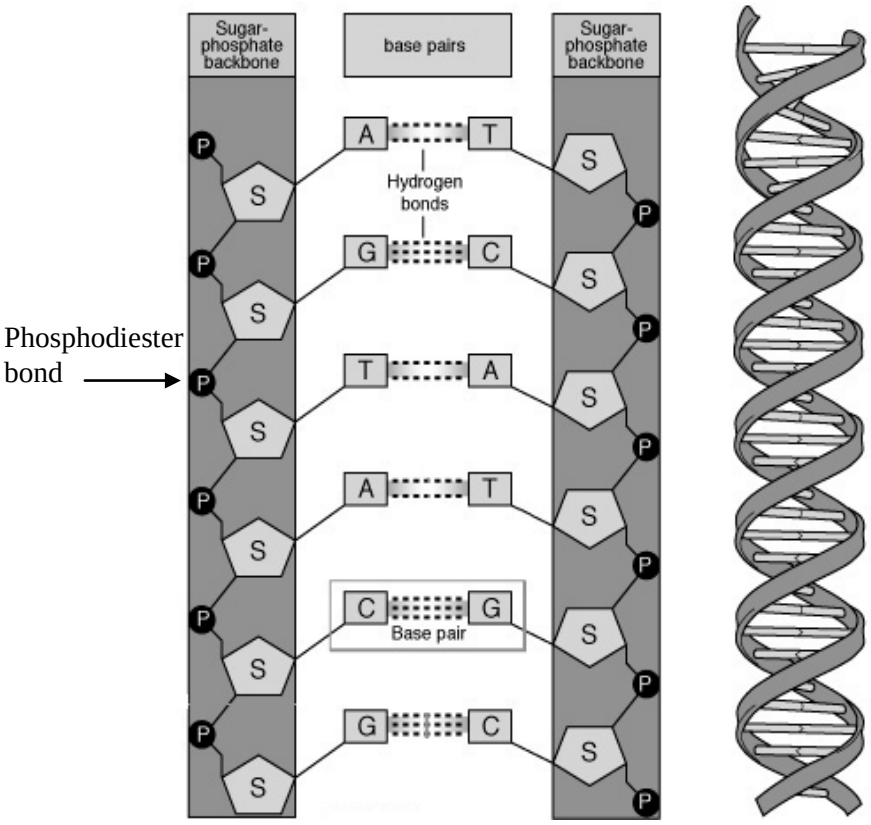

Figure 1.5: Schematic diagram showing DNA double helix formed by hydrogen bonds between a purine and a pyrimidine. An A binds to a T with two hydrogen bonds whereas a G binds to a C with three hydrogen bonds. Nucleotides in sugar phosphate backbone are linked by phosphodiester bonds (image was taken from Education Portal, 2013).

The two strands of the double helix are held together by hydrogen bonds between the purine and pyrimidine bases. The precise conformation of the double helix is maintained by pairing between a purine and a pyrimidine. In native DNA, an A always binds with a T, and a G with a C. The specificity of A:T and G:C pairing is accomplished by the

number of hydrogen bonds that can be formed between a purine and pyrimidine. There are three hydrogen bonds formed between G and C pairing, whereas, two hydrogen bonds formed between A and T (Figure 1.2). The base pairing specificity allows the genetic information to be copied accurately and passed onto new generations (Cooper and Hausman, 2009).

In a eukaryotic cell, DNA is tightly packaged into nucleus in the form of a nucleoprotein structure called chromatin, which is composed of repeating units of nucleoprotein known as nucleosome. A nucleosome is composed of a segment of DNA and an octamer of a protein called Histone (Figure 1.6). Nucleosomes act as barriers to the enzymes involved in various metabolic processes, such as gene transcription, DNA replication, and DNA damage repair mechanisms and therefore the chromatin structure needs to be remodeled for any of such event to take place (Grabarz et al, 2012).

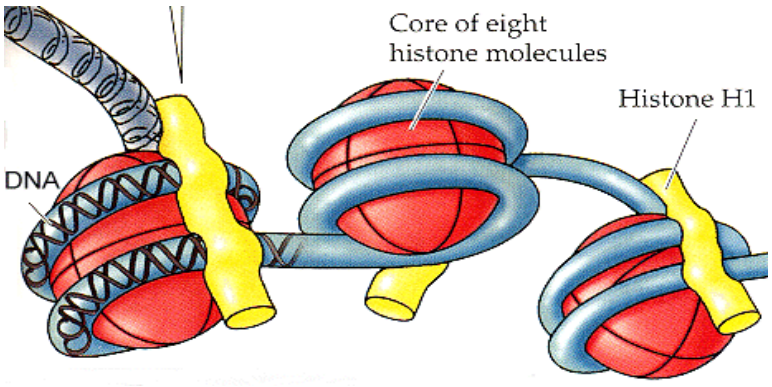

Figure 1.6: Showing the structure of nucleosomes. The DNA double helix wraps around a central core of eight histone molecules to form a single nucleosome. A second histone (H1 in the illustration) fastens the DNA to the nucleosome core (image taken from Purves et al, 1997).

1.6.2 How genetic integrity may be compromised

Although, DNA, containing the genetic information, is stored relatively safely in the cells, various endogenous and exogenous genotoxic agents continuously threaten its functional integrity. Reactive oxygen species (ROS), generated spontaneously from the

essential cellular functions such as oxidative respiration and lipid peroxidation, are the major endogenous genotoxic agents (Dinant et al, 2008). ROS are known to exert their harmful effects by chemically binding to the DNA bases. The binding of ROS to the DNA bases results in distortion of the helical structure of DNA and modification of the bases (Cooke et al, 2003). If the structural modification falls in a protein encoding region, otherwise known as gene, it leads to alteration of the genetic information, in which case, the gene is said to be mutated. ROS can also cause damage to the DNA bases resulting in lesions such as abasic sites, where a purine or pyrimdine group is removed, and single strand break (SSB). Exogenous genotoxic agents, on the other hand, include ultraviolet light, ionising radiation, various chemicals present in food, and combustion product present in the air, which can induce a wide variety of lesions in DNA including base damage, SSBs and double strand break (DSB) (Dinant et al, 2008). The consequence of DNA damage is often adverse. Lesions affecting a single strand may block the progression of replication leading to DSBs (Negritto, 2010). DSBs are invariably lethal for cells if left un-repaired and mutagenic if not repaired correctly (discussed in a later section). If mutations are introduced into the genes that control cell growth, uncontrollable growth or neoplasms may result (Dinant et al, 2008).

1.6.3 DNA damage response

Since genetic integrity is a prerequisite for an organism to survive and function properly, eukaryotic cells have evolved a complex but subtle network of surveillance mechanisms known as DNA damage response (DDR). The function of the DDR is to make sure that damaged DNA is not replicated and passed on to daughter cells during cell division. In the heart of a DDR, there are several cell cycle checkpoints known as DNA damage checkpoints, and DNA repair mechanisms. DNA damage checkpoints arrest cell cycles to provide DNA repair mechanisms with a time window to repair the lesions before cell division can take place (Dinant et al, 2008).

1.6.3.1 Cell cycle

Cell cycle denotes a series of events occurring in a cell resulting in its division. There are two types of cell division operative in eukaryotes, mitosis and meiosis. Mitosis is the

process by which somatic cells are proliferated by producing two daughter cells with identical nuclei. Meiosis, on the other hand, is the process by which germ cells are divided to produce haploid gamets or spores. Meiosis consists of two distinct cell divisions, meiosis I and meiosis II. Mitosis and both meiotic divisions are divided into four stages, prophase, metaphase, anaphase and telophase. Mitosis and meiosis form only a small part of the respective cell cycle. The rest of the cell cycle is known as interphase, which consists of three distinct parts, termed as G_1 (gap 1) phase, S (synthesis) phase, G_2 (gap 2) phase (Figure 1.7). However, when cells are differentiated to become specialised cell types, for example, hepatocytes, they cease to divide, becoming quiescent, and remain so throughout their lifetime. This phase of the cell cycle is denoted as late $G_{1\ or}$ G_0 phase.

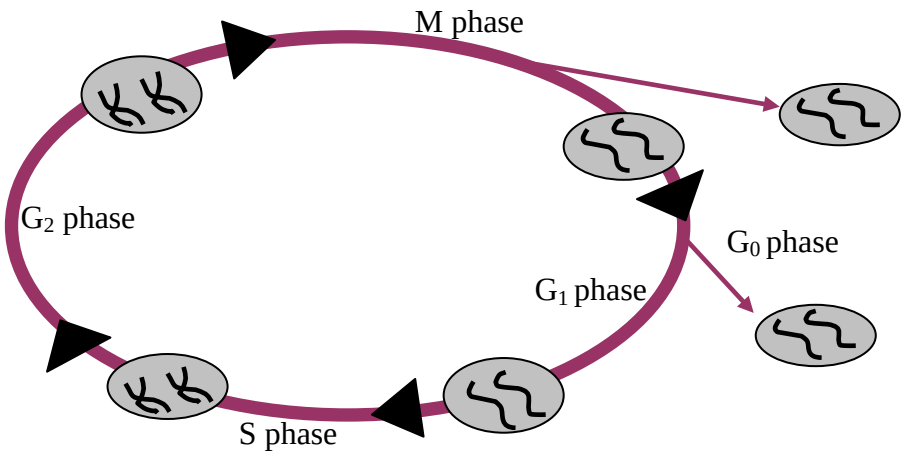

Figure 1.7: Schematic diagram of a eukaryotic cell cycle. A division competent cell spends most of the time in interphase, in which DNA replication takes place. The interphase is divided into three sub-phases, G_1 phase, S phase, and G_2 phase. The terminally differentiated cells rest in the G_0 phase.

1.6.3.2 Cell Cycle Checkpoints

DNA replication and synthesis take place only during the interphase of a cell cycle. Consequently, the DNA damage checkpoints are functional in the G_1, S, and G_2 phases of the cell cycle. The function of G_1 phase checkpoint is to ensure that damaged DNA is repaired before a cell enters the S phase, during which DNA replication takes place. The functions of S phase checkpoint include, a) monitoring the integrity of the DNA to be replicated and initiating the repair process if there is any damage, b) monitoring the

quality of the replicated DNA and initiating the repair of any errors occurred during replication. The function of G_2 phase checkpoint is to initiate cell cycle arrest if the cell contains damaged or partially replicated DNA. G_2 phase arrest is not relieved until such damage is repaired or the genome is completely replicated. DNA damage checkpoint is also present in G_0 phase of the cell cycle. Transition of cells through the cell cycle checkpoints is facilitated by the combined actions two proteins known as cell division control 25 (Cdc25) and cyclin dependant kinase 2 (Cdk2). Cdk2 promotes the progression of cells from one phase of the cell cycle to the next. In a resting cell, Cdk2 remains inactive via inhibitory phosphorylation at threonine and tyrosine on position 14 and 15 respectively. During cell cycle, the inhibitory phosphorylations on Cdk2 are removed by Cdc25 (Uto et al, 2008). Cdc25 is a phosphatase, an enzyme that removes phosphate group from its substrates. There are three isoforms of Cdc25 in eukaryotes, Cdc25A, Cdc25B and Cdc25C. Cdc25A and Cdc25C are active in G1 phase and S phase, respectively, whereas, Cdc25B is active in M phase of the cell cycle checkpoint (Mordes, 2005). In the event of DNA damage, cell cycle arrest is accomplished via inactivation of Cdk2. In the G_1 phase, cell cycle arrest is accomplished by direct inactivation of Cdk2 by a protein called p21. The S phase and G2 phase arrests, on the other hand, are accomplished indirectly via inactivation of Cdc25 (Uto et al, 2008).

1.6.3.3 DNA Repair Mechanisms

There are five major DNA repair mechanisms operative in eukaryotic cells: a) base excision repair (BER), b) nucleotide excision repair (NER), c) mismatch repair (MMR), d) homologous recombination (HR), and e) non-homologous end joining (NHEJ) (Gudmundsdottir et al, 2006). The former three, namely the NER, the BER, and the MMR, repair lesions affecting only one of the two strands of DNA. In all three cases, the lesions are excised and the resulting gaps are filled by DNA polymerases, which simply insert correct nucleotides using the intact complementary strand as a template. Hence, these three mechanisms are collectively known as the excision repair mechanisms (ERMs). Although partly overlapping, these mechanisms are lesions specific. The BER mechanism deals with small chemical alterations in the DNA bases, the NER mechanism targets helix-distorting single strand lesions, and the MMR mechanism corrects mismatched DNA bases (Fleck and Nielsen, 2004). HR and NHEJ, on the other hand,

repair double strand breaks simply by joining the broken strands, and thus are known as recombination repair mechanisms, too.

1.6.3.4 Base excision repair (BER)

The BER is responsible for correcting most spontaneous, alkylative, and oxidative DNA lesions that do not significantly distort the double helix backbone of DNA (Ataian and Krebs, 2006).

There are two types of BER mechanism in eukaryotes, long patch BER and short patch BER. Long patch BER removes and replaces up to 10 bases at a time, whereas, short patch BER removes and replaces only one base at a time. The short patch BER and long patch BER differ only in the way the damage is recognised; the underlying principle of the damage repair is common to both pathways. The damaged base or bases are identified, removed, replaced with correct base (Cox et al., 2012).

In short patch BER, the damaged bases are identified by a family of enzymes known as DNA glycosylases. Eukaryotic cells have several different types of DNA glycosylases that recognise different types of damaged bases. DNA glycosylases scan for damaged bases that remain buried in the double helix, base-paired and stacked with adjacent bases. If a damaged base is identified, the DNA glycosylase kinks the DNA and flips the damaged base out of the helix and into its active site (Cox et al., 2012). Once the damaged base is into the active site, the enzyme hydrolyses the N-glycosidic bond that links the damaged base to the sugar-phosphate backbone of the DNA, which results in an apurinic or apyrimidinic (AP) site in the DNA. The AP site generated thus is then processed by an enzyme called AP endonuclease 1 (APE1), which incise the DNA by hydrolysing the phosphodiester bond immediately 5' or 3' to the AP site. The incised ribose-phosphate backbone is then removed from the DNA by an enzyme called deoxyribophosphodiesterase or dRpase, and the correct nucleotide is incorporated in to the repair site by a DNA polymerase, Polβ. In the final step, the nicks in the DNA strand is sealed by a DNA ligase, Ligase III, in the presence of X-ray cross complement 1 (XRCC1) protein and the integrity of the DNA is restored (Figure 1.8 A).

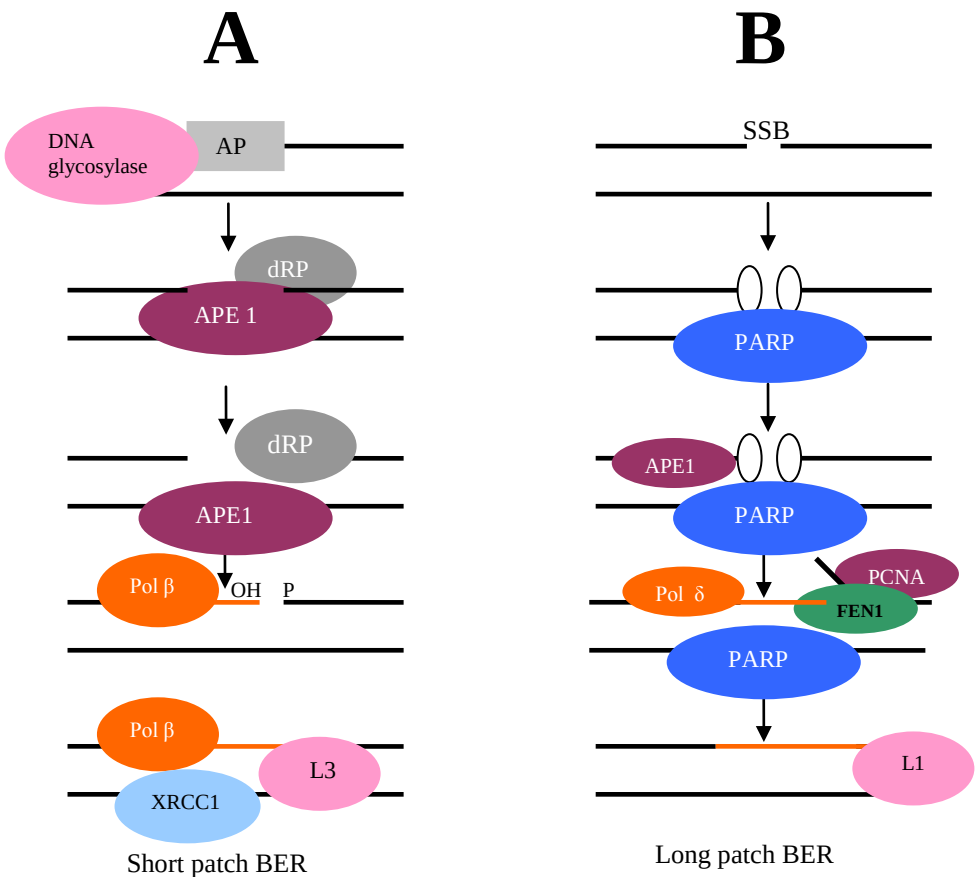

Figure 1.8: Schematic representation of BER. **(A)** Short-patch BER. Base-specific DNA glycosylase recognises the damaged base and generates an AP site. APE 1 then incises the ribose-phosphate backbone, which is removed by the enzyme dRpase. Polβ then inserts the correct nucleotide and the nicks are sealed by Ligase III (L3). (B) Long-patch BER. The damage is recognised by the enzyme PARP, which then recruits APE 1 and PNK to the damage site. APE 1 and PNK process the two ends of DNA. Pol δ, then, inserts 2-8 nucleotides creating a flap structure. The flap structure is then removed by the enzyme FEN 1. Finally, the nicks in the DNA are sealed by *Ligase 1 (*L1*).*

The long patch BER is implicated in the repair of SSBs that lack in ligatable junctions and, therefore, require processing of 3´ or 5´ end for ligation (Fortini et al., 2000). In this process, the damage is recognised by an enzyme called *poly (ADP-ribose) polymerase* (PARP). On recognition of the damage, PARP recruits APE1 and another protein called *polynucleotide kinase* (PNK) for the processing of two ends of the DNA. A DNA polymerase, Polδ, then adds 2 to 8 more nucleotides generating a flap structure. The flap structure is then removed by an enzyme called flap endonuclease 1 (FEN 1) in the presence of a protein called proliferating cell nuclear antigen (PCNA). Finally, the nick in the DNA is sealed by a DNA ligase, *Ligase I* (Figure 1.8 B).

1.6.3.5 Nucleotide excision repair (NER)

NER repairs large and bulky DNA lesions that significantly distort the double helix. Unlike BER, NER does not require specific recognition of the damaged nucleotides rather it recognises lesions based on abnormal structure and chemistry (Cox et al., 2012). The DNA lesions repaired by NER include UV induced 6-4 photoproducts (6-4PPs), cyclobutane pyrimidine dimers (CPDs) and benzo[a] pyrene-guanine caused by exposure to cigarette smoke (Cox et al., 2012). Eukaryotic NER functions in two modes. In one mode, it acts throughout the genome and therefore is referred to as Global genome NER (GG-NER). In the second mode, it targets damaged template nucleotide with stalled RNA polymerase and therefore, is referred to as transcription-coupled NER (TC-NER). The difference between the two types of NER lies in the way the damaged site is recognised. In GG-NER, the damaged nucleotide is recognised by a complex of two enzymes, XPC and hHR23B, whereas, in TC-NER, the damaged site is recognised by way of the stalled RNA polymerase II.

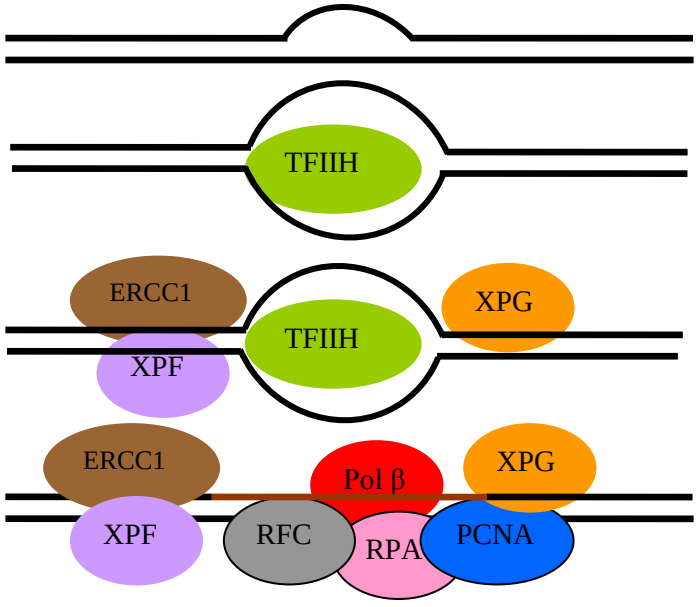

Figure 1.9: Schematic diagram showing a summary of NER pathway. Once the damage is recognised, the enzyme TFIIH unwinds around 25 base pairs of DNA surrounding the damage. XPG and ERCC1/XPF then makes incision on 5´ and 3´sides of the damaged site to remove around 30 nucleotides including the damaged ones. The enzyme *Pol β* then fills the gap by incorporating correct nucleotides using the intact strand as a template in the presence of RPA, RFC and PCNA.

The rest of the process leading to the repair of the damage is similar in both sub-pathways (Cox et al., 2012). Following recognition of the damaged site, TFIIH, a multi-subunit transcription factor composed of XPB and XPD, is recruited to the damaged site. The subunits of TFIIH, XPB and XPD, act as helicases, enzymes that break open two strands of DNA, to unwind approximately 25 base-pairs of DNA surrounding the damaged site for incision (Cooper and Hausman, 2009). Two endonucleases, XPG and a hetero-dimer of XPF and ERCC1, are then recruited to the repair site. XPG and XPF/ERCC1 incise the DNA on 5´ and 3´sides of the damaged site (Cooper and Hausman, 2009). As a result, around 30 nucleotides including the damaged ones are removed from the DNA. The resulting gap is then filled by the replicative DNA polymerase in the presence of replication protein C (RFC), replication protein A (RPA) and proliferative cell nuclear antigen (PCNA). Finally, the nicks in the DNA are sealed by a DNA ligase (Figure 1.9).

1.6.3.6 Mismatch repair (MMR)

Eukaryotic DNA replication is error prone; a wrong base is incorporated every 10^8 bases inserted (Kunkel, 2004). Most mismatched bases are removed by the proofreading activity of the DNA polymerase. The mismatched bases that escape the proofreading activity of DNA polymerase are corrected by MMR adding to the fidelity of the eukaryotic replication process (Cooper and Hausman, 2009). MMR is also responsible for the repair of mismatched bases that arise during homologous recombination and that arise from DNA damage by various genotoxic agents (Ataian and Krebs, 2006). One interesting feature of MMR system is the distinction between the parental DNA and newly synthesised DNA. In *E. coli*, the distinction between the parental strands and the newly synthesised strands is made by the methylation tags on the parental strands. In E. Coli DNA, following replication, adenine residues are methylated within the sequence GATC, forming 6-methyladenine. Since newly synthesised strands are not methylated, MMR enzymes leave the parental stands alone and make corrections in the newly synthesised strands. The enzymes involved in the *E. coli* MMR system comprised of MutS, MutL, and MutH families. The heterodimer of MutS and MutL families scans through the DNA for any mismatches. Once a mismatch is found, MutH is recruited to the repair site to identify the newly synthesised strand and make incision on GATC sequence. In Eukaryotes, however, such distinction can not be made by way of methylation tags on the parental strand since there is no eukaryotic homologue for MutH.

In eukaryotic cells, the lagging strand is synthesised as short fragments known as Okazaki fragments. Eukaryotic MMR enzymes distinguish the lagging strand from the leading strand by the nicks at the either end of the Okazaki fragments (Cox et al., 2012). The identification of the newly synthesised strands is performed by a tetra-heteromeric complex MLH1/MLH3 and MSH2/MSH3, homologues of MutL and MutS, respectively. The repair process following identification of the newly synthesised strands is very similar in both prokaryotes and eukaryotes. An exonuclease enzyme called Exo1 removes the mis-paired base in the presence of RPA, RFC and PCNA. DNA polymerase then incorporates the correct base and finally the nicks on the DNA are sealed by ligase (Figure 1.10).

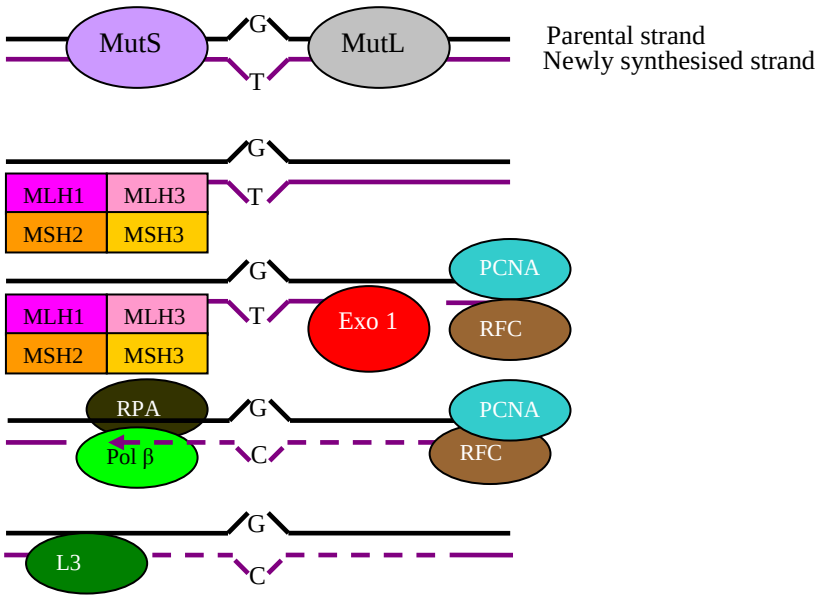

Figure 1.10: **Schematic diagram showing a summary of MMR.** The tetra-heterodimer of MLH1/MLH3 and MSH2/MSH3 recognises the newly synthesised DNA strand. The enzyme EXO 1 removes the mismatched base. Finally, Pol β inserts the correct base in the presence of RPA, RFC and PCNA using the parental strand as a template. Finally, the nicks in the DNA are sealed by Ligase 3 (L3).

1.6.3.7 Homologous recombination (HR)

DSBs are the most dangerous of all DNA lesions. Unlike other lesser forms of DNA lesions that lead to mutation, DSBs typically lead to cell death if not repaired and promote mutations and genomic instability if not repaired accurately. Ability to repair DSBs is inherent to all living organisms. In dividing human cells, each day around 10

DSBs occur as a result of metabolic processes such as replication, V(D)J recombination, and meiosis, or endogenously generated ROS (Lindahl, 1993). Without a competent DSBs repair mechanism, a eukaryotic cell would die after a few divisions (Cox et al., 2012).

HR is the predominant pathway for repairing replication associated DSBs. As the name suggests it is based on the genetic information from either the identical chromatid or the homologous chromosome (Gudmundsdottir et al., 2006). Consequently HR is found to be active in S and G2 phase of the cell cycle where it can utilize the undamaged sister chromatid as the template for restoring the genetic information (Cox et al., 2012). Because of the very nature, HR is an error free mechanism, no genetic information is lost due to missing nucleotides at the site of the DSBs. HR begins with the selective degradation of 5' end of the broken DNA to generate 3' overhangs by a protein complex involving MRE11, RAD50 and NBS1 (MRN). In the resultant 3' overhangs, replication protein A (RPA), facilitated by RAD52, binds to prevent degradation. Then, a protein called RAD51 is recruited to the site which displaces RPA from the ssDNA.

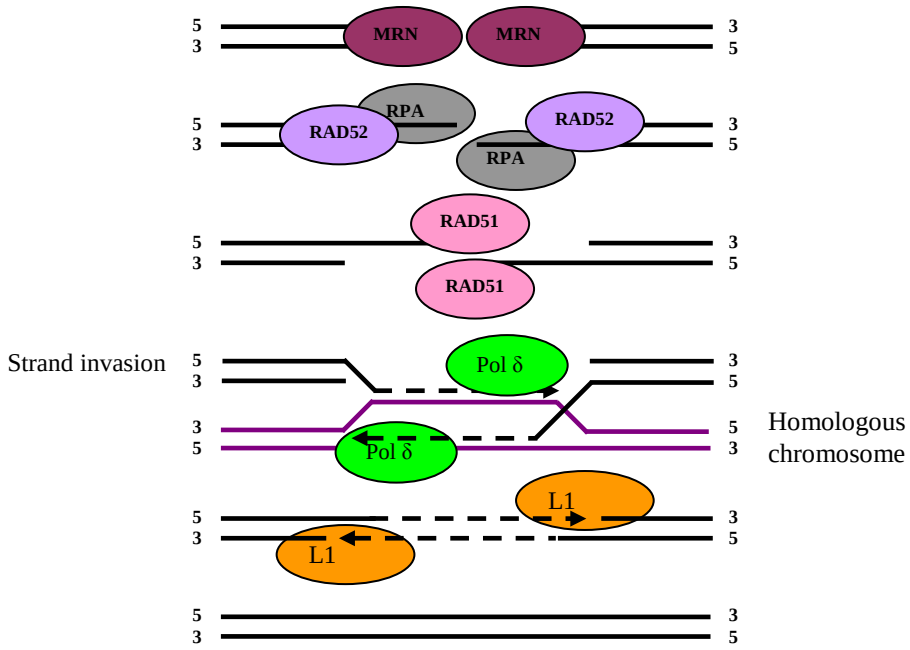

Figure 1.11: Schematic diagram of HR repair. MRN complex generates 3´ overhangs in the broken DNA ends. RPA binds the 3´ overhangs in the presence of RAD52 to prevent degradation. RAD51 displace RPA and binds to 3´ overhangs. The resulting RAD51-SSDNA complex then invades a homologous chromosome and Pol δ extends 3´ overhangs using the strands of homologous chromosome as templates. Finally, the nicks in the DNA are sealed by L1.

Next, the resulting RAD51-ssDNA complex invades a homologous sequence on the sister chromatid or homologous chromosome, which is then used by a DNA polymerase, Pol δ, as a template to extend the 3' end of the ssDNA. Finally, the repaired ends are joined by a DNA ligase, Ligase 1 (L1) (figure 1.11) (Gudmundsdottir et al., 2006, Fleck and Nielsen, 2004).

1.6.3.8 Non-homologous end joining (NHEJ)

Although HR restores genetic information accurately, it is complicated. Moreover, DSBs also occur when HR mediated repair is not possible (Cox et al., 2012). For example, during the G_1 phase and late G_1 or G_0 phase of the cell cycle the homologous chromosomes are not readily aligned and DSBs repair via HR is not feasible. Consequently, NHEJ is found to responsible DSBs repair in the G_1 phase and late G_1 or G_0 phase of the cell cycle. As NHEJ repair is not based on a sequence homology it is an error-prone repair mechanism (Cox et al., 2012).

Central to NHEJ is the multi-meric DNA-dependant protein kinase, DNA-PK. This holo-enzyme consists of a catalytic subunit, DNA-PKcs and a hetero-dimer of Ku70 and Ku80. The hetero-dimer Ku70/Ku80 binds to the termini of a DSB to protect the ends from degradation, and signals the catalytic subunit, DNA-PKcs to form the active complex DNA-PK. The activated DNA-PK then phosphorylates a protein called Artemis. Artemis is generally active as an exonuclease, an enzyme that digests nucleotides from one end. Phosphorylation of Artemis by DNA-PK transforms it into an endonuclease, an enzyme that makes incision on DNA at an internal sequence (Cox et al., 2012). However, the DNA-bound DNA-PKcs then juxtapose the DNA ends and any unpaired DNA sequences are cleaved by Artemis. Finally, the juxtaposed ends are ligated by a DNA ligase, Ligase IV, facilitated by a protein called *x-ray cross* complementation group (XRCC4) (Figure 1.12). Since nucleotides are added or deleted at the broken ends of the DNA during NHEJ repair, it is a mutagenic process. However, NHEJ is a very important DSB repair mechanism for the differentiated somatic cells of higher eukaryotes even at expense of mutation.

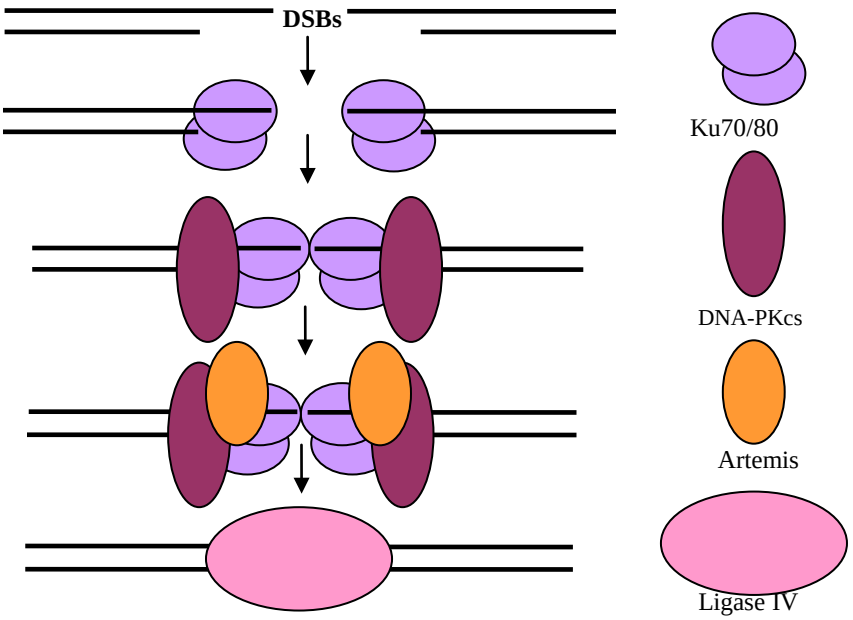

Figure 1.12: Schematic diagram showing events in NHEJ repair. Hetero-dimer of Ku70/80 binds to the DSB ends and signals DNA-PKcs to site to form the active complex DNA-PK. The active DNA-PK complex recruits Artemis, which incises the unpaired nucleotides. Finally, the ends of the DSBs are joined bu *Ligase IV*.

1.6.4 Sensor of DNA damage

To initiate a DDR, a cell must first recognise the DNA damage (Gudmundsdottir et al, 2006). How cells recognise DNA damage has been the topic of many studies. The outcomes of these studies have led to the comparison of the DDR to a signal transduction system consisting of proteins acting as sensors, transducers, mediators and effectors (Yang et al, 2004). In this system, DNA damage acts as signal, which is detected by sensor proteins. The mediator proteins bring the sensor proteins and the transducer proteins together. Then the transducer proteins pass the signal to effector proteins, which finally initiate the response (figure 1.13) (Wood and Chen, 2007). Since sensor proteins are the first to be activated following DNA damage, detection and quantification of these proteins may give valuable insights into a DDR.

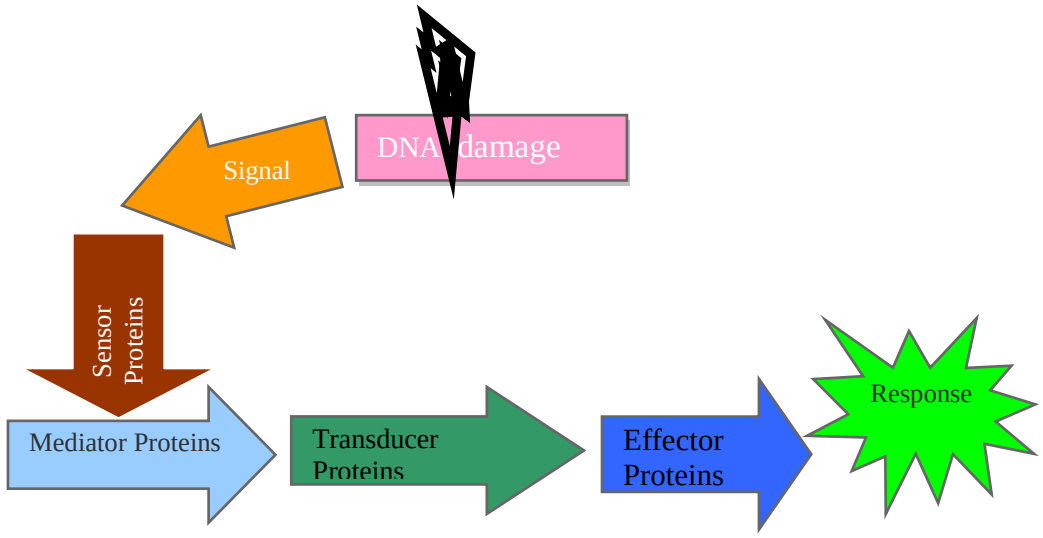

Figure 1.13: Showing DDR as a signal transduction system. Sensor proteins detect the damage signal. The mediator proteins convey the signals to the transducer proteins, which signal the effecter proteins to consummate the response.

Although studies are still underway to identify specific DNA damage sensors, several proteins have been implicated as candidates. Two mammalian proteins, Ataxia Telangiectasia, Mutated (ATM) and ATM and Rad3- related (ATR) are the most studied of them.

1.6.4.1 ATM and ATR

ATM and ATR belong to a family of protein known as phosphoinositide 3-kinase like kinase (PIKK). A kinase is a protein that transfers phospho groups onto other proteins in a process known as phosphorylation. ATM and ATR are structurally very similar containing four conserved domains that regulate their kinase activity (Lempiainen and Halazonetis, 2009). The four conserved domains of the kinases are the FRAP-ATM-TRRAP (FAT) domain, the Kinase domain (KD), the PIKK-regulatory domain (PRD) and the FAT-C-terminal (FATC) domain (figure 1.14).

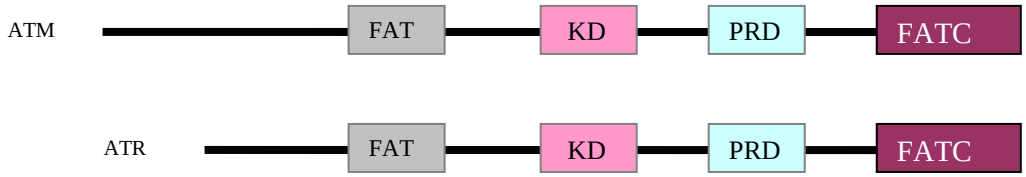

Figure 1.14: Schematic diagram showing structural similarity between ATM and ATR. Both of the kinases contain four conserved domains, namely FAT, KD, PRD and FATC (adapted from Lempiainen and Halazonetis, 2009).

In addition to the structural similarity, the kinases are also marked by a similarity in the way they phosphorylate their substrates. It is a common consensus that both ATM and ATR phosphorylate their substrates in the sequence context of serine/threonine-glutamine (S/TQ) motif (Kim et al, 1999; Kastan and Lim, 2000; Abraham, 2001; Zhao and Piwnica-Worms, 2001, Mordes and Cortez, 2008). ATM and ATR are activated at the very early stages of a DDR in eukaryotic cells, relaying the DNA damage signal onwards by phosphorylating many regulatory proteins downstream (Yang et al, 2003). Nevertheless, these kinases are found to be damage specific. ATM is predominantly activated in response to DSBs whereas ATR responds to both DSBs and SSBs (Yang et al, 2003). However, ATR activation following the occurrence of DSBs probably takes place as a SSB response when one strand in the DSB segment is repaired (Yang et al, 2003).

1.6.4.2 Role of ATM and ATR in the cell cycle checkpoints and DNA repair mechanisms

As mentioned earlier, in the event of DNA damage, cell cycle checkpoints arrest the replication process to allow DNA repair mechanism time to repair the damage. Studies on many human diseases over the years have shown that an intrinsic connection exists between the cell cycle check points and DNA repair mechanisms.

ATM and ATR are ubiquitously present in inactive forms. On recognition of an insult to DNA, the kinases are activated via autophosphorylation. ATM becomes activated via autophosphorylation at the serine residue on position 1981 (So et al., 2009), whereas, ATR becomes activated via autophosphorylation at the threonine residue on position 1989 (Liu et al., 2011). Following activation, the kinases are relocated to the respective

sites of damage to form nuclear foci (So et al, 2009; Liu et al, 2011; Mordes and Cortez, 2008), which is a characteristic feature of DDR proteins (Wood and Chen, 2007). It is evident from studies that ATM and ATR phosphorylate a number of proteins with critical functions in both cell cycle checkpoints and DNA repair mechanisms (Balajee and Geard, 2006), and thus coordinating the two events of a DDR.

1.6.4.2.1 Role of ATM and ATR in the cell cycle check points

1.6.4.2.1.1 G_1 phase checkpoint

Tumor suppressor protein, P53 plays a pivotal role in the activation of G_1 phase DNA damage checkpoint. It has been shown that in p53 null cells the G_1 phase DNA damage checkpoint is completely abrogated (Abraham, 2001). Activated P53 is responsible for the transcriptional activation of p21, a protein with a critical role in G_1 phase cell cycle arrest. P21 is an inhibitor of cyclin dependant kinase, Cdk2. Cyclin E and cyclin A-associated Cdk2 activities promote the progression of cells from G_1 phase to S phase. p53 mediated activation of p21 thus arrests cells in G_1 phase (Figure 1.15). In a normally growing cell, p53 is negatively regulated by a protein called MDM2, which transports the former to cytoplasm for proteosomal degradation.

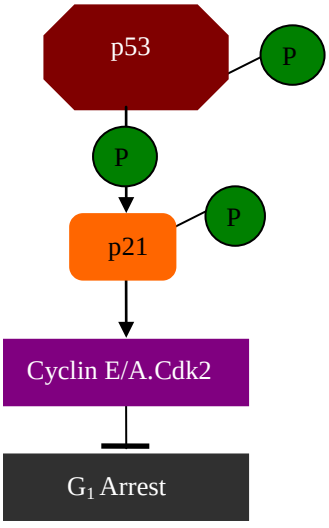

Figure 1.15: Role of p53 in G_1 phase arrest. Activated p53 phosphorylates a protein called p21, which is responsible for inhibiting Cdk2. Cdk2 in association with Cyclin E/A promotes cells to progress to S phase. p53 mediated inhibition of Cdk2 via p21, thus, results in cell cycle arrest in G_1 phase of the cell cycle

1.6.4.2.1.2 ATM and G_1 phase checkpoint

ATM plays multiple roles in activating and stabilizing p53 in the G_1 phase checkpoint of the cell cycle. Following the occurrence of DSBs, ATM directly phosphorylates MDM2 at the serine residue on position 395 (Ser 395). ATM mediated phosphorylation of MDM2 modifies the affinity of the later for p53. ATM, then, phosphorylates a protein called checkpoint Kinase 2 (Chk2) at the threonone residue on position 68 (Thr 68), which in turn, phosphorylates p53 at Ser 20. Chk2 mediated phosphorylation facilitates the accumulation of p53 by removing the MDM2 binding site. Next, ATM directly activates p53 by phosphorylating it at the serine residue on position 15 (Ser15) (Abraham, 2001) (Figure 1.16). Interplay of these three events, modification of Mdm2 affinity for p53 by ATM and Chk2 and subsequent activation of p53 by ATM, enables a cell to go through either the G_1 phase of cell cycle or apoptosis based on the extent of DNA damage (Balajee and Geard, 2006).

1.6.4.2.1.3 ATR and G_1 phase checkpoint

ATR also phosphorylates p53 at Ser 15. It has been shown that in ATM null cells that incurred DSBs, p53 phosphorylation at Ser 15 is significantly decreased but not completely suppressed (Abraham, 2001). This suggests that ATR serves as backup kinase for ATM with respect to DSB response. It has also been shown that in response to DSBs, ATR null cells significantly deficient in maintaining Ser 15 phosphorylation of p53 (Tibbets et al., 1999), suggesting a role for ATR in maintenance of p53 phosphorylation. However, in response to SSBs causing agents such UV, ATR has been shown to be the sole kinase for p53 phosphorylation at Ser 15 during G_1 phase checkpoint (Tibbets et al., 1999). Nevertheless, how ATR dependant G1 phase checkpoint is activated is not well understood as yet (Abraham, 2001). It has been suggested that a parallel ATR-Chk1 pathway may exist (Figure 1.16).

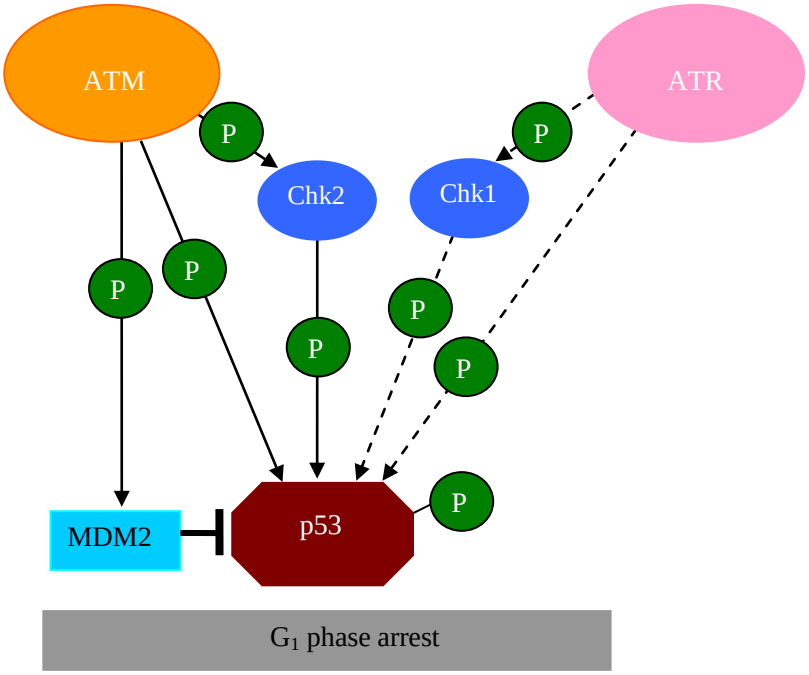

Figure 1.16: The roles of ATM and ATR in G_1 phase arrest. ATM inhibits MDM2, which is an inhibitor of p53 in a normally growing cell. ATM, then, directly activates p53 via phosphorylation. ATM also phosphorylates Chk2, which in turn phosphorylates p53 to enhance the activity of the later. It has been suggested that ATR mediated activation of G_1 phase checkpoint (shown as dotted lines) is identical to that of ATM.

1.6.4.2.1.4 S phase checkpoint

Central to S phase checkpoint is the activation of two proteins, checkpoint kinase 1 (Chk1) and checkpoint kinase 2 (Chk2). Both Chk1 and Chk2 phosphorylate Cdc25, Cdc25A in this instance, to facilitate its nuclear export and proteosomal degradation. Degradation of Cdc25A thus delays DNA synthesis in S phase (Abraham, 2001) (figure 1.17).

1.6.4.2.1.5 ATM in S phase checkpoint

Studies have shown that ATM plays an important role in activating the S phase checkpoint (Balajee and Geard, 2006). In response to DNA damage in the form of DSBs, ATM phosphorylates Chk2 at Thr 68. Chk2, in turn, phosphorylates the serine residue on position 123 (Ser 123) in Cdc25A. This phosphorylation facilitates the ubiquitin dependant degradation of Cdc25A.

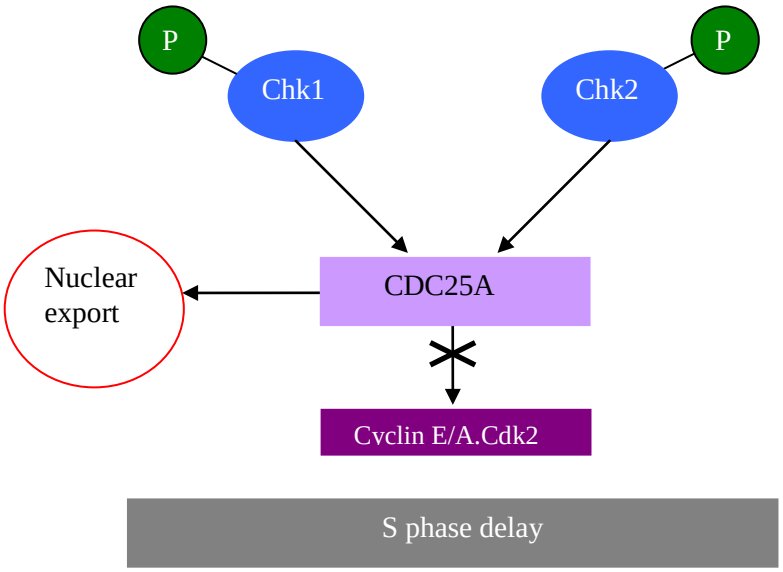

Figure 1.17: Functions of Chk1 and Chk2 in S phase delay. Both Chk1 and Chk2 phosphorylate Cdc25A to inhibit its phosphatase activity. Cdc25A is responsible for activating Cdk2 by removing the inhibitory phosphorylation. Inhibition of Cdc25 by Chk1 and Chk2, thus, results in S phase delay.

1.6.4.2.1.6 ATR in S phase checkpoint

The function ATR in activating S phase checkpoint in the event of single strand lesions is well characterised. ATR mediated S phase checkpoint activation is very similar to that of ATM. Following DNA damage in the form of SSBs, ATR phosphorylates Chk1 at the serine residue on position 345 (Ser 345). Chk1 then phosphorylates CDC25A on Thr 504 (Uto et al., 2008). Chk1 mediated phosphorylation facilitates the nuclear export and ubiquitin mediated degradation of Cdc25A resulting in S phase delay (Flynn and Zou, 2011) (Figure 1.17).

1.6.4.2.1.7 G_2 Checkpoint

G_2 phase checkpoint is the final gatekeeper that stops cells with damaged DNA from going through nuclear division. As in the case of S phase checkpoint, the G_2 phase arrest is also facilitated via inactivation of Cdc25, Cdc25C in this case, by Chk1 and Chk2.

1.6.4.2.1.8 ATM and G_2 Checkpoint

Following the occurrence of DSBs, ATM phosphorylates Chk2 at Thr 68 Thr 68, which in turn phosphorylates Cdc25C, creating a binding site in the phosphatase for a protein complex known as 14-3-3. The resulting complex of 14-3-3/Cdc25C proteins are exported to the cytoplasm, and thus Cdc25C can not activate Cdk2 (figure 1.18). These events keep Cdk2 in an inactive state and thus halting the cells from entering mitotic division (Flynn and Zou, 2011).

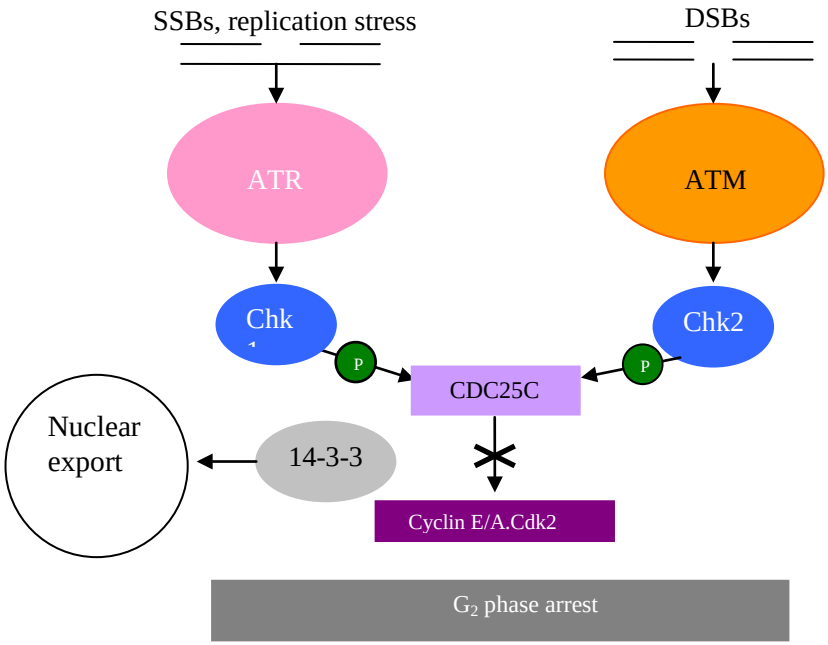

Figure 1.18: Showing the functions of ATM and ATR in G_2 phase arrest. In the event of DSBs and SSBs, ATM and ATR phosphorylate Chk2 and Chk1, respectively. Chk2 and Chk1, in turn, generate a binding site in Cdc25C for 14-3-3. The complex of Cdc25C and 14-3-3 is exported to the cytoplasm for ubiquitin mediated degradation of Cdc25C. Degradation of Cdc25C result in cell cycle arrest in G_2 phase of the cell cycle.

1.6.4.2.1.9 ATR and G2 Checkpoint

In response to SSBs, ATR phosphorylates Chk1 at Ser 345. Chk1 then phosphorylates Cdc25C, creating a binding site for the 14-3-3 protein complex. The resulting complex of 14-3-3/Cdc25C proteins are thus exported to the cytoplasm for ubiquitin mediated degradation (Flynn and Zou, 2011) (Figure 1.18).

1.6.4.2.2 Role of ATM and ATR in DNA repair mechanism

Although the main function of ATM and ATR is to activate cell cycle checkpoint, there is evidence as regards to the role of these kinases in the actual repair processes. In the event of DSBs, H2AX, one of the five types of histone proteins in eukaryotes, is phosphorylated to provide access to the proteins of DNA repair mechanisms to the damage sites (Derheimer and Kastan, 2010).

Numerous studies have shown that in the event of DSBs, ATM phosphorylates H2AX at the serine residue on position 139 (Ser 139) (Derheimer and Kastan, 2010) suggesting a direct role for ATM DSBs repair. However, it is also evident that ATM is not the sole kinase for H2AX. ATR has also been shown to phosphorylate H2AX at Ser139 in response to replication stress (Chanoux et al., 2009).

1.6.4.2.2.1 ATM and ATR in HR

MRN complex responsible for the processing of blunt ends of DSBs is a direct substrate for ATM kinase (Derheimer and Kastan, 2010). It has also been shown that MRN complex generates small DNA fragments at the site of DSBs, which further stimulate the activation of ATM (Derheimer and Kastan, 2010). ATM and MRN complex, therefore, act in concert for the efficient repair of DSBs.

RPA, one of the key proteins in HR, NER and MMR, is also phosphorylated by both ATM and ATR (Zou and Elledge, 2003; Shell et al., 2009). It has been shown that ATM and RPA co-localises along the length of synapsed meiotic chromosomes (Balajee and Geard, 2006). RPA has also been shown to be phosphorylated by Mecl, a homologue of ATM in Yeast (Cox et al., 2012). Moreover, it has been shown that in ATM null human cells, RPA phosphorylation is attenuated, which suggests that RPA phosphorylation by ATM is a conserved DNA repair pathway in eukaryotes (Balajee and Geard, 2006).

1.6.4.2.2.1.2 ATM and ATR in NHEJ

The catalytic subunit of DNA-PK, DND-PKcs is activated via auto-phosphorylation upon association with Ku70 and Ku80. However, studies have shown that DNA-PKcs can also be phosphorylated by both ATM and ATR, suggesting the existence of an NHEJ repair mechanism independent of Ku70 and Ku80 (Chen et al., 2007; Yajima et al., 2009). ATM has also been shown to interact with Artemis which is responsible for cleaving any unpaired nucleotides during NHEJ repair of DSBs (Derheimer and Kastan, 2010).

1.6.4.2.2.1.3 ATR in single strand lesion repair mechanism

Since ATR is predominantly activated following single strand affecting lesions, it is expected to have significant roles in the repair of such lesions, too. Numerous studies have shown that ATR directly interacts with a number of enzymes with significant functions in NER. A study carried out by Li et al., (2011) showed that ATR facilitates the nuclear import of XPA, a protein with critical function in both GG-NER and TC-NER, in a cell cycle checkpoint-dependant fashion. In another study by Auclai et al (2008), it has been shown that in ATR null cells, GG-NER is completely abrogated during the S phase of the cell cycle, suggesting an indispensable role of ATR in the maintenance of GG-NER.

As mentioned earlier, RPA is a multi-faceted protein with significant functions in most of the eukaryotic DNA repair mechanisms, except for BER and NHEJ. However, in an earlier study, RPA has been shown to stimulate the long-patch BER sub-pathway (Demott et al., 1998). As previously discussed, this single strand binding protein is directly activated by ATR, further suggesting the importance of the kinase in genome maintenance.

1.6.4.2.3 Activated ATM indicates the occurrence of DSBs and activated ATR indicates that of both DSBs and SSBs

With the respective roles of both ATM and ATR in the activation of the DNA damage checkpoints and DNA repair mechanisms, as summarized in table as follows, in

perspective, it is clear that the activated forms these kinases are very good markers of the initiation of a DDR. ATM activation is as an indication of the initiation of a DDR in the event of DSBs. ATR activation, on the other hand, may be regarded as an indication of the initiation of a DDR in response to both DSBs and SSBs.

Table 1.1: A summary of the roles of ATM and ATR in cell cycle checkpoints and DNA repair mechanisms

Event	Kinase	
Cell cycle checkpoints	ATM	ATR
	1. Deactivates MdM2	1. Activates p53
	2. Activates p53 directly	2. Activates Chk1, which in
	3. Activates Chk2, which in	turn activates p53
G_1 phase arrest	turn activates p53	
	Activated p53, in turn, activates p21, which deactivates CDK2 to arrest cell cycle	
	1. Activates Chk2, which in	1. Activates Chk1, which in
	turn deactivates CDC25A	turn deactivates CDC25A
S phase Delay	Deactivation of CDC25A leads to delay in cell cycle progression	
	1. Activates Chk2, which in	1. Activates Chk1, which in
G_2 phase arrest	turn deactivates CDC25B	turn deactivates CDC25B
	Deactivation of CDC25A leads to cell cycle arrest	
DNA repair mechanisms		
BER	1. Activates RPA	1. Activates RPA
	RPA stimulates long-patch BER sub-pathway	
	1. Activates RPA	1. Activates RPA
		2. Facilitates nuclear export
NER		of XPA
MMR	1. Activates RPA	Activates RPA
	1. Activates MRN complex	1. Activates RPA
HR	2. Activates RPA	
	1. Activates DNA-PKcs	1. Activates DNA-PKcs
NHEJ	2. Activates Artemis	2. Activates Artemis

1.6.5 Fates of cells sustaining DNA damage beyond repair

In the foregoing section, the common knowledge of how the eukaryotes deal with DNA damage has been elaborated. In the event of DNA damage, the cell cycle checkpoints arrest the cell cycle for the damage to be repaired by the DNA repair mechanisms. If the damage is beyond repair, the cell cycle checkpoints facilitate the elimination of the cell by initiating a "programmed cell death" called apoptosis.

1.6.5.1 Apoptosis

Apoptosis is a genetically controlled elimination process of unwanted, potentially harmful cells from a biological system. It takes place during normal development as in the formation of the digits in the limbs, and to maintain homeostasis of cell populations in tissues as in the case of the maintenance of B lympocytes and T lymphocytes in the bone marrow (Lawen, 2003, Elomre, 2007). Apoptosis also acts as a defence mechanism to eliminate cells that are damaged by noxious agents or invaded by pathogens (Elmore, 2007). It is a means by which eukaryotes eliminate cells that are capable of becoming neoplastic.

Apoptosis is characterised by a number of biochemical events, which lead to morphological features attributed to an apoptotic cell. Once a cell is committed to apoptosis, a group of proteases, enzymes that break down proteins, known as initiator caspases are activated via dimerisation. Activated initiator caspases, in turn, cleave the catalytic domains of a second group of proteases known as executor caspases to activate them (Pop and Salvesen, 2009). The executor caspases are responsible for cleaving proteins that are essential for maintaining the structural integrity of the cells. The caspases mediated cleavage of the structural proteins lead to cell shrinkage and membrane blebbing, the characteristic morphological features of an apoptotic cell (Lawen, 2003; Elomre, 2007). The executor caspases also facilitate the cleavage of the nuclear DNA by inactivating an enzyme called inhibitor of caspase-activated DNase (ICAD). Inactivation of ICAD by caspases allows caspases-activated DNase (CAD) to relocate to the nucleus and cleave the DNA into smaller fragments leading to cell death (Lawen, 2003, Elomre, 2007).

Another characteristic feature of apoptosis is the externalisation of phosphatidylserine, an inner membrane protein. The movement of phosphatidylserine to the outer surface allows the identification of apoptotic cells by the phagocytes, which are specialised cells responsible for removing harmful cells or objects from a biological system. Phagocytic recognition and removal of the apoptotic cells mark the final phase in the apoptotic process (Elomre, 2007).

1.6.5.2 Senescence

However, there is a third scenario, in which a cell sustaining DNA damage beyond repair escapes apoptosis by adopting an adaptive mode known as senescence. The term senescence means "to grow old". It was coined about four decades ago to describe a process by which eukaryotic cells, at the end of their replicative life span, cease to grow (Rodier and Campisi, 2011). At the end of each cell division, telomere, the end of a chromatid, gets progressively shortened because of the inability of DNA polymerases to replicate DNA at the very end. Germ cells and stem cells possess telomerase, an enzyme that can restore the telomeric region, which enables these specialised cells to divide throughout their lifetime. However, progressive telomere shortening is the major cause of replicative senescence in somatic cells as prevalent in aged organisms. To date, senescence refers to a …"*irreversible growth arrest…*"in eukaryotic cells in response to a myriad of stimuli which include damage to chromatin structure, oxidative stress, DNA damage, and activation of various oncogenes (Kong et al, 2011, Rodier and Campisi, 2011).

In senescence state, the cells are irreversibly arrested in the G_0 phase of the cell cycle. They remain metabolically active and become resistant to apoptosis. Senescent cells undergo characteristic morphological and biochemical changes. They increase in size, almost doubling in terms of size compared to non-senescent cells. Senescence is usually accompanied by a persistent DDR (Rodier and Campisi, 2011).

1.6.5.2 A summary of the fates of cells sustaining DNA damage

The fate of a cell sustaining DNA damage is decided in the various cell cycle checkpoints. If the repair of the damage is feasible, the repair process is initiated and the cell goes through the cell cycle as usual. In the event of DNA damage that is beyond repair, cells are faced with two fates. If the elimination of cells with such damage is beneficial for the organism as a whole, the apoptotic pathway is activated. On the other hand, if the physical presence of the cells with un-repairable damage is beneficial for the organism as whole, the cells enter G_0 phase of the cell cycle and senesce (Figure 1.19).

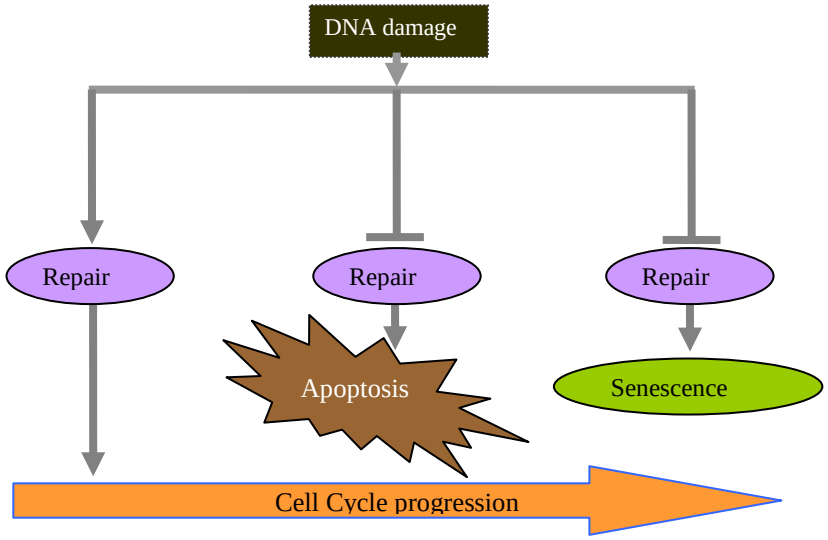

Figure 1.19: Schematic diagram summarising the fates of a cell sustaining DNA damage. If the damage is repaired, the cell cycle proceeds as normal. If the damage is beyond repair, the cell either goes through apoptosis or senesce in an adaptive mode.

1.6.6 Evidence as regard to the effects of cryopreservation on genetic material

It has been shown that the DNA damage resulting from cryopreservation occurs in the form of various mutations, chromatin structure break, and DNA fragmentations. In a study carried out by Kopeika, et al (2005), it has been shown that the frequency of base pair mutation is increased in the mitochondrial DNA of cryopreserved zebrafish (*Danio rerio*) blastomere cells. In a recent study on human semen, Dejarkom, and Kunathikom (2007) have shown that cryopreservation decreases the motility of spermatozoa. Since

mitochondria, the powerhouse of a cell, is responsible for generating ATP needed for motility, this finding suggests mitochondrial damage in cryopreserved spermatozoa.

The study of Dejarkom and Kunathikom (2007) has also shown that the chromatin integrity of spermatozoa is significantly decreased following cryopreservation. In an earlier study, a research group working with ram spermatozoa have shown that cryopreservation facilitates DNA fragmentation by destabilising the chromatin structure (Peris et al., 2004). Since chromatin is the building blocks of the eukaryotic chromosomes (as discussed earlier), these findings suggest that cryopreservation may have an impact on genomic DNA, too.

Numerous studies have shown that cryopreservation is responsible for increased DNA fragmentations. An earlier study looking at the effects of ROS and cryopreservation on equine spermatozoa showed that both of the factors promoted DNA fragmentations in the cells (Baumber et al., 2003). In a more recent work, cryopreservation has been found responsible for increased DNA fragmentations in the spermatozoa of sex-reversed rainbow trout (Perez et al, 2008). In this study, Perez et al, (2008) has shown that short-term chilled storage facilitates nucleotide oxidisation rather than DNA fragmentation whereas cryopreservation causes DNA fragmentation rather than nucleotide oxidisation.

Fragmented DNA is a major hallmark of apoptosis (Dash, 2009), and therefore, it has been suggested that cryopreservation may induce apoptosis in the cells, which contributes to a reduced post thaw survival rate. An earlier study, attempted to investigate the effects of cryopreservation on nuclear DNA of bull spermatozoa, found that cryopreservation induced an apoptosis like mechanism in the cells (Martin et al, 2004). In this study active caspases, which are the early markers of apoptosis in somatic cells, were found in both dead and live cryopreserved sperms. In a more recent study, Ortega-Ferrusola et al, (2008) also found an increased caspases activity in cryopreserved equine spermatozoa. Translocation of phosphatidylserine, an inner membrane protein, onto the outer surface is another classic marker of apoptosis; and cryopreservation has been linked to this classic marker, too (Duru et al, 2001).

1.6.7 Potential source of DNA damage during cryopreservation

Cryopreservation is a multi-step process, and damage to the genome can take place during any or all of the steps involved. In fact, numerous studies have implicated all of the four steps involved in cryopreservation, namely, chilling, CPA treatment, freezing and thawing as the potential sources of cryopreservation induced DNA damage.

As mentioned earlier, CPAs are thought to affect cells indirectly via osmotic stress during freezing and thawing. However, it is now evident that CPAs can exert direct biochemical injury to the genomic DNA. In study carried out by Rajaei et al, (2005), it has been shown that CPAs increased DNA fragmentations significantly decreasing the cell survival. In this study, the porcine embryos were treated with ethylene glycol, 1, 2-propanediol and glycerol and the result showed a decreased survival rate in the embryos treated with 1, 2- propanediol and glycerol; and increased DNA fragmentations in all three cases. In another study, Rajaei et al, (2006), have shown that ethylene glycol, 1, 2-propanediol and glycerol increased DNA fragmentation in the porcine blstocysts, too.

The chilling process involved in cryopreservation may also have damaging effects on the genome of the biological objects. It has been shown that chilling exerts oxidative stress on cells leading to increased endogenous ROS generation (Scandalios, 1993; Tsang et al, 1991). Chilling-induced increased ROS formation has been linked to lipid peroxiadation (Prasad, 1996) and apoptosis, too (Wood and Youle, 1995).

Freezing and thawing process involved in cryopreservation have long been implicated with an increased endogenous ROS (Ball et al., 2001). As mentioned earlier, ROS chemically modifies the DNA bases; and increased DNA fragmentations were found to be proportional to the freeze-thaw cycles involved in the process (Linfor and Meyers, 2002). In a recent study, cryopreservation has been found to increase lipid peroxidation in goat spermatozoa (Gogol et al, 2006). Lipid peroxidation as well as ROS may damage mitochondrial and nuclear DNAs resulting in chromatin cross-linking, mutations and DNA strand breaks (Baumber et al, 2003).

1.6.8 Shortcomings of the evidence implicating cryopreservation with compromised genetic integrity

Evidence associating cryopreservation with DNA damage and apoptosis is also not well grounded. The studies of Martin et al, (2004) and Ortega-Ferrusola et al, (2008), which found increased caspases activity in cryopreserved bull spermatozoa and equine spermatozoa, respectively, failed to detect either the nuclear condensation or the DNA fragmentation, which mark the final stages of apoptotic process. In addition, a recent study by Thomson et al, (2009) has shown that cryopreservation induced DNA fragmentation in human spermatozoa is facilitated by oxidative stress rather than apoptosis.

What is more, most of the studies investigating the effects of cryopreservation on DNA employed either the Comet assay, also known as single cell gel electrophoresis, or the TUNEL (Terminal deoxynucleotidyl transferase dUTP nick end labelling) assay to detect DNA damage. The reliability of both the assays to detect apoptotic DNA has been called into question.

The comet assay is based on the electrophoretic movement of DNA through a gel matrix i.e. agarose. To detect DNA damage using comet assay, cells are fixed and embedded in a thin agarose gel layer on a microscope slide. Cells are then lysed to break open DNA and remove proteins. Next, the DNA is unwounded under alkaline or neutral pH. The unwounded DNA is then electrophoresed. During electrophoresis, the DNA, being negatively charged, moves from the cathode to the anode. The movement of DNA is modified by its size, with the shorter fragment moving faster. In Comet assay, this differential movement generates a comet like structure with the intact DNA forming a head and fragmented DNA a tail, hence called the comet assay (Collins et al, 2008).

Based on the way the DNA is unwounded, comet assay is divided into two types, alkaline comet assay, which is used to detect SSBs, and neutral comet assay, which is used to detect DSBs and apoptosis for that matter. It is believed that alkaline condition is required to break the hydrogen bond between the two strands to release the single stranded DNA, whereas, neutral condition will not affect the DNA strand and only the DSB fragments will be detected (Collins et al, 2008). However, it is now evident that comet assay is not a reliable method for detecting DNA damage. The detection range of comet assay is limited

to approximately 3 breaks per 10^9 Dalton of DNA and the length the human genome is 2.15 x 10^{12} Dalton. Therefore, with the comet assay…"*only a fairly narrow range of break frequencies*" can be detected, which invariably…"*coincides with the levels of DNA lesions seen in normal cells"* (Collins et al, 2008). By the same token, it is not possible to detect mitochondrial DNA damage using the comet assay since the mitochondrial genome is approximately 11 x 10^6 Dalton in size (Collins et al, 2008). The use of the comet assay to detect apoptotic DNA fragmentation has been under severe scrutiny. In a study carried out by Rundell et al., (2003), it has been shown that DNA fragmentations detected with the comet assay disappear if the cells are provided with an appropriate recovery time. Apoptosis is not an immediate consequence of severe DNA damage, it is initiated only after attempts to repair such damage; and apoptosis, once initiated, is an irreversible process. Moreover, apoptotic DNA is cleaved into small nucleosome-sized fragments of approximately 200 base pairs, which are too small to be detected with the comet assay (Collins et al, 2008). Therefore, the association of the comet assay-detected DNA fragmentation to Apoptosis may not be appropriate.

TUNEL assay is a microscopic technique to detect DNA fragmentation *in situ*. It relies on the ability of an enzyme called Terminal deoxynucleotydil Transferase (TdT), which can catalyze the addition of fluorescently-labelled dUTP to free 3'-OH termini of broken DNA strands (Kyrylkova et al., 2012). To detect strand breaks using the TUNEL assay, the cells are first fixed using a suitable fixative such as paraformaldehyde and pemeabilised using an alcohol such as ethanol. Following fixation and pemeabilisation, the cells are incubated with the fluorescently-labelled dUTPs in the presence of TdT to facilitate the incorporation of the former into the nicks in the DNA. Finally, the extent of DNA breaks is assessed by visualising the fluorescently labelled dUTP by fluorescence microscopy. However, TUNEL assay is also not a reliable method for detecting apoptotic DNA fragmentation. As dUTP can be incorporated into any 3'-OH termini, TUNEL assay also labels SSBs, DNA during the repair process, and RNA, significantly overestimating the extent of DNA fragmentation (Valen, 2003).

1.7 Rationale for the current study

In the light of the evidence accumulated, however, it goes beyond saying that cryopreservation may cause damage to the genetic material. However, the nature of such

damage is yet to be fully elucidated. As mentioned earlier, DNA damage in the form of DSBs is a major stimulus for apoptosis, if DNA damage resulting from cryopreservation is severe enough to initiate apoptosis merits investigation. It is clear from the foregoing discussion that the comet assay and the TUNEL assay are not reliable methods for identifying the nature of DNA damage. Since cells react differently to different types of DNA damage, it is only by investigating the response of the cells to cryopreservation that the nature of such damage can be characterised. Attempts have been made in the past to study the DDR in cryopreserved cells using various methods but with very limited success. In a study carried out by Kopeika et al, (2003), an indirect approach was made to study DDR in loach (*Misgurnus fossilis*) sperm. In the study of Kopeika et al., (2003) embryos derived from cryopreserved sperms were treated with caffeine, an inhibitor of DNA repair system. It was expected that if a DDR were initiated in the embryos, caffeine would impair it resulting in decreased embryo survival rate. Surprisingly, caffeine treatment of the embryos resulted in an increased survival rate. The apparent incongruity might be due to the indirect manner of the investigation; and a direct approach to investigate the DDR by way of detecting the proteins involved may shed some light on the nature of DNA damage in cryopreserved cells. If the DNA fragmentation observed in cryopreserved cells represents apoptotic event, it can be assumed that cells sustain extensive DNA damage, such as DSBs, during cryopreservation, and in the cells that survive cryopreservation, such damage is repaired. Since most of the eukaryotic DNA repair mechanisms are error prone, the cells that survive cryopreservation would be susceptible to increased sequence alteration in the genome. To date, no studies have been carried out to investigate the occurrence of various forms of sequence alteration in the genome of cryopreserved biological objects. In these settings, the current study set out to bridge these gaps in the knowledge regarding the effects of cryopreservation on the genetic material of biological objects.

1.7.2 Zebrafish (*Danio rerio*) was identified as a potential model organism for the study

In the past few decades, zebrafish (*Danio rerio*) has been used as a model animal mainly in the field of developmental biology due to its transparent embryos and rapid organogenesis (Hill et al., 2005). However, in recent years, it has emerged as an ideal

vertebrate model in a variety of other biological disciplines, such as cancer research, toxicology study, environmental monitoring.

Zebrafish (*Danio rerio*) share 80% gene homology with human (Barbazuk et al., 2000) and it has been shown that the vertebrate model is susceptible to almost all types of neoplasm known to date (Kent et al, 2002, Matthews, 2004, Smolowitz et al, 2002). It has also been shown that various types of neoplasm can be induced in zebrafish (*Danio rerio*) via chemical exposure (Mizgireuev et al, 2006, Spitsbergen et al, 2000, Haramis et al, 2006, Shepherd et all, 2007, Beckwith et al, 2000), which makes it an ideal model organism for studying human diseases. The incidence of neoplastic disorders has been correlated not only to the occurrence of lesions in the genetic material but also to the impaired DDR in the organism concerned. All of the key proteins functional in eukaryotic DDR are known to be conserved in zebrafish (*Danio rerio*) (Misun et al., 2007), which further reiterates that vertebrate is an ideal model system for studying human diseases resulting from compromised genetic integrity. By the same token, the vertebrate organism also becomes an ideal model system for studying DDR, and therefore, zebrafish (*Danio rerio*) appeared to be the ideal model system for the current study.

Zebrafish (*Danio rerio*) sperms have been successfully cryopreserved (Morris et al., 2003) and used to investigate the effects of cryopreservation on the genetic material (Hagedorn et al., 2012). However, the sperms would not serve the purpose of the current study since sperm, being haploid cells with only the paternal genome, are not likely to possess all the component of a DDR. An appropriate model for the current study would be a biological object containing both the paternal and maternal genomes. To that end, zebrafish (*Danio rerio*) embryos appeared to be an ideal test material for the current study.

1.7.3 Late blastula (5¼ hpf) stage zebrafish (*Danio rerio*) embryos were selected as the test material for the study

Different types of cells respond differently to DNA damage (Blanpain, 2010). There is even a slight heterogeneity in the intensity of DDR from the cells of the same tissue (Farnandez-Capetillo and Murga, 2008). Therefore, to detect a DDR as uniform as possible, it is ideal to carry out the experimental work with embryos at a developmental

stage in which the cells are not irreversibly committed to a specific fate. It has been shown that cells in zebrafish (*Danio rerio*) embryos become irreversibly committed to specific fates in the mid-gastrula period (8 hpf) (Ho and Kimmel, 1993). Ho and Kimmel (1993) have shown that cells in zebrafish (*Danio rerio*) embryos at the onset of gastrula period (5 hpf) are not committed to a specific fate and still retain pluripotency. Ho and Kimmel (1993) also shown that although cells in the embryos at mid gastrula period are irreversibly committed, the commitment of the cells to specific fates begin at $6^1/_2$ hpf. Therefore, the embryos at the onset of gastrula period or earlier would generate a uniform DDR. However, it has been shown that the zebrafish (*Danio rerio*) embryos become capable of generating a complete DDR only at the end of the blastula ($5^1/_2$ hpf) period following mid blastula transition (MBT) (Ikegami et al, 1997). Therefore, the zebrafish (*Danio rerio*) embryos at onset of the gastrula period (5¼ hpf) were chosen as the model organism for the current study.

1.7.4 Scope of the study

With the potential sources of cryopreservation induced damage to the genome in perspective, the experimental work of the current study was spanned into three areas, namely, chilling treatment, cryoprotectant treatment, and freezing and thawing. The study investigated the effects of chilling temperature on the genome of 5¼ hpf zebrafish (*Danio rerio*) embryos by analysing such effect of short-term chilled storage. It was expected that the effects of short term chilling would shed some light on the effects of chilling injury sustained by biological objects during controlled slow cooling cryopreservation. However, zebrafish (*Danio rerio*) embryos have not been successfully cryopreserved to -196°C as yet, which posed a difficulty in studying the effects of cooling and warming on genetic integrity using the teleost embryos. Nevertheless, in the current study, a protocol for cooling 5¼ hpf zebrafish (*Danio rerio*) to -35°C was devised, and the investigation of the effect of cooling and warming on the genome was carried out on the embryos cooled to -35°C.

1.8 The aim of the study

The aim of the current study was to investigate the effects of short-term chilling, CPA treatment, and cooling and warming on the genome of 5¼ hpf zebrafish (*Danio rerio*) embryos.

1.8.1 Objectives

a. Development of the assays for DDR proteins activated in the event of DSBs and SSBs in the genome of 5¼ hpf zebrafish (*Danio rerio*) embryos.

b. Investigation of the effects of short term chilling and different cryopreservation parameters on the genome of 5¼ zebrafish (*Danio rerio*) embryos in terms of the occurrence of DSBs and SSBs.

c. Investigation of the effects of short term chilling and different cryopreservation parameters on the genome of 5¼ zebrafish (*Danio rerio*) embryos in terms of the occurrence of various forms of sequence alteration.

1.9 Techniques employed in the study

1.9.1 Technique employed in the investigation DSBs and SSBs

In the current study, substrate specificity of ATM and ATR was utilised to investigate the nature of DNA damage in terms of strand breaks in 5¼ hpf zebrafish (*Danio rerio*) embryos treated with the experimental conditions. It is apparent that DDR mediated by both of the kinases are propagated via phosphorylation. Upon DNA damage, the kinases become activated via auto-phosphorylation. Once activated, the kinases phosphorylate a number of downstream proteins with critical functions in both cell cycle arrest and damage repair. Therefore, phosphorylation is the molecular switch that dictates the activation of the DNA damage checkpoints and the damage repair, in other words, the DDR. As mentioned earlier, both ATM and ATR phosphrylate their substrate at a sequence motif known as S/TQ motif. The current study utilised an antibody against the

phosphorylated S/TQ motif (Cell Signalling, 2851) (referred to hereafter as S*/T*Q, in which * denotes phosphorylation) to detect the downstream substrates of the kinases. It was hypothesised that the use of the antibody against the S*/T*Q motif would allow the detection of all the substrates for the respective kinases at the same time, facilitating the characterisation of the pathway involved.

Phosphorylation status of a protein could be investigated by a number of techniques such as such as Western blot, Enzyme linked immunosorbent assay (ELISA), Immunocytochemistry (ICC), and Immunohistochemistry (IHC). The underlying principle for the detection of protein is common to all of these techniques. The protein of interest is probed with a specifically directed antibody known as the primary antibody. The complex of the primary antibody and the protein of interest is then probed with a secondary antibody raised against the species in which the primary antibody was raised. Finally, the complex of the protein of interest, the primary antibody and the secondary antibody is detected via a reporter molecule which either binds to the secondary antibody or is modified by it. However, Western blot is the most commonly utilised of the techniques for its simplicity and high sensitivity (discussed in chapter 3 in details) and for the very reasons, the current study utilised the technique to investigate the phosphorylated substrate proteins for ATM and ATR.

1.9.2 Technique used in the investigation of the occurrence of various forms of sequence alteration in the genome 5¼ hpf zebrafish (*Danio rerio*) embryos

As discussed in section 1.5.3.3, the ERMs are responsible for repairing DNA lesions such as chemical modifications of the DNA bases, helix-distorting lesions and mismatched DNA bases that do not result in strand breaks. The present study utilised the expression profiles of a number genes from the ERMs as indications of the occurrence of various forms of sequence alteration in the genome of 5¼ hpf zebrafish (*Danio rerio*) embryos.

A gene is a DNA sequence that contains the code for a protein. During protein synthesis in a biological system, the code in a gene is transcribed into a sequence of RNA called messenger RNA (mRNA). The transcription of the genetic code into mRNAs takes place in the nucleus. Following synthesis, mRNAs are exported to the cytoplasm, where the

information in the mRNAs is translated into proteins. An mRNA contains three parts – a 5' noncoding region, a protein-coding region and a 3' noncoding region. In the coding region, the information for protein synthesis is carried in the form of nucleotide triplets, with one triplet coding for one amino acid. In the cytoplasm, the amino acids occur as covalently bound to an RNA molecule called transfer RNA (tRNA). A tRNA represents a specific amino by way of a nucleotide triplet, with a given triplet always carrying a specific amino acid. Thus, the amino acid sequence for a protein is determined by the complementarily between the mRNAs and tRNAs. However, the mRNAs and tRNAs are brought together by an organelle called ribosome, which is the primary site for biological protein synthesis. A ribosome consists of two subunits, one smaller and one relatively larger. The smaller subunit reads the mRNA triplet sequence, whereas, the lager subunit imports tRNAs complementary to the mRNA sequence and chain the amino acids via peptide bonds to generate a protein (Cox et al., 2012).

There are a number of techniques available for investigating gene expression profiles such as Northern blotting, DNA microarrays, nuclease protection assays and quantitative real time polymerase chain reaction (qRT-PCR). Among them, qRT-PCR is the most advanced and commonly used technique. In qRT-PCR, total RNAs from the cells are extracted and only the messenger RNAs (mRNAs), which contain the codes for the proteins, are converted into complementary DNA (cDNA) using an enzyme called reverse transcriptase. cDNA is then amplified in a PCR reaction and the amplification products are monitored and quantified in real time. qRT-PCR is a very sensitive method for quantifying amplification products. It can quantify the minute amount of DNA (Palmer et al., 2003) and detect even the slightest variation in the amplification products (Gentle et al., 2001). In the light of the advantages of qRT-PCR, the current study utilised the technique to investigate the expression profiles of the genes of the ERMs.

.

1.9.4 Experimental designs

The experimental works undertaken in this study can be grouped under the following headings.

1.9.4.1 Optimisation, development and validation of techniques and method used in the study

This part of the study began with an empirical optimisation of various parameters of Western blot. The parameters of Western blot optimised are: a) extraction of total proteins from the embryos, b) amount of total protein to be probed, c) transfer of proteins onto the membrane, and d) antibody incubation protocol. The optimised Western blot protocol was then employed to generate assays using S*/T*Q antibody for the DDR proteins activated in 5¼ hpf zebrafish (*Danio rerio*) embryos treated with DSB-inducing chemical camptothecin and SSB inducing chemical hydrogen peroxide (H_2O_2), respectively. The assays for DSB-activated DDR proteins and SSB-activated DDR proteins were used in the subsequent experiment to investigate the occurrence DSBs and SSBs in the genome of 5¼ hpf zebrafish (*Danio rerio*) embryos treated with different cryopreservation parameters. This part of the study also investigated if the genes chosen from the individual excision repair mechanisms were expressed in 5 ¼ hpf zebrafish (*Danio rerio*) embryos. In addition, the experimental works in this part of the study comprised of an evaluation of two ubiquitously expressed genes, *ACTB* and *EF1-α,* to be used as endogenous control in qRT-PCR analysis of the expression of the genes of the excision repair mechanisms. The findings of this part of the study are presented and discussed in chapter 3.

1.9.3 Effects of chilling on the genome

In this part of the study, the effects of short-term chilling on the genome of 5¼ hpf zebrafish (*Danio rerio*) embryo in terms of the occurrence of DSBs, SSBs and various forms of sequence alteration were investigated by utilising the assays and method developed and optimised, as described in chapter 3. The findings of this part of the study are presented and discussed in chapter 4.

1.9.4.3 Effects of CPAs on the genome

In this part of the study, the assays and method developed and optimised, as described in chapter 3, were utilised to investigate the effects of two CPAs, namely, MeOH and

DMSO, on the genome of 5¼ hpf zebrafish (*Danio rerio*) embryos in terms of the occurrence of DSBs, SSBs and various forms of sequence alteration outlined. The findings of this part of the study are presented and discussed in chapter 5.

1.9.4.5 Effects freezing on the genome

The experimental works in this part of the study were carried out in two phases. In the first phase, a protocol for cooling 5¼ hpf zebrafish (*Danio rerio*) embryos to subzero temperature as low as -35°C was developed. In the second phase, the assays and methods developed and optimised, as described in chapter 3, were utilised to investigate the effects of cooling to -35°C and subsequent warming on the genome of the embryos in terms of the occurrence DSBs, SSBs, and various forms of sequence alteration. The findings of this part of the study are presented and discussed in chapter 6.

CHAPTER 2: MATERIALS AND METHOD

2.1 Background

The current study investigated the effects of different cryopreservation parameters on the genome of 5¼ hpf zebrafish (*Danio rerio*) embryos. The study was the focussed on the investigation of: a) the occurrence of DSBs, b) the occurrence of SSBs, c) the occurrence of sequence alteration in the genome. The experimental conditions under which the aforementioned investigations were carried out were, a) chilling of the embryos at 0˚C for 30, 60, and 120 minutes, b) treatment of the embryos with two penetrating cryoprotectants, namely methanol (MeOH) and dimethylsulfoxide (Me_2SO) for 30 minutes, and c) cooling of the embryos to -35˚C using 2M MeOH and 1.5M Me_2SO as CPAs, and subsequent warming.

The experimental works for the study were performed at the Institute of Biological and Environmental Science and Technology (IBEST), University of Bedfordshire, UK.

2.2 General Methods

2.2.1 Fish maintenance

12-14 weeks old zebrafish (*Danio rerio*) were obtained from Aquascape Ltd., Birmingham, UK. The fish were reared in a 40 L glass tank (30 x 30 x 60 cm). The water in the tank was continuously aerated and filtered using an electric pump connected to an upright funnel contained in a cushion of filter floss in a 1 L beaker immersed in the tank. The funnel and the floss were covered with pebbles and small stones. The temperature of water in the tank was maintained at 28±1°C. A light/dark cycle of 12 h each was maintained using an automatic timer switch controlling the electric current. The water in the tank was replaced twice a week.

2.2.2 Fish breeding and embryo collection

The fish were fed three times a day with TetraMin® (Tetra, Germany) flake food (ingredients: processed fish and fish derivatives, cereals, yeast, vegetable protein extracts, molluscs and crustaceans, oils and fats, derivatives of vegetable origin, algae, various sugars containing permitted colorants). To prevent overfeeding, the flake food per feeding was limited to an amount that could be consumed by the fish within 5 minutes. The fish were also fed with live brine shrimps in the afternoon. Live brine shrimps were produced by culturing the brine shrimp cysts for 24 hours in salty water made up of 52.5 gm sea salt (ZM systems, UK) in 1.5 L distilled water. The water was continuously aerated and the temperature of water was maintained at 28±1° C.

Female and male fish were kept together in a ratio of 1:2-3. Every morning, spawning was induced by first light. Eggs were fertilized by the male fish as and when they were released by the female fish. The plastic beaker containing the upright funnel covered with pebbles was used to collect embryos. Embryos collected in the morning were incubated at 28±1° C until they had developed into the desired stage.

2.2.3 Determination of the embryo development stage

5¼ hpf embryos were isolated using light microscopy (Leica MZ95, Leica Microsystems, Germany) according to the characteristic morphological features (Figure 2.2) described by Kimmel et al., (1995) (Figure 2.1).

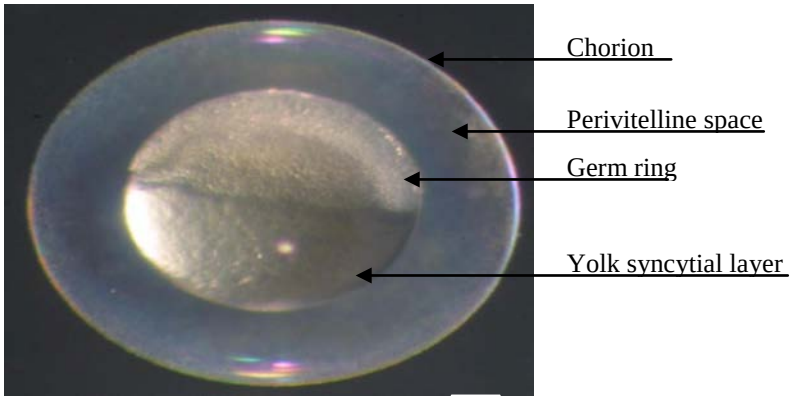

Figure 2.1: Representative image 5¼ hpf zebrafish (*Danio rerio*) embryos used in the present study (scale 1 cm= 100 µm). Picture was taken using a light microscopy (Leica MZ 95 stereomicroscope) and 5¼ hpf developmental stages was determined based on the characteristic morphological features (Kimmel et al., 1995).

2.3 Treatment of the embryos

Following is a description of the treatment of the embryos under the experimental conditions chosen for the current study.

2.3.1 Short-term chilling of the embryos

Desired number of 5¼ hpf embryos were isolated and washed three times with embryo medium 2 (E2) (15 mM NaCl, 0.5 mM KCl, 0.27 mM $CaCl_2$, 1 mM $MgSO_4$, 0.27 mM $NaHCO_3$, 0.15 mM KH_2PO_4, 0.05 mM Na_2HPO_4). The embryos were then transferred into a multi-well cell culture plate containing E2 and chilled at 0°C by placing and keeping the plate in a crushed ice bath for 30, 60 and 120 minutes, respectively. In all cases, a second set of embryos were kept incubating as non-treated control at 28±1°C for the duration of the chilling treatment. At the end of the respective chilling periods, the chilled embryos together with the non-treated control embryos were subjected to subsequent treatment as required by the technique in question.

2.3.2 CPA treatment of the embryos

5¼ hpf embryos were isolated and washed as described in section 2.3.1. The embryos were then transferred into a multi-well cell culture plate containing E2. CPA treatment was initiated by replacing the E2 in the wells with 10 ml solution of the desired concentration of the respective CPA. The plate containing the embryos in CPA solution was then incubated at ambient temperature for 30 minutes. In all cases, a second set of embryos were kept incubating at ambient temperature for the duration of the CPA treatment as non-treated control. At the end of the incubation period, the CPA-treated embryos together with the non-treated control embryos were subjected to the subsequent treatment as required by the technique concerned.

2.3.3 Cooling of the embryos to subzero temperature

5¼ hpf embryos were incubated in the solution of the respective CPA of the desired concentration using the method described in section 2.3.2. Following CPA incubation, the

multi-well plate containing the embryos in CPA solution was placed in the cooling chamber of a programmable cooler (Planer KRYO10 Series II). Embryos were then cooled to seeding temperature at a cooling rate of 0.75°C/minute. Ice nucleation was induced at -7.5°C (when the CPA was 2 M MeOH) and at -6°C (when the CPA was 1.5 M Me_2SO) by touching the cryoprotectant solution with the tips of a pair of tweezers previously cooled in liquid nitrogen. The plates were maintained at the seeding temperature for 10 minutes and then cooled to -35°C at a rate cooling rate of 0.75°C/minute the plates were held at -35°C for 10 minutes. Following holding at -35°C, the plates were thawed immediately in a water bath set at 37°C (~420°C/min). CPA solution was then removed progressively in a five-step dilution method. When the CPA was MeOH, the embryos were introduced for 1 minute each in 1M, 0.5M, 0.25M, 0.125M, 0M MeOH (five steps), respectively. When the CPA was 1.5M Me_2SO, the embryos were introduced for 1 minute each in 1M, 0.5M, 0.25M, 0.125M, 0M Me_2SO (five steps), respectively. The embryos were now ready for the subsequent treatment as required by the technique in question.

2.4 Technique Specific Methods

2.4.1 Investigation on the survival of the embryos

In current study, the survival of 5 ¼ hpf zebrafish (*Danio rerio*) embryos treated with different parameters of cryopreservation was assessed by monitoring the hatching rates. Following treatment under the respective experimental conditions, the embryos were washed three times with E2 and incubated at 28±1°C for 5 days. Embryo survival was monitored daily and any dead embryos were removed from the experiment. At the end of the 5 day period, the embryo survival was recorded and evaluated in terms of percentage hatched. Embryos were considered hatched if they showed natural swimming movements with functional heart and had no obvious signs of malformation (Lahnsteiner 2009).

2.4.2 Western Blot specific methods

2.4.2.1 De-chorination and de-yolking of the embryos

Zebrafish (*Danio rerio*) embryos at early developmental stage such as 5¼ hpf contain a high volume of yolk proteins, which interfere with the proteomic applications such as

Western blot and mass spectrometry. In the current study, the embryos were de-chorinated and de-yolked prior to extracting the total proteins in order to avoid such inference from the yolk proteins.

2.4.2.1.1 Dechorination of embryos

The embryos were de-chorinated according to the method described by Westerfield (2000). Following the respective treatment of the experimental conditions, embryos were washed three times with E2 and incubated in a heated solution of 2 mg/ml protease (Sigma-Aldrich, 81748) in E2 for 10 min for partial digestion of the chorion. Partially digested chorions were removed using pipette suction and the embryos were then washed three times with E2 to remove the traces of protease, which would otherwise result in protein degradation. The de-chorinated embryos were then transferred into a 1.5 ml eppendorf tube for de-yolking.

2.4.2.1.2 De-yolking of embryos

Deyolking of the embryos was carried out using ½ Ginzburg Fish Ringer solution without calcium (55 mM NaCl, 1.8 mM KCl, 1.25 mM $NaHCO_3$) as described by Link et al, (2006). Briefly, 1 ml of Ginzburg Fish Ringer solution was added to the tube containing de-chorinated embryos and the tube was shaken for 5 minutes at 1100 rpm to disrupt and dissolve the yolk proteins. The tube was then centrifuged for 30 sec at 300g to pellet the cells of the embryo proper. Following centrifugation, the supernatant containing the dissolved yolk proteins was discarded. The de-yolked cells of the embryo proper were then washed twice by adding 1 ml of Wash Buffer (110 mM NaCl, 3.5 mM KCl, 2.7 mM $CaCl_2$, 10 mM Tris-HCl pH 8.5), shaking for 2 minutes at 1100 rpm, and pelleting the cells at 300g for 30 seconds.

2.4.2.2 Protein extraction

In the current study, total proteins from 5¼ hpf embryos were extracted using RIPA buffer (Sigma-Aldrich, R0278), supplemented with 1% protease inhibitor cocktail

(Sigma-Aldrich) and 1% phosphatase inhibitor cocktail (Sigma-Aldrich), according to the manufacturer's instructions. Briefly, 100 µl of RIPA buffer mix was added to the tube containing de-chorinated and de-yolked cells of the embryo proper and the tube was cooled on ice for 5 minutes. Following cooling, the tube was vortexed briefly to homogenise the cells, and centrifuged at 8000 rpm for 5 minutes to palette the cell debris. Finally, the supernatant containing the soluble proteins was collected into a fresh tube. The extracted proteins were used straightaway or stored at -80˚C for later use.

2.4.2.3 Protein Quantification

Extracted total proteins were quantified using QuantiPro™ Bicinchoninic Acid (BCA) Assay Kit (Sigma-Aldrich, QPBCA) according to manufacturer's instructions. This is a detergent-compatible method for colorimetric detection and quantitation of total proteins. This method is based on the reduction of cupric ions (Cu^{+2}) to cuprous ions (Cu^{+1}) by proteins in an alkaline medium (i.e. biuret reaction) and a selective and sensitive colorimetric detection of the Cu^{+1}ions. BCA forms a purple-colour complex with Cu^{+1}, which is the basis for monitoring the reduction of Cu^{+2} ions by proteins (Smith et al., 1985). The complex exhibits a strong absorbance at 562 nm and the absorbance is directly proportional to protein concentration. To quantify a protein of interest using the BCA assay, a standard curve is generated by plotting the absorbance readings of the BCA-Cu^{+1} complex derived from the reduction reaction of Cu^{+2} by a known concentration series of a generic protein. The concentration of the protein of interest is then calculated from the equation for the best fit line of the standard curve.

In the current study, bovine serum albumin (BSA) was used to generate the standard curve for the BCA assay. The BSA standard concentrations were prepared as shown in table 2.3 from 1mg/ml stock solution of BSA. All proteins were diluted using distilled water.

Table 2.1 Concentrations of BSA standards used to generate a standard curve

Sample	Protein standard	Final protein
Buffer (µl)	(1 mg/ml) (µl)	concentration (µg/ml)
1000	0	0
999.5	0.5	0.5
995	5	5
990	10	10
980	20	20
970	30	30

The QuantiPro™ BCA Assay Kit used in the study is comprised of three components, QuantiPro Buffer QA, QuantiPro QB and QuantiPro QC. QuantiPro Buffer QA contains sodium carbonate, sodium tartate, and sodium bicarbonate in 0.2 M NaOH, pH 11.25, QuantiPro QB contains 4% (w/v) bicinchoninic acid and QuantiPro QC contains 4% (w/v) copper(II) sulphate solution, pH 8.5, pentahydrate solution. The desired volume of BCA working solution was prepared by mixing QA, QB and QC according to manufacturer's instructions. BSA of known concentrations and unknown protein solutions were mixed with 1 mL of BCA working solution and incubated on a rotary incubator for 1 h at 60°C. Following incubation, absorbance reading for each protein sample was taken by Biophotometer (Eppendorf, UK) at 562 nm (i.e. measured absorbance – blank absorbance). All readings were taken three times and the mean value was used to generate the standard curve. Standard curves with an R^2 value (a measure of linearity of BSA standard concentrations) of 99% or better were used for quantification of the protein of interest. A representative BCA protein standard curve is shown in figure 2.2.

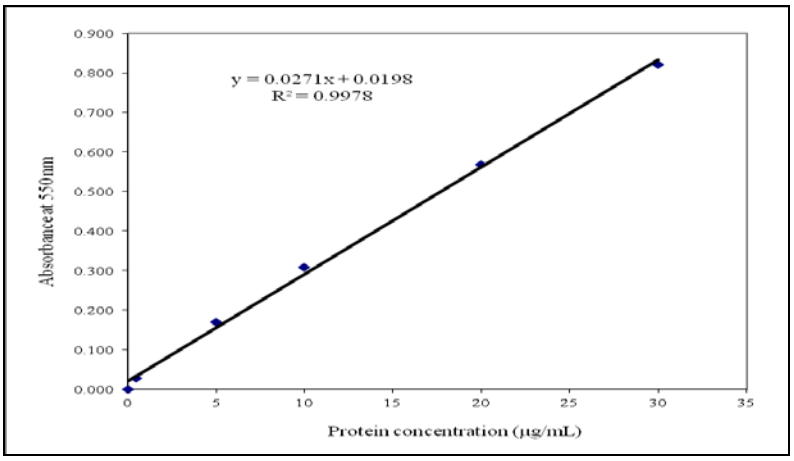

Figure 2.2: A representative BCA standard curve. The equation (y= mx + b) from this standard curve was used to calculate the concentration of the protein of interest

2.4.2.4 Polyacrylamide gel electrophoresis

Total proteins were separated using sodium Dodecyl sulphate Polyacrylamide gel electrophoresis (SDS-PAGE). Concentrations of acrylamide in SDS-PAGE gels vary according to the molecular weight of the protein of interest (table 2.2). The molecular weights of most of the proteins of interest of the current study were within the range of 20-220 kDa, and therefore, all Western blot experiment in the study were carried out using 8% SDS-PAGE gels.

Table 2.2: SDS-PAGE gels are prepared based on the size of the protein of interest

Protein size (kDa)	Gel percentage (%)
4-40	20
12-45	15
10-70	12.5
15-100	10
25-200	8

The resolving and stacking gels were prepared on Bio-Rad Mini-PROTEAN II casting stand (Bio-Rad, UK). For preparation of 5 ml (enough for one gel) of a 8% resolving gel, the following components were mixed in order listed: distilled water (2.03 ml), 30% Protogel contains 37.5:1 Acrylamide: Bisacrylamide (1.67 ml, National Diagnostics, USA), 4X resolving buffer contains 1.5 M Tris HCl and 10% SDS, pH 8.8 (1.5 ml, National dignistics, USA), 10% ammonium persulfate (APS) (0.025ml, Sigma-Aldrich,

UK) and N,N,N′,N′-tetramethylethylenediamine (TEMED) (0.005ml, Sigma-Aldrich, UK) .

Once polymerization of the resolving gel was complete, 2 ml of 4% stacking gel was prepared by adding the following components in order: distilled water (1.22 ml), 30 % Protogel contains 37.5:1 Acrylamide: Bisacrylamide (0.26 ml, National Diagnostics, USA), 4X stacking buffer contains 0.5 M Tris HCl and 0.4% SDS, pH 6.8 (0.5 ml, National Diagnostics, USA), 10% ammonium persulfate (APS) (0.01ml, Sigma-Aldrich, UK) and N,N,N′,N′-tetramethylethylenediamine (TEMED) (0.002ml, Sigma-Aldrich, UK). The stacking gel was layered on top of the resolving gel and allowed to polymerise.

The gel was transferred to a Bio-Rad Mini-PROTEAN II (Bio-Rad, UK) electrophoresis tank. 1x electrophoresis buffer was prepared from a 10X stock consisting of: 30.28 gm/L of Tris base (0.25M, pH 8.3), 144.0 gm/L of glycine (1.92M), 100ml of 10% SDS (1%). Sufficient volume of 1x electrophoresis buffer was added to the tank to cover the top of the gel. Proteins of interest along with a 3 µl MagicMark™ XP Western Protein Standard (Life Technologies, UK) were heated at 95°C for 5 min prior to loading onto the gel. The gel was run at a constant voltage of 200V for 45 minutes or until the bromophenol blue dye front migrated to the bottom of the gel. Negatively charged protein with low molecular weight migrated faster and reached the bottom half of the gel while high molecular weight proteins migrated slower and remained at the top half of the gel (Figure 2.3). .

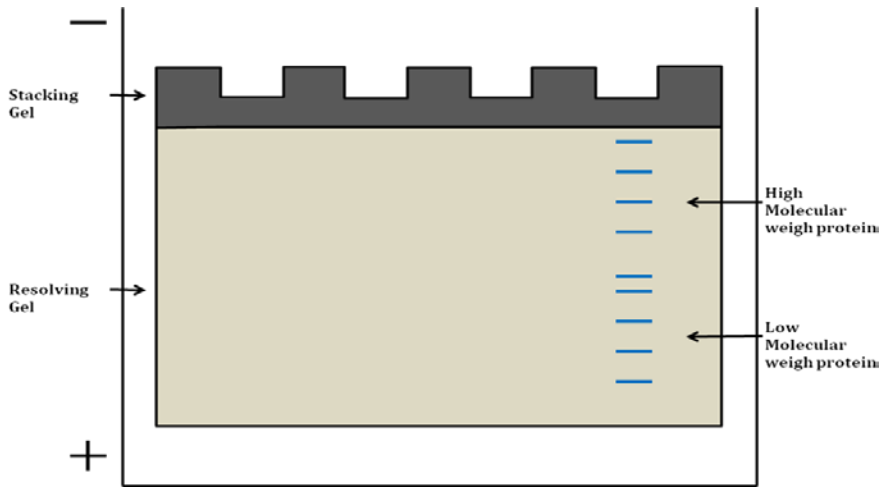

Figure 2.3: Schematic representation of SDS-PAGE gel. Proteins were loaded onto each wells on stacking gel and electrophoresed. Proteins were separated according to their molecular weight; low molecular weight proteins migrate faster and reached at the bottom half of the gel while high molecular weight proteins remained at the top half of the gel.

2.4.2.5 Blotting

Blotting of proteins from gels was performed in polyvenylfluoride (PVDF) membrane (Thermo Scientific, 88518) using the Semi-Dry blotting method (BioRad, 170-3940). Following SDS-PAGE, the gel was equilibrated in blotting buffer (48 mM Tris, 39 mM glyicine, 0.04% SDS, 10% methanol) for 10 minutes. PVDF membrane was activated in 100% methanol for 1 min and equilibrated in blotting buffer for 10 min. A sandwich was prepared by placing the membrane onto a filter paper pre-soaked in the blotting buffer, the gel was then placed onto the membrane and a second pre-soaked filter paper was placed on top of the gel. The sandwich was then blotted for 45 minutes at 15 volts.

2.4.2.6 Membrane staining with Ponceau S solution

The membrane was incubated with Ponceau S solution (Sigma-Aldrich) for 5 minutes which was followed by washing in milliQ water until the desired contrast was achieved. Following washing the membrane was air dried and the efficiency of protein transfer was analysed by visual monitoring.

2.4.2.7 Membrane staining with Sypro Ruby solution

The blotted membrane was incubated with gentle agitation in 10 ml solution of 7% acetic acid and 10% methanol for 10 minutes at room temperature. The membrane was then washed four times for 5 minutes each in MilliQ water to remove traces of acetic acid and methanol. Following washing, the membrane was incubated in Sypro Ruby stain (Life technogies, UK) for 15 minutes at room temperature with gentle agitation. Then, the membrane was washed 3 times for 1 minute each with MilliQ water to remove excess stain. Finally, the membrane was air-dried, viewed under UV light and image was taken.

2.4.2.8 Immuno-detection and visualisation

Immuno-detection was performed using WesternDot^{tm}625 Western Blot Kits (Life Technologies, W10132). The membrane was blocked in 10 ml of WesternDot blocking buffer for 1 hour at room temperature. After blocking, the membrane was incubated with

10 ml of 1mg/ml primary antibody solution (dilution 1:1000) overnight at 4˚C. The membrane was then washed 3 times for 5 minutes each in WesternDot Wash buffer. Following washing, the membrane was incubated with the pre-hybridised complex of Biotin-XX-Goat anti-rabbit and Qdot 625 Streptavidin conjugate in 10 ml of WesternDot blocking buffer for 2 hours at room temperature. The membrane was then washed 3 times as previously, followed by a final wash in MilliQ water for 5 minutes. The membrane was completely dried using 100% methanol and visualised under an UV trans-illuminator using exposure of 0.48 seconds and image was taken. .

2.4.2.9 Densitometry and data analysis

The intensity of protein bands were quantified using ImageJ software (Maryland, USA) according to the method described by Sheffield (2007). Where appropriate, the intensity of the bands of the proteins in a sample were normalised to that of *β-actin* in the same sample. The *β-actin-normalised* intensity of protein bands were presented as relative to that of the non-treated control, unless specified otherwise.

2.4.3 PCR specific methods

2.4.3.1 RNA extraction

RNA extraction from 5¼ hpf zebrafish (*Danio rerio*) was carried out using RNAqueous-Mico RNA Isolation Kit (Ambion, UK, AM1931) according to the manufacturer's instructions. The procedure involved 3 steps, lysis of the embryos to release the nucleic acid, washing, and elution of the RNA. A summary of the protocol used in RNA extraction is incorporated in table 2.2.

Table 2.3: A summary of the protocol used to extract RNA from the embryos

Step 1	A total of 5 embryos from each treated group were lysed in 100 µL of Lysis solution with vigorous vortexing
Step 2	50 µl of 100% ethanol was added to the lysate and the mix was briefly vortexed. The lysate mixture was transferred into a spin column containing silica based filter and the whole assembly was centrifuged at 13,000 x g for 10 seconds
Step 3	RNA bound in the filter was washed with Washing solution 1, Washing solution 2/3, respectively, which was followed by centrifugation at 13,000 x g to remove excess ethanol.
Step 4	The filter was transferred onto a collection tube and 10 µl of Elution solution pre-warmed at 72 °C was added to filter. RNA was eluted to the collection tube by centrifuging the assembly at 13,000 x g for 30 seconds. The process was repeated with a second aliquot of 10 µl of Elution solution.

2.4.3.2 DNase treatment

The eluted RNA was subjected to DNase treatment in order to eliminate contamination from genomic DNA; as such contamination of RNA may lead to misleading results. The procedure involved incubation of the eluted RNA solution with *DNase* enzyme and subsequent deactivation of the enzyme. A summary of the procedure used in *DNase* treatment is incorporated in table 2.3.

Table 2.4: A summary of the protocol used in *DNase* treatment

Step1	0.1 volume of *DNase* I buffer (100mM Tris, 25 mM MgCl2, 1 mM CaCl2) and 1 µl DNase I enzyme was added to the tube containing eluted RNA solution and the tube was incubated at 37°C for 20 min.
Step 2	0.1 volume of *DNase* Inactivation reagent was added to the tube and the tube was incubated for 2 min at room temperature. The tube was vortexed briefly during incubation.
Step3	The tube was centrifuged at 13,000 x g to pallet the inactivation reagent and genomic DNA. The supernatant containing the purified RNA was collected into a fresh *RNase* free tube and used straightaway or stored at -80°C for later use.

2.4.3.3 RNA quantification

Total RNA was quantified using Biophotometer™ (Eppendorf, Germany). RNA was diluted by 50-fold with PCR water (Sigma-Aldrich, UK,) in UVette (Eppendorf, Germany). The absorbance readings were taken at 260 nm and 280 nm. The Biophotometer™ automatically calculated the RNA concentration in the original sample using the following equation:

(Absorbance at 260nm x RNA coefficient) X Dilution factor = µg/ml of RNA

pure RNA falls in the range of 1.7 – 2.1. In the current study, only the RNA samples showing purity within the specified range were subjected to subsequent treatment.

2.4.3.4 cDNA synthesis in reverse transcription reaction

RNA was converted into cDNA in reverse transcription reaction using Precision nanoScript Reverse Transcription Kit (Primerdesign, Southampton, UK) according to the manufacturer's instructions. The reverse transcription reaction was carried out in two steps. In the first step, 1 µg of total RNA was mixed with oligodT primers (1 µl) in a tube. The mixture volume in the tube was made up to 10 µl using RNAse/DNAse free water. The tube containing the mixture was then incubated at 65°C for 5 minutes. Following incubation at 65°C, the tube was chilled on ice for two minutes. In the second step, RNA sample from the first step was mixed with nanoscript buffer (2 µl), dNTP mix (10 mM each -1 µl), DTT (100 mM – 2 µl), nanoscript reverse transcriptase (1 µl). The final volume of the mixture was made up to 20 µl using DNAse/RNAse free water. The tube containing the reaction mixture was incubated at 55 °C for 20 minutes to facilitate the reverse transcription reaction. Finally, the reaction was terminated by inactivating the enzyme at 75° C for 15 minutes. Thermocycler PCR machine (Techne, UK) was used for

all incubation steps. No RNA template control and no reverse transcriptase reactions were also performed to check for the reaction purity. For conventional PCR, undiluted cDNA was used subsequently. For qRT-PCR experiment, cDNA was diluted at ratio of 1:2 in molecular biology grade water (Sigma-Aldrich, UK) and stored at -80°C.

2.4.3.5 Conventional Polymerase Chain Reaction (PCR)

Conventional PCR was performed using the primers designed to be specific for the gene of interest. The PCR reaction was performed in 50 µl reaction volume consisting of NH_4 PCR buffer (Bioline, UK), 200 µM dNTPs (Bioline, UK), 1.5 mM MgCl2 (Bioline), 2 U BIOTAQ™ DNA polymerase (Bioline, UK), 0.5 µM each primer (forward and reverse) (see Table 2.5), 1 µg RNA template and PCR water (Sigma, UK). Standard conditions for PCR were: initial denaturation at 94 °C for 5 min (1 cycle), amplification step consisting of 45 cycles consisting of denaturation at 94° C for 30 seconds, annealing for 30 seconds at temperature optimum for the primer in question (see Table 2.5 for details), extension at 72° C for 30 seconds followed by 1 cycle of additional extension step at 72 °C for 10 min. A housekeeping gene, either *ACTB* or *EF1-alpha*, was amplified as an endogenous control in the same sample but in separate reaction.

Table 2.5: Details of the primers used in the study together with the annealing temperature and product size

Gene	Forward (F)/Reverse (R) primers	Annealing temp.	Product size (bp)
ACTB	F: CCAGCTGTCTTCCCATCCA	59	86
	R: TCACCAACGTAGCTGTCTTTCTG	59	
EF1-α	F: CTGGAGGCCAGCTCAAACAT	60	87
	R: ATCAAGAAGAGTAGTACCGCTAGCATTAC	60	
UDG	F: AGTGTTCAGAGACCTGTGCC	60	130
	R: GCAGGACACCTTGATTTGCC	60	
TDG	F: AATGGGTTCAGTCGGCTCAG	60	186
	R: CTTTAGCAGGTGCTGTCTGC	60	
ERCC1	F: GGAGAGGTGGTGCCAGACTA	60	165
	R: AGGGTCTTTCACGTCCACCT	61	
MSH2	F: CAGGAAACTTGGTGTGTGCG	60	147
	R: CGCTGCACCACCTGTTTAAG	60	

2.4.3.6 Analysis of PCR product

PCR products were analysed using agarose gel electrophoresis method and Ethidium Bromide (EtBr) staining. 2 % agarose gel was prepared in sterile TAE buffer (T4038, Sigma, UK) by warming the solution. 0.5 µg/mL EtBr (E1510, Sigma, UK) was added to warm agarose solution, the solution was swirled and poured onto gel cast and left to set. Samples were mixed with gel loading buffer (G2526, Sigma, UK) and loaded into the wells of the gel along with the product size marker, HyperLadder™ V (Bioline, UK). Electrophoresis was carried out at 100V for 2 hours. At the end of the electrophoresis run, the gel was visualised under UV light using Genosmart UV Gel Documentation System (VWR, UK).

2.4.3.7 Standard generation

The standards for real time PCR of the gene of interest along with the housekeeping genes *EF1-alpha* and *ACTB* were generated by conventional PCR using the primers specific for the gene of interest. PCR reaction was performed according to the procedure described in the Section 2.4.2.5. PCR product was run on 2% agarose gel and the DNA bands of the expected product size were excised. DNA was then isolated from excised bands using EZNA Gel Extraction Kit (Omega Bio-Tek) according to manufacturer's instructions. An overview of the protocol is incorporated in table 2.6. Isolated DNA was quantified using BioPhotometer (Eppendorf , UK) at 260 nm. The DNA was diluted to 2 ng/µl followed by 10- fold serial dilutions to generate standards for q-RT PCR.

Table 2.6 Steps involved in the EZNA Gel Extraction Kit protocol

Step 1	400 µl of the Binding Buffer was added to 1.5 ml tube contain agarose of DNA fragment and incubated with the agarose at 55-60° C for 7 mins.
Step 2	Solution was applied to the spin column containing 2 mL collection tubes and the whole assembly was centrifuged at 13000 x g for 1 min.
Step 3	Column was washed with 300 µl of Binding buffer and followed by two washes of 700 µl of Wash Buffer and air dried by centrifugation for 2 min at 13000 x g
Step 4	DNA was eluted with 30µl and 20µl of elution buffer

2.4.3.8 Quantification of the expression levels of genes

q-RT PCR was performed on RotorGene 6000 cycler (Corbett Research, UK) using a 72 well rotor to quantify the expression levels of the gene of interest. Reaction mixture comprised of 7.5 µl of sensimix 2X Reaction buffer (containing heat activated DNA polymerase, Ultrapure dNTPs, $MgCl_2$, SYBR® Green I), 333 nM of each primers and 2 µl of cDNA sample diluted in PCR water (sigma, UK). The reaction condition were 1 cycle at 95° C for 10 min, followed by 45 cycles at 95° C for 10 sec, at appropriate annealing temperature (see Table 2.5) for 15 sec and extension at 72° C for 15 sec. Data were acquired on FAM/SYBR channel at the end of the each extension step. At the end of the amplification run, melt curves were analysed to check for mispriming and amplification efficiency were calculated from a standard curve (for each amplification reaction the R^2 was close to 1). The relative gene expression data were obtained using RotorGene software (Version 1.7, Corbett research) and Microsoft Excel. Relative gene expression levels were calculated using relative quantification method. *EF1-alpha* and *β actin* were used for this study as endogenous control genes.

2.4.3.9 Relative quantification

Relative gene expression levels were calculated using the two standard curve quantification method with kinetic PCR efficiency correction (see equation below) using Rotorgene software (Pfaffl 2003). Expression levels of the genes of interest were normalised with the expression levels of *EF1-alpha a*nd *ACTB* and presented as relative to the expression level of the gene of interest in the non-treated control.

$$\text{Relative quantification} = \frac{(E_{\text{target}})^{\Delta CP\,(\text{target})\,(\,control - sample\,)}}{(E_{\text{ref}})^{\Delta CP\,(\text{ref})\,(\,control - sample\,)}}$$

Where, E is the real time PCR efficiency and ΔCP is the crossing point difference between the unknown sample and the control sample.

2.5 Statistical analysis

Statistical analysis was carried out using SPSS V.19 software (IBM, USA) and Microsoft Excel (Microsoft Corp. USA). The one-sample Kolmogorov-Smirnov test was performed to determine if the data for each gene were normally distributed. All data were normally distributed either before or after logarithmic transformation. Differences in the hatching rates, gene and protein expression levels were analysed using one-way ANOVA along with Tukey's post hoc tests or where appropriates using student's t-test.

CHAPTER 3: OPTIMISATION, DEVELOPMENT AND VALIDATION OF TECHNIQUES AND METHODS USED IN THE INVESTIGATION OF THE EFFECTS OF DIFFERENT CRYOPRESERVATION PARAMETERS ON THE GENOME OF 5¼ hpf ZEBRAFISH (*Danio rerio*) EMBRYOS

3.1 Introduction

The current study set out to investigate the effects of different cryopreservation parameters on the genome of 5¼ hpf zebrafish (*Danio rerio*) embryos in terms of the objectives laid out in section 1.8.1. This part of the study describes and discusses the experimental works undertaken to optimise, develop and validate the techniques and methods employed in such investigation. The experimental works presented in this part of the study was carried out in two phases. For the reasons described in chapter 1, the current study intended to investigate the effects of the cryopreservation parameters on the genome of the embryos in terms of strand breaks by analysing the activation of DDR proteins and Western blot was selected as the technique for such detection. Western blot is a very sensitive technique for detecting and identifying proteins of interest. However, it is essential to optimise various parameters of the technique for a successful detection of the protein of interest of a particular study. To that effect, the first phase of this part of the study was dedicated to an empirical optimisation of a number of parameters that contribute to successful Western blot detection. In the second phase, the Western blot protocol optimised in the first phase was employed to generate S*/T*Q antibody-mediated assays for DDR proteins activated in the event of DSBs and SSBs in the genome of 5¼ hpf zebrafish (*Danio rerio*) embryos. DNA damage in the form of various mutations can occur indirectly as a result of error during the repair of DSBs and SSBs or directly from lesser forms of DNA damage other than strand breaks. Therefore, the current study also set out to investigate the occurrence of sequence alteration in 5¼ hpf zebrafish (*Danio rerio*) embryos treated with different cryopreservation parameters. As discussed in chapter 1, the current study set out to investigate the occurrence of sequence alteration in the embryos treated with the parameters of cryopreservation by analysing the expression profiles of a number of genes with critical functions in the individual ERMs. However, the expression of the chosen genes in 5¼ hpf zebrafish (*Danio rerio*) embryos needed to be validated before they could be analysed in the subsequent parts of the study. To that end, the experimental works in the second phase of this part of the study also comprised of an investigation into the expression of the genes selected from the ERMs. In

addition, the experimental work in this phase also included the validation process of two house-keeping genes (HKGs), namely, *ACTB* and *EF1 alpha*, for their subsequent utilisation as endogenous controls in the expression analysis of the genes of the ERMs.

3.2 Optimisation of different parameters of Western blot

To detect a protein using Western blot, total proteins extracted from cells are first separated according to the molecular weight in a process called sodium dodecyl sulphate polyacrylamide gel electrophoresis (SDS-PAGE). Following SDS-PAGE, the separated proteins on the gel are transferred onto a second matrix, usually a nitrocellulose or polyvinyldene difluoride (PVDF) membrane. The free binding sites in the membrane are then blocked using a suitable protein such as bovine serum albumin (BSA) solution. The protein of interest in the membrane is then probed with the primary antibody; and the resulting complex, in turn, is probed with a secondary antibody raised against the species in which the primary antibody was raised. The complex of the primary antibody and the secondary antibody is visualised via a reporter molecule coupled to the secondary antibody. The reporter molecule either actively generates a detectable signal or is modified by enzymatic reaction to generate a signal. Compared to other key immunological laboratory techniques, Western blot readily provides important information regarding the protein of interest. Since proteins are separated according to the molecular weight and then detected with a specifically directed antibody, the technique essentially confirms the identity of a target protein. In addition, Western blot also provides important information about the post-translation modification (PMT) of proteins. PMTs, such as glycosylation, methylation and cleavage, modify the molecular weight of a protein resulting in band size higher or lower than that expected (Moore, 2009).

Western blot is a multi-parametric technique; and as mentioned earlier, various parameters of the technique need to be optimised for a successful detection of the protein of interest. Moreover, during the onset of the current study, there was no published protocol available for Western blot detection of phosphorylated proteins from 5¼ hpf zebrafish embryos. In this phase of the experimental works, therefore, a number of brief experiments were carried out to determine the optimum conditions of some of the important Western blot parameters to facilitate successful detection of phosphorylated

DDR proteins from 5¼ hpf embryos. The parameters taken into consideration were: a) amount of protein to be probed, b) blotting buffer formulation, c) blotting duration, and d) antibody incubation protocol. All experiments were carried out three times using total proteins extracted from 5¼ hpf zebrafish (*Danio rerio*) embryos according to the methods described in section 2.4.1.2.

3.2.1 Determination of the amount of total proteins to be probed

In SDS-PAGE, it is important not to load too less or too much total proteins. Under-loading results in resolution of only the most abundant of proteins; and if the protein of interest is not abundant, the immuno-detection process fails. Overloading, on the contrary, results in protein aggregation and precipitation producing a narrowing and then widening stretches in the separation trace (Jensen, 2012). Overloading is also one of the many causes of non-specific binding in immuno-detection step. However, there is no gold standard as regard to what amount of protein should be loaded in a SDS-PAGE gel. The appropriate load amount needs to be determined empirically. In this experiment, the optimum amount of total proteins that would result in clear resolution of the individual proteins was determined.

3.2.1.1 Experimental design

5 µg, 10 µg, 20 µg, 30 µg, 40 µg, and 50 µg of total proteins were resolved in SDS-PAGE according to the method described in section 2.4.2.4. The gel was then equilibrated in blotting buffer containing 20% MeOH for 10 minutes. Following equilibration, the proteins were blotted from the gel onto a PVDF membrane for 30 minutes according to the method described in section 2.4.2.5. After blotting, the membrane was stained with Sypro Ruby according to the method described in section 2.4.2.7. Two clearly visible bands were then analysed according to the method described in section 2.4.2.9.

3.2.1.2 Result

Resolution of the individual protein bands was significantly improved with the increasing load amount. Two clearly visible bands, referred to as band 1 and 2, became sharper with the increased amount of total proteins loaded (Figure 3.1 A). However, there was no statistically significant ($p<0.05$) difference in the intensity of band 1 resulting from the load amount of 40 µg and 50 µg (Figure 3.1 B). Similarly, there was no statistically significant ($p<0.05$) difference in the intensity of band 2 resulting from load amount of 30 µg, 40 µg and 50 µg of total proteins (Figure 3.1 C). Nevertheless, it is desirable to load the lesser amount of protein possible to avoid spillage into surrounding wells of the gel and overloading effects. Therefore, based on the finding of the current experiment, it was decided that 40 µg of total protein would be used as loading amount for the subsequent Western blot experiments in the study.

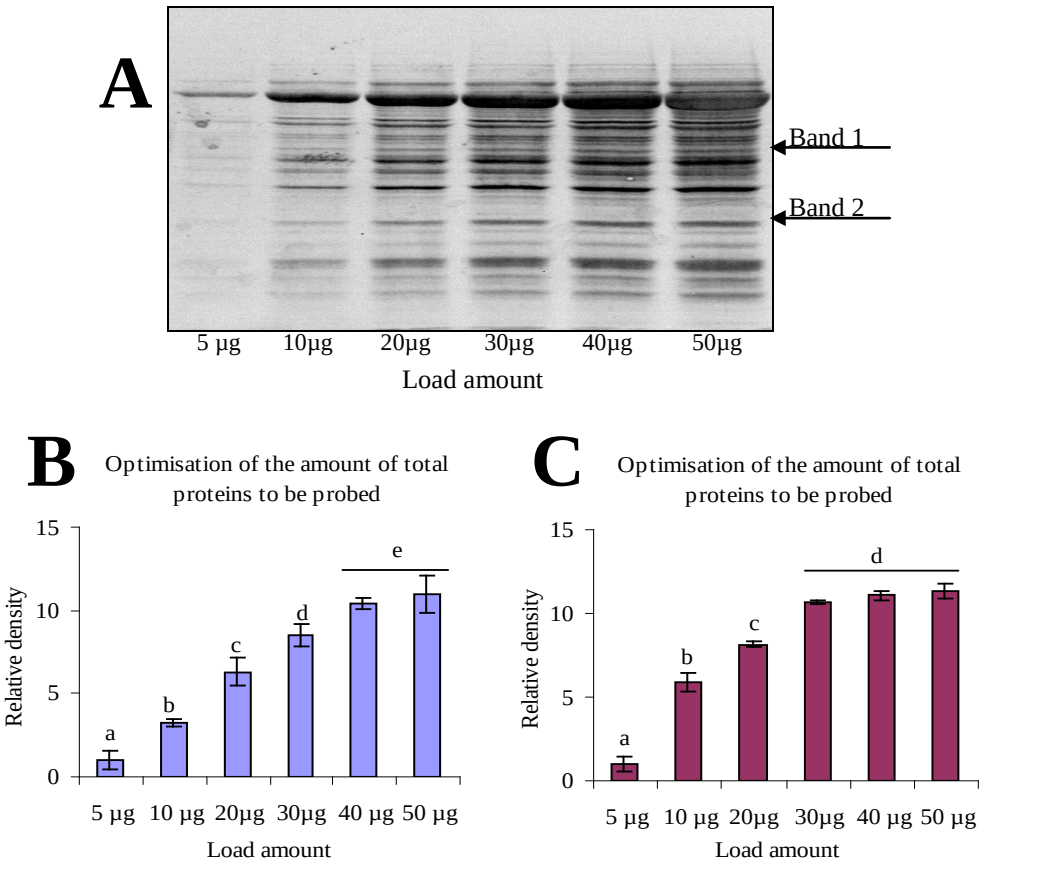

Figure 3.1: A load amount of 40 µg of total proteins results in clear resolution of individual protein bands. (A) Representative blot of three independent experiments showing resolution of individual protein bands. Total proteins, ranging 5-50 µg, were resolved in SDS-PAGE, blotted onto membrane for 30 min and stained with Sypro Ruby. The image was taken under UV light. Intensity of the bands was quantified using Image J software (Maryland, USA) **(B)** Graphical

presentation of the intensity of band 1. **(C)** Graphical presentation of the intensity of band 2. Values shown are mean ± SEM of the band intensity obtained from three replicates. Different letter indicates statistically significant ($p<0.05$) difference among the groups being compared.

3.2.2 Optimisation of the blotting protocol

While optimising the blotting protocol, two parameters namely, transfer buffer composition and transfer duration, were taken into consideration.

3.2.2.1 Effects of MeOH on protein transfer

Blotting buffer is traditionally supplemented with an appropriate concentration of MeOH, which plays two important roles in efficient transfer of proteins from a gel onto a membrane. Firstly, MeOH restores the gel to its original dimensions. During electrophoresis, polyacrylamide, being a hydrogel, absorbs water and increases in size in all dimensions (Millipore, 2012). An un-uniformed gel compromises protein resolution during blotting. MeOH stabilises gel dimensions by drying water off the gel. Secondly, MeOH removes SDS from protein molecules (Millipore, 2012). SDS imparts negative charge onto proteins. It is added to the electrophoresis and blotting buffers so that proteins are masked in negative charges and migrate towards the anode in an electric field. However, SDS also causes protein molecules to migrate faster through the membrane minimising protein-membrane interaction. MeOH facilitates protein-membrane interaction by removing SDS from protein molecules (Millipore, 2012). Nevertheless, stripping of SDS by MeOH from relatively larger proteins leads poor transfer of the proteins (Abcam, 2012). Therefore, a balance between MeOH and SDS concentration is essential for efficient protein transfer. In this experiment, the optimum concentration of MeOH in blotting buffer for efficient protein transfer was empirically determined.

3.2.2.2 Experimental design

Based on the finding in the previous experiment, 40 µg of total proteins were resolved in three gels using the method described in section 2.4.2.4. The gels were equilibrated for 10

minutes in blotting buffer without methanol, blotting buffer containing 10% MeOH, and blotting buffer containing 20% methanol, respectively. The gels were then blotted onto PVDF membranes for 30 minutes at 15 volt using the respective blotting buffer. After blotting, the membranes were stained with Sypro Ruby according to the method described in section 2.4.2.7. Following staining, the membranes were imaged and two clearly visible bands in the membranes were analysed according to the method described in section 2.4.2.9.

3.2.2.3 Results

Result of this experiment clearly shows the benefits of methanol in transfer buffer (Figure 3.2 A, B and C). Resolution of individual protein bands improved in the membranes blotted using the transfer buffer containing MeOH (B and C) compared to that in the membrane blotted using the buffer without MeOH (A). The intensity of band 1 and 2 in the membranes blotted using the buffers containing 10% and 20% MeOH, respectively, significantly ($p<0.05$) improved relative to that of the bands in the membrane blotted using the buffer without MeOH. However, the intensity of the bands in the membrane blotted using 20% MeOH was decreased compared to the intensity of the bands in the membrane blotted using the buffer containing 10% MeOH (Figure 3.2 D and E), with the decrease being statistically significant ($p<0.05$) for band 2 (Figure 3.2 E). Since 20% MeOH in blotting buffer appeared to have interfered with protein transfer, it was decided that a blotting buffer containing 10% MeOH would be used in the subsequent Western blot experiments in the study.

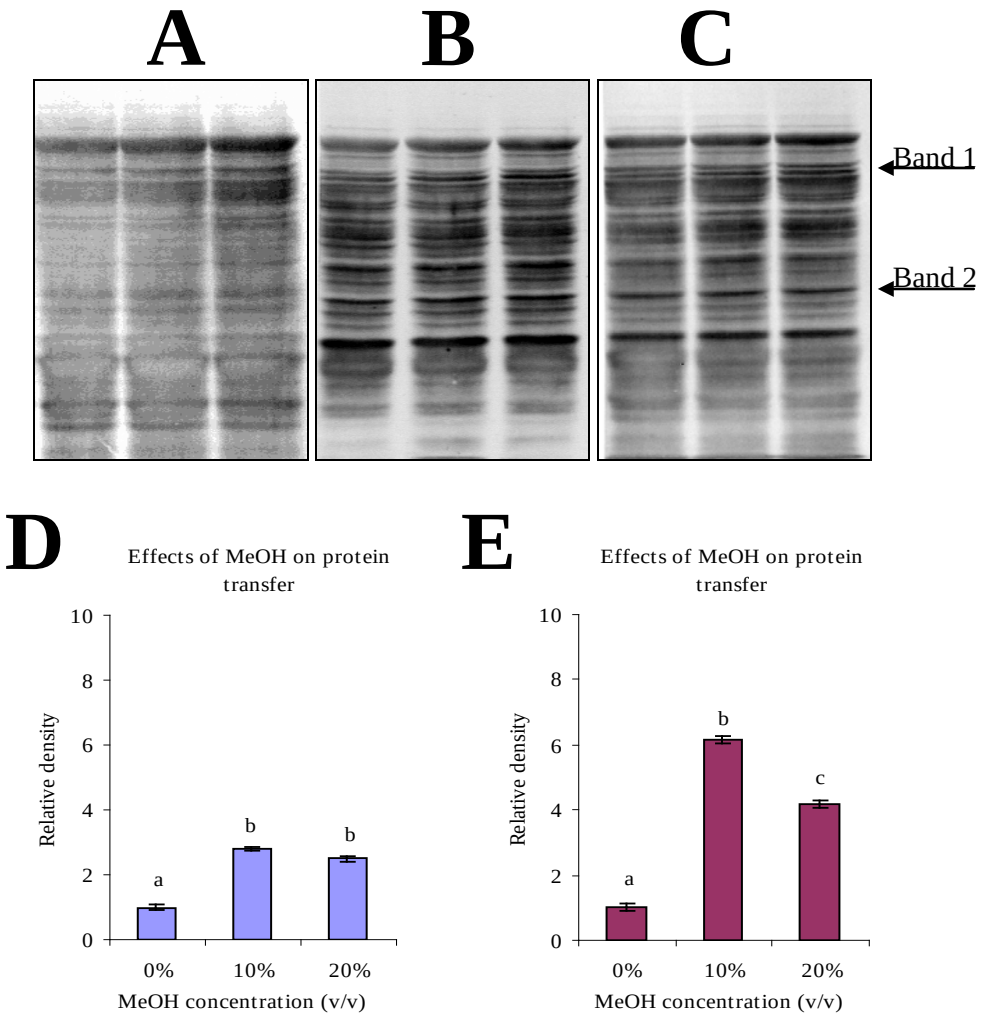

Figure 3.2: **Effects of MeOH on the efficiency of protein transfer**. 40 µg of total proteins were resolved in three gels and equilibrated in and blotted with blotting buffer without MeOH, blotting buffer containing 10% MeOH and blotting buffer containing 20% MeOH, respectively. The membranes were stained with Sypro Ruby and images were taken. Band intensity was quantified using ImageJ software (Maryland USA). Representative blots of three independent experiments, (A) membrane blotted using buffer without MeOH, (B) membrane blotted using buffer containing 10% MeOH and (C) membrane blotted using buffer containing 20% MeOH. (D) Graphical presentation of the intensity of band 1. (E) Graphical presentation of the intensity of band 2. Values shown are mean ± SEM of the band intensity obtained from three replicates. Different letter indicates statistically significant ($p<0.05$) difference among the groups being compared.

3.2.2.4 Effects of blotting duration on protein transfer

Efficiency of protein transfer is affected by blotting duration too. Larger proteins require longer time to elute from the gel. Longer time on the other hand, causes smaller proteins to disappear from membranes. Therefore, an appropriate blotting time is often

experimentally established based on the molecular weight of the protein of interest. In this experiment, the optimum blotting duration that would improve transfer of proteins onto the membrane was empirically determined.

3.2.2.5 Experimental design

40 µg of total proteins were resolved in three gels according to the method described in section 2.4.2.4. Based on the finding in the previous experiment, the gels were equilibrated in blotting buffer containing 10% MeOH for 10 minutes and blotted onto PVDF membranes for 30, 45 and 60 minutes, respectively. Following blotting, the membranes were stained with Sypro Ruby, according to the method described in section 2.4.2.7. The gels and the membranes were then imaged and two clearly visible bands in the membranes were analysed according to the method described in section 2.4.2.9.

3.2.2.5 Results

Blotting duration showed a two-way effect on protein transfer. Blotting for 45 and 60 minutes improved transfer of proteins onto the membranes compared to that for 30 minutes (Figure 3.3 A, B and C). The intensity of band 1 in the membranes blotted for 45 and 60 minutes was significantly ($p<0.05$) increased relative to the intensity of the band in the membrane blotted for 30 minutes. However, the intensity of the band in the membrane blotted for 60 minutes was significantly decreased compared to that in membrane blotted for 45 minutes (Figure 3.3 D). Conversely, the intensity of band 2 was not significantly increased in the membrane blotted for 45 minute relative to that of the band in the membrane blotted for 30 minutes. However, the intensity of the band in the membrane blotted for 60 minutes was significantly decreased compared to the intensity of that in the membrane blotted for 45 minutes (Figure 3.3 E). A similar pattern was observed in other protein bands, too (circled in Figure 3.3 A, B and C). The finding indicates that blotting for 60 minutes causes proteins to migrate through the membrane and 45 minute blotting is optimum for the range of proteins analysed. Therefore, it was decided that in all subsequent Western blot experiment in the current study, protein blotting would be carried out for a duration of 45 minutes.

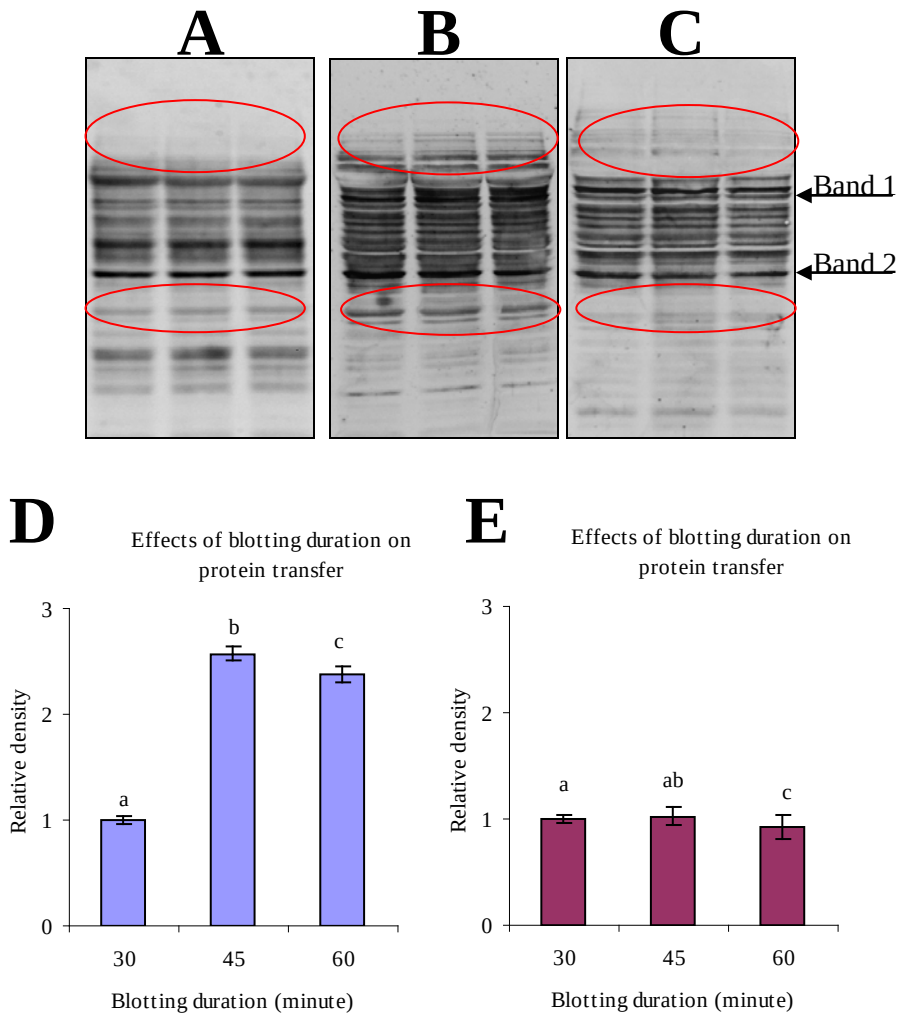

Figure 3.3: Effects of blotting duration on protein transfer. 40 µg of total proteins were resolved in three gels and equilibrated in and blotted with blotting buffer containing 10% MeOH for 30, 45, and 60 minutes, respectively. The membranes were stained with Sypro Ruby and images were taken. Band intensity was quantified using ImageJ software (Maryland, USA). Representative blots of three independent experiments, (A) membrane blotted for 30 minutes (B) membrane blotted for 45 minute and, (C) membrane blotted for 60 minutes. (D) Graphical presentation of the intensity of band 1. (E) Graphical presentation of the intensity of band 2. Values shown are mean ± SEM of the band intensity obtained from three replicates. Different letter indicates statistically significant ($p<0.05$) difference among the groups being compared.

3.2.3 Optimisation of Immuno-detection protocol

In the imuno-detection step, a specific antibody is used to identify an antigen of interest in the blotted membrane. Successful Western blot detection largely depends on binding of the primary antibody with the antigen. Therefore, the optimum conditions needs to be determined and adopted to facilitate such binding. The parameters that are considered

while adopting optimum conditions for immuno-detection step include detection systems, antibody concentrations, buffer compositions, blocking agents, and incubation time and temperature. Invariably, the optimum conditions for a given antibody are suggested by the supplier. In the current experiment, *anti-β actin* (Anaspec, 5542), an antibody specific for the ubiquitously expressed protein β-actin, and WesternDot kits (Invitrogen, W10142), a set of commercially available Western blot kits, were used to optimise the immuno-detection protocol. The optimum conditions for all the parameters except for the incubation time and temperature were suggested by the suppliers. Traditionally, primary antibody incubation is carried out for either 2 to 3 hour at ambient temperature or overnight at 4°C. At higher temperature an antibody becomes overly sensitive and binds to non-specific sites. Similarly, longer incubation time also results in non-specific binding. Consequently, antibody binding is inversely related to the time and temperature of incubation (Boenisch, 2009). In this experiment, the optimum time and temperature for the primary antibody incubation was empirically determined.

3.2.3.1 Experimental design

40 µg of total proteins were resolved in two gels and blotted onto PVDF membrane using the method described sections 2.4.2.4 and 2.4.2.5, respectively. The membranes were blocked using WesternDot blocking buffer for 1hour at ambient temperature. Following blocking, one of the membranes was incubated with 1µg/ml of *anti-β actin* in wash buffer for 2 hours at ambient temperature and the second membrane was incubated with 1µg/ml of *anti-β actin* in wash buffer overnight at 4°C. After primary antibody incubation, the membranes were incubated with 0.1µg/ml Biotin-XX-Goat anti-rabbit in wash buffer for 2 hours and with 0.1µg/ml Qdot 625 Streptavidin conjugate in WesternDot blocking buffer for 1 hour, respectively, at ambient temperature. Finally, the membranes were visualised and documented according to the method described in section 2.4.2.8.

3.2.3.2 Results

Anti-β actin used in the experiment detects a protein band of approximately 42 kDa, and a band of the expected size was detected in both conditions of the primary antibody incubation (Figure 3.4 A and B). However, the intensity of the band for β-actin in the membrane incubated at 4°C was significantly ($p<0.05$) increased relative to that in the

membrane incubated at ambient temperature (Figure 3.4 C). Nevertheless, the primary antibody incubation in both conditions resulted in non-specific bindings also. There were two very intense bands of approximately 75 kDa and 150 kDa in both of the membranes. However, the extent of non-specific binding in the membrane incubated through overnight at 4°C was lesser compared to that in the membrane incubated for 2 hour at ambient temperature (Figure 3.4 A and B).

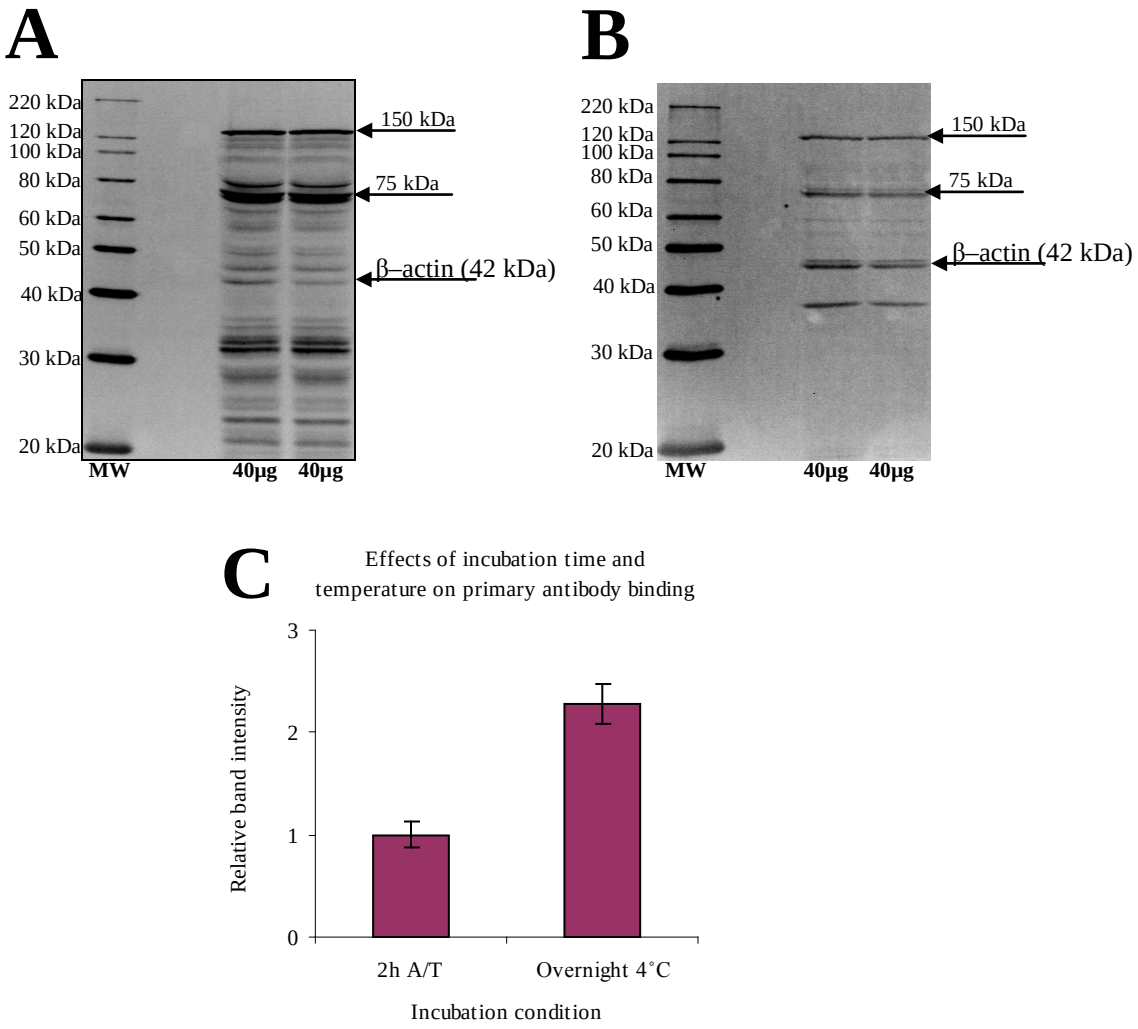

Figure 3.4: Primary antibody incubation overnight at 4˚C resulted increased specific binding. 40µg of total proteins were resolved in two SDS-PAGE gels, blotted onto PVDF membranes and blocked for 1 hour. One of the membranes was incubated with *anti-β actin* for 2 h at ambient temperature, followed by incubation at ambient temperature with Biotin-XX-Goat anti-rabbit for 2 h and Qdot streaptavidin for 1 h. the second membrane was incubated with anti-β-actin through overnight at 4˚C, followed by incubation at ambient temperature with Biotin-XX-Goat anti-rabbit for 2 h and Qdot streaptavidin for 1 h. (A) Representative Western blot of three independent experiments on primary antibody incubation at ambient temperature for 2 hours. (B) Representative Western blot of three independent experiments on primary antibody incubation overnight at 4˚C. (C) Graphical presentation of the intensity of the band for *β-actin* in both membranes. Values shown are mean +/- SEM of the band intensities obtained from three replicates and presented as relative to that in the membrane incubate at ambient temperature for 2h. Different

letter indicates statistically significant ($p<0.05$) difference between the groups being compared. MW represents MagicMark^{TM} XP Western protein standards (Invitrogen, LC5602).

Based on the finding of the current experiment, it was decided that in the subsequent Western blot experiments in the study, the primary antibody incubation would carried out through overnight at 4°C.

3.2.4 Identification of the source of non-specific binding

The most common source of non-specific binding in immunological techniques is the secondary antibody. Secondary antibodies are generated against a pooled population of immunoglobulins (invariably IgG) from a target species. Consequently, the secondary antibody recognises both heavy and light chains of the IgG molecule, resulting in enhanced signal. However, since light chains are shared by all immunoglobulin classes, the use of secondary antibody generated against the whole IgG molecule from a target species would result in non-specific binding (Thermo Scientific, 2013). Since the non-specific binding from a secondary antibody is unavoidable, signals generated from such binding is excluded from data analysis. Non-specific signal may also be generated from the reporter molecule. Reporter molecules are often coupled to a bio-molecule which binds to the secondary antibody to facilitate the detection of the antigen of interest. The bio-molecule coupled to the reporter molecule may react with cellular proteins resulting in non-specific signal (Minard and Cawley, 1978). Therefore, it is essential to identify the source of the non-specific binding before steps could be taken to eliminate such binding or exclude the resulting non-specific signals from data analysis. This experiment was carried out to identify the source of the non-specific binding observed in the previous experiment.

3.2.4.1 Experimental designs

40 µg of total proteins were resolved in two gels and blotted onto PVDF membranes according to the methods described sections 2.4.2.4 and 2.4.2.5, respectively. The membranes were blocked using WesternDot blocking buffer for 1 hour. Following blocking, one of the membranes was incubated with 0.1µg/ml Biotin-XX-Goat anti-rabbit in wash buffer for 2 hours and then with 0.1µg/ml Qdot 625 streptavidin conjugate in

WesternDot blocking buffer fore 1 hour. The second membrane was incubated with 0.1µg/ml Qdot 625 streptavidin conjugate in WesternDot blocking buffer for 1 hour. The membranes were then visualised and documented according to the method described in section 2.4.2.8.

3.2.4.2 Results

The protein bands detected in the membrane probed with the secondary antibody was marked by a very similar pattern to that detected in the membrane probed with *anti-β actin* in the previous experiment. However, in this experiment, the 42 kDa band of *β actin* was not detected (Figure 3.5 A), which confirms that the 42 kDa band detected in the preceding experiment was due to specific binding of *anti β actin*. Nevertheless, the 75 kDa and 150 kDa bands were very intense as in the previous experiment. There were a number of bands in the range of 20 kDa to 60 kDa detected in the membrane. Conversely, in the membrane probed with Qdot 625 streptavidin conjugate alone, only the 75 kDa and 150 kDa bands were detected (Figure 3.5 B).

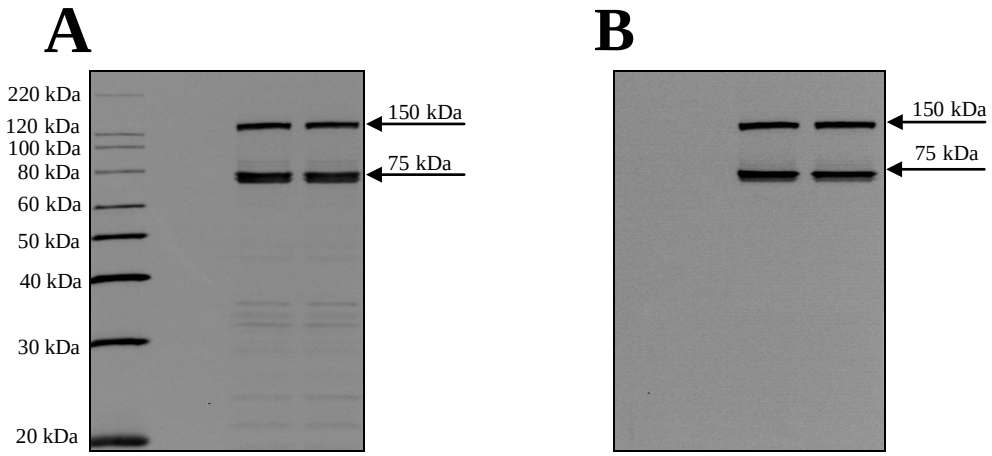

Figure 3.5: Identification of the source of non-specific bands. (A) Showing PVDF membrane incubated with secondary antibody followed by incubation with Qdot streptavidin conjugate**.** Two very intense bands at 75 kDa and 150 kDa, together with a number of bands ranging 20-60 kDa were detected in the membrane. **(B)** Showing membrane incubated with Qdot streptavidin conjugate. Only the 75 kDa and 150 kDa bands were detected in the membrane. MW represents MagicMark^{TM} XP Western protein standards (Invitrogen, LC5602).

The finding indicates that the bands in the range of 20-60 kDa were due to non-specific binding of the secondary antibody and 75 kDa and 150 kDa bands were due to non-specific binding of Qdot 625 streptavidin conjugate.

3.2.5 Pre-hybridisation of the biotinylated secondary antibody and the streptavidin conjugate eliminated non-specific binding

The interaction of biotin and streptavidin or avidin is the strongest known non-covalent bond between a protein and a ligand. Streptavidin and avidin are tetrameric proteins with four biotin binding sites (Figure 3.6). The streptavidin/avidin-biotin interaction is very rapid and the resulting complex is unaffected by the extremes of pH, temperature, organic solvents and detergents (Thermo Scientific, 2013). The strong affinity of avidin/streptavidin-biotin complex has been exploited in many protein and DNA detection techniques such as Western blot, Northern blot, Southern blot, ELISA, Immunohistochemistry (IHC), immunocytochemistry (ICC), immunoprecipitation (IP), cell surface labeling, and fluorescence-activated cell sorting (FACS).

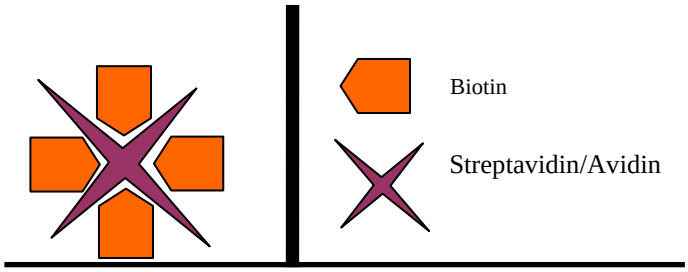

Figure 3.6: Schematic diagram showing biotin, streptavidin/avidin and biotin binding sites in streptavidin/avidin. Biotin has one binding site and streptavidin has four binding sites. Four biotin molecules bind to one streptavidin or avidin molecule to generate a saturated complex.

Biotin, a 244 Da protein, can be easily incorporated into other molecules such as protein and DNA without significantly altering their biological activity. Once a molecule is biotinylated, it can then be detected or purified using a biotin-binding protein such as streptavidin or avidin. In the context of immunohistochemical and immunoblotting techniques, biotin is most commonly incorporated onto primary or secondary antibodies, which are then detected with a biotin-binding protein conjugated to an enzyme such as Horse Radish Peroxidase (HRP) or fluorophore such as Qdot. Western blot, IHC and ELISA are based on a common procedure of detecting a target protein. In each case, the protein of interest is immobilized by adsorption, fixed or captured on a surface and then probed with a biotinylated antibody. The biotinylated antibody bound to the protein of interest is then detected or localized using a biotin-binding protein conjugated to a reporter molecule (Figure 3.7 A). The Westerndot Western blot kits used in the current study is based on the interaction of biotin and streptavidin. The secondary antibody in the kits is biotinylated and the reporter molecule Qdot is coupled to streptavidin.

Biotin is present in all living cells, where it plays critical roles in a number of biological processes such as cell growth and the citric acid cycle. Since biotinylated molecule will bind to any biotin-binding protein, techniques which employ streptavidin/avidin-biotin interaction to detect biological analytes suffer from a major setback. Biotin-binding proteins conjugated to reporter molecule binds to endogenous biotin or biotinylated proteins resulting in non-specific signal (Figure 3.7 B). This results in false positive signals in immunohistochemical method and non-specific bands in immunoblotting method such as western blot. In western blot, such non-specific bands usually appear in the form of a 75 kDa and a 150 kDa protein bands (Yu et al., 2009;) as observed in the preceding experiments.

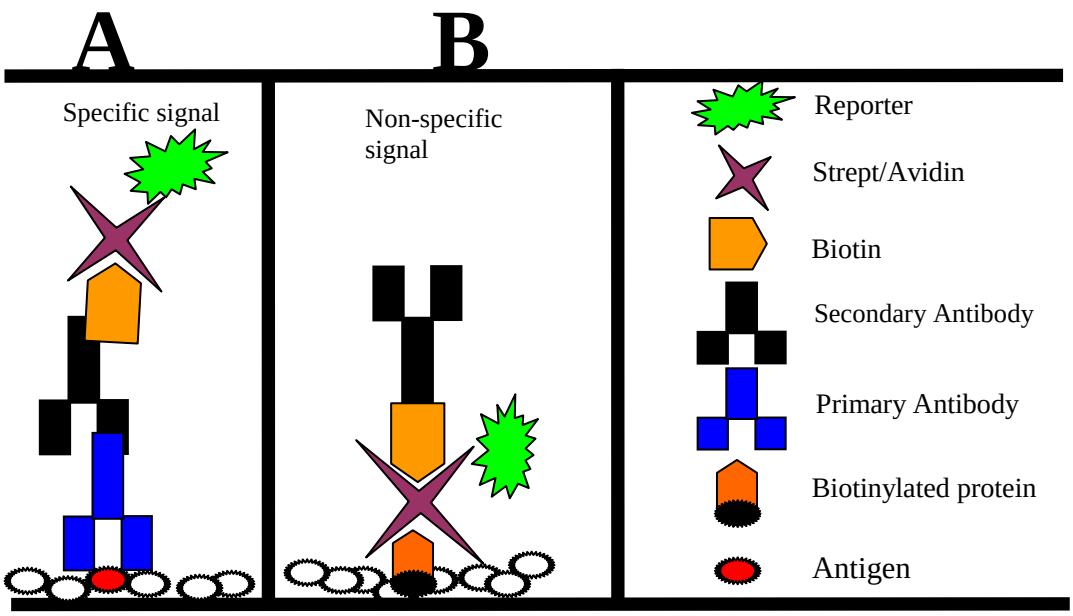

Figure 3.7: Schematic diagram showing specific and non-specific signals generated from streptavidin/avidin-biotin detection system. (A) Specific signal is generated when streptavidin/avidin molecule coupled to reporter molecule binds to biotinylated secondary antibody. **(B)** Non-specific signal is generated when streptavidin/avidin molecule coupled to reporter molecule binds to endogenous biotin or biotinylated proteins.

To eliminate such non-specific binding a second blocking step is incorporated into the methods in question. In this blocking step, endogenous biotin or biotinylated protein is blocked using a tetrameric biotin binding protein such as avidin. The free binding sites on the biotin-binding proteins are then blocked using free biotin molecules. However, this blocking method often compromises the specific signals. The method is also time consuming and often adds to the extra cost depending on the extent of endogenous biotin or biotinylated protein in biological samples.

In this experiment, a unique method was developed that efficiently eliminated non-specific binding inherent to streptavidin/avidin-biotin detection system without the need for a second blocking step. The method is based on pre-hybridisation of the biotinylated secondary antibody and the streptavidin/avidin-coupled reporter molecule, Qdot 625 in this case of the current study. It was hypothesised that prior hybridisation of streptavidin/avidin conjugate with the biotinylated secondary antibody would eliminate the non-specific binding of the biotin-binding protein with the endogenous biotin or biotinylated proteins. In such hybridisation, the biotin binding sites in the streptavidin/avidin conjugate would be blocked by the biotinylated secondary antibody and thus any localised signal generated would be a result the interaction between the secondary antibody and the primary antibody bound to the antigen (Figure3.8).

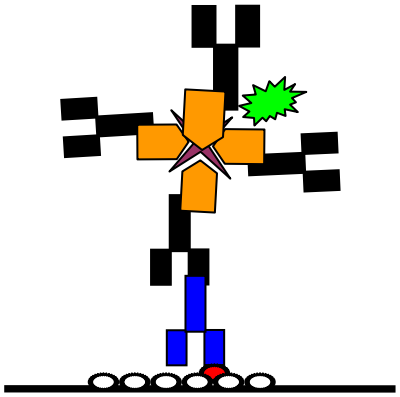

Figure 3.8: Schematic diagram showing pre-hybridisation of streptavidin/avidin-reporter molecule and biotinylated secondary antibody. Four biotin binding sites in streptavidin/avidin will be blocked by biotinylated secondary antibody and therefore any signal generated will be the result of an interaction between the secondary antibodies bound to streptavidin/avidin molecule.

3.2.5.1 Experimental designs

One part Qdot-streptavidin Conjugate was mixed with five parts biotinylated secondary antibody in a tube and incubated at ambient temperature for 1 hour. The resulting complex was then incubated with equal volume of 1mg/ml biotin in wash buffer for 30 minutes to ensure any free biotin-binding sites in the streptavidin conjugate were blocked. The complex of the secondary antibody and Qdot-streptavidin Conjugate was then diluted in 10 ml blocking buffer and stored at 4°C. 40 µg of total proteins were resolved, blotted onto PVDF membrane according to the methods described in sections 2.4.2.4 and 2.4.2.5, respectively. The membrane was blocked with WesternDot blocking buffer for 1 hour and incubated with the complex of the secondary antibody and Qdot-streptavidin Conjugate in

blocking buffer for 2 hours at ambient temperature. Finally, the membrane was washed and visualised according to the method described in section 2.4.2.8.

3.2.5.2 Results

Pre-hybridisation of the secondary antibody and Qdot streptavidin conjugate efficiently eliminated the 75 kDa and 150 kDa bands observed in the previous experiment (Figure 3.9). The finding indicates that the method could be utilised to detect antibody-antigen complex in the subsequent Western blot experiment. In the next experiment, therefore, the use of the newly developed method to detect antibody-antigen complex was validated.

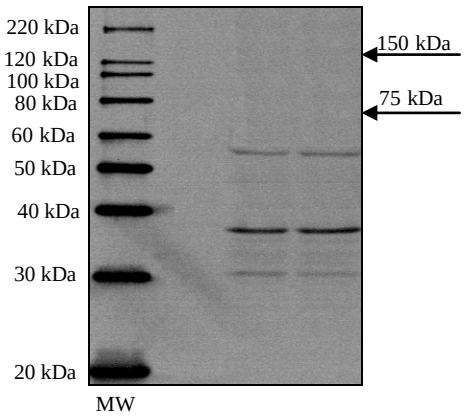

Figure 3.9: Pre-hybridisation of the secondary antibody with Qdot streptavidin conjugate eliminated the 75 kDa and 150 kDa bands. 40 µg total proteins were resolved and blotted onto PVDF membrane. The membrane was blocked and incubated with the pre-hybridised complex of Qdot streptavidin conjugate and biotinylated secondary antibody for 2 h at ambient temperature. Finally, the membrane was washed and image was documented under UV light. MW represents MagicMark^{TM} XP Western protein standards (Invitrogen, LC5602).

3.2.6 Validation of the newly developed method to detect antibody-antigen complex

40 µg of total proteins were resolved and blotted onto PVDF membrane according to the methods described in sections 2.4.2.4 and 2.4.2.5, respectively. The membrane was blocked and incubated with 1 mg/ml of anti-β-actin according to the method described in section 2.4.2.8. Following primary antibody incubation, the membrane was incubated with the complex of the biotinylated secondary antibody and Qdot-streptavidin Conjugate in blocking buffer for 2 hours at ambient temperature. The membrane was washed and visualised according to the method described in section 2.4.2.8.

3.2.6.1 Result

Use of the pre-hybridised complex of the biotinylated secondary antibody and Qdot-streptavidin conjugate resulted in successful detection of the ubiquitously expressed protein β actin. An intense band of the expected size (42 kDa) was detected in the membrane. As in the preceding experiments, protein bands of apparent molecular weights of 21 kDa, 23 kDa, 28 kDa, 32 kDa, 36 kDa, and 58 kDa were also detected in the membrane. It is apparent that the bands were due to non-specific binding of the secondary antibody to various intracellular proteins.

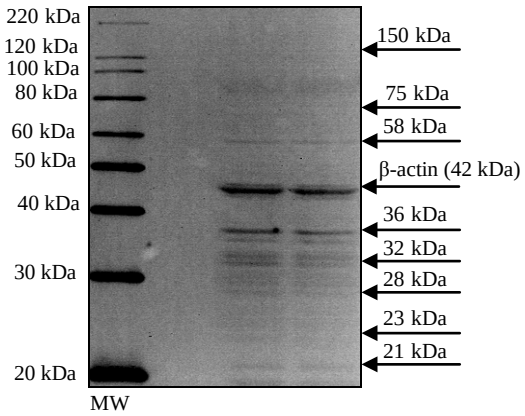

Figure 3.10: Pre-hybridised complex of the biotinylated secondary antibody and Qdot streptavidin conjugate successfully detected β actin. 40 µg total proteins were resolved and blotted onto PVDF membrane. The membrane was blocked and incubated and incubated with 1 mg/ml of anti-β-actin in wash buffer through overnight at 4°C. The membrane was then incubated with the pre-hybridised complex of Qdot streptavidin conjugate and biotinylated secondary antibody for 2 h at ambient temperature. Finally, the membrane was washed and image was documented under UV light. MW represents MagicMark^{TM} XP Western protein standards (Invitrogen, LC5602).

Nevertheless, the finding of the current experiment indicates that the pre-hybridised complex of the biotinylated secondary antibody and Qdot-streptavidin conjugate could be utilised to detect the primary antibody-antigen complex. Therefore, it was decided that the pre-hybridisation method developed in this part of the study would be used in all subsequent Western blot experiments in the subsequent parts of the study. Since the bands ranging 20-60 kDa were due to non-specific binding of the secondary antibody, these bands will not be included in the data analysis unless they are differently expressed in the treated samples.

This work is being prepared for publication.

3.3 Development of the assays for zebrafish (*Danio rerio*) DDR proteins activated by DSBs and SSBs

As discussed in chapter 1, the protein kinases, ATM and ATR are activated at a very early stage of a eukaryotic DDR. Activation of ATM is regarded as an indication of DNA damage in the form of DSBs, whereas, that of ATR may be an indication of the occurrence of both DSBs and SSBs. Therefore, a concurrent analysis of the kinases can be utilised to characterise the nature of DNA damage sustained by a biological object. Detection of only the activated form of ATM would be an indication of the occurrence of DSBs, whereas, detection of the activated form of ATR, in the absence of activated ATM, would be indicative of that of SSBs. However, a direct detection of the phosphorylated ATM or ATR using antibodies specific for the respective kinases was deemed not ideal for the reasons discussed in chapter 1; and the current study intended to utilised an antibody against the common substrate motif (S*/T*Q) of the kinases to indirectly investigate the activation of the parental kinases. Antibody against the S*/T*Q motif has previously been utilised to investigate DNA damage in adult zebrafish (*Danio rerio*) (Santoriello et al., 2009). To some extent, the use of a motif antibody provides greater benefit than that of the specific antibody against the parental proteins. For example, in addition to serving as an indication of the activation of parental proteins, it also provides an overview of the metabolic pathway involved in a specific biological process by detecting the downstream substrate proteins. However, in the context of the present study, utilisation of the S*/T*Q antibody has one limitation, that is how to distinguish between the activation of ATM and that of ATR. The limitation can be overcome by a careful observation of the substrates unique to the respective kinases, which is made easier by Western blot as the technique is based on the separation of proteins according to their molecular weights. The substrates unique to ATM and ATR are Chk2 and Chk1, respectively. However, much of the knowledge of the ATM/ATR pathway is gained from the studies carried out in human and mice. Zebrafish (*Danio rerio*) is known to possess all the components of a DDR. It is, however, not known, if the DDR in the teleost thoroughly follows the established ATM/ATR pathway in terms of the downstream substrate proteins such as Chk1 and Chk2. In these settings, the objective of this part of the study was to investigate if the activation of ATM and ATR in zebrafish (*Danio rerio*) embryos can be distinguished by analysing the substrates specific for the respective kinases. To that effect, the experiments described in this section were carried out to

generate S*/T*Q antibody-mediated Western blot assays for DDR proteins activated in the event of DSBs and SSBs in the genome of 5¼ hpf zebrafish (*Danio rerio*) embryos.

3.3.1 Development of the assay for zebrafish embryonic DDR proteins affected in the event of DSBs in the genome

DNA topoisomerases are a family of enzymes that facilitate the unwinding and rewinding process of supercoiled DNA structure during replication, transcription, recombination and chromatin remodelling. There two types of topoisomerases in eukaryotes, *topoisomerase* 1 (*Top I*) and *topoisomerase II* (*Top II*). *Top I* causes relaxation of the supercoiled DNA by inducing a transient SSB and passing the intact DNA strand through the SSB. The SSB is then resealed to form a structure with the same chemical bonds as the starting DNA. *Top II*, on the other hand, relaxes the supercoiled DNA by inducing a transient DSB, passing another portion of the double stranded DNA through the DSB. The DSB is then resealed by the enzyme in an ATP dependant manner (Cox et al., 2012). Because of their mode of action, topoisomerases have become attractive targets of anti-cancer agents. To date, the inhibitors of topoisomerases are among the most effective and widely used drugs in cancer treatment. The inhibitors of *Top I* act by stabilising the otherwise transient complexes formed between the enzyme and DNA. Collisions of such stabilised complexes with the progressing DNA replication fork result in the formation DSBs, leading to the initiation of a DDR. The inhibitors of *Top II*, on the other hand, act by stabilising the otherwise transient DSB generated as part of the enzymatic cycle (Zhao et al, 2012). Inhibitors of the topoisomerases have widely been used to induce DSBs in the genome in studies investigating activation of eukaryotic DDR proteins such as ATM and ATR (Siu et al., 2004; Muslimovic et al., 2009; Rojas et al., 2009; Zuco et al., 2010). In an early study based on phenotype investigation, etoposide, an inhibitor of *Top I*, and camptothecin, an inhibitor of *Top II*, have been shown to activate cell cycle checkpoints in zebrafish (*Danio rerio*) embryos (Ikegami et al, 1997). Guided by the findings of the study of Ikegami et al, (1997), this part of the study utilised the drugs, etoposide and camptothecin, to induce DSBs in the genome of zebrafish (*Danio rerio*) and thereby activate the DDR proteins.

3.3.1.1 Etoposide treatment

5¼ hpf zebrafish (*Danio rerio*) embryos were incubated for a period of 2 hours in 60 µM etoposide (Ikegami et al., 1997) prepared in 1M Me_2SO. A second group of 5¼ hpf embryos were incubated in E2 for 2 hours at ambient temperature as non-treated control. Following incubation, total proteins were extracted from each group of embryos according to the method described in section 2.4.2.2. 40 µg of total proteins from each lysate were resolved alongside two known control lysates, 293 cells$^-$ and 293 cells$^+$ (Cell Signalling, 9253) for the S*/T*Q antibody using the method described in section 2.4.1.4. The resolved proteins were then blotted onto PVDF membrane using the method described in section 2.4.2.5. Finally, the membrane was probed with anti-S*/T*Q using Western blot according to the method described in section 2.4.2.8.

3.3.1.2 Results

In the 293 cell$^+$ lysate, two bands of approximately 90 kDa and 300 kDa were detected (Figure 3.11 A, + lane). These bands were not present in the 293 cell$^-$ lysate (figure 3.6 A, – lane). A band of approximately 150 kDa was present in both 293 cell$^-$ and 293 cell$^+$ lysates. However, there was no significant ($p<0.05$) difference in the β-actin-normalised intensity of the bands. Etoposide treatment did not result in phosphorylation of any DDR protein in 5¼ hpf zebrafish (*Danio rerio*) embryos. None of the protein bands detected in the 293 cell$^+$ lysate alone was present in the embryo lysates. The 150 kDa band was present in the zebrafish embryo lysates also (Figure 3.11A, lane 3-6). However, the β-actin -normalised intensity of the band in the etoposide-treated embryo lysates was not significantly different ($p>0.05$) from that of the non-treated control (Figure 3.11 C). There was a band of approximately 38 kDa present in the embryo lysates only. Nevertheless, the *β-actin* normalised intensity of the band was not significantly different ($p>0.05$) from that of the non-treated control. Bands of apparent molecular weight of 21 kDa, 23 kDa, 32 kDa, 36 kDa, 52 kDa and 58 kDa were due to non-specific binding of the secondary antibody (as discussed in section 3.4 in detail) and were not further analysed for the reason described in section 3.2.6.

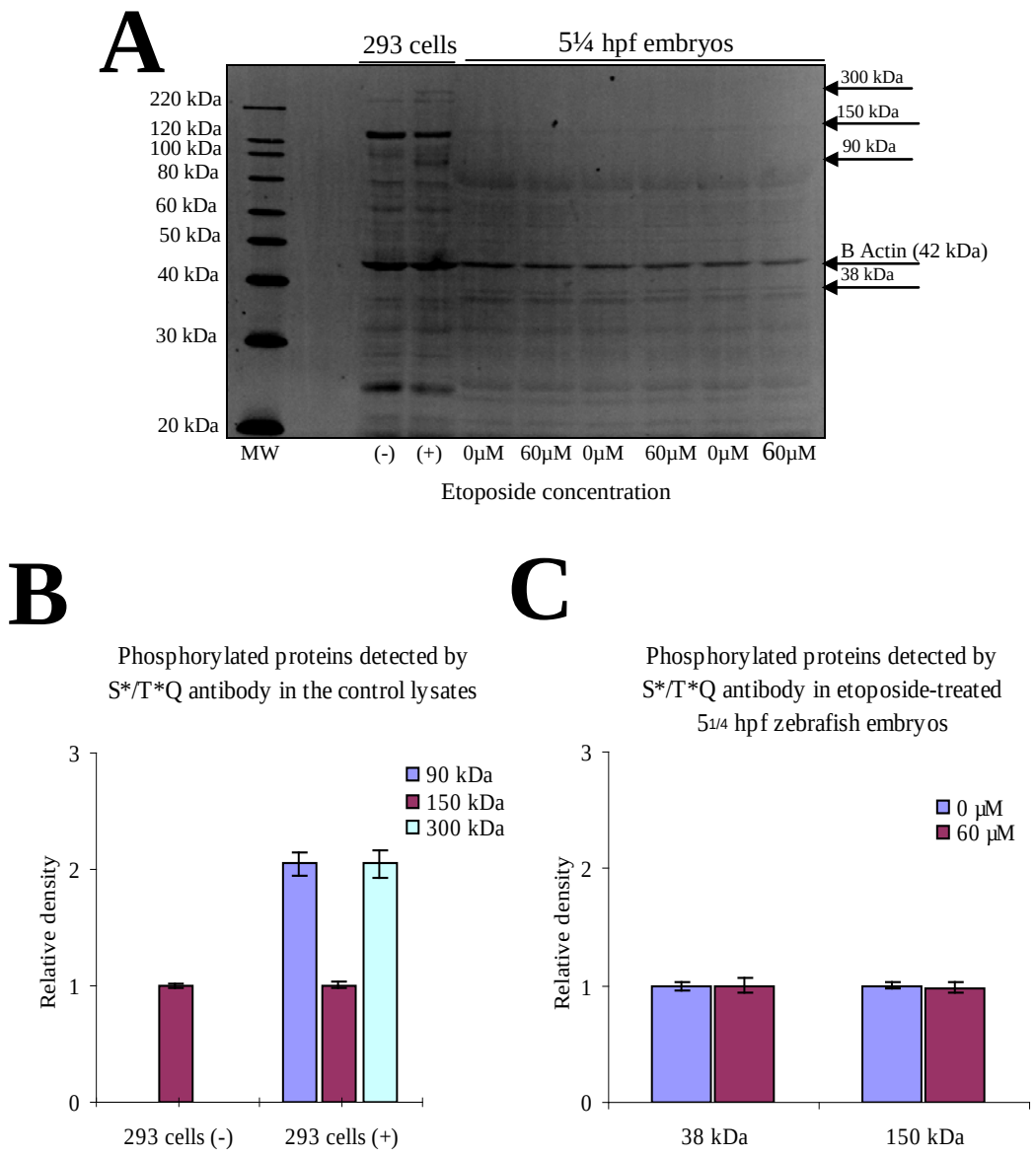

Figure 3.11: Zebrafish (*Danio rerio*) DDR proteins were not affected by etoposide treatment. **(A)** Western blot showing DDR proteins detected by S*/T*Q antibody. $5^{1/4}$ hpf embryos were incubated for 2 h in 0 and 60 µM etoposide. Total proteins were extracted from each treated group and probed alongside 293 cell lysates, negative and positive controls for S*/T*Q motif, with anti-S*/T*Q, and anti-β-*actin* simultaneously. β-*actin* served as a control for variations in protein loading. (B) Graphical presentation of the intensity of the bands detected in the 293 cells^{-} and 293 cell^{+} lysates. Values shown are mean +/- SEM of β-*actin* normalised band intensities obtained from three replicates and presented as relative to those in the 293 cells^{-} lysate. (C) Graphical presentation of the intensity of the bands detected in the lysates prepared from the embryos treated with 0 and 60 µM etoposide. Values shown are mean +/- SEM of β-*actin* normalised band intensities obtained from three replicates and presented as relative to those in the lysate prepared from the embryos exposed to 0 µM etoposide. Different letters, where appropriate, indicate statistically significant ($p<0.05$) difference among the groups being compared. MW represents MagicMark^{TM} XP Western protein standards (Invitrogen, LC5602).

3.3.1.3 Discussion

Contrary to the expectation, etoposide treatment did not activate any DDR proteins in 5¼ hpf zebrafish (*Danio rerio*) embryos as detected by ATM/ATR substrate motif (S*/T*Q) antibody (Figure 3.11 A-C). Successful detection of the activated DDR proteins in the 293^{+} lysates (Figure 3.11, A and B) confirmed the sensitivity and specificity of the antibody for the S*/T*Q motif. Nevertheless, the finding of this part of the study regarding etoposide treatment is in agreement with that of Ikegami al, (1997). Ikegami et al, (1997) have shown that treating zebrafish (*Danio rerio*) embryos at a developmental stage earlier than 5¼ hpf with etoposide resulted in activation of the cell cycle checkpoint, whereas, treating the 5¼ hpf or later developmental stage embryos did not result in activation of the cell cycle checkpoints. The author put forward the highly efficient zebrafish DDR as the reason for etoposide treatment not resulting in the activation of cell cycle checkpoints in 5¼ hpf zebrafish embryos. Ikegami et al (1997) concluded that the zebrafish DDR in early developmental stage embryos is not as efficient as to repair DNA damage; hence, etoposide treatment resulted in the activation of cell cycle checkpoints, whereas, in the later developmental stage embryos, the zebrafish DDR becomes efficient enough to repair the damage as quickly as it is generated. However, the finding of this part of the current study contradicts the hypothesis put forward by Ikegami et al, (1997). As discussed in chapter 1, cell cycle checkpoints are an essential component of an effective DDR. The function of the cell cycle checkpoints is to slow down or arrest the cell cycle for the DNA repair mechanisms to repair the damage. In the event of DNA damage, the sensor protein ATM or ATR bridge the cell cycle checkpoints and the DNA repair mechanisms by activating a number of proteins from both of the events. Therefore, a technique based on an antibody against ATM/ATR substrate motif, such as S*/T*Q antibody, would detect proteins activated from the cell cycle checkpoints as well as from the repair mechanisms. To that end, the failure of this part of the current study to detect activated DDR proteins in the etoposide-treated embryos indicates that the drug failed to induce DSBs in the genome and thereby failed to initiate a DDR. The reason for the etoposide treatment not resulting in the activation of any DDR proteins in 5 ¼ hpf zebrafish (*Danio rerio*) could be explained by the fact that not all proteins present in an embryo are native to the embryo itself. It is possible that *Top II* is preloaded in the embryos from the oocyte to carry out the essential biological functions, and at later developmental stages, it becomes redundant by an

enzyme of the same family, such as *Top I*. This scenario explains the finding of Ikegami et al (1997) as well as that of this part of the current study.

3.3.1.4 Camptothecin treatment

5¼ hpf zebrafish (*Danio rerio*) embryos were incubated for a period of 2 hours in 60 µM camptothecin (Ikegami et al., 1997) prepared in 1M Me_2SO. A second group of 5¼ hpf embryos were incubated in E2 as non-treated control. Total proteins were extracted from each group of embryos according to the method described in section 2.4.2.2. 40 µg of total proteins from each lysate were resolved and blotted using the methods described in sections 2.4.2.4 and 2.4.2.5, respectively. The membrane was probed with anti-S*/T*Q using the method described in section 2.4.2.8.

3.3.1.5 Result

A total of seven proteins were affected in 5¼ hpf zebrafish (*Danio rerio*) in response to camptothecin treatment. Five proteins of apparent molecular weight of 22 kDa, 31 kDa, 34 kDa, 62 kDa, and 100 kDa were detected only in the lysates prepared from the embryos treated with camptothecin (Figure 3.7 A and C). 150 kDa protein, which was found phosphorylated in the 293 cell lysates, non-treated and etoposide treated embryos in the previous experiment, was phosphorylated in the non-treated embryos in this experiment too. However, the protein was found dephosphorylated in the embryos treated with camptothecin (Figure 3.7 A). Similarly, the 38 kDa protein which was phosphorylated in the non-treated and etoposide treated embryos in the previous experiment was found phosphorylated in the non-treated and camptothecin-treated embryos in this experiment. Nevertheless, the protein was hypophosphorylated in the camptothecin treated embryos, with the β-actin normalised intensity of the band being significantly ($p<0.05$) decreased relative to that of the non-treated control. Bands of apparent molecular weight of 21 kDa, 23 kDa, 32 kDa, 36 kDa, 52 kDa and 58 kDa were not further analysed for the reason described in section 3.2.6.

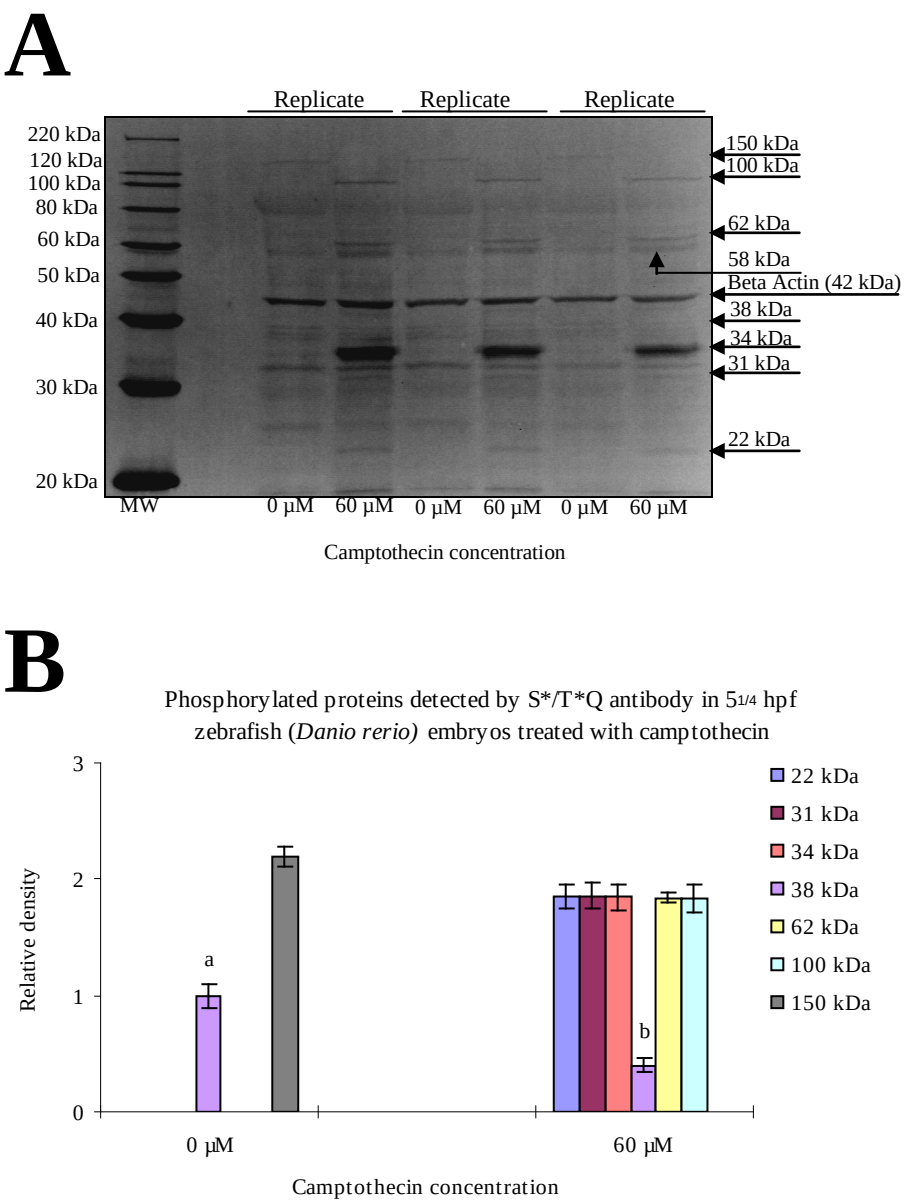

Figure 3.12: Zebrafish (*Danio rerio*) DDR proteins were affected by camptothecin treatment. **(A)** Western blot showing zebrafish DDR initiated by camptothecin treatment in three independent treatments. Total proteins were extracted from the embryos treated with 0 µM and 60 µM camptothecin for 2h and probed with anti-S*/T*Q. β-*actin* was probed as a loading control. **(B)** Graphical presentation of the intensity of the bands detected in the embryo lysates. Values shown are mean +/- SEM of β-*actin* normalised band intensities relative to those in the lysates prepared from non-treated embryos. Different letter indicates statistically significant ($p<0.05$) difference among the groups being compared. MW represents MagicMark™ XP Western protein standards (Invitrogen, LC5602).

3.3.1.6 Discussion

In the study of Ikegami et al, (1997), camptothecin has been shown to activate cell cycle checkpoints in both early and later developmental stage zebrafish (*Danio rerio*) embryos. Based on the finding of Ikegami et al (1997), it was expected that the drug would activate DDR proteins in 5¼ hpf zebrafish (*Danio rerio*) embryos; and this part of the study found that camptothecin treatment activated a number of proteins in the embryos as detected by the S*/T*Q antibody (Figure 3.12 A and B). However, the DDR proteins detected in the lysates prepared from the camptothecin-treated embryos are different from those detected in the 293^{+} cell lysate (Figure 3.11 A, + lane and B) by S*/T*Q antibody. The 293 cell lysates were sourced as the known controls for the S*/T*Q antibody and according to the supplier, the lysates were prepared by treating 293 cells with UV light, which usually causes DNA damage other than DSBs (De Gruijl et al., 2001; Rochette et al., 2010). Therefore, DDR from 293 cells would be different to that from the cells treated with DSB inducer, such as camptothecin. Moreover, the 293 cell lines are derived from human embryonic kidney cells and the response from such cells will not be identical to that from zebrafish (*Danio rerio*) embryonic cells, which is one of the reasons why the this part of the study set out to assay zebrafish DDR proteins activated in response to DSBs and SSBs. The 293 cell control lysates were used only to validate the sensitivity and specificity of the S*/T*Q motif antibody and the results obtained justified the use of such controls by clearly showing the sensitivity and specificity of the antibody for S*/T*Q moiety. Nevertheless, this part of the study showed the benefit of using ATM/ATR substrate motif antibody by providing an overview in a single Western blot of the DSB-mediated DDR in 5 ¼ hpf zebrafish (*Danio rerio*) embryos. The finding of this part of the study indicates that the eukaryotic DDR in terms off DSB-mediated activation of ATM is conserved in the vertebrate model.

As discussed in chapter 1, ATM-dependant DDR is mediated by Chk2, a 62 kDa protein. In the event of DSBs in the G_1 phase of the cell cycle, ATM activates Chk2 and p53. Chk2 in turn phosphorylates p53 to enhance the level of the tumour suppressor protein. Once activated, p53 phosphorylates a 21 kDa protein, p21, which inhibits cell cycle promoter protein, Cdk2. Inhibition of Cdk2 results in cell cycle arrest for the repair process to take place or apoptosis to be initiated. On the other hand, in the event of DSBs in both S phase and G_2 phase of the cycle, ATM activates only Chk2. In the S phase, activated Chk2, in turn, deactivates Cdc25A via inhibitory phosphorylation. In a normal

cell, the function of Cdc25A is to activate Cdk2 by removing its inhibitory phosphorylation. Deactivation of Cdc25A thus arrests the cell cycle for the repair process to take place. In G_2 phase, Chk2 deactivates CDC25C, which functions the same way as CDC25A. Since the activation of Chk2 is specific to ATM, the presence of a 62 kDa protein in the camptothecin treated embryo lysates indicates that the DDR was initiated by ATM. By the same token, the presence of the 62 kDa protein also confirms that camptothecin treatment induced DSBs in the genome of the 5¼ hpf zebrafish (*Danio rerio*).

ATM is known to have a large number of substrates (Kastan and Lim, 2000), which according to recent study is around 500 in number (Stokes, 2007), indicating that the kinase may play significant roles in various biological processes. Not surprisingly, the current study found a number of proteins activated in the zebrafish (*Danio rerio*) in response camptothecin induced DSBs. As discussed in chapter 1, ATM phosphorylates a number of proteins from the cell cycle checkpoints as well as from the DNA repair mechanisms, the proteins detected in the camptothecin-treated zebrafish (*Danio rerio*) embryos likely to represent proteins from both of the events. For example, the 34 kDa protein detected in the camptothecin-treated embryo lysates is most likely to be the smaller subunit of RPA, which is responsible for DNA repair. To that end, the finding of the current experiment reiterates the notion that ATM plays significant roles both cell cycle checkpoints and DNA repair.

As mentioned earlier, in the event of DSBs, ATM facilitates the cell cycle arrest indirectly via phosphorylation of Chk2. However, the finding of the current study indicates that ATM may play a direct role in cell cycle arrest as the 150 kDa protein is evidently deactivated in the camptothecin-treated embryo lysates. This observation is further supported by the finding that the 38 kDa protein is down-regulated in such lystaes. In the vast array of published literature focussed on eukaryotic DDR, there is no mention of a 150 kDa protein that promotes cell cycle progression and, therefore, is deactivated in the event of extensive DNA damage to facilitate cell cycle arrest. In that regard, the finding suggests that the eukaryotic DDR, as elucidated by studies carried out mainly in human cells, is not thoroughly conserved in zebrafish (*Danio rerio*). This observation is further added to by the presence in DSB-mediated DDR in 5¼ hpf zebrafish (*Danio rerio*) embryos of 100 kDa, 31 kDa and 22 kDa proteins, which are not described in the eukaryotic DDR. In a study carried out by Wu et al, (2008), it has been shown that

MSH2, a 100 kDa protein known to be active in the MMR, plays an important role in DSB repair in human cells. The 100 kDa protein detected in the camptothecin-treated embryo lysates in this part of the study may represent the mismatch detecting protein MSH2, in which case it would be an indication that MSH2 is a substrate for ATM, which in turn would be yet another evidence that zebrafish (*Danio rerio*) DDR is not identical to that elucidated in human. The 22 kDa and 31 kDa proteins detected in the camptothecin-treated embryos may be unique to zebrafish as it is already apparent that the DDR in the teleost is different to the common notion of the eukaryotic DDR. However, it is not possible to draw a firm conclusion as regards to the DDR proteins appeared to be unique to zebrafish without further investigation, which is beyond the scope of the current study. For the purpose of the current study the pattern of activation and deactivation of the substrate proteins by ATM would be suitable to investigate the occurrence of DSBs in the genome of 5¼ hpf zebrafish (*Danio rerio*) embryos treated with different cryopreservation parameters.

3.3.2 Development of the assay for SSB-activated DDR proteins

H_2O_2 is a well known inducer of SSBs in the genome of biological objects. It has been utilised as an SSB inducer in a large number of studies involving a wide range of test materials (Ananthaswamy, and Eisenstark, 1977; Mello Filho et al, 1984; Schraufstatter et al., 1986; Fortini et al., 2000, Wang et al., 2009; Grudzenski et al., 2010). H_2O_2 readily penetrates cells and is thought to exert its effects by generating a flux of highly reactive ROS, hydroxyl radical (◦OH) through superoxide mediated Fenton reaction (Mello Filho et al, 1984):

$$Fe^{2+} + H_2O_2 \rightarrow Fe^{3+} + {\circ}OH + OH^-$$
$$Fe^{3+} + H_2O_2 \rightarrow Fe^{2+} + OOH\cdot + H^+$$

As described in chapter 1, ROS chemically binds to the bases in DNA resulting in SSBs and structural alteration of the bases. H_2O_2 has been previously utilised to induce SSBs in the genome of early and late developmental stage zebrafish (*Danio rerio*) embryos (Garcia-Kaeufer et al., 2009; Kosmehl et al., 2006).

3.3.2.1 H_2O_2 treatment

Guided by the published studies, 5¼ hpf zebrafish (*Danio rerio*) embryos were incubated in 30 mM H_2O_2 prepared in E2 for 1 hour. A second group of embryos were incubated in E2 as non-treated control. Total proteins were extracted from the treated and non-treated embryos according to the method described in section 2.4.2.2. 40 µg of total proteins from each lysate were separated in SDS-PAGE and blotted onto PVDF membrane using the method described in section 2.4.2.5. Finally, the membrane was probed with anti-S*/T*Q using Western blot according to the method described in section 2.4.2.8.

3.3.2.2 Results

The result of the experiment showed that DDR proteins were affected in 5¼ hpf zebrafish (*Danio rerio*) embryos in response to H_2O_2 treatment. The 150 kDa protein, which was phosphorylated in the non-treated embryos in the previous two experiments, was phosphorylated in the non-treated embryos in this experiment too. However, as in the case of camptothecin-treated embryos in the preceding experiment, the 150 kDa protein was dephosphorylated in the H_2O_2 -treated embryos. Similarly, the 38 kDa protein, which was phosphorylated in the non-treated, etoposide-treated and camptothecin-treated embryos, was phosphorylated in the non-treated and H_2O_2-treated embryos in this experiment. Nevertheless, unlike in the camptothecin-treated embryos, the protein was hyperphosphorylated in the H_2O_2–treated embryos, with the β-actin-normalised intensity of the band being significantly ($p<0.05$) increased relative to that of the non-treated control. Bands generated from the non-specific binding of the secondary antibody were ignored, as usual.

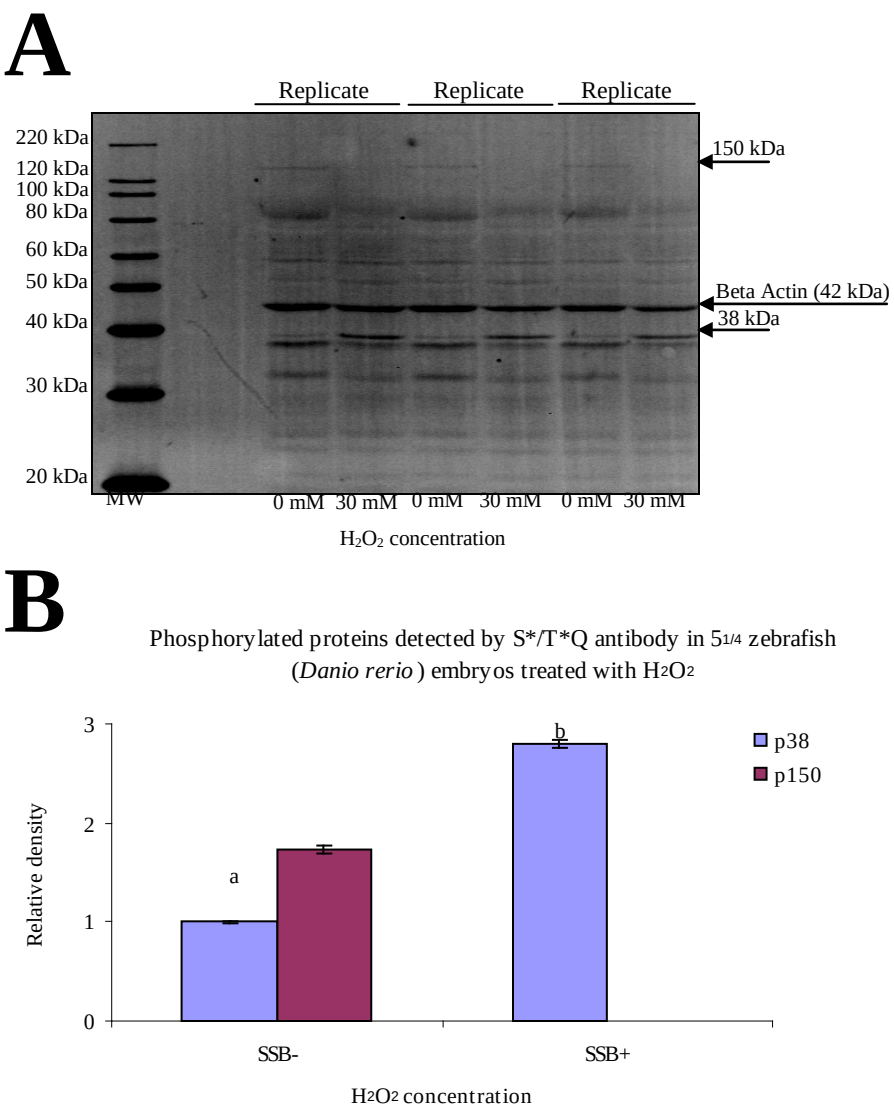

Figure 3.13: H_2O_2 treatment affected DDR protein phosphorylation in 5¼ hpf zebrafish (*Danio rerio*) embryos. (A) Western blot showing zebrafish DDR initiated by H_2O_2 in three independent treatments. Total proteins were extracted from the embryos treated for 1h with 0 mM and 30 mM H_2O_2 and probed with anti-S*/T*Q and anti- β-*actin*, as before. β-*actin* was probed as a loading control. **(B)** Quantification of the bands detected in the embryo lysates. Values shown are mean +/- SEM of β-*actin* normalised band densities relative to those in the lysate prepared from the embryos exposed to 0 mM H_2O_2. MW represents MagicMark^{TM} XP Western protein standards (Invitrogen, LC5602).

3.3.2.3 Discussion

According to the common notion of eukaryotic DDR, ATR-dependant DDR is mediated by Chk1, a 56 kDa kinase. In the event of SSBs in the genome, ATR activates Chk1 to bring about cell cycle arrest or delay so that the damage could be repaired. Activated Chk1, in turn, activates p53 if the cell sustaining DNA damage is in the G_1 phase, deactivates Cdc25A if the damage sustaining cell is in the S phase, or Cdc25C, if such cell is in the G_2 phase of the cell cycle. With that perspective, it was expected that the treatment of 5¼ hpf zebrafish (*Danio rerio*) embryos with SSB inducer H_2O_2 would result in the activation of ATR, which in turn would result in the activation of Chk1. In the context of the current study, activation of Chk1 would be manifested in the form of a 56 kDa protein band as detected by the S*/T*Q antibody.

However, the S*T*Q antibody did not detect any protein corresponding to the molecular weight of Chk1 in the H_2O_2-treated embryos; indicating that ATR mediated phosphorylation of Chk1 may not be conserved in zebrafish (*Danio rerio*) embryos. Nevertheless, the DDR proteins affected in the H_2O_2–treated embryos were marked by an interesting pattern. It was of great significance to observe that the 150 kDa protein found deactivated in camptothecin-treated embryos was found deactivated in H_2O_2-treated embryos too. According to the elucidated eukaryotic DDR, in the event of DNA damage such as DSBs and SSBs, cell cycle promoter proteins, such as Cdk2, are deactivated to facilitate cell cycle arrest. The finding that the 150 kDa protein was deactivated in both camptothecin-treated and H_2O_2-treated embryos indicates that the 150 kDa protein is a zebrafish homologue for the cell cycle promoter protein Cdk2. The finding also indicates that the DSB-mediated DDR and the SSB-mediated DDR in zebrafish (*Danio rerio*) embryos share a common protein, the 150 kDa protein. According to the common knowledge of eukaryotic DDR, ATM and ATR accomplish cell cycle arrest or delay deactivating the cell cycle promoter protein Cdk2 indirectly via a combined action of a number of downstream substrates. The finding in this part of the study, however, suggests that the kinases play a direct role in cell cycle arrest in zebrafish (*Danio rerio*) embryos. It was even of greater significance to observe that the 38 kDa protein, which was hypophosphorylated in the camptothecin-treated embryos, was hyperphosphorylated in the H_2O_2–treated embryos. The finding indicates that the 38 kDa protein is differentially expressed depending on the nature of the DNA damage. As it was established from the findings of the previous experiment that ATM mediated phosphorylation of 62 kDa

protein is conserved in zebrafish (*Danio rerio*) embryos, the absence of a 62 kDa band in the H_2O_2-treated embryo lysates confirms that the DDR initiated in such embryos was mediated by a kinase other than ATM, which in the case of the current study was ATR since the motif antibody utilised was specific for the downstream substrates of ATM and ATR. With this perspective, the finding regarding the differential expression of the 38 kDa protein in camptothecin-treated embryos and H_2O_2-treated embryos indicates that ATM kinase selectively down-regulates 38 kDa protein, whereas ATR kinase selectively up-regulates the protein. The finding also suggests that the 38 kDa protein is unique to zebrafish (*Danio rerio*) as there is no mention of such a protein in any of the databases recording the substrate proteins for ATM and ATR kinases.

Nevertheless, it is apparent from the overall findings in this part of the study that the S*/T*Q antibody successfully detected the selective activation of ATM and ATR in the event of DSBs and SSBs, respectively, as evident from the distinctive patterns of DDR protein activation in 5¼ hpf zebrafish (*Danio rerio*) embryos treated with DSB-inducer camptothecin and SSB inducer H_2O_2.. Based on the findings in this part of the study, therefore, it was decided that the S*/T*Q antibody would be used in the subsequent parts of the study to detect DDR proteins in 5¼ hpf zebrafish embryos treated with different cryopreservation parameters, and the distinctive patterns of DDR protein activation and deactivation in response to DSBs and SSBs would be utilised to analyse the nature of DNA damage in such embryos. For the convenience of analysis, the DDR proteins detected in this part of study will be referred to hereafter as p22, p31, p34, p38, p62, p100, and p150.

This work is being prepared for publication.

3.3.3 Investigation in zebrafish (*Danio rerio*) of the expression of genes unique to the individual ERMs

In the eukaryotic genome, various forms of sequence alteration occur spontaneously as a result of errors during replication. As discussed in details in chapter 1, the ERMs play indispensable roles in maintaining the genome integrity by correcting the altered sequences, which may otherwise result in various mutations. Since, the primary function of the ERMs is to maintain the genomic integrity in terms of structural alteration, an up-

regulation of any of the repair mechanisms would be an indication of an increased occurrence of the types of lesions repaired by the particular pathway. However, the potential of these DNA repair mechanisms as a means to investigate the occurrence of sequence alteration in zebrafish (*Danio rerio*) has not been explored. As part of the investigation of the effects of various cryopreservation parameters on the genome of 5¼ hpf zebrafish (*Danio rerio*) embryos, the current study utilised the expression levels of four genes unique to the individual ERMs as an indication of the occurrence of sequence alteration. The genes analysed are *Uracil DNA gycosylase* (*UDG)* and *Thymine DNA glycosylase* (*TDG)* from the BER, *ERCC 1* from the NER and *MSH2* from the MMR. The functions of the proteins encoded by these genes are discussed in chapter 1 in detail. Briefly, *UDG* and *TDG* remove misincorporated uracil and mismatched thymine, respectively, from DNA (Figure 1.5). *ERCC1* is responsible for making incision in DNA in the NER pathway (Figure 1.6), whereas, *MSH2* is responsible for detecting the mismatched bases in the MMR pathway (Figure 1.7). The objective of this experiment was to investigate if the aforementioned genes are expressed in 5¼ hpf zebrafish (*Danio rerio*) embryos.

3.3.3.1 Experimental designs

Total RNA from 5¼ hpf zebrafish (*Danio rerio*) embryos were extracted and converted into cDNA using the methods described in section 2.4.3.1 and 2.4.3.4, respectively. cDNA was then subjected to PCR reactions using the method described in section 2.4.3.5 to amplify the selected genes, namely *UDG, TDG, ERCC1* and *MSH2*. Finally, the amplicons were analysed according to the method outlined in section 2.4.3.6. House keeping gene *ACTB* was amplified separately in the sample as a loading control.

3.3.3.2 Results

Agarose gel analysis of the amplicons generated a single band with the expected product size for each of the genes (Figure 6 A-D), which is an indication that the primers used in the amplification reactions were specific for the respective gene. The HKG, *ACTB*, was amplified alongside the gene of interest, which served as a loading control as well as a confirmation of the efficiency of the reaction. The specificity of primers was further

confirmed by analysis of the melt curves from the cDNA standards prepared for the respective genes analysis in the subsequent experiments.The melt curve for each of the genes amplified produced a single peak indicating a single amplicon (Figure 6 E-H).

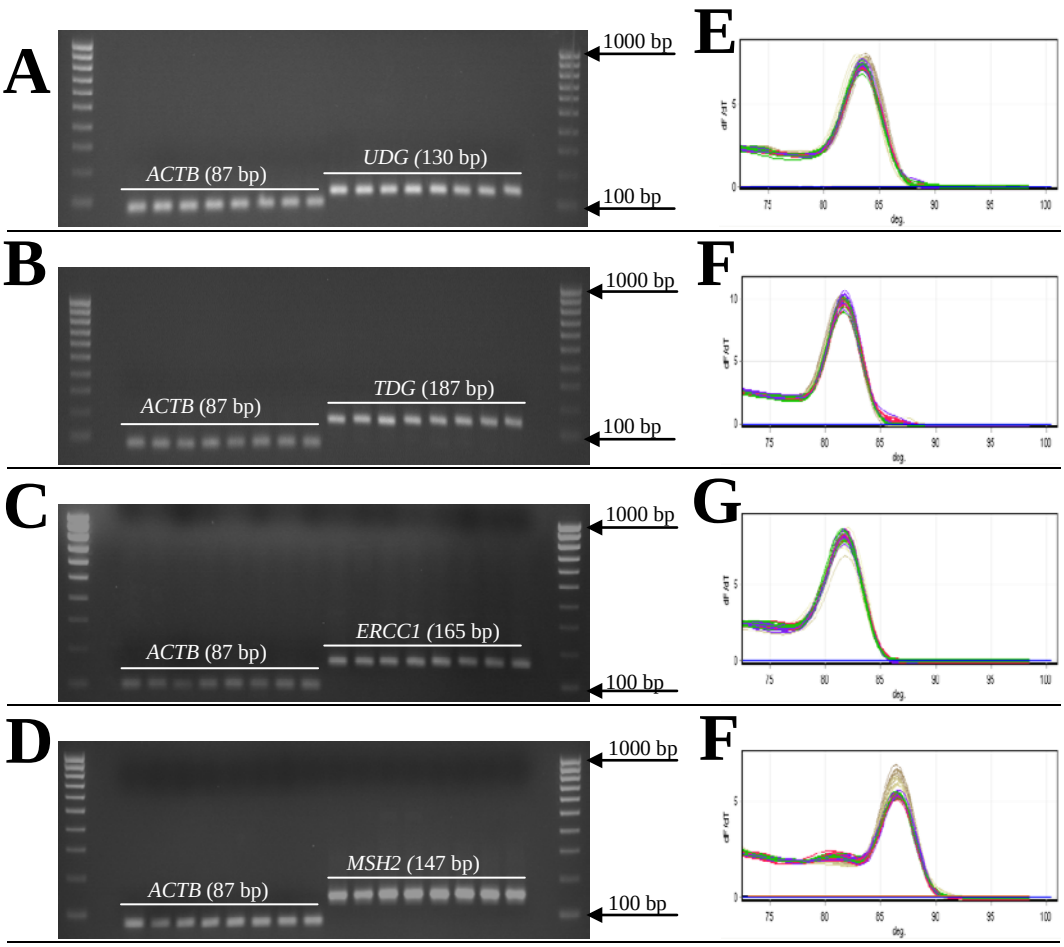

Figure 3.14: Amplification reaction for each gene produced a single band of the expected size. (A-D) Agarose gel electrophoresis (2% agarose) of *UDG*, *TDG*, *ERCC1* and *MSH2* amplicons. *ACTB* was used as an internal control. Hyperladder IV (100 bp ladder) was used to estimate the product size. **(E-F)** Showing the melt curves for the corresponding genes

3.3.3.3 Discussion

The ERMs are the first line of defence against the non-lethal structural alteration in the eukaryotic genome. As mentioned earlier, the potential of these mechanisms as indicators of the frequency of various types of sequence alteration of DNA has not been explored in zebrafish (*Danio rerio*). Zebrafish is known to possess a competent DDR (Sussman, 2007; Zeng et al., 2009), indicating that the teleost would also possess the ERMs.

However, it was not known if the repair pathways in terms of the proteins involved are thoroughly conserved in the vertebrate model. Analysis of the transcript level of a gene gives an overview of the protein encoded by the particular gene. To that end, this part of the study investigated the expression of the selected genes in 5¼ hpf zebrafish (*Danio rerio*) embryos. The agarose gel analysis of the PCR products resulted in a single band for each of the genes indicating that the amplicons were specific for the respective genes (Figure 3.9 A-D). The melt curve analysis (Figure 3.9 B) for the amplified products for each gene also confirmed the specificity of the primers used in the amplification reactions. Therefore, the finding of this part of the study indicates that each of the genes selected from the individual ERMs were expressed in 5¼ hpf zebrafish (*Danio rerio*) embryos. The expression of the selected genes, as detected, is evidence that the eukaryotic excision repair mechanisms are conserved at transcriptional level in the vertebrate model. Based on the finding of this part of the study, therefore, it was decided that the expression profiles of the selected genes would be utilised in the subsequent parts of the study to investigate the occurrence of various forms of sequence alteration in the genome of 5¼ hpf zebrafish (*Danio rerio*) embryos treated with different cryopreservation parameters.

3.3.4 Validation of the expression stability of *ACTB* and *EF1 alpha* in 5¼ hpf zebrafish (*Danio rerio*) embryos treated with different cryopreservation parameters

The raw data from qRT-PCR requires normalisation against an endogenous invariant control gene in order to account for sample to sample variations, which may be introduced during RNA purification, cDNA synthesis, dilutions and pipetting or from variations in the enzyme activities. To normalize the raw data from qRT-PCR, a second set of PCR reactions is carried out for the endogenous control gene on all experimental samples. The abundance value of the target gene is divided by that of the endogenous control gene and the normalized values for different samples thus can be directly compared. An ideal endogenous control gene would be a gene that is co-expressed with the target gene and is not transcriptionally altered by the specific experimental conditions. Housekeeping genes (HKGs), so called for their key roles in cellular processes, are thought to be expressed at constant levels, and therefore, are commonly used as endogenous controls in qRT-PCR. However, recent studies have shown that the expression levels of HKGs are not always stable and no single gene has a constant level

under all experimental conditions (Jain et al, 2006; Wan et al., 2011; Du et al., 2013). Using as an endogenous control, a HKG, which is affected by the experimental conditions, would yield misleading results. Therefore, it is necessary to validate the expression stability of a HKG under the experimental conditions prior to using it as an endogenous control. In a study carried out to validate a number of HKGs for their potential use as endogenous controls in qRT-PCR, Lin et al., (2009) has shown that the expression levels of *ACTB* and *EF1 alpha* remain stable in the chilled and cryopreserved blastomere cells from zebrafish (*Danio rerio*) embryos. Guided by the findings of Lin et al, (2009) the HKGs, *ACTB* and *EF1 alpha*, were chosen as the potential endogenous controls for qRT-PCR analysis in the current study. The objective of this experiment was to validate the expression stability of *ACTB* and *EF1 alpha* in the embryos treated with different cryopreservation parameters.

3.3.4.1 Experimental designs

3.3.4.2 Stability of *ACTB* and *EF1 alpha* expression in the chilled embryos

Total RNAs from 5¼ hpf zebrafish embryos chilled for 0, 30, 60 and 120 minutes were extracted using the method described in section 2.4.3.1. Concentration and purity of the extracted RNA were determined using the method described in section 2.4.3.3. Concentrations of RNA across the samples were made the same by diluting the samples, where necessary. RNA from each treated group was converted to cDNA using the method described in section 2.4.3.4. cDNA was then subjected to PCR reaction for the amplification of *ACTB* and *EF1 alpha* using primers specific for the respective genes according to the method described in section 2.4.3.8. A standard curve was generated using the known concentration series of the amplified cDNA. The absolute concentration of the respective gene transcript was then determined from the standard curve. To evaluate the expression stability, the data was then normalised against the non-treated control (0 min).

3.3.4.3 Stability of *ACTB* and *EF1 alpha* expression in the embryos treated with MeOH and Me_2SO

Total RNAs from 5¼ hpf zebrafish (*Danio rerio*) embryos treated with 1M, 2M and 3M MeOH for 30 minutes, and 1M, 1.5M, and 2M Me_2SO for 30 minutes were extracted using the method described in section 2.4.3.1. Concentration and purity of the extracted RNA were determined using the method described in section 2.4.3.3. Concentrations of RNA across the samples were made the same by diluting the samples. The RNA was then converted to cDNA and the genes were amplified as per method described in sections 2.4.3.4 and 2.4.3.8. Evaluation of the expression stability of the genes was then carried out according to the method described in section 3.3.4.2.

3.3.4.4 Stability of *ACTB* and *EF1 alpha* expression in the embryos cooled to -35°C

Total RNAs were extracted from the 5¼ hpf zebrafish embryos cooled to -35°C using 2M MeOH and 1.5M Me_2SO, separately, using the method described in section 2.4.3.1. Evaluation of the expression stability of *ACTB* and *EF1 alpha* was carried out as per the method described in section 3.5.1.2.

3.3.4.5 Results

3.3.4.5.1 Analysis of PCR efficiency

Following amplification of the HKGs, *ACTB* and *EF1 Alpha*, in the embryos subjected to the experimental conditions of the study, the amplification efficiency and the correlation coefficient were determined from the standard curves (Figure 3.10) generated from the serial dilutions of cDNA (Figure 3.11). The efficiency and correlation coefficient of the amplification of the genes under all experimental conditions were within the acceptable range of 0.99 and 0.7 to 1.1, respectively (Pfaffl, 2004). The melt curve analysis of the amplicons showed a single peak for each of the gene amplified indicating that the primers were specific for the genes and there was no contamination in the PCR reactions (Figure 3.12).

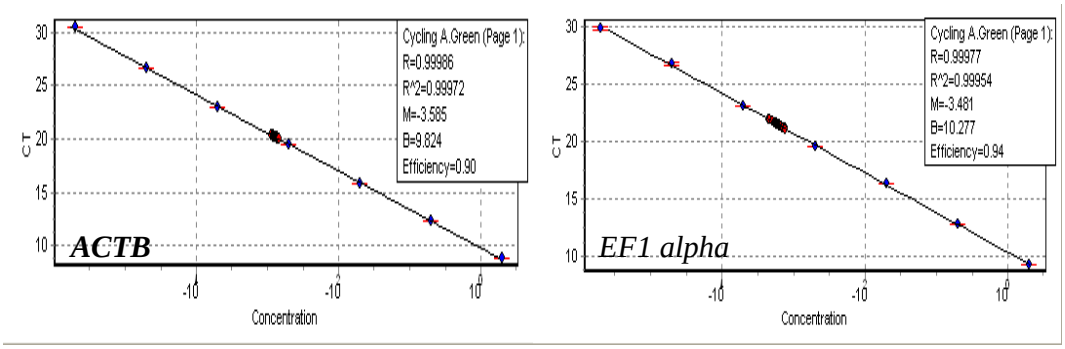

Figure 3.15: Example of standard curves for *ACTB* and *EF1 alpha*. Mean ± SEM Ct values were plotted against the log concentration of 10-fold dilutions of cDNA. Each standard curve had an R^2 value > 0.99 due to an equal number of cycles separating standards of 10-flod dilution concentration difference. Each curve had an efficiency value within acceptable range of 0.7 and 1.1 (Pfaffl 2004).

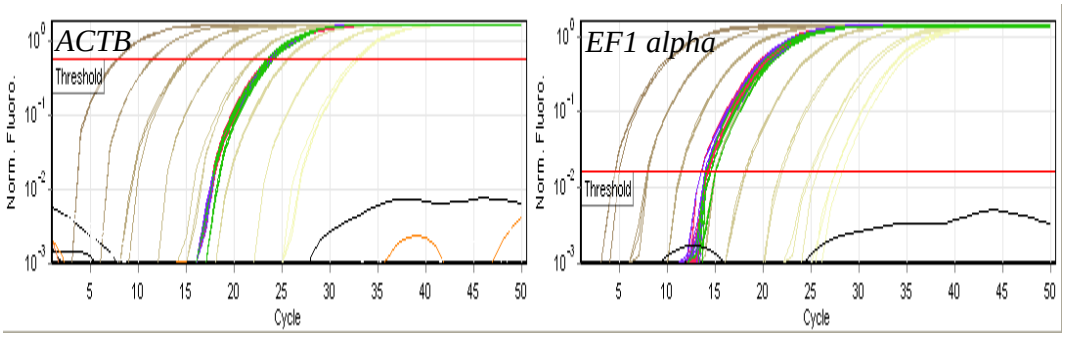

Figure 3.16: Example of fluorescence measurement of *ACTB* and *EF1 alpha*. Fluorescence graphs showing fluorescence measurements obtained for standards (brown), negative control (light blue and orange) and other colours related to embryos samples.

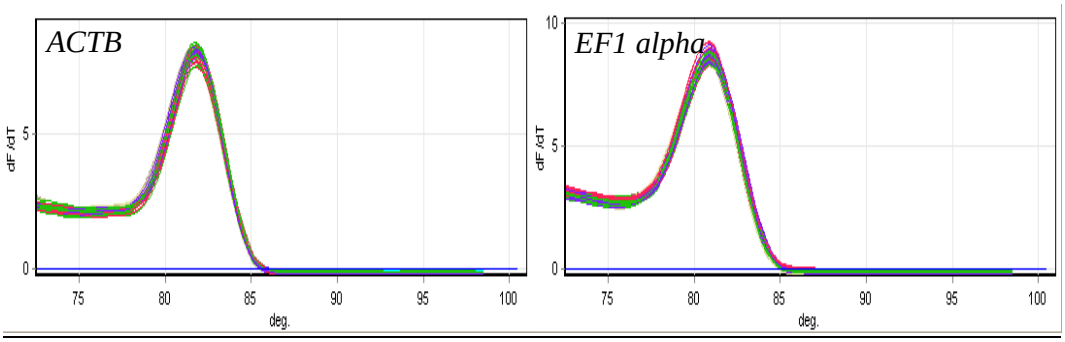

Figure 3.17: Example of melting curve profile for *ACTB* and *EF1 alpha*. Standard (brown), negative control (light blue) and samples (other colours. All samples produced a single melting peak indicating that the samples had no contamination, mispriming and primer-dimers.

3.3.4.5.2 Expression of *ACTB* and *EF1 alpha* remained stable in the chilled embryos

Comparison of the expression profiles of *ACTB* and *EF1 alpha* in the 5¼ hpf zebrafish embryos chilled at 0C for 30, 60, 120 minutes to those in the fresh embryos (0 min) shows that the expression of the genes were not significantly ($p<0.05$) affected by chilling (Figure 3.13 A and B).

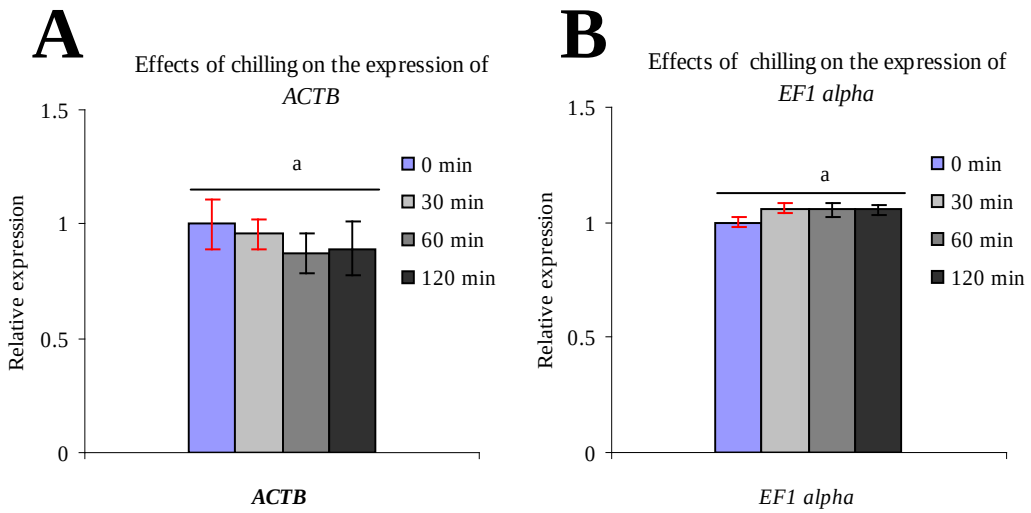

Figure 3.18: Expression of *ACTB* and *EF1 alpha* was not affected by chilling. Graphical presentation of the expression profiles of *ACTB* (A) and *EF1 alpha* (B) in the embryos chilled for different periods. **5¼** hpf zebrafish (*Danio rerio*) embryos were chilled at 0˚C for 30, 60 and 120 min. Total RNAs were extracted from each treated group and a group of fresh embryos and converted to cDNA from which *ACTB* and *EF1 alpha* were amplified and quantified using qRT-PCR. Values shown are mean-/+ SEM of the expression level relative to that in the fresh embryos. Different letter indicates statistically significant ($p<0.05$) difference among the groups being compared.

3.3.4.5.3 Expression of *ACTB* and *EF1 alpha* remained stable in the embryos incubated in MeOH

The expression of *ACTB* and *EF1 alpha* in the 5¼ hpf zebrafish embryos incubated in 1M, 2M, and 3M MeOH for 30 min was not significantly ($p<0.05$) different from that in the fresh embryos (0 min) (Figure 3.14 A and B)

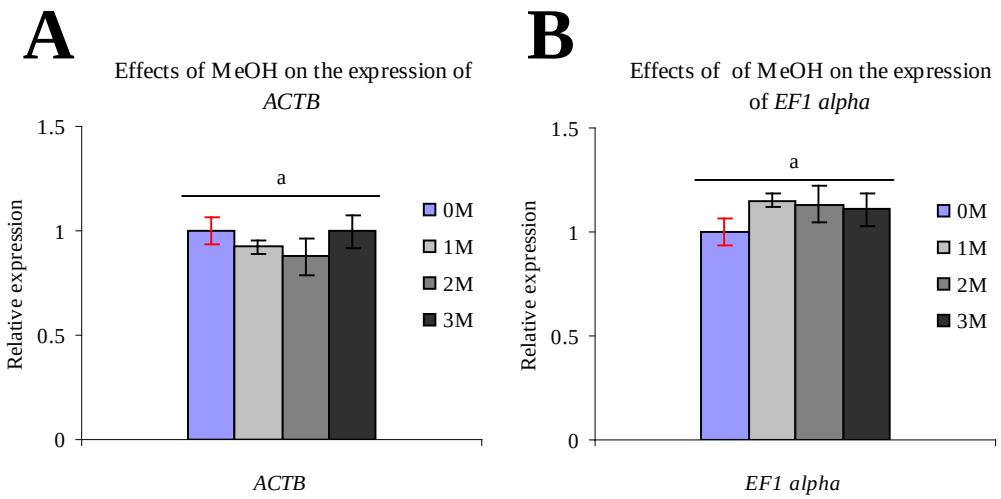

Figure 3.19: Expression of *ACTB* and *EF1 alpha* was not affected by MeOH incubation. Graphical presentation of the expression profiles of *ACTB* (A) and *EF1 alpha* (B) in the embryos treated with MeOH. 5¼ hpf zebrafish (*Danio rerio*) embryos were incubated with 1M , 2M and 3M MeOH for 30 min. Total RNAs were extracted from each treated group and a group of fresh embryos and converted to cDNA from which *ACTB* and *EF1 alpha* were amplified and quantified using qRT-PCR. Values shown are mean-/+ SEM of the expression levels relative to that in the fresh embryos. Different letters indicate statistically significant ($p<0.05$) difference among the groups being compared.

3.3.4.5.4Expression of *ACTB* and *EF1 alpha* remained stable in the embryos incubated in Me_2SO

The expression profiles of *ACTB* and *EF1 alpha* in the embryos incubated with different concentrations of Me_2SO was not significantly different from those in the non-treated (0M) embryos (Figure 3.15 A and B).

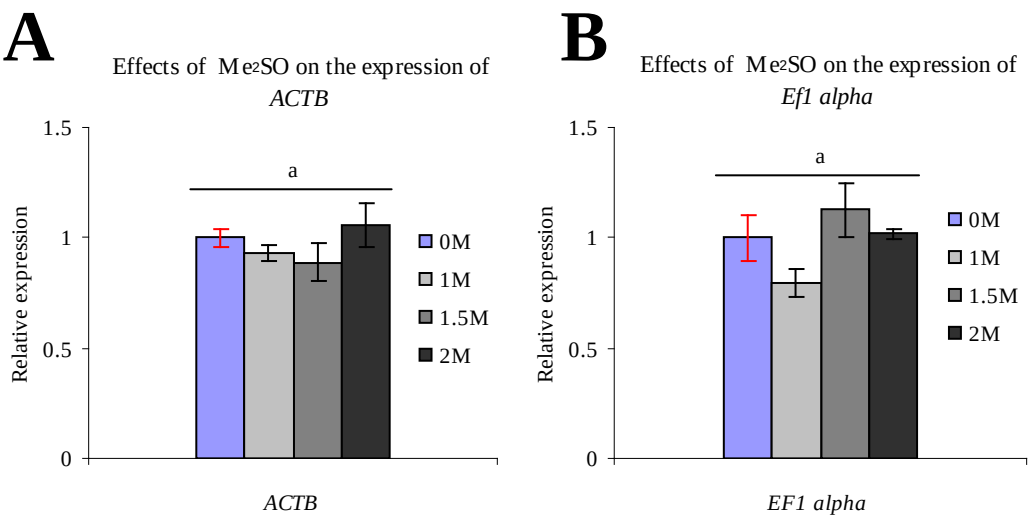

Figure 3.20: Expression of *ACTB* and *EF1 alpha* was not affected by Me_2SO incubation. Graphical presentation of the expression profiles of *ACTB* (A) and *EF1 alpha* (B) in the embryos treated with different concentrations of Me_2SO. 5¼ hpf zebrafish (*Danio rerio*) embryos were incubated in 1M, 1.5M and 2M Me_2SO for 30 min. Total RNAs were extracted from each treated group and a group of fresh embryos and converted to cDNA from which *ACTB* and *EF1 alpha* were amplified and quantified using qRT-PCR. Values shown are mean-/+ SEM of the expression levels relative to that in the fresh embryos. different letters indicate statistically significant ($p<0.05$) difference among the groups being compared.

3.3.4.5.5Expression of *ACTB* and *EF1 alpha* remained stable in the frozen embryos

The expression profiles of *ACTB* and *EF1 alpha* in the **5¼** hpf zebrafish embryos cooled to -35C using MeOH and Me_2SO as CPAs were not significantly ($p>0.05$) different from those in the fresh embryos (Figure 3.16 A and B).

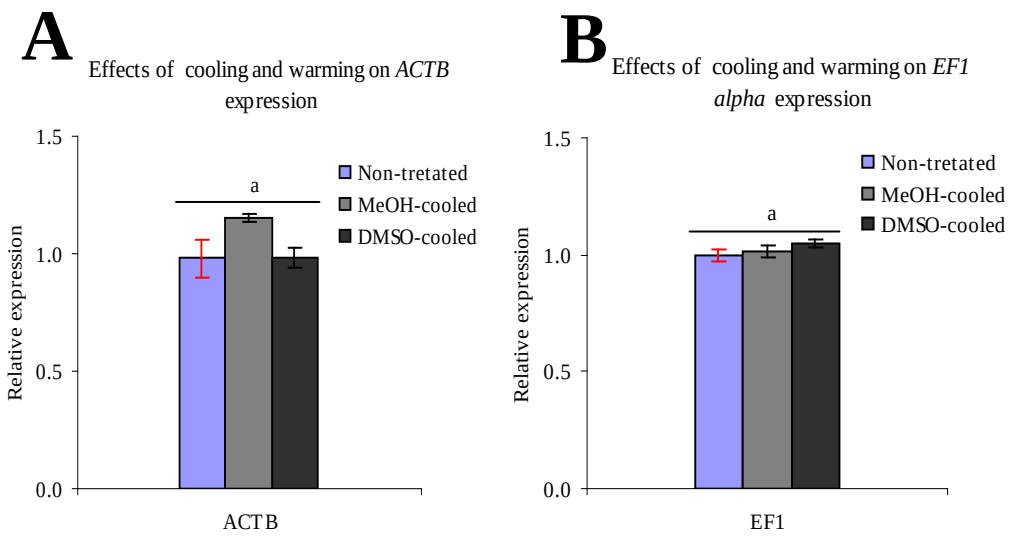

Figure 3.21: Expression of *ACTB* and *EF1 alpha* was not affected by cooling to -35°C. Graphical presentation of the expression profiles of *ACTB* (A) and *EF1 alpha* (B) in the embryos cooled to **-35°C.** 5¼ hpf zebrafish (*Danio rerio*) embryos were cooled to **-35°C** using MeOH and Me_2SO as CPAs. Total RNAs were extracted from each treated group and a group of fresh embryos and converted to cDNA from which *ACTB* and *EF1 alpha* were amplified and quantified using qRT-PCR. Values shown are mean-/+ SEM of the expression levels relative to that in the fresh embryos. different letters indicate statistically significant ($p<0.05$) difference among the groups being compared.

3.3.4.6 Discussion

Normalisation to a stable endogenous control gene adds to the reliability of the data for profiling gene expression using qRT-PCR. However, normalisation against a gene that is affected by the experimental conditions would significantly skew the data resulting in incorrect conclusion being drawn. HKGs are widely used as endogenous control gene in relative gene expression analysis using qRT-PCR. There was a misconception circling among the scientific community that the expression of a HKG is stable irrespective of the experimental conditions. In recent years, the misconception has been eliminated through findings a large number of studies that showed that there is not a single gene that is stable in all experimental conditions (Jain et al, 2006; Wan et al., 2011; Du et al., 2013). The findings of these studies also called for an appropriate validation of a gene before it can be utilised as an endogenous control. Guided by the study of Lin et al, (2009), the HKGs, *ACTB* and *EF1 alpha* were chosen as endogenous control genes for the current study. However, recognising the significance and legitimacy of the call from the growing number of studies for validating the stability of the endogenous control gene, the

expression stability of the selected HKGs under the experimental conditions of the current study was validated. It was observed that the expression levels of the genes were slightly affected by the experimental conditions (Figure 3.13-3.16). However, the observed variations were considered negligible as the expression levels of the genes in the embryos under experimental conditions were not significantly different ($p>0.05$) from those in the non-treated embryos. It is evident from the findings that the HKGs, *ACTB* and *EF1 alpha*, could be utilised as endogenous control genes for the expression analysis of the genes of the ERMs under the experimental conditions of the current study.

3.4.5 Summary

In this part of the study a number of parameters that contribute to successful Western blot detection of proteins of interest were empirically optimised. The optimisation work in this part of the study led to the development of a novel method that efficiently eliminated non-specific binding inherent to streptavidin-biotin detection system. The optimised Western blot protocol was then utilised to validate the use of S*/T*Q antibody to detect the activation of ATM and ATR in 5¼ hpf zebrafish (*Danio rerio*) embryos. It was found that the S*/T*Q antibody detected a number of activated DDR proteins and one deactivated DDR protein in the embryos treated with DSB-inducing drug camptothecin. Since DSB-initiated DDR is mediated by ATM, the finding indicated that the DDR proteins affected by camptothecin-induced DSBs were the downstream substrates of ATM rather than that of ATR. Moreover, one of the DDR proteins activated in camptothecin-treated embryos corresponded to the molecular weight of Chk2 (62 kDa) which is a substrate specific for ATM. The S*/T*Q antibody also successfully detected an activated DDR protein and a deactivated DDR protein in the embryos treated with SSB-inducing chemical H_2O_2. As SSB-activated DDR is mediated by ATR, the finding indicated that the DDR proteins affected in H_2O_2-treated embryos were substrates of ATR. However, in the H_2O_2-treated embryos no protein corresponding to the molecular weight of ATR-specific substrate Chk1 was detected, indicating that ATR-mediated DDR, in terms of the downstream substrates involved, may not be thoroughly conserved in 5¼ hpf zebrafish (*Danio rerio*) embryos. Nevertheless, the pattern of DDR proteins affected in the H_2O_2-treated embryos was distinctively different from that of the DDR proteins in the camptothecin-treated embryos, which indicated the S*/T*Q antibody could be utilised to distinguish between the activation of ATM and ATR, and thereby, to distinguish between the events of DSBs

and SSBs in the genome. This part of the study showed that the genes selected from the individual ERMs were expressed in zebrafish 5¼ hpf zebrafish (*Danio rerio*) embryos, and therefore, an analysis of the expression profiles of the genes could be utilised to investigate the occurrence of the types of sequence alteration repaired by the proteins encoded by the respective genes. This part of the study also showed that the expression levels of *ACTB* and *EF1 alpha* remained stable under all of the experimental conditions of the current, and therefore, the HKGs could be utilised as endogenous control genes in the expression analysis of the genes of the ERMs in the subsequent parts of the study.

CHAPTER 4: EFFECTS OF CHILLING ON THE GENOME OF 5¼ hpf ZEBRAFISH (*Danio rerio*) EMBRYOS

4.1 Introduction

Chilled storage is an effective method for preserving biological objects for limited period of time when cryopreservation is not feasible. In aquaculture, chilled storage is routinely used to facilitate transportation of biological objects from facility to facility and even from country to country for research purposes (Komrakova and Holtz, 2009). However, biological objects are known to be sensitive with varying degrees to the chilling temperature. It has been shown that chilling temperature caused protein denatauration in mulberry (Ukaji et al., 1999) and tomato (Sabehat et al., 1998), leakage of solutes from liposome (Hays et al., 2001), increased endogenous ROS formation in plant cells (Tsang et al., 1991, Prasad, 1996) and apoptosis in Burkitt lymphoma cells (Gregory and Milner, 1994). In a recent study, chilling temperature has also been shown to decrease the expression of two transcription factors, *Sox2* and *Sox3*, in zebrafish (*Danio rerio*) embryos (Desai et al., 2011).

Despite the accumulated evidence regarding the damaging effects of chilling temperature, no study has been carried out to investigate the effects of chilling temperature in the context of the occurrence of DSBs, SSBs or sequence alteration in the genome of a biological object. Sensitivity to chilling temperature has also been identified as one of the limiting factors to successful cryopreservation of biological objects (Valdez et al, 2005). In controlled slow cooling cryopreservation, which is the most commonly used cryopreservation method, biological objects are cooled slowly from the physiological temperatures to the seeding temperature at which ice formation is manually induced. It is a common knowledge that biological objects are sensitive to this temperature shift (Zhang and Rawson, 1995; Valdez et al, 2004). The sensitivity of the biological objects to the decreasing temperature during controlled slow cooling satisfies the common definition of the chilling injury (Pollard and Leibo, 1994), as used in this study. Therefore, an investigation into the effects of short-term chilling on the genome will also help understanding the chilling injury sustained by biological objects during controlled slow cooling cryopreservation. Moreover, the sensitivity of a biological object to the chilling temperature appears to correlate with its sensitivity to cooling temperature (Pollard and

Leibo, 1994). Understanding the nature of the injury sustained by biological objects during short-term chilling, therefore, will also shed some light on the nature of the injury sustained during cooling.

In these perspectives, the experimental work presented in this part of the study were undertaken to investigate the effects of short-term chilling on the genome of 5¼ hpf zebrafish (*Danio rerio*) embryos in terms of the occurrence of DSBs, SSBs, and various forms of sequence alteration.

4.2 Experimental design

4.2.1 Investigation of the effects of chilling on the hatching of 5¼ hpf zebrafish (*Danio rerio*) embryos

The experimental work in this part of the study began with the investigation of the effects of different chilling periods on the survival of 5¼ hpf zebrafish (*Danio rerio*) embryos. Four groups of 30 embryos were chilled at 0˚C for 0, 30, 60, and 120 minutes according to the method described in section 2.3.1. Following chilling, the embryos were incubated at 28±1˚C in E2 for 5 days. At the end of the 5-day period, the embryo survival was assessed using the method described in section 2.4.1.

4.2.2 Investigation of the occurrence of DSBs and SSBs in the genome of 5¼ hpf zebrafish (*Danio rerio*) embryos chilled for different time points

5¼ hpf zebrafish embryos in groups of 120 were chilled at 0C for 0, 30, 60, and 120 minutes according to the method described in section 2.3.1. Following chilling, total proteins were extracted from each treated group of the embryos using the method described in section 2.4.2.2. 40 µg of total proteins from each group of embryos and DSB^- and DSB^+ embryo lysates was resolved in SDS-PAGE and blotted onto PVDF membrane using the methods described in sections 2.4.2.4 and 2.4.2.5, respectively. The membrane was then probed according to the method described in section 2.4.2.8. Data analysis was carried out using the method described in section 2.4.2.9.

Investigation of the occurrence of SSBs in the genome of the chilled embryos was carried out by analysing the phosphorylated proteins detected in the blot against the activation and deactivation pattern of DDR proteins in the SSB^{+} 5¼ hpf zebrafish (*Danio rerio*) embryo lysate.

4.2.4 Investigation of the occurrence of various forms of sequence alteration in the genome of 5¼ hpf zebrafish (*Danio rerio*) embryos chilled for different time points

5¼ hpf zebrafish embryos in groups of five were chilled at 0°C for 0, 30, 60, and 120 minutes. Following chilling treatment, total RNAs were extracted from each group of embryos using the method described in section 2.4.3.1 and converted cDNA using the method described in section 2.4.3.4. The cDNA was then subjected to PCR reaction to amplify the genes selected from the individual ERMs using the method described in section 2.4.3.8. The expression profiles of each of the genes were then generated using the method described in section 2.4.3.9

4.3 Results

4.3.1 Short-term chilling did not affect the hatching of 5¼ hpf zebrafish (*Danio rerio*) embryos

In this experiment, the effect of chilling temperature on the survival of 5¼ hpf zebrafish embryos was investigated. The mean value of the hatching rates of three replicates were plotted against the exposure times to chilling temperature and presented in figure 4.1. The result showed that chilling at 0°C for 30, 60, and 120 minutes did not have significant ($p>0.05$) effect on the hatching rates of the embryos compared to that of the 0 minute control (referred to as non-treated control hereafter) (Figure 4.1).

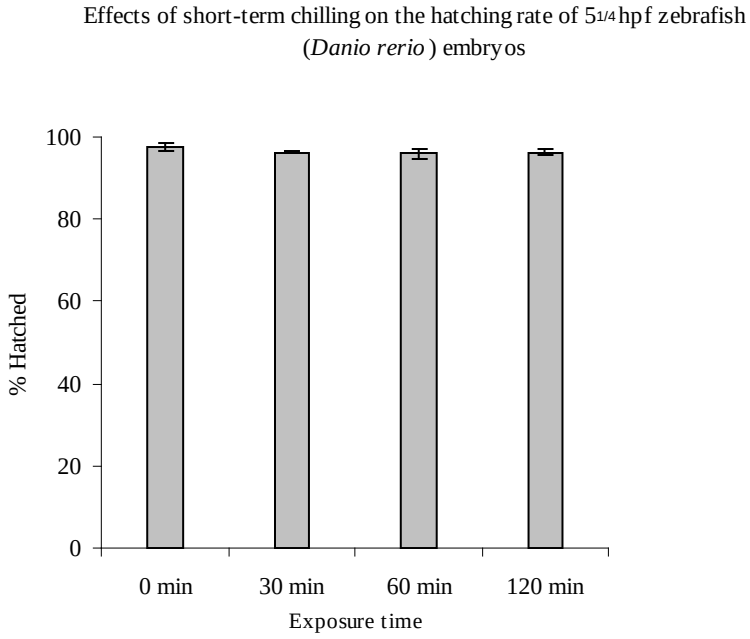

Figure 4.1: Short-term chilling did not affect the hatching of the 5¼ hpf zebrafish (*Danio rerio*) embryos. (A) Graphical presentation of the hatching rates of 5¼ hpf zebrafish (*Danio rerio*) embryos chilled at 0°C for 30, 60, and 120 minutes. Values shown are mean +/- SEM of the hatching rates from three independent experiments. Different letters, where appropriate, indicate statistically significant ($p<0.05$) difference among the groups being compared.

4.3.2 Short-term chilling did not affect the expression of DSB-affected or SSB-affected DDR proteins in 5¼ hpf zebrafish (*Danio rerio*) embryos

Representative Western blot together with the analysis of phosphorylation and dephosphorylation pattern of DDR proteins detected in DSB^+ 5¼ hpf zebrafish (*Danio rerio*) embryos, SSB^+ 5¼ hpf zebrafish (*Danio rerio*) embryos, and in 5¼ hpf zebrafish (*Danio rerio*) embryos chilled for different time points are presented in figure 4.2. It was apparent from the analysis that the chilling treatment did not affect the expression of DSB-affected or SSB-affected DDR proteins in 5¼ hpf zebrafish (*Danio rerio*) embryos. In the event of DSBs in the genome of 5¼ hpf zebrafish (*Danio rerio*) embryos, the proteins p38 and p150 are hypophosphorylated and dephosphorylated, respectively, whereas, the proteins p22, p31, p34, p62, p100 are phosphorylated. On the other hand, in the event of SSBs in the genome of 5¼ hpf zebrafish (*Danio rerio*) embryos, the protein p38 is hyperphosphorylated and the protein p150 is dephosphorylated (Figure 4.2 C, refer to section 3.3.2 for details). In the current experiment, the S*/T*Q antibody successfully detected the hypo-phosphorylation of the p38 protein, de-phosphorylation of the p150 protein and the phosphorylation of the proteins p22, p31, p34, p62, p100 in the DSB^+ 5¼ hpf zebrafish (*Danio rerio*) embryos relative to the DSB^- 5¼ hpf zebrafish (*Danio rerio*) embryos (Figure 4.2 A and B). However, none of the proteins phosphorylated in the DSB^+ embryos was phosphorylated in 5¼ hpf zebrafish (*Danio rerio*) embryos chilled for different time points. Moreover, the p150 protein was found phosphorylated in the non-treated (0 minute) and chilled 5¼ hpf zebrafish (*Danio rerio*) embryos; and the normalised intensity of phosphorylation of the protein in the chilled embryos was not significantly ($p>0.05$) different from that in the non-treated embryos (Figure 4.2 D). Similarly, the p38 protein was also found phosphorylated in the non-treated and chilled 5¼ hpf zebrafish (*Danio rerio*) embryos (Figure 4.2 A); and there was no significant ($p>0.05$) difference in the normalised intensity of phosphorylation of the protein in the chilled embryos relative to that in the non-treated embryos (Figure 4.2 D).

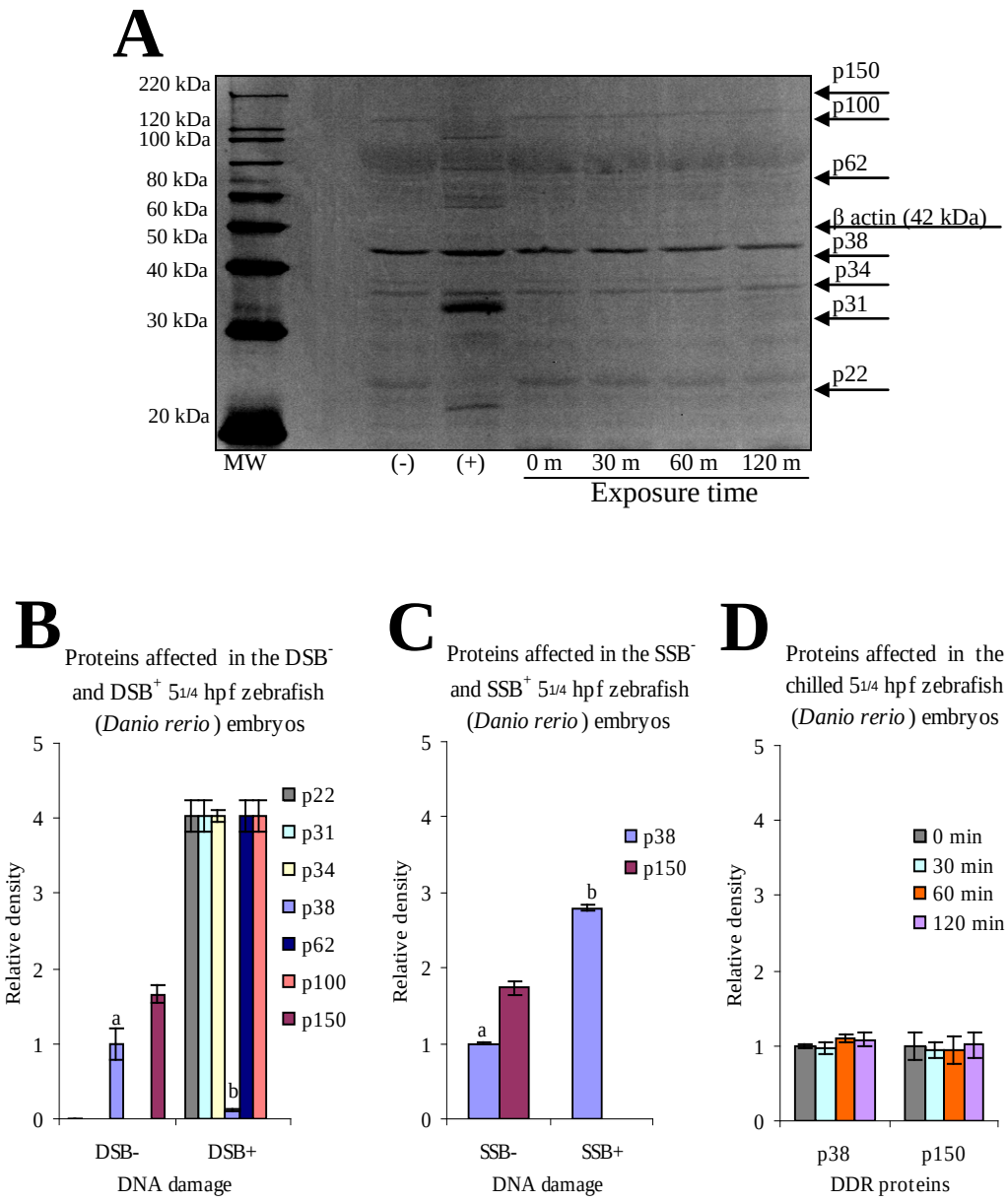

Figure 4.2: DSB-affected and SSB-affected DDR proteins were not affected in 5¼ hpf zebrafish (*Danio rerio*) embryos chilled for time points (A) Representative blot of three independent experiments. 5¼ hpf zebrafish (*Danio rerio*) embryos were chilled at 0˚C for 0, 30, 60, and 120 minutes. Total proteins were extracted from each treated group and probed alongside DSB^- and DSB^+ embryo lysates with anti-S*/T*Q and anti-β-*actin* simultaneously. *β actin* served as a control for variations in protein loading. **(B)** Graphical presentation of the intensity of phosphorylation of the proteins detected in the $DSB^-$and DSB^+ embryos. Values shown are mean +/- SEM of β-*actin* normalised band intensities obtained from three replicates and presented as relative to those in the DSB^- lysate **(C)** Graphical presentation of the intensity of phosphorylation of the proteins affected in the $SSB^-$and SSB^+ embryos. Values shown are mean +/- SEM of β-*actin* normalised band intensities obtained from three replicates and presented as relative to those in the SSB^- embryos. (**D**) Graphical presentation of the intensity of phosphorylation of the proteins detected in the embryos chilled at 0˚C for different time points. Values shown are mean +/- SEM of β-*actin* normalised band intensities obtained from three replicates and presented as relative to those in the non-treated embryos (0 min). Different letters, where appropriate, indicate statistically significant ($p<0.05$) difference among the groups being compared. MW represents MagicMark™ XP Western protein standards (Invitrogen, LC5602).

4.3.3 Short-term chilling affected the expression in 5¼ hpf zebrafish (*Danio rerio*) embryos of the *MSH2* gene from the MMR mechanism

4.3.3.1 Analysis of PCR efficiency

The expression profiles of the genes encoding proteins with critical functions in BER, NER and MMR were investigated by relative gene expression analysis using qRT-PCR. Following PCR amplification, the amplification efficiency and correlation coefficient for each gene amplified were determined from the standard curves derived from the fluorescence measurements of the amplification products of a 10-fold dilution series of the cDNA for the corresponding genes. The amplification efficiency and correlation coefficient for each gene were within the acceptable range, 0.7 to 1.1 (Pfaffl, 2003). In addition, at the end of the amplification reaction for each gene, melt curve analysis was performed to check for the primer specificity and to rule out any primer-dimer formation. The melt curve analysis shows that the amplicons for each of the genes generated a single peak indicating a single product and no contamination.

4.3.3.2 Expression level of the *MSH2* gene from the MMR mechanism was increased in 5¼ hpf zebrafish (*Danio rerio*) embryos chilled for 120 minutes

After monitoring the amplification efficiency and the specificity of the primer, the raw data generated was processed using Rotor-Gene 600 analytical software to carry out relative gene expression analysis. The mRNA levels of each gene was normalised against the expression levels of *ACTB* and *EF1-alpha*, the two endogenous controls selected for the current study. The mean of two normalised values were then plotted against the exposure times to chilling temperature and presented in figure 4.3. The results showed that the expression level of *MSH2* was increased as the chilling period increased, with the expression level in the embryos chilled for 120 minutes becoming significantly different from that in the non-treated control (Figure 4.3 D). No significant difference was noticed in the expression levels of *ERCC1*, *UDG*, and *TDG* in the chilled embryos relative to those in the non-treated control (Figure 4.3 B, C, and D).

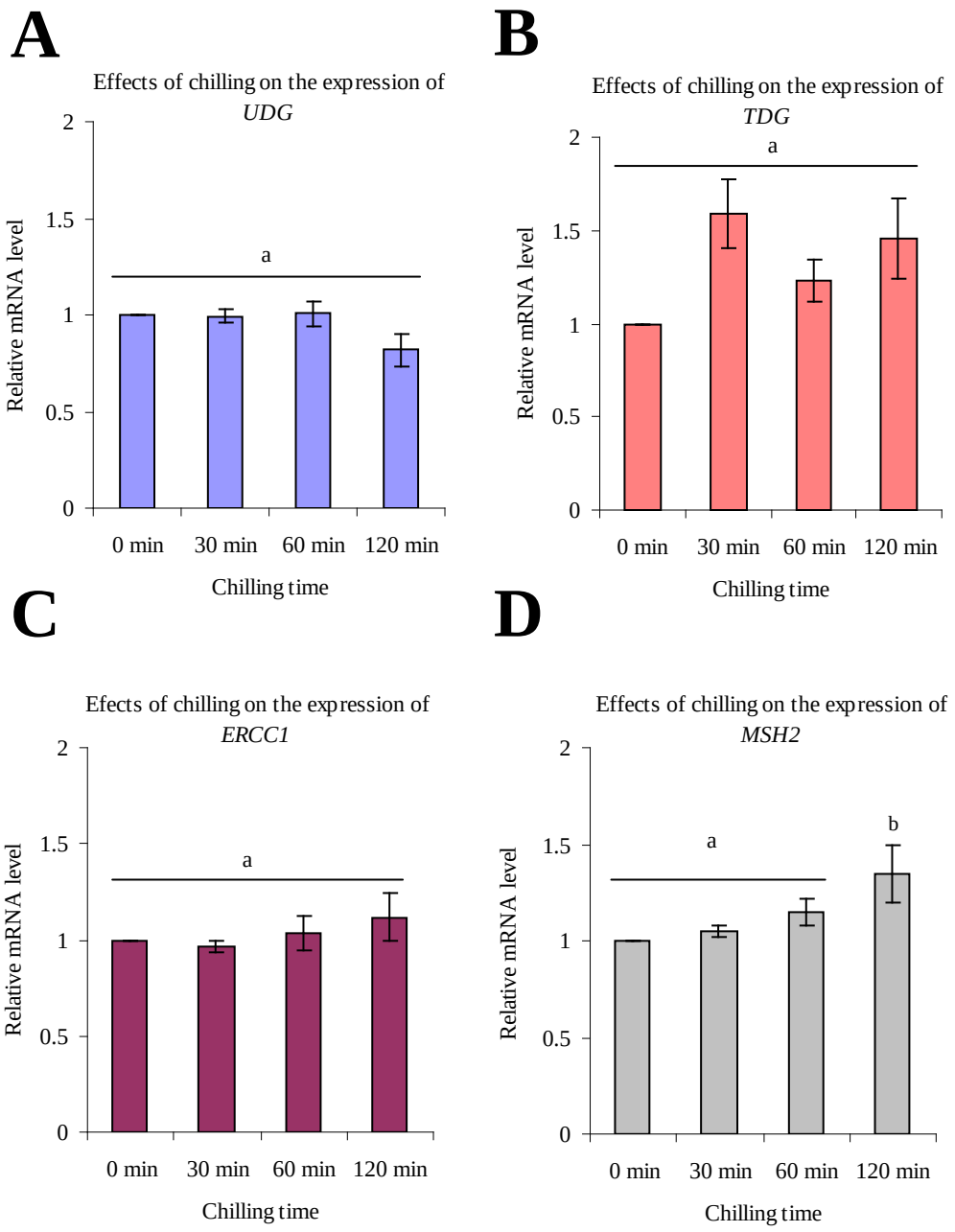

Figure 4.3: Short-term chilling affected the expression of the *MSH2* gene from the MMR mechanism. Graphical presentation of the expression profiles of the gene *UDG* **(A)**, the gene *TDG* **(B)** the gene *ERCC1* **(C)**, and the gene *MSH2* **(D).** Total RNA from the embryos chilled for different time points extracted, converted to cDNA, from which the genes of interest were amplified in qRT-PCR using the gene-specific primers. Values shown are mean +/- SEM of the *ACTB* and *EF1 alpha*-normalised expression levels of the genes obtained from three independent replicates and presented as relative to those in the corresponding non-treated embryos. Different letter indicates statistically significant (p>0.05) difference among the groups being compared.

4.4 Discussion

4.4.1 Short-term chilling did not have any effect on the survival of $5^{1}/_{4}$ hpf zebrafish (*Danio rerio*) embryo

Assessment of the hatching rate is a widely used method for investigating the effects of experimental conditions on embryos. It provides useful information about the effects of a specific experimental condition on the development of an organism. Severe DNA damage such as DSBs, if left un-repaired, is lethal for an organism. A cell with persistent DSBs usually dies after few cell cycles (Cox et al., 2012). Therefore, in a developing embryo, in which the cells are continuously dividing such DNA damage will result in the death of the organism. DNA damage in the form of various mutations can also result in cell death when the alteration occurs in the genes encoding proteins with critical functions in essential metabolic process such as replication. As discussed earlier in chapter 1, chilling temperature is capable of causing increased endogenous ROS (Scandallios, 1993; Tsang et al, 1991), which are a potential source of severe DNA damage (Wood and Youle, 1995). As part of the investigation into the effects of short-term chilling on the genomic DNA, the present study assessed the hatching rates of 5¼ hpf zebrafish (*Danio rerio*) embryos. It was found that short-term chilling did not have any significant effect on the survival of 5¼ hpf zebrafish embryos (Figure 4.1). The finding of this part of the study is in line with that of the study of Desai et al., (2011), which showed that short-term chilling of 5¼ hpf zebrafish embryos for up to 180 minutes did not affect the hatching rates of the embryos. However, the finding of this part of the current study is in contrast with that of the study of Valdez et al, (2004), which showed that short-term chilling resulted in reduced hatching rates of medaka (*Oryzias latipas*) embryos.

Although the hatching rate is an effective method of assessing the survival of embryos of specific experimental conditions, it fails to provide information about the events taking place at the molecular level. Therefore, it is not possible to rule out the possibility of severe DNA damage during short-term chilling based on hatching rate alone. The short-term chilling conditions used in this part of the study might have caused severe DNA damage, which might have been repaired with the passage of time leading to successful hatching of the embryos. Moreover, other forms of DNA damage, such SSBs and various mutations, which do not affect the survival of an organism, but affect the quality of survival, can not be ruled out either.

4.4.2 Short-term chilling did not cause the occurrence of DSBs or SSBs in the genome of 5¼ hpf zebrafish (*Danio rerio*) embryos

Zebrafish (*Danio rerio*) embryos possess a very competent DDR (discussed in chapter 1 in detail) and the teleost embryos can repair most forms of DNA damage if provided with an appropriate recovery time. Since the objective of this part of the study was to investigate if short-term chilling causes the occurrence of DSBs in the genome, total proteins from the embryos were extracted immediately at the end of the respective chilling treatment and probed for the DSB-affected DDR proteins.

As discussed in chapter 3, in the event of DSBs in the genome of 5¼ hpf zebrafish (*Danio rerio*) embryos, the p38 and p150 proteins are down-regulated and deactivated via dephosphorylation, respectively, probably to facilitate cell cycle arrest, whereas, the p22, p31, p34, p62, p100 proteins are activated via phosphorylation probably to facilitate both cell cycle arrest and repair of the damage. The pattern of down-regulation, deactivation and activation of DDR proteins characteristic of the occurrence of DSBs in the genome of 5¼ hpf zebrafish (*Danio rerio*) embryos was maintained in the DSB^{+} embryos in this experiment too (Figure 4.2 A), which confirmed that the S*/T*Q antibody was still sensitive against the ATM/ATR substrate motif. However, none of the DDR proteins activated in the DSB^{+} embryos was activated in the chilled embryos (Figure 4.2 A and D). Moreover, the p150 protein, which is deactivated in the event of DSBs in the genome of the embryos, remained activated in the chilled embryos, and the expression level of the p38 protein, which is down-regulated in the event of DSBs in the genome of the embryos, remained at the baseline level in the chilled embryos. The findings of this part of the study indicate that the DSB-activated kinase ATM was not activated in the embryos chilled for different time points. Based on the finding of this part of the study, therefore, it can be concluded that the short-term chilling conditions did not cause the occurrence of DSBs in the genome of 5¼ hpf zebrafish (*Danio rerio*) embryos.

DSBs are not the only form of DNA damage that compromises the genetic integrity of a biological object. Persistent SSBs are also detrimental to the genome of biological objects. However, unlike DSBs, SSBs are not lethal to biological objects. These single stranded lesions are usually readily repaired in a cell capable of generating a DDR (Grafstrom et al., 1984; O'connell et al., 2010). Nevertheless, since most of the eukaryotic DNA repair mechanisms are error prone (Dinant et al., 2008; Cox et al., 2012), SSB

repair may also lead to various mutations being introduced into the genome. As discussed in chapter 3, in the event of SSBs in the genome of 5¼ hpf zebrafish (*Danio rerio*) embryos, the p150 protein is deactivated probably to facilitate cell cycle arrest, whereas, the p38 protein is hyper-activated probably to facilitate the repair of the damage. However, as discussed above, this part of the study found that in 5¼ hpf zebrafish (*Danio rerio*) embryos chilled for different time points, the p150 protein was not deactivated and the p38 protein was not hyper-activated. The findings indicate that the chilling conditions did not cause increased occurrence of SSBs in the genome of 5¼ hpf zebrafish (*Danio rerio*) embryos.

The findings of this part of the study suggest that the chilling step involved in the controlled slow cooling cryopreservation may also not cause the occurrence of DSBs or SSBs in the genome of 5¼ hpf zebrafish (*Danio rerio*) embryos.

4.4.3 Short-term chilling caused increased occurrence of mismatched based in $5^1/_4$ hpf zebrafish (*Danio rerio*) embryos

The findings that the short-term chilling conditions did not cause the occurrence of DSBs or SSBs in the genome of 5¼ hpf zebrafish (*Danio rerio*) indicate that the occurrence of any form of mutation secondary to the repair of DSBs and SSBs is unlikely in such embryos. However, chilling temperature has been shown to increase the endogenous ROS formation (Tsang et al., 1991, Prasad, 1996). Since ROS can alter the genetic code by chemically modifying the DNA bases (Cooke et al, 2003), the findings that chilling conditions used in this part of the study did not cause DSBs or SSBs in the genome of 5 ¼ hpf zebrafish (*Danio rerio*) embryos do not rule out the possibility of the occurrence of various sequence alterations independent of DSB and SSB repair. As discussed earlier in chapter 1 and chapter 3, the ERMs, namely, the BER, the NER and the MMR mechanisms, are responsible for correcting any post replication alteration in the genome. This part of the study investigated indirectly the effect of the chilling conditions in terms of the occurrence of various forms of sequence alteration in the genome by quantifying the expression levels of four genes, namely, *MSH2* from the MMR, *ERCC1* from the NER, *UDG* and *TDG* from the BER mechanisms. An up-regulation of a gene from a particular repair pathway was regarded as an indication of an increased occurrence of the sequence alteration corrected by the pathway. It was found that chilling at 0°C for 120

minutes significantly increased the expression level of *MSH2* in 5¼ hpf zebrafish (*Danio rerio*) embryos (Figure 4.3 D). The finding indicates that the MMR mechanism was up-regulated in such embryos. As discussed in chapter 1, the MMR mechanism is responsible for correcting mismatched bases in the replicated DNA. Therefore, the finding that the MMR was up-regulated in 5¼ hpf zebrafish (*Danio rerio*) chilled for 120 minutes suggests that the chilling condition caused an increased occurrence of mismatched bases in the genome of the embryos. However, it was also found that chilling of 5¼ hpf zebrafish (*Danio rerio*) embryos for 30 and 60 minutes did not affect the expression of the genes of ERMs. During slow cooling cryopreservation biological objects are exposed to chilling temperature for a limited period of time, which rarely exceeds 30 minutes. Therefore, the finding suggests that the chilling step involved in controlled slow cooling cryopreservation may not cause increased occurrence of sequence alteration in the genome of 5¼ hpf zebrafish (*Danio rerio*) embryos. This is the first study to investigate the effects of short-term chilling on the genes of the ERMs. By the same token, this is also the first study to indicate that the short-term chilling could cause an increase in the occurrence of mismatched base pairing in the genome of biological objects.

4.5.6 Summary

This is the first study to investigate the effects of short-term chilling on the genome of 5¼ hpf zebrafish (*Danio rerio*) embryos in the context of the occurrence of DSBs, SSBs and various forms of sequence alteration. In this part of the study, it was found that chilling at 0˚C for 30, 60, and 120 minutes did not cause DSBs or SSBs in the genome of 5¼ hpf zebrafish (*Danio rerio*) embryos. However, it was also found that chilling at 0˚C for 120 minutes up-regulated the MMR mechanism in 5¼ hpf zebrafish (*Danio rerio*) embryos, which indicates that the embryos were susceptible to an increased occurrence of mismatched bases in the genome. Nevertheless, the overall findings in this part of the study suggest that the chilling step involved in controlled slow cooling cryopreservation may not cause increased occurrence of DSBs, SSBs or sequence alteration in the genome of 5¼ hpf zebrafish (*Danio rerio*) embryos.

Treatment of biological with a CPA of choice is the first step in controlled slow cooling cryopreservation. However, CPAs are also known to have detrimental effects on

biological objects. Therefore, in the next part of the study, the effects of the different concentrations of two CPAs, namely, MeOH and Me_2SO, on the genome of 5¼ hpf zebrafish (*Danio rerio*) embryos were investigated by utilizing the methods developed and validated in the previous part of the study (chapter 3).

This work is being prepared for publication

CHAPTER 5: INVESTIGATION OF THE EFFECTS OF CPA TREATMENT ON THE GENOME OF 5 ¼ hpf ZEBRAFISH (*Danio rerio*) EMBRYOS

5.1 Introduction

CPAs are added to the cryopreservation solution to counteract the harmful effects sustained by biological objects during chilling and cooling. How CPAs exert the protective effect is discussed in chapter 1 in detail. It is a well established fact that all CPAs, in concentrations adequate to protect, have some harmful effects, too, as manifested in relatively reduced survival rates of the CPA-treated biological objects. It was thought that CPAs damage biological objects mainly via osmotic stress (Mazur and Sceider, 2006). It has also been shown that CPAs bind to the phospholipids in the bilayer membrane causing structural disorientation (Hotlemans, 2001, Lindhi 2001). CPAs have been implicated in protein denaturation too (Arakawa et al, 1990). However, emerging evidence indicates that CPAs may cause direct biochemical injury to the genome of the biological object in question (Rajaei et al, 2005, Rajaei et al, 2006, Tasdemir et al, 2013). Nevertheless, the exact mechanism by which CPAs exert the harmful effects is yet to be fully characterised.

Before a CPA can be added to the cryopreservation solution, the optimum concentration of the CPA that does not result in toxic effect on cells is empirically determined. However, the conventional methods of assessing the toxicity of CPAs fall short of giving insights into the mechanism of damage. For example, Trypan blue staining and FDA+PI staining, two of the most commonly used methods to assess CPA toxicity, are based on membrane integrity. These methods utilise membrane integrity as an indication of cell viability. However, the membrane integrity does not rule out the possibility of damage at the molecular level. It has been shown that CPA treatment results in increased DNA fragmentation in porcine blastocysts (Rajaei et al, 2005, Rajaei et al, 2006) and in Eastern Anatolian red bull sperm (Tasdemir et al, 2013). Therefore, a cell can sustain damage to its genome from CPA toxicity and depending on the extent of the damage may survive with an intact membrane, in which case the conventional method would fail to detect such damage. However, Rajaei et al, (2005) and Tasdemir et al, (2013) have used TUNEL assay and Comet assay, respectively, to detect DNA fragmentations. Reliability of both of the techniques has been called into question for the reasons described in chapter 1. With

that perspective, the experimental works described in this part of the study were undertaken to investigate the effects of CPA treatment on the genome of 5¼ hpf zebrafish (*Danio rerio*) in the context of the occurrence of DSBs, SSBs and various forms of sequence alteration utilising the methods developed and optimised previously, as described in chapter 3.

To carry out the investigation, two permeable CPAs, namely, MeOH and Me_2SO have been chosen to treat the embryos with. MeOH and Me_2SO have been shown to be ideal CPAs for zebrafish (*Danio rerio*) embryos (Zhang et al, 1993), blastomeres (Lin et al, 2009), and ovarian follicles (Tsai et al, 2009). MeOH and Me_2SO at 2M and 1.5M concentrations, respectively, have been shown to have no significant effect on blastomeres cells derived from 5¼ hpf zebrafish (*Danio rerio*) embryos (Lin et al., 2009). Guided by the finding of Lin et al., (2009), the embryos were treated in this part of the study with three concentrations of the CPAs, namely, 1M, 2M, and 3M of MeOH and 1M, 1.5M and 2M of Me_2SO, spanning the optimum concentrations mentioned above.

5.2 Experimental designs

All experiments were carried out three times unless stated otherwise

5.2.1 Investigation of the effects of MeOH and Me_2SO on the hatching of 5¼ hpf zebrafish (*Danio rerio*) embryos

The experimental work for this part of the study was initiated by investigating the effects of the CPAs on the survival of the embryos. Four groups of 30 embryos were incubated in 0, 1, 2, and 3M MeOH according to the method described in section 2.3.2. Treatment of the embryos with 1, 1.5 and 2M Me_2SO was carried out in the same way. Following CPA incubation, the embryos were washed to remove the CPA and left incubating at 28±1°C for 5 days. At the end of the 5-day period, the embryo survival was assessed in terms of the hatching rate using the method described in section 2.4.1.

5.2.2 Investigation of the occurrence of DSBs and SSBs in the genome of 5¼ hpf zebrafish (*Danio rerio*) embryos treated with MeOH and Me_2SO.

5¼ hpf zebrafish (*Danio rerio*) embryos in groups of 120 were treated with 0, 1, 2, and 3M MeOH, and 0, 1, 1.5 and 2M Me_2SO according to the method described in section 2.3.2. Following CPA treatment, total proteins were extracted from each treated group of the embryos using the method described 2.4.2.2. The extracted proteins were then resolved alongside DSB^- and DSB^+ embryo lysates in SDS-PAGE and blotted onto PVDF membrane using the methods described in sections 2.4.2.4 and 2.4.2.5, respectively. The membrane was then probed for DSB-affected DDR proteins using the method described in section 2.4.2.8. Finally, the data analysis was carried out using densitometry as described in section 2.4.2.9.

Investigation of the occurrence of SSBs in the genome of 5¼ hpf zebrafish (*Danio rerio*) embryos treated with different concentrations of MeOH and Me_2SO was carried out by analysing the proteins detected in the blots against the DDR proteins affected in 5¼ hpf zebrafish (*Danio rerio*) embryos in response to the occurrence of SSBs in the genome.

5.2.3 Investigation of the occurrence of various forms of sequence alteration in the genome of 5¼ hpf zebrafish (*Danio rerio*) embryos treated with the CPAs

5¼ hpf zebrafish embryos in groups of five were treated with 0, 1, 2, and 3M MeOH and 0, 1, 1.5 and 2M Me_2SO according to the method described in section 2.3.2. Following CPA treatment, total RNAs were extracted from the embryos using the method described in section 2.4.3.1 and converted to cDNA using the method described in section.2.4.3.4. The cDNA was then subjected to PCR reaction to amplify the genes of the excision repair mechanisms using the method described in section 2.4.3.8. The expression profiles of each of the genes were then generated using the method described in section 2.4.3.9.

5.3 Results

5.3.1 MeOH and Me_2SO treatment did not affect the hatching rates of 5¼ hpf zebrafish (*Danio rerio*) embryos

The effects of different concentrations of MeOH and Me_2SO on the hatching of 5¼ hpf zebrafish (*Danio rerio*) are presented in figure 5.1. The results showed that the increased concentrations of both of the CPAs slightly reduced the hatching rates of the embryos. Nevertheless, the hatching rates of the MeOH-treated and Me_2SO-treated embryos were not significantly different from the hatching rates of the respective non-treated embryos (Figure 5.1 A and B).

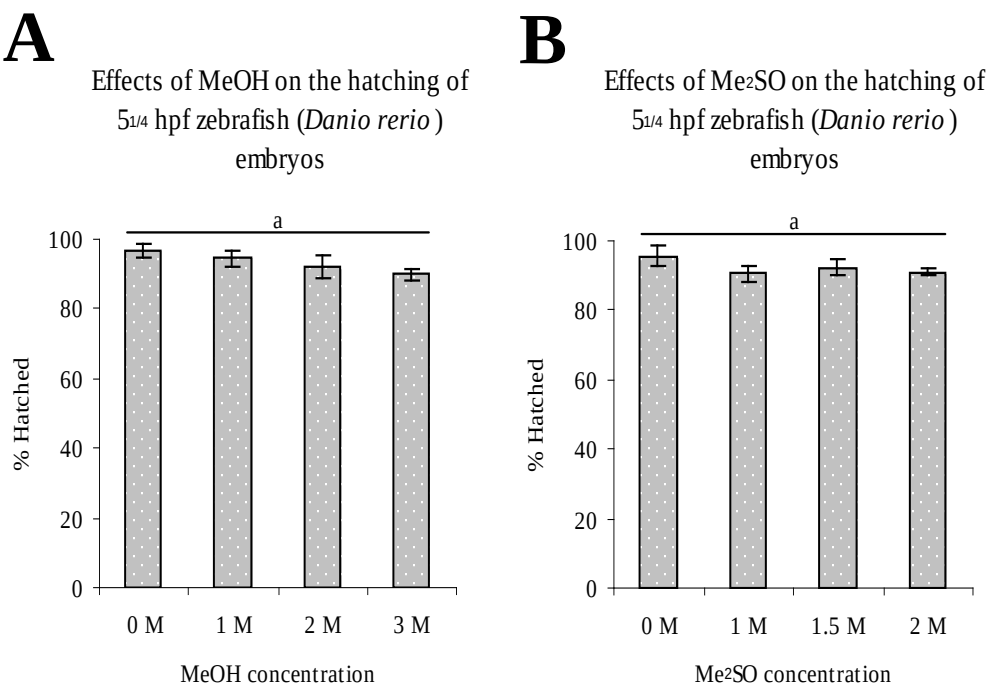

Figure 5.1: MeOH and Me_2SO did not affect the hatching of the $5^1/_4$ hpf zebrafish (*Danio rerio*) embryos. (A) Graphical presentation of the hatching rates of 5¼ hpf embryos incubated for 30 minutes in 0, 1, 2, and 3M MeOH. **(B)** Graphical presentation of the hatching rates of 5¼ hpf embryos incubated for 30 minutes in 0, 1.5 and 2 M Me_2SO. Values shown are mean +/- SEM of the hatching rates obtained from three independent experiments. Different letters, where appropriate, indicate statistically significant ($p<0.05$) difference among the groups being compared.

5.3.2 Investigation of the occurrence of DSBs and SSBs in the genome of 5¼ hpf zebrafish (*Danio rerio*) embryos treated with MeOH and Me_2SO

5.3.2.1 MeOH treatment did not affect the expression of DSB-affected and SSB-affected DDR proteins in 5¼ hpf zebrafish (*Danio rerio*) embryos

The result of the experiment shows that MeOH treatment did not affect the expression of DSB-affected and SSB-affected DDR proteins in 5¼ hpf zebrafish (*Danio rerio*) embryos. The S*/T*Q antibody successfully detected the phosphorylation of the p22, p31, p34, p62, p100 proteins, hypo-phosphorylation of the p38 protein and de-phosphorylation of p150 protein in the DSB^+ embryo lysate relative to the DSB^- embryo lysate (Figure 5.2 A). None of the proteins phosphorylated in the DSB^+ embryos was phosphorylated in the MeOH-treated embryos (Figure 5.2 A). The p150 protein, which dephosphorylated in the DSB^+ embryos (Figure 5.2 B) and SSB^+ embryos (Figure 5.2 C), was found phosphorylated in the non-treated (0M) and MeOH-treated embryos (Figure 5.2 A); and there was no significant difference ($p>0.05$) in the *β actin* normalised intensity of phosphorylation of the protein in the treated embryos relative to that in the non-treated embryos (Figure 5.2 D). In addition, the p38 protein, which was significantly ($p<0.05$) hypo-phosphorylated in the DSB^+ embryos relative to the DSB^- embryos (Figure 5.2 B), and significantly hyperphosphorylated in the SSB^+ embryos relative to the SSB^- embryos (Figure 5.2 C), was found phosphorylated in the non-treated and MeOH-treated embryos (Figure 5.2 A). However, there was no significant difference ($p>0.05$) in the *β actin* normalised intensity of phosphorylation of the protein in the treated embryos relative to that in the non-treated embryos (Figure 5.2 D).

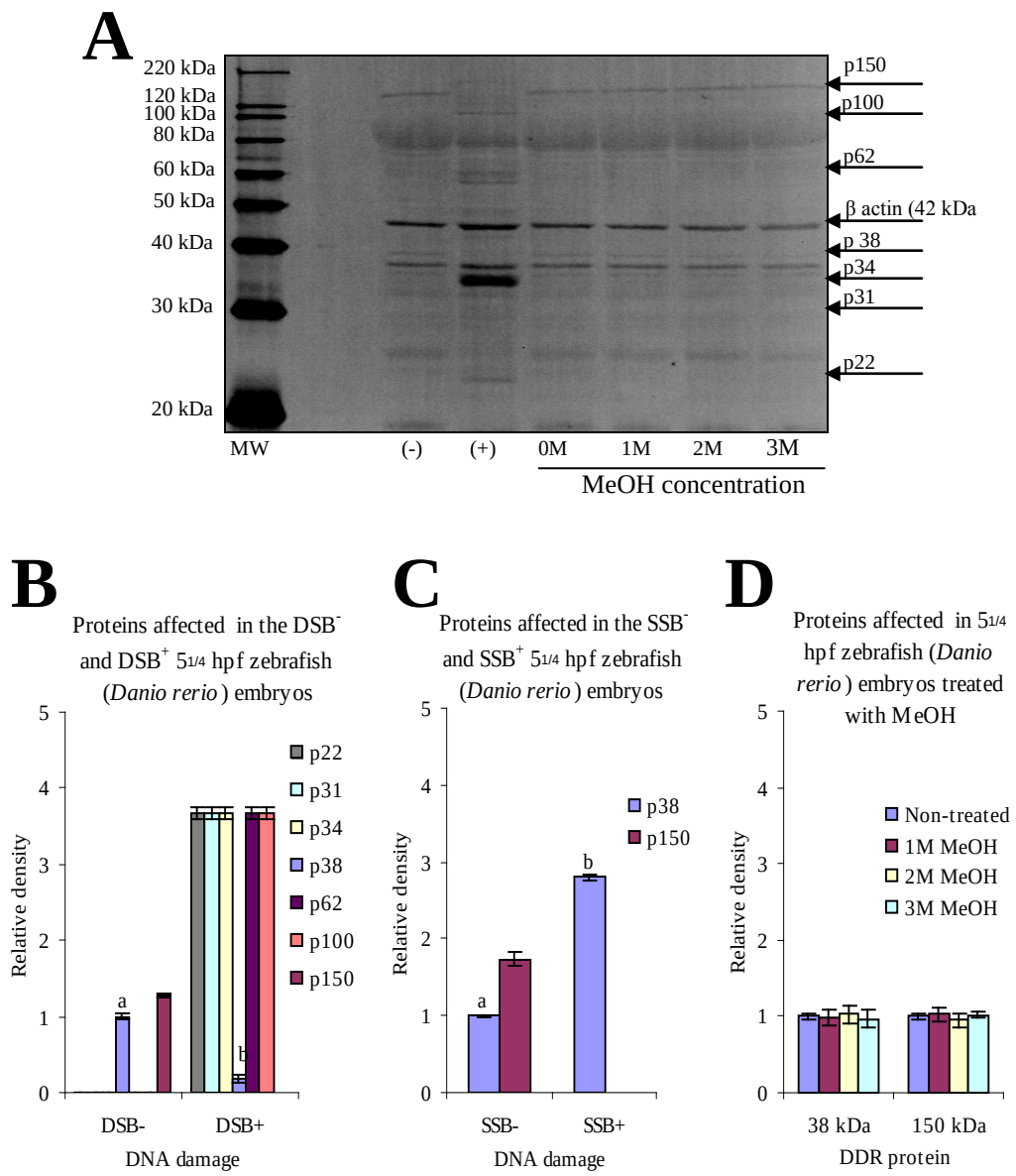

Figure 5.2: DSB-affected and SSB-affected DDR proteins were not affected in 5¼ hpf zebrafish (*Danio rerio*) embryos treated with MeOH. (A) Representative blot of three independent experiments. 5¼ hpf embryos were incubated for 30 minutes in 0, 1, 2, and 3M MeOH. Total proteins were extracted from each treated group and probed alongside DSB^- and DSB^+ embryo lysates with anti-S*/T*Q, and anti-β-*actin* simultaneously. *β actin* served as a control for variations in protein loading. **(B)** Graphical presentation of the intensity of phosphorylation of the proteins detected in the $DSB^-$and DSB^+ embryos. Values shown are mean +/- SEM of β-*actin* normalised band intensities obtained from three replicates and presented as relative to those in the DSB^-embryos **(C)** Graphical presentation of the intensity of phosphorylation of the proteins affected in the $SSB^-$and SSB^+ embryos. Values shown are mean +/- SEM of β-*actin* normalised band intensities obtained from three replicates and presented as relative to those in the SSB^- embryos. **(D**) Graphical presentation of the intensity of phosphorylation of the proteins detected in the lysates prepared from the embryos treated with different concentrations of MeOH. Values shown are mean +/- SEM of β-*actin* normalised band intensities obtained from three replicates and presented as relative to those in the lysate prepared from the non-treated embryos (0M). Different letters, where appropriate, indicate statistically significant ($p<0.05$) difference among the groups being compared. MW represents MagicMark^{TM} XP Western protein standards (Invitrogen, LC5602).

5.3.2.2 Me_2SO treatment did not affect the expression of DSB-affected and SSB-affected DDR proteins in 5¼ hpf zebrafish (*Danio rerio*) embryos

As in the case of MeOH treatment, Me_2SO treatment did not affect the expression of any of the DSB-affected or SSB-affected DDR proteins in 5¼ hpf zebrafish (*Danio rerio*) embryos. The patterns of hypo-phosphorylation, de-phosphorylation and phosphorylation of the DDR proteins in the DSB^- and DSB^+ embryo lysates were replicated in this experiment, too (Figure 5.3 A). None of the DDR proteins phosphorylated in the DSB^+ embryos was phosphorylated in the Me_2SO -treated embryos (Figure 5.3 A). The p150 protein, which was dephosphorylated in the DSB^+ embryos (Figure 5.3 B) and SSB^+ embryos (Figure 5.3 C), was found phosphorylated in the non-treated (0M) and Me_2SO-treated embryos (Figure 5.2 A). Moreover, there was no significant difference ($p>0.05$) in the *β actin* normalised intensity of phosphorylation of the protein in the treated embryos relative to that in the non-treated embryos (Figure 5.3 D). Furthermore, , the p38 protein, which was significantly ($p<0.05$) hypo-phosphorylated in the DSB^+ embryos relative to the DSB^- embryos (Figure 5.3 B), and significantly hyperphosphorylated in the SSB^+ embryos relative to the SSB^- embryos (Figure 5.3 C), remained phosphorylated in the non-treated and Me_2SO-treated embryos (Figure 5.3 A); and there was no significant difference ($p>0.05$) in the *β actin* normalised intensity of phosphorylation of the protein in Me_2SO-treated embryos relative to that in the non-treated embryos (Figure 5.3 D).

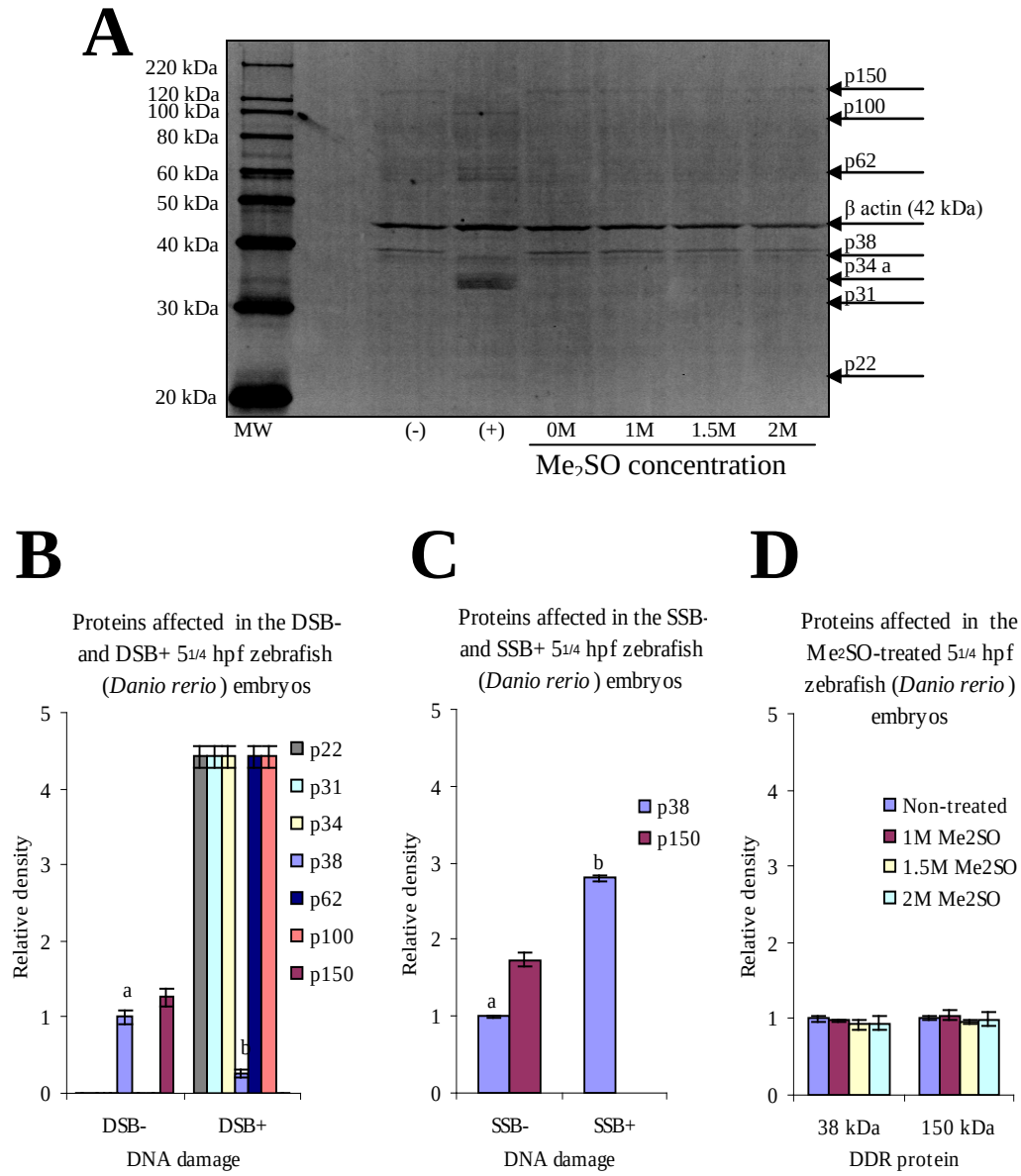

Figure 5.3: DSB-affected DDR proteins were not affected in 5¼ hpf zebrafish (*Danio rerio*) embryos treated with Me_2SO. (A) Representative blot of three independent experiments. 5¼ hpf embryos were incubated for 30 minutes in 0, 1, 1.5 and 2M Me_2SO. Total proteins were extracted from each treated group and probed alongside DSB^- and DSB^+ embryo lysates with anti-S*/T*Q, and anti-β-*actin* simultaneously. *β actin* served as a control for variations in protein loading. **(B)** Graphical presentation of the intensity of phosphorylation of the proteins detected in the $DSB^-$and DSB^+ embryos. Values shown are mean +/- SEM of β-*actin* normalised band intensities obtained from three replicates and presented as relative to those in the DSB^- embryos. **(C)** Graphical presentation of the intensity of phosphorylation of the proteins detected in the $SSB^-$and SSB^+ embryos. Values shown are mean +/- SEM of β-*actin* normalised band intensities obtained from three replicates and presented as relative to those in the SSB^- embryos. **(D)** Graphical presentation of the intensity of phosphorylation of the proteins detected in the lysates prepared from the embryos treated with different concentrations of Me_2SO. Values shown are mean +/- SEM of β-*actin* normalised band intensities obtained from three replicates and presented as relative to those in the lysate prepared from the non-treated embryos (0M). Different letters, where appropriate, indicate statistically significant ($p<0.05$) difference among the groups being compared. MW represents MagicMark™ XP Western protein standards (Invitrogen, LC5602).

5.3.2.3 MeOH treatment affected the expression levels of each of the genes of the ERMs.

Expression profiles of the genes from the individual ERMs in 5¼ hpf zebrafish (*Danio rerio*) embryos treated with different concentrations of MeOH are presented in figure 5.5. The result showed that the relative expression levels of the gene *TDG* from the *TDG*-dependant BER mechanism, *ERCC1* from the NER mechanism and *MSH2* from the MMR mechanism were significantly decreased ($p<0.05$) with the increased concentrations of MeOH (Figure 5.5 B, C and D). The expression levels of the gene *UDG* from the *UDG*-dependant BER mechanism, on the other hand, were initially decreased and then significantly increased ($p<0.05$) amounting to 1.6 fold above the expression level of the gene in the non-treated embryos (Figure 5.5 A).

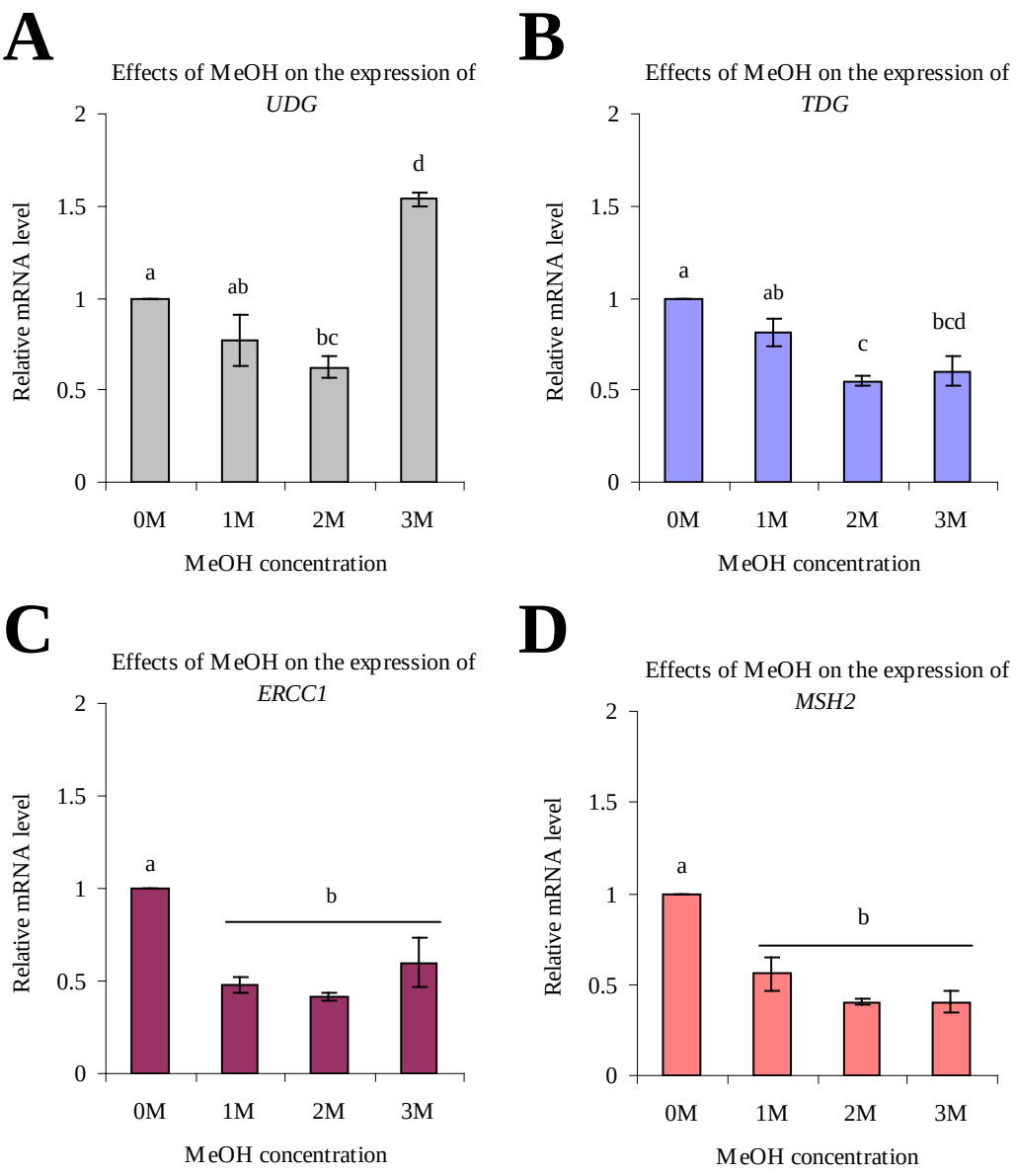

Figure 5.4: Expression levels of the genes from the ERMs were affected in the embryos treated with MeOH. **(A)** Graphical presentation of the expression profiles of the gene *UDG* from the BER mechanism. **(B)** Graphical presentation of the expression profiles of the gene *TDG* from the BER mechanism. **(C**) Graphical presentation of the expression profiles of the gene *ERCC1* from the NER mechanism. **(D)** Graphical presentation of the expression profiles of the gene *MSH2* from the MMR mechanism**.** Values shown are mean +/- SEM of the *ACTB* and *EF1 alpha*-normalised expression levels of the genes obtained from three independent replicates and presented as relative to those in the corresponding non-treated embryos. Different letters, where appropriate, indicate statistically significant ($p<0.05$) difference among the groups being compared.

5.3.2.4 Me_2SO treatment affected the expression levels of each of the genes of the ERMs.

The expression profiles of the genes from the individual ERMs in the Me_2SO-treated embryos were marked by a similar pattern to that observed in the MeOH-treated embryos. The relative expression levels of the gene *TDG* from the *TDG*-dependant BER mechanism, the gene *ERCC1* from the NER mechanism, and the gene *MSH2* from the MMR mechanism were significantly decreased ($p<0.05$) with the increased concentrations of Me_2SO. As in the case of MeOH-treated embryos, the relative expression levels of the gene *UDG* from the *UDG*-dependant BER were decreased initially and then significantly increased ($p<0.05$) resulting in 1.4 fold above the expression level of the gene in the non-treated embryos (Figure 5.5 A).

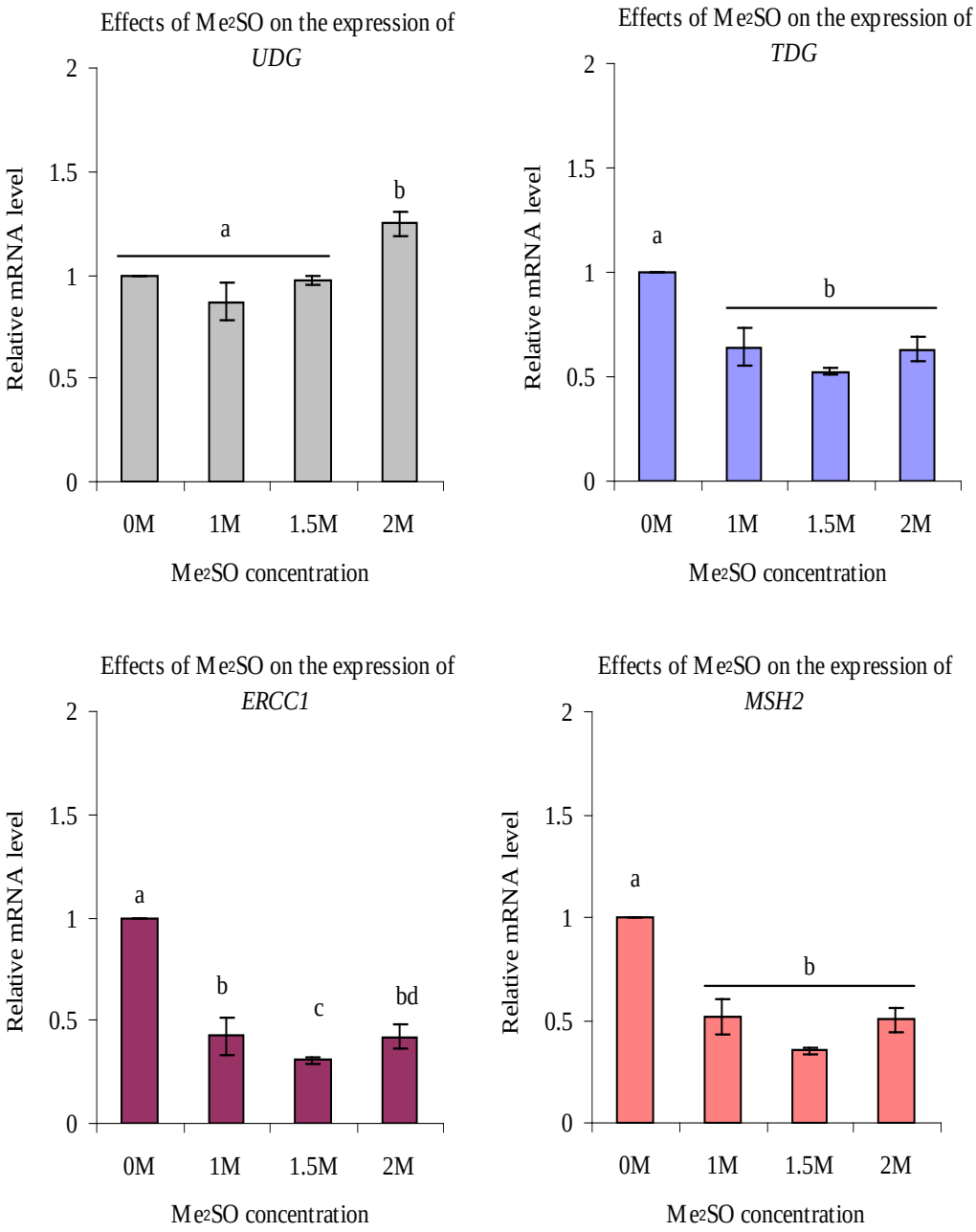

Figure 5.5: Expression levels of the genes from the ERMs were affected in the embryos treated with Me_2SO. **(A)** Graphical presentation of the expression profiles of the gene *UDG* from the BER mechanism. **(B)** Graphical presentation of the expression profiles of the gene *TDG* from the BER mechanism. **(C**) Graphical presentation of the expression profiles of the gene *ERCC1* from the NER mechanism. **(D)** Graphical presentation of the expression profiles of the gene *MSH2* from the MMR mechanism**.** Values shown are mean +/- SEM of the *ACTB* and *EF1 alpha*-normalised expression levels of the genes obtained from three independent replicates and presented as relative to those in the corresponding non-treated embryos. Different letters, where appropriate, indicate statistically significant ($p<0.05$) difference among the groups being compared.

5.4 Discussion

5.4.1 MeOH and Me_2SO treatment did not affect the survival of 5¼ hpf zebrafish (*Danio rerio*) embryos

CPAs have been implicated in the increased DNA fragmentations in biological objects (Rajaei et al, 2005, Tasdemir et al, 2013). As discussed in chapter 1, DNA fragmentation is representative of either increased number of DSBs or the final phase of apoptosis resulting from the increased number of DSBs. Since biological objects sustaining severe DNA damage such as DSBs do not survive longer unless the damage is repaired, an assessment of the survival rate appeared to be an ideal method to investigate the effects of an experimental condition on the genome of the biological objects. To that end, this part of the study investigated the hatching rate as an overall indication of the effects of MeOH and Me_2SO on the genome of 5¼ hpf zebrafish (*Danio rerio*) embryos. The result showed that the CPAs did not affect the survival of the teleost embryos (Figure 5.1). The reason for such finding could be twofold. Firstly, MeOH and Me_2SO treatment at concentrations used did not result in severe damage in the genome of 5¼ hpf zebrafish (*Danio rerio*) embryos, which explains the unaffected hatching rates of the CPA-treated embryos. Alternatively, it is possible that the CPA treatment did result in severe DNA damage but as zebrafish (*Danio rerio*) embryos have a very competent DDR, the damage has been repaired during the development leading to the successful hatching. Since most of the eukaryotic DNA repair mechanisms are known to be error prone, the event of the second scenario would mean that the genome of the teleost embryos would be susceptible to increased occurrence of sequence alteration. In the subsequent experiments, therefore, the effects of the CPAs in terms of different types of DNA damage in 5¼ hpf zebrafish (*Danio rerio*) embryos were investigated by analysing the DDR.

5.4.2 MeOH and Me_2SO treatment did not cause increased occurrence DSBs or SSBs in the genome of 5¼ hpf zebrafish (*Danio rerio*) embryos

As 5¼ hpf zebrafish (*Danio rerio*) embryos have been shown to possess a very competent DDR, the investigation of DSB-mediated DDR was carried out immediately following the treatment of the embryos with the CPAs. The results showed that DSB-affected and SSB-affected zebrafish DDR proteins were not affected in the embryos treated with

MeOH and Me_2SO. The p38 protein, which is down-regulated in the event DSBs and up-regulated in the event of SSBs in the genome of 5¼ hpf zebrafish (*Danio rerio*) embryos, was stable in the embryos treated with both of the CPAs. Similarly, the p150 protein, which is deactivated in the event of both DSBs and SSBs in the genome of 5¼ hpf zebrafish (*Danio rerio*) embryos, remained activated in the embryos treated with the CPAs. Moreover, the proteins p22, p34, p62 and p100, which are activated in the event of DSBs in the genome of 5¼ hpf zebrafish (*Danio rerio*) embryos, were not activated in the embryos treated with the CPAs. The finding indicates that neither the DSB-activated kinase ATM, nor the SSB-activated kinase ATR was activated in the embryos treated with the CPAs. The findings, in the light of the fact that the embryos were not provided with a recovery time for any damage to be repaired, suggest that the CPAs, MeOH and Me_2SO at concentrations used, did not cause DSBs or SSBs in the genome of 5¼ hpf zebrafish (*Danio rerio*) embryos. As discussed earlier, increased occurrence of DSBs may be manifested as DNA fragmentation, and therefore, the finding of this part of the study is in disagreement with those of Rajaei et al, (2005) and Tasdemir et al, (2013), which have linked CPA treatment to increased DNA fragmentation in porcine blastocysts and Eastern Anatolian red bull sperm.

However, DNA damage other than strand breaks, such as various forms of sequence alteration, can not be ruled out based on these findings. As part of the objective of this part of the study, therefore, the effects of the CPAs on the genome of 5¼ hpf zebrafish (*Danio rerio*) embryos in terms of the occurrence of various forms sequence alteration was investigated in the next experiment.

5.4.3 MeOH and Me_2SO affected the expression levels of the genes of the ERMs in 5¼ hpf zebrafish (*Danio rerio*) embryos

As discussed in chapter 1 and chapter 3, the ERMs may provide an overview of the occurrence of various forms of sequence alteration in eukaryotic genome. As part of the investigation of the effects of MeOH and Me_2SO on the genome of 5¼ hpf zebrafish (*Danio rerio*) embryos, this part of the study analysed the expression profiles of the genes selected from the individual ERMs in the CPA-treated embryos. It was found that the gene *UDG* from the *UDG*-dependant BER mechanism was up-regulated in the embryos treated with 3M MeOH and 2M Me_2SO. The finding indicates that the occurrence of

uracil in DNA was increased in the embryos treated with 3M MeOH and 2M Me_2SO. However, it was of great significance to observe that the gene *TDG* from the *TDG*-dependant BER, the gene *ERCC1* from the NER and the gene *MSH2* from the MMR mechanisms were suppressed in the embryos treated with both of the CPAs. The pattern of gene suppression observed in the CPA-treated embryos is similar to that observed following DNA methylation (Choi et el., 2012), which is an epigenetic event responsible for regulating gene transcription to facilitate various metabolic processes such as normal development, X-chromosome inactivation, and genetic imprinting (Robertson and Jones, 2000).

DNA methylation is a covalent chemical modification in which a methyl group (CH_3) is added to the carbon molecule at position 5 in the cytosine ring by a group of enzymes known as *DNA methyltransferases* (DNMTs) (Robertson and Jones, 2000, Das and Singal, 2004, Thaler et al, 2012). Most cytosine methylation occurs in the sequence context ´5CpG´3, in which C denotes a cytosine, p denotes a phosphodiester bond, and G denotes a guanine. Approximately 70% of CpG residues in eukaryotes are epigenetically methylated. The remaining CpG residues occur in or near the transcription start sites, promoters, of 70% of the eukaryotic genes and are known as CpG islands. In normal cells, CpG islands are protected from methylation by mechanisms which are yet to be established. However, it is now evident that the CpG islands can undergo methylation *de novo*, resulting in reduced expression of the gene concerned (Blackledge and Klose, 2011).

Regulation of gene transcription by DNA methylation is accomplished via a number of mechanisms. It has been shown that DNA methylation interferes with the binding of specific transcription factors to their recognition sites in the respective promoters (Singal and Ginder, 1999, Tate and Bird, 1993). DNA methylation has also been shown to facilitate the binding of transcriptional repressors to the promoter regions to prevent gene transcription (Prokhortchouk and Hendrich, 2002, Singal et al, 1997, Singal et al, 2001). It has also been shown that DNA methylation can affect histone modification and chromatin structure to alter gene transcription (Bender et al, 1998). DNA methylation patterns are established during embryogenesis *de novo* via DNMTs and are very tightly controlled during development via an interplay of DNMTs responsible for maintenance methylation and *DNA demethyltransferases* (DNDMTs), enzymes that actively remove CH_3 group from DNA (Bird, 2002, Das and Singal, 2004). An imbalance between the

maintenance methylation and de-methylation may lead to hyper-methylation or hypo-methylation of DNA resulting in abnormal gene transcriptions, which might have been the case in the CPA-treated embryos in this part of the study. Both MeOH and Me_2SO have acidic properties, and therefore, are capable of dissociating to generate free CH_3 groups. In fact, there is evidence regarding the methylating properties of both of the CPAs. Me_2SO has been shown to cause hyper-methylation by increasing the expression of DNMTs in mouse embryonic stem cells (Iwatani et al, 2006). It has also been shown to stimulate the activity if DNMTs *in vitro* (Yokochi and Robertson, 2004). Similarly, MeOH has been to shown to methylate bovine serum albumin, ovalbumin, 20S proteosome (Chen et al, 2010), and benzene (Van Der Mynsbrugge et al, 2012) *in vitro*. Therefore, it is possible that MeOH and Me_2SO stimulated the activity of DNMTs in the embryos by generating free CH_3 groups, which resulted in *de novo* DNA methylation leading to repression of the expression of the genes as observed (Figure 5.4 and 5.5). The up-regulation of *UDG* expression in the embryos treated with 3M MeOH and 2M Me_2SO may be explained by the fact that DNA methylation in eukaryotes is very tightly controlled via the action of DNMTs and DNDMTs. The putative stimulation of DNMTs by MeOH and Me_2SO might have, in turn, stimulated the activity of DNDMTs as a counter mechanism to maintain the homeostasis of methylation. The function of DNDMTs, as mentioned earlier, is to remove CH_3 group from DNA, and the enzyme may not have the ability to distinguish between the native methylated bases and *de novo* methylated bases; removed CH_3 group from cytosine converting it to a uracil resulting in the up-regulation of *UDG* which code for the enzyme responsible for replacing misincorporated uracil from DNA. Nevertheless, the hypothesised DNA methylation by MeOH and Me_2SO needs to be further investigated before a firm conclusion can be drawn.

However, as the ERMs are responsible for maintenance of the genome following replication, suppression of the genes with key roles in the individual ERMs would mean that the activity of the proteins encoded by the genes will also be suppressed resulting in compromised genetic integrity. In this perspective, the findings of this part of the study, irrespective of the mechanism by which the expression of the genes *TDG*, *ERCC1*, and *MSH2* was suppressed, suggests that the CPA-treated embryos were more susceptible to increased occurrence of various forms of sequence alteration in the genome.

5.5 Summary

This is the first study to investigate the effects of MeOH and Me_2SO on the genome of zebrafish (*Danio rerio*) embryos in the context of the occurrence of DSBs, SSBs, and various forms of sequence alteration. This part of the study found that CPA treatment did not cause increased occurrence of DSBs or SSBs in the genome of 5¼ hpf zebrafish (*Danio rerio*) embryos, which is in contrast with those of Rajaei et al, (2005) and Tasdemir et al, (2013), which showed that CPA treatment caused increased DNA fragmentation. This part of the study also clearly showed the shortcoming of the utilisation of embryo survival as a parameter of assessing CPA toxicity. The study found that the survival of the embryos in terms of hatching rate was unaffected following CPA treatment but found CPA treatment to cause up-regulation of the *UDG*-dependant BER mechanism and down-regulation of the *TDG*-dependant BER, the NER and the MMR mechanism indicating an increased occurrence of various forms of sequence alteration in the genome.

In controlled slow cooling cryopreservation, CPA treatment of biological objects is followed by cooling to subzero temperature. Cooling and subsequent warming have been shown to cause various forms of damage to the genetic material of biological objects (discussed in chapter 1 in detail). In the next part of the current study, therefore, the effects of cooling and warming on the genome of 5¼ hpf zebrafish (*Danio rerio*) embryos in terms of the occurrence of DSBs, SSBs and various forms of sequence alteration were investigated.

This work is being prepared for publication.

CHAPTER 6: INVESTIGATION ON THE EFFECTS OF COOLING AND WARMING ON THE GENOME OF 5¼ hpf ZEBRAFISH (*Danio rerio*) EMBRYOS

6.1 Introduction

As discussed in chapter 1 in detail, the damaging effects of cryopreservation on biological objects of are attributed to different cryopreservation parameters such as CPA treatment, chilling, cooling and warming, and thereafter classified as CPA toxicity, chilling injury, and, cooling and warming injury. The injury sustained by biological objects during cooling and warming is thought to result from IIF, which is invariably lethal to cells. In recent years, cryopreservation has also been implicated in various forms of DNA damage. Evidence implicating cryopreservation in DNA damage has been discussed in chapter 1 in detail. Studies have shown that cryopreservation as a whole causes increased mutations in mitochondrial DNA zebrafish (*Danio rerio*) blastomeres cells (Kopeika et al, 2005), and increased DNA fragmentation in equine spermatozoa (Baumber et al, 2003), ram spermatozoa (Peris et al, 2004) and rainbow trout spermatozoa (Perez, 2008). Cryopreservation has also been implicated in the onset of apoptosis in human spermatozoa (Duru et al, 2001), bull spermatozoa (Martin et al, 2004) and equine spermatozoa (Ortega-Ferrusola, 2008).

The experimental works presented in this part of the study was dedicated to investigate the effects of cooling and warming on the genome of 5¼ hpf zebrafish (*Danio rerio*) embryos in the context of the occurrence of DSBs, SSBs and various forms of sequence alteration. The experimental works in this part of the study were carried out in two phases. Since zebrafish embryos have not been successfully cryopreserved to -196°C as yet, there was no protocol available for the current study to cool the teleost embryos to -196°C and thereby carry out the intended investigation. However, in a study carried out by Zhang et al, (1993), the heartbeat stage zebrafish (*Danio rerio*) embryos were cooled to a range of subzero temperatures with relatively good post warming survival rates. In the first phase of the experimental works in this part of the study, a number of parameters of the protocol devised by Zhang et al, (1993) were optimised to cool 5¼ hpf zebrafish (*Danio rerio*) embryos. Using the optimised method, this part of the study succeeded to cool the teleost embryos to -35˚C with a notably improved post warming survival rate than that achieved with the original protocol of Zhang et al., (1993). In the second phase

of the experimental works, the effects of cooling to -35°C and subsequent warming on the genome of 5¼ hpf zebrafish (*Danio rerio*) embryos in terms of the objectives laid out in chapter 1 were investigated by utilising the method devised earlier in the study (discussed in chapter 3).

6.2. Optimisation of the cooling protocol

The experimental work in the first phase began with the application of the protocol devised by Zhang et al, (1993) to cool 5¼ hpf zebrafish (*Danio rerio*) embryos, the test material of the current study. Cooling of 5¼ hpf zebrafish (*Danio rerio*) embryos using the established protocol resulted in relatively a reduced post warming survival rate. Two parameters of the established protocol, namely, warming rate and CPA removal, were then optimised to achieve a significantly higher post warming survival rate.

6.2.1 Application of the established protocol to cool 5¼ hpf zebrafish (*Danio rerio*) embryos.

6.2.1.1 Experimental design

Embryos in groups of 30 were incubated in either 2M MeOH or 1.5M Me_2SO using the method outlined in section 2.3.2. The embryos were then cooled to -10˚C, -15˚C, -20˚C, -25˚C and -30˚C using the protocol outlined in section 2.3.3. Following cooling, the embryos were warmed at a rate of approximately ~300˚C/min in a water bath set at 28±1˚C. After warming, the CPA solution was replaced with E2 and the embryos were incubated at 28±1˚C for 5 days. At the end of the 5-day period, the survival of the embryos was monitored by assessing the hatching rates as described in section 2.4.1.

6.2.1.2 Result

Hatching rates of 5¼ hpf zebrafish (*Danio rerio*) cooled to a range of subzero temperatures using the method devised by Zhang et al, (1993) are presented in Figure 6.1.

Hatching rates of the embryos cooled using MeOH and Me_2SO as the CPAs were significantly decreased ($p<0.05$) with the decreasing cooling temperature relative to that of the corresponding non-treated embryos. Embryos cooled with MeOH did not survive cooling at-30˚C, whereas, those cooled with Me_2SO did not survive cooling at -25˚C and beyond. 5¼ hpf zebrafish (*Danio rerio*) embryos are known to be more sensitive than the embryos at later developmental stages, such as heart beat stage, to subzero temperature (Zhang et al, 1993), which might have been reflected in the relatively reduced post-warming hatching rates, as the cooling method used was devised for the heart beat stage embryos.

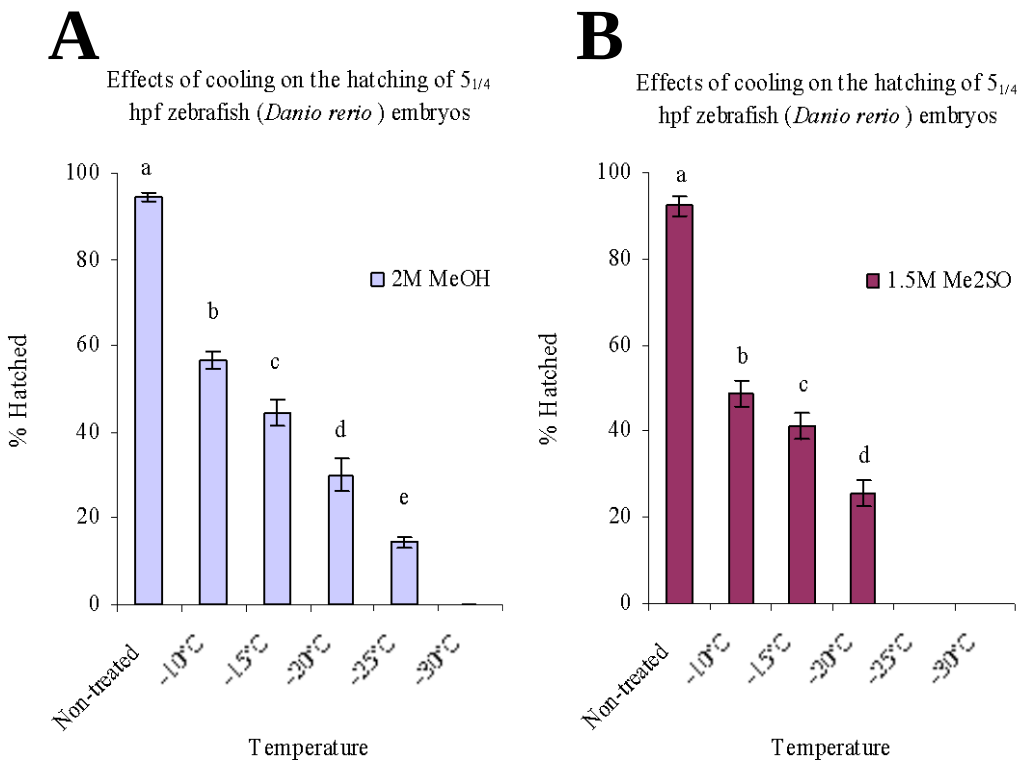

Figure 6.1: The method of Zhang et al, (1993) resulted in relatively reduced hatching of 5¼ hpf zebrafish (*Danio rerio*) embryos. (A) Graphical presentation of the hatching rates of 5¼ hpf embryos cooled with 2M MeOH. **(B)** Graphical presentation of the hatching rates of 5¼ hpf embryos cooled with 1.5M Me_2SO. Values shown are mean +/- SEM of the hatching rates from three independent experiments. Different letters indicate statistically significant difference ($p<0.05$) among the groups being compared.

However, during the course of the current experiment it was noticed that on warming, the embryos were suddenly becoming opaque from being transparent, leading to death. As

discussed in section 1.4 in chapter 1, warming process has significant effects on the survival of the cooled embryos. A relatively slow warming rate for slowly cooled cells results in re-crystallisation of ultramicroscopic ice crystals to form larger ice crystals, which is lethal (Mazur, 1984). Cells may also die from excessive swelling caused by increased water influx during a relatively slow warming process (Mazur, 1984). Hence, slowly cooled cells are usually warmed rapidly to minimise such injuries. However, the optimum warming rate is relative to the biological objects in question. The warming rate, ~300°C/min, used by Zhang et al, (1993) was optimum for the heart beat stage embryos; it might not have been optimum for 5¼ hpf embryos. Therefore, in the subsequent experiment, the effects of a relatively faster warming rate of approximately 425°C/min on the survival of the cooled embryos were investigated.

6.2.2 Optimisation of warming rate

6.2.2.1 Experimental design

Embryos in groups of 30 were incubated in either 2M MeOH or 1.5M Me2SO using the method described in section 2.3.2. The embryos were then cooled to -10˚C using the protocol outlined in section 2.3.3. Following cooling, one group of the embryos was warmed at a rate of ~300˚C/min. The second group of embryos was warmed at a relatively faster rate of ~425˚C/min in a water bath set at 37˚C. Following warming, CPA solution was replaced with E2 and the embryos were incubated at 28±1˚C for 5-days. At the end of the 5-day period, the survival of the embryos was monitored by assessing the hatching rates as described in section 2.4.1.

6.2.2.2 Result

Effects of two warming rates on the hatching of 5¼ hpf zebrafish (*Danio rerio*) cooled to -10˚C using 2M MeOH and 1.5M Me_2SO as CPAs, respectively, are compared in figure 6.2. The relatively rapid warming rate of ~425˚C/min significantly improved ($p<0.05$) the hatching rate of the embryos cooled with both MeOH and Me_2SO (6.3.1.2 A and B, respectively).

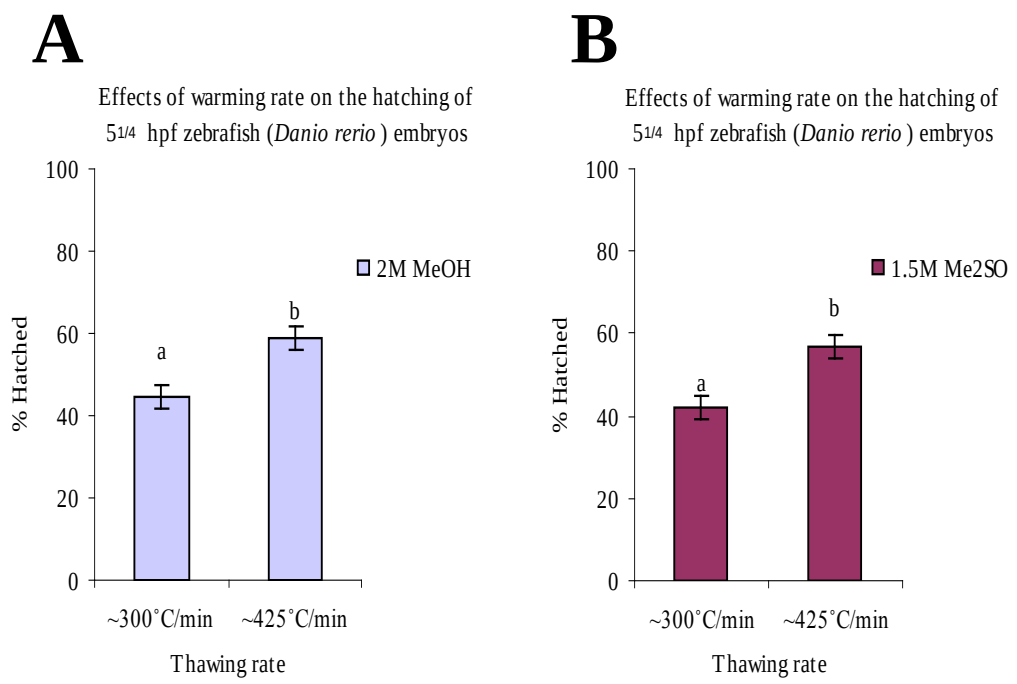

Figure 6.2: Rapid warming rate significantly improved the post warming hatching of 5¼ hpf zebrafish (*Danio rerio*) embryos. (A) Graphical presentation of the effects of two warming rates on hatching of 5¼ hpf embryos cooled with 2M MeOH. **(B)** Graphical presentation of the of the effects of two warming rates on hatching of 5¼ hpf embryos cooled with 1.5M Me_2SO. Values shown are mean +/- SEM of the hatching rates from three independent experiments. Different letters indicate statistically significant ($p<0.05$) difference among the groups being compared.

During the course of this experiment, it was noticed that the embryos were lysing immediately after the CPA solution was replaced with MilliQ water. CPA removal plays a critical role on the post warming survival of cryopreserved biological objects (Muldrew et al, 2004). When CPA solution is removed, the cells are exposed to a hypotonic solution and a high osmotic gradient is generated across the membrane. To maintain osmotic equilibrium extracellular water moves into the intracellular space swelling the cells, this may cause cell rupture. To reduce osmotic stresses CPA solution is usually removed in stepwise manner by serial dilution of the CPA to allow cells enough time between steps to reach an osmotic equilibrium. In the current experiment, CPA solution was replaced with E2 in one step, which might have caused osmotic stress leading to embryo death as observed. In the next experiment, therefore, the effects of stepwise dilution of the CPA solution on the survival of cooled embryos were investigated.

6.2.3 Optimisation of stepwise removal of CPA solution

6.2.3.1 Experimental design

Embryos in groups of 30 were incubated in either 2M MeOH or 1.5M Me2SO using the method described in section 2.3.2. The embryos were then cooled to -10˚C using the protocol outlined in section 2.3.3. Based on the finding of the previous experiment, the embryos were warmed at a rate of ~425˚C/min in a water bath set at 37˚C. Following warming, CPA solutions were diluted in stepwise manner using E2. When the CPA was 2M MeOH, the embryos were introduced for 1 minute each in 0M MeOH (one step), 1M and 0M MeOH (two step), 1M, 0.5M, 0M MeOH (three step), 1M, 0.5M, 0.25M, 0M MeOH (four step), and 1M, 0.5M, 0.25M, 0.125M, 0M MeOH (five steps), respectively. When the CPA was 1.5M Me_2SO, the embryos were introduced for 1 minute each in 0M Me_2SO (one step), 1M and 0M Me_2SO (two step), 1M, 0.5M, 0M Me_2SO (three step), 1M, 0.5M, 0.25M, 0M Me_2SO (four step), and 1M, 0.5M, 0.25M, 0.125M, 0M Me_2SO (five steps), respectively. Following CPA solution removal, the embryos were incubated in E2 at 28±1˚C for days and the hatching rates were monitored at the end of the 5-day period as per the method outlined in section 2.4.1.

6.2.3.2 Result

The effects of stepwise removal of CPA solution on the survival of 5¼ hpf embryos cooled to -10˚C are graphically presented in figure 6.3.1.2. Increased number of CPA removal step significantly improved the hatching rates of the embryos cooled with MeOH for up to three step and the embryos cooled with Me_2SO for up to four step (Figure 6.3.1.3 A and B, respectively). No significant difference ($p>0.05$) in the hatching rates of the embryos was noticed following four and five step removal of the CPAs.

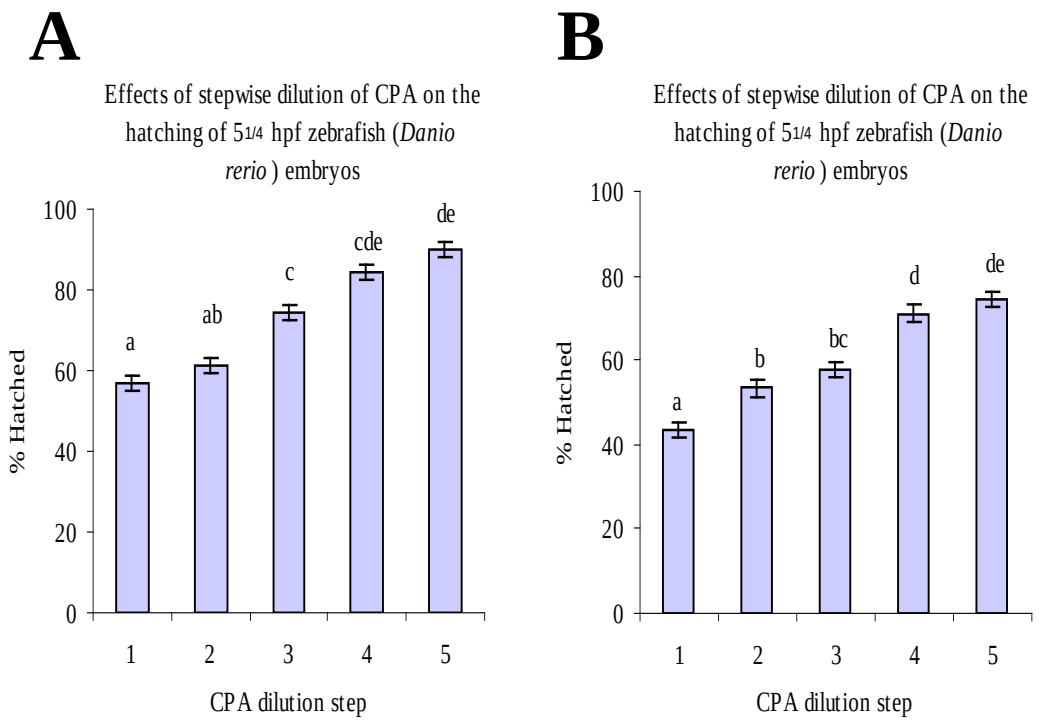

Figure 6.3: Post warming survival of the cooled embryos was improved with the increased number of CPA removal step. (A) Graphical presentation of the effects of stepwise removal of CPA solution on hatching of 5¼ hpf embryos cooled with 2M MeOH. **(B)** Graphical presentation of effects of stepwise removal of CPA solution on hatching of 5¼ hpf embryos cooled with 1.5M Me_2SO. Values shown are mean +/- SEM of the hatching rates from three independent experiments. Different letters indicate statistically significant ($p<0.05$) difference among the groups being compared

However, the relative hatching rates of the embryos following CPA solution removal in five steps were slightly higher than those following CPA solution removal in four step, and therefore, it was decided that CPA solution removal in all subsequent experiment would be carried out using five-step dilution method. The findings of the current experiment and the previous experiment described in section 6.2.2 indicate that a warming rate of ~425°C/min and a five-step dilution of the CPA solution were optimum conditions for cooling 5¼ hpf zebrafish (*Danio rerio*) embryos. In the next experiment, therefore, the optimised cooling protocol was applied to investigate the lowest subzero temperature to which 5¼ hpf zebrafish (*Danio rerio*) embryos could be cooled to with a reasonably good survival rate.

6.2.4 Application of the optimised protocol to cool 5¼ hpf embryos to the lowest possible subzero temperature

6.2.4.1 Experimental design

Embryos in groups of 30 were incubated in either 2M MeOH or 1.5M Me2SO using the method described in section 2.3.2. The embryos were then cooled to -10°C, -15°C, -20°C, -25°C, -30°C, -35°C, 40°C and -45°C using the protocol described in section 2.3.3. Following cooling, the embryos were warmed at ~425C/min based on the finding of the experiment described in section 6.2.2. After warming, the CPA solution was removed using the five-step dilution method based on the finding of the experiment described in section 6.2.3. Finally, the embryos were incubated at 28±1°C in E2 for 5 days. At the end of the 5-day period, survival of the embryos was assessed by monitoring the hatching rates as described in section 2.4.1.

6.2.4.2 Result

Hatching rates of the embryos cooled to different subzero temperatures using the optimised protocol are presented in figure 6.4. The post warming hatching rates of the embryos cooled using the optimised protocol was notably improved compared to those of the embryos cooled with the original method devised by Zhang et al, (1993) (compare Figure 6.1 and 6.4). However, the survival rates of the embryos cooled using the optimised method were also significantly decreased ($p<0.05$) with the decreasing cooling temperature (Figure 6.4 A and B). Nevertheless, the optimised protocol resulted in successful cooling of the embryos, using both 2M MeOH and 1.5M Me_2SO, to subzero temperature as low as -40°C. No embryo survived cooling to -45C.

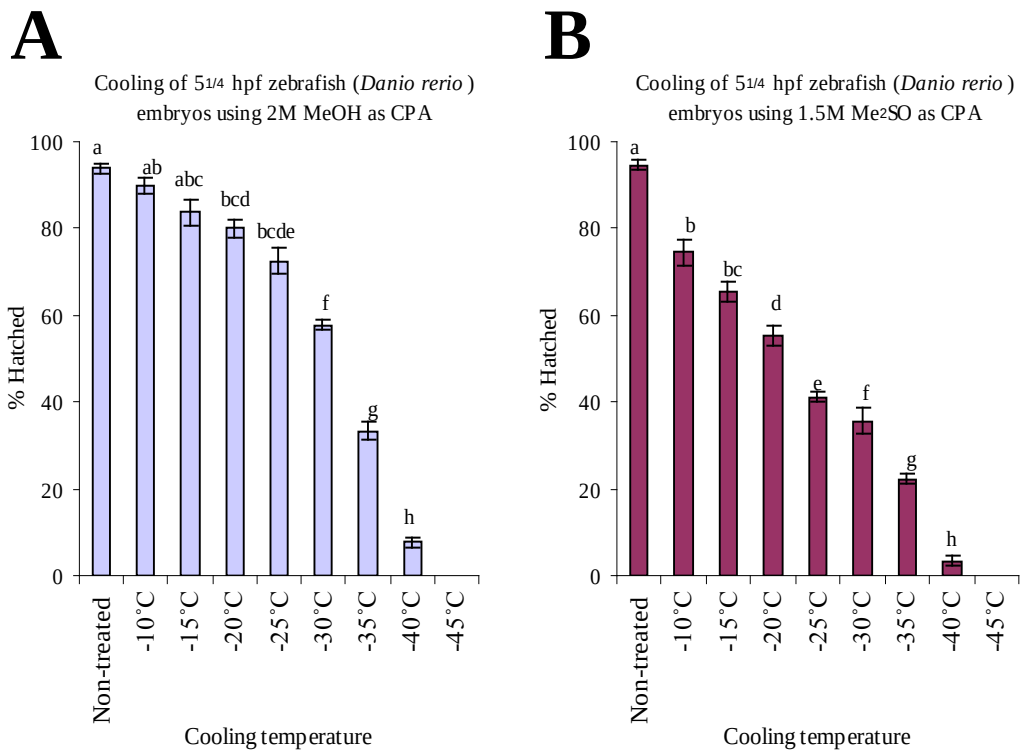

Figure 6.4: The optimised protocol resulted in cooling of the embryos to subzero temperature as low as -40°C. **(A)** Graphical presentation of the hatching rates of 5¼ hpf embryos cooled with 2M MeOH as CPA. **(B)** Graphical presentation of the hatching rates of 5¼ hpf embryos cooled with 1.5M Me_2SO as CPA. Values shown are mean +/- SEM of the hatching rates obtained from three independent experiments. Different letters indicate statistically significant ($p<0.05$) difference among the groups being compared.

However, the number of embryos survived cooling to -40°C was considered too low to facilitate the experimental procedures of the current study. The number of embryos survived cooling to -35°C appeared to be sufficient to carry out the experimental procedures. Moreover, most of the embryos cooled to -35°C died on warming. If damage to the genome is to be responsible for embryo death, the damage must have taken place before cooling to this critical subzero temperature. Therefore, in the subsequent experiments, the investigation of the effects of cooling and warming on the genome was carried out on the embryos cooled to -35°C.

6.3 Investigation of the occurrence of DSBs and SSBs in the genome of MeOH-cooled embryos

A total of 200 embryos were cooled to -35˚C using MeOH as CPA according to the method described in section 2.3.3. A second group of 120 embryos were incubated in E2 at 28±1˚C as non-treated control. The cooled embryos were warmed at rate of ~425˚C/min and the CPA solution was removed using in 5-step dilution method. Then, total proteins were extracted from the cooled and warmed embryos and non-treated control embryos using the method described in section 2.4.2.2. The extracted proteins from each group were probed alongside DSB^- and DSB^+ embryo lysates for DSB-affected DDR proteins using the S*/T*Q antibody according to the method described in section 2.4.2.8.

6.2.2.1 Investigation of the repair of SSBs in MeOH-cooled embryos provided with recovery time

A total of 200 embryos were cooled to -35˚C using 2M MeOH as CPA. A second group of 120 embryos were incubated in E2 at 28±1˚C as non-treated control. The cooled embryos were warmed at a rate of ~425C/min and the CPA solution was removed in 5-step dilution method. Based on the finding of the experiment described in section 6.3, the embryos were provided with a recovery time by incubating them at 28±1˚C in E2 for 30 minutes. At the end of the recovery time, total proteins were extracted from the cooled and warmed embryos and non-treated control embryos using the method described in section 2.4.2.2. The extracted proteins were then probed, alongside SSB^- and SSB^+ embryo lysates, for SSB-affected DDR proteins using S*/T*Q antibody according to the method outlined in section 2.4.2.8.

6.2.3 Investigation of the occurrence of DSBs and SSBs in Me_2SO-cooled embryos

A total of 120 embryos were cooled to -35C using Me_2SO as CPA according to the method outlined in section 2.3.3. A second group of 120 embryos were incubated in E2 at 28±1˚C as non-treated control. Total proteins from the cooled and warmed embryos and non-treated control embryos were extracted using the method described in section 2.4.2.2.

The extracted proteins were then probed alongside DSB^- and DSB^+ embryos lysates for DSB-mediated DDR proteins using S*/T*Q antibody according to the method described in section 2.4.2.8.

Investigation of the occurrence of SSBs in the genome of the embryos cooled with Me_2SO was carried out by analysing the proteins detected in the Me_2SO -cooled embryos against the patterns of activation and deactivation of DDR proteins detected in SSB^+ 5¼ hpf zebrafish (*Danio rerio*) embryos.

6.2.4 Investigation of the occurrence of various forms of sequence alteration in the genome of 5¼ hpf zebrafish (*Danio rerio*) embryos following cooling and warming

Embryos in groups of 30 were cooled to -35˚C using either 2M MeOH or 1.5M Me_2SO as CPA. A second group of embryos was incubated in E2 at 28±1˚C as non-treated control. Total RNAs were extracted from the cooled and warmed embryos and the non-treated control embryos using the method described in section 2.4.3.1 and converted to cDNA using the method described in section 2.4.3.4. The cDNA was then subjected to PCR reaction to amplify the genes selected from the individual ERMs using the method described in section 2.4.3.8. The expression profiles of each of the genes were then generated using the method described in section 2.4.3.9.

6.3 Results

6.3.2 Expression of DSB-affected DDR proteins were not affected in the embryos cooled using MeOH as CPA

Cooling of 5¼ hpf embryos to -35˚C using 2M MeOH as CPA did not affect the expression of DSB-affected DDR proteins. The S*/T*Q antibody successfully detected the dephosphorylation and phosphorylation patterns of DSB-affected DDR proteins in the DSB^+ embryo lysate relative to the DSB^- embryo lysate (Figure 6.5 A and B). None of the proteins phosphorylated in the DSB^+ lysate was phosphorylated in the MeOH-cooled embryos. However, the patterns of the expression of DDR proteins in the MeOH-cooled embryos were in line with those in the SSB^+ embryo lysate. The p150 protein, which is de-phosphorylated in the event of both DSBs and SSBs, was found de-phosphorylated in the MeOH-cooled embryos (Figure 6.5 A). In addition, the p38 protein, which is relatively hypo-phosphorylated and hyper-phosphorylated in the event of DSBs and SSBs, respectively, was phosphorylated in both non-treated embryo lysate and MeOH-cooled embryo lysate but the normalised intensity of phosphorylation of the protein was significantly increased ($p<0.05$) in the MeOH-cooled embryo lysate relative to that in the non-treated embryo lysate (Figure 6.5 C).

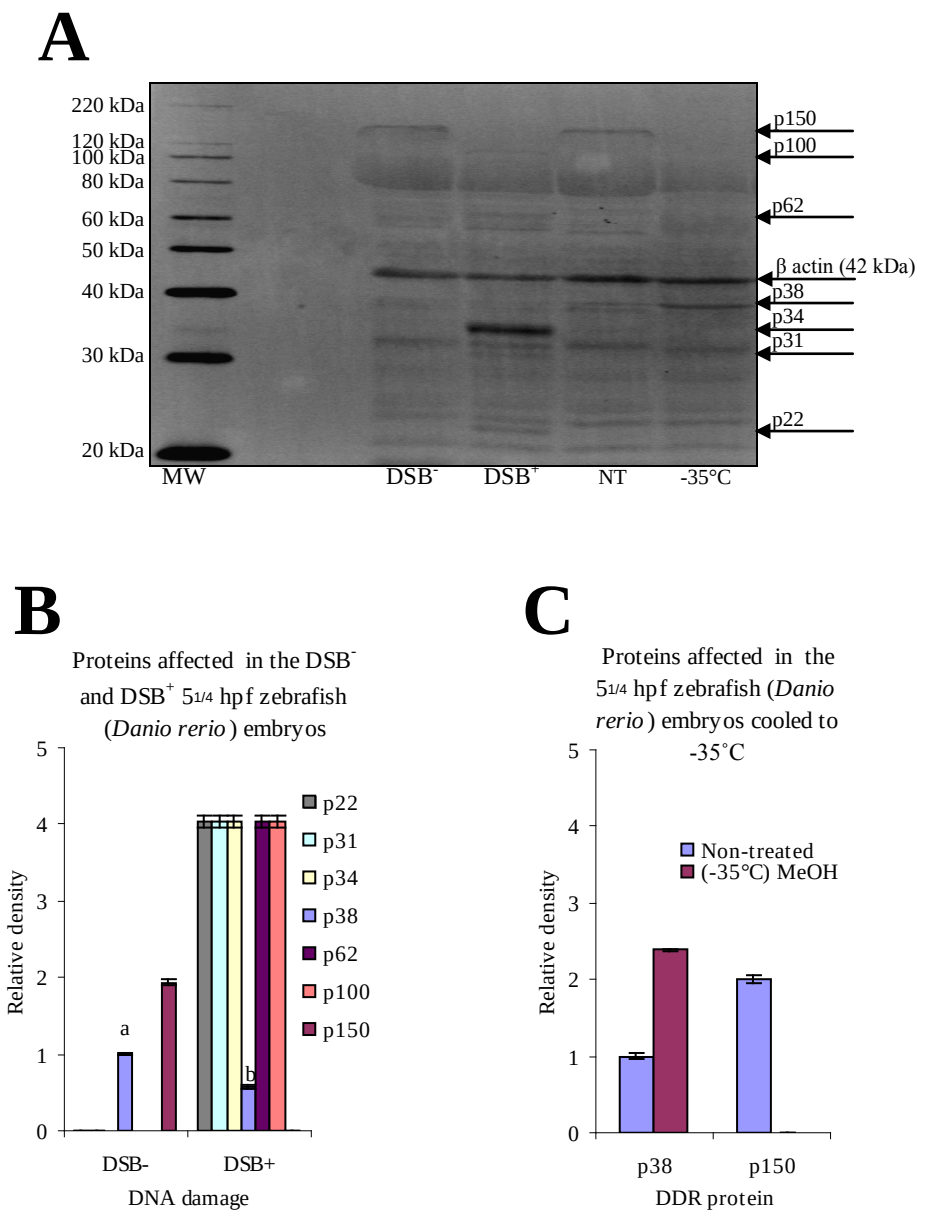

Figure 6.5: SSB affected DDR proteins were affected in 5¼ hpf zebrafish (*Danio rerio*) embryos cooled with MeOH. (A) Representative blot of three independent experiments. 5¼ hpf embryos were cooled to -35°C using MeOH as CPA. Total proteins were extracted from the non-treated (NT) and cooled embryos (-35°C), and probed alongside DSB$^-$ and DSB$^+$ embryo lysates with anti-S*/T*Q, and anti-β-*actin* simultaneously. *β actin* served as a control for variations in protein loading. **(B)** Graphical presentation of the intensity of phosphorylation of the proteins detected in the DSB$^-$and DSB$^+$ lysates. **(C)** Graphical presentation of the intensity of phosphorylation of the proteins detected in the lysates prepared from the embryos cooled with MeOH. Values shown are mean +/- SEM of β-*actin* normalised band intensities obtained from three replicates and presented as relative to those in the lysate prepared from non-treated embryos. Different letters, where appropriate, indicate statistically significant ($p<0.05$) difference among the groups being compared. MW represents MagicMark^{TM} XP Western protein standards (Invitrogen, LC5602).

6.3.2.2 Expression of SSB-mediated DDR proteins returned to the base line level in the MeOH-cooled 5¼ hpf embryos provided with recovery time

The effect of recovery time on the expression of SSB-affected DDR proteins in 5¼ hpf embryos cooled with MeOH is presented in figure 6.6. The characteristic expression patterns of SSB-affected DDR proteins, as established and discussed in chapter 3, was successfully detected in the SSB^+ embryo lysates (6.6 A and B). The p150 and p38 proteins were dephosphorylated and hyperphosphorylated, respectively, in the SSB^+ embryo lysate relative to those in the SSB^- embryo lysate. However, the expression of both p150 and p38 proteins in cooled embryos provided with time to recover returned to the base line level. Both p150 and p38 were phosphorylated in the non-treated and MeOH-cooled embryo lysates (6.6 A) and there was no significant difference ($p>0.05$) in the intensity of phosphorylation of the proteins in the non-treated and cooled embryo lysates (Figure 6.6 C).

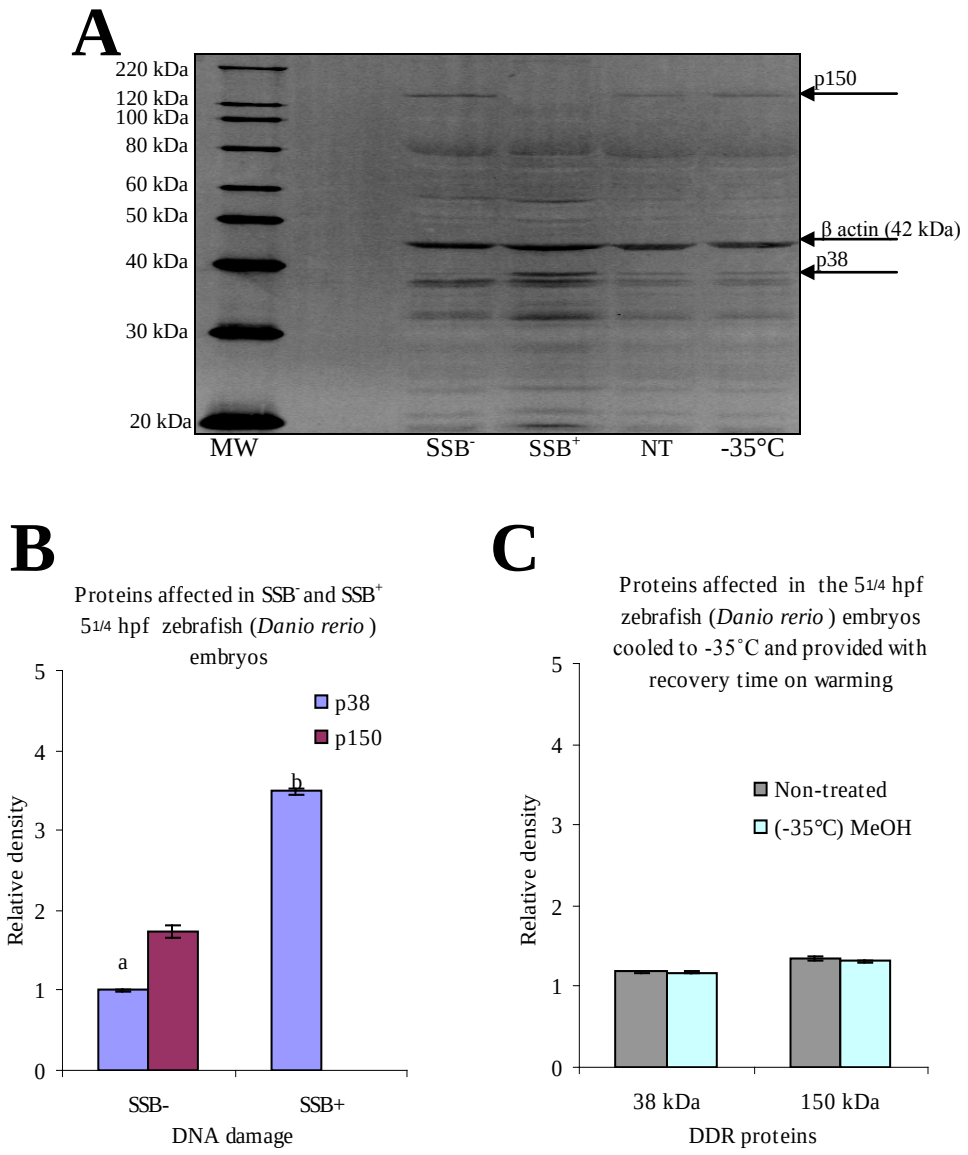

Figure 6.6: Expression of SSB-affected DDR proteins returned to base line levels in MeOH-cooled embryos provided with a recovery time. (A) Representative blot of three independent experiments. 5¼ hpf embryos were cooled to -35°C using MeOH as CPA. Embryos were warmed and incubated in E2 at 28±1°C for 30 minutes. Total proteins were extracted from the non-treated embryos (NT) and the cooled embryos (-35°C), and probed alongside SSB^- and SSB^+ embryo lysates with anti-S*/T*Q, and anti-β-*actin* simultaneously. *β actin* served as a control for variations in protein loading. **(B)** Graphical presentation of the intensity of phosphorylation of the proteins detected in the $SSB^-$and SSB^+ embryo lysates. **(C)** Graphical presentation of the intensity of phosphorylation of the proteins detected in the lysates prepared from the embryos cooled using MeOH and warmed subsequently. Values shown are mean +/- SEM of β-*actin* normalised band intensities obtained from three replicates and presented as relative to those in the lysate prepared from non-treated embryos. Different letters, where appropriate, indicate statistically significant ($p<0.05$) difference among the groups being compared. MW represents MagicMark^{TM} XP Western protein standards (Invitrogen, LC5602).

6.3.3 Expression of DSB-affected and SSB-affected DDR proteins were not affected in 5¼ hpf zebrafish (*Danio rerio*) embryos cooled with Me_2SO

The result of the experiment shows that none of the DDR proteins phosphorylated in DSB^+ embryo lysate (Figure 6.7 A and B) was phosphorylated in the Me_2SO-cooled embryo. Moreover, the p150 protein, which is dephosphorylated in the DSB^+ 5¼ hpf zebrafish (*Danio rerio*) embryos (Figure 6.7 A and B) and in the SSB^+ 5¼ hpf zebrafish (*Danio rerio*) embryos, was found phosphorylated in both non-treated and Me_2SO-cooled embryos. In addition, the normalised intensity of phosphorylation of the protein in the embryos cooled to -35°C using Me_2SO as the CPA was not significantly different ($p>0.05$) from that in the non-treated embryos (N/T). Similarly, the p38 protein, which is relatively hypo-phosphorylated in the DSB^+ embryos (Figure 6.7 A and B) and relatively hyperphosphorylated in the SSB^+ embryos (Figure 6.7 C), was found phosphorylated in embryos cooled to -35C (Figure 6.7 A); and the normalised intensity of phosphorylation of the protein in the cooled embryos was not significantly different ($p>0.05$) from that in the non-treated embryos (Figure 6.7 D).

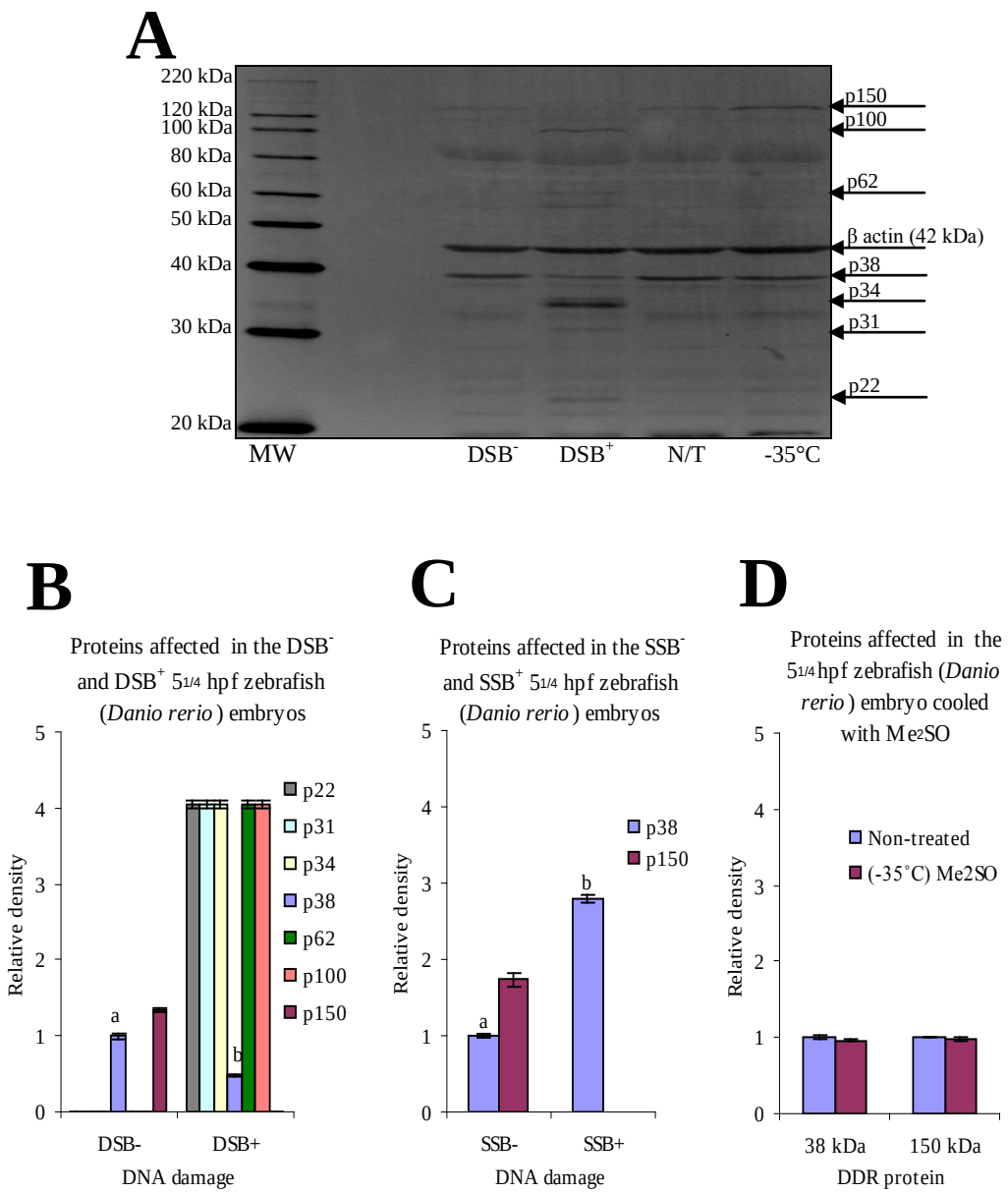

Figure 6.7: DSB affected DDR proteins were not affected in 5¼ hpf zebrafish (*Danio rerio*) embryos cooled with Me_2SO. (A) Representative blot of three independent experiments. 5¼ hpf embryos were cooled to -35°C using Me_2SO as CPA. Total proteins were extracted from the non-treated (NT) and cooled (-35°C) embryos and probed alongside DSB^- and DSB^+ embryo lysates with anti-S*/T*Q, and anti-β-*actin* simultaneously. *β actin* served as a control for variations in protein loading. **(B)** Graphical presentation of the intensity of phosphorylation of the proteins detected in the $DSB^-$and DSB^+ embryos. Values shown are mean +/- SEM of β-*actin* normalised band intensities obtained from three replicates and presented as relative to those in the DSB^- embryos. **(C)** Graphical presentation of the intensity of phosphorylation of the proteins detected in the $SSB^-$and SSB^+ embryos**.** Values shown are mean +/- SEM of β-*actin* normalised band intensities obtained from three replicates and presented as relative to those in the SSB^- embryos. **(D)** Graphical presentation of the intensity of phosphorylation of the proteins detected in the embryos cooled with Me_2SO. Values shown are mean +/- SEM of β-*actin* normalised band intensities obtained from three replicates and presented as relative to those in the non-treated embryos. Different letters, where appropriate, indicate statistically significant ($p<0.05$) difference among the groups being compared. MW represents MagicMark^{TM} XP Western protein standards (Invitrogen, LC5602).

6.3.4 Cooling of 5¼ hpf zebrafish (*Danio rerio*) embryos using MeOH and Me_2SO affects the expression of the genes of the ERMs

The expression profiles of the genes of the ERMs in 5¼ hpf zebrafish (*Danio rerio*) embryos cooled to -35°C are presented in figure 6.9. The expression of each of the genes in both MeOH-cooled and Me_2SO-cooled embryos were affected relative to that of the genes in the corresponding non-treated embryos. In MeOH-cooled embryos, the relative expression of the gene *UDG* from the *UDG*-dependant BER and the gene *MSH2* from the MMR mechanisms were significantly decreased ($p<0.05$), whereas, that of the gene the gene *ERCC1* from the NER mechanism was significantly increased ($p<0.05$) by 1.6 fold above of that of the gene in the non-treated embryos (Figure 6.9 A). In the Me_2SO-cooled embryos, on the other hand, the expression of the gene *UDG* from the *UDG*-dependant BER was significantly decreased, whereas, that of the gene *TDG* from the *TDG*-dependant BER was significantly increased ($p<0.05$) by 1.8 fold above of that of the gene in the non-treated embryos (Figure 6.9 B).

A

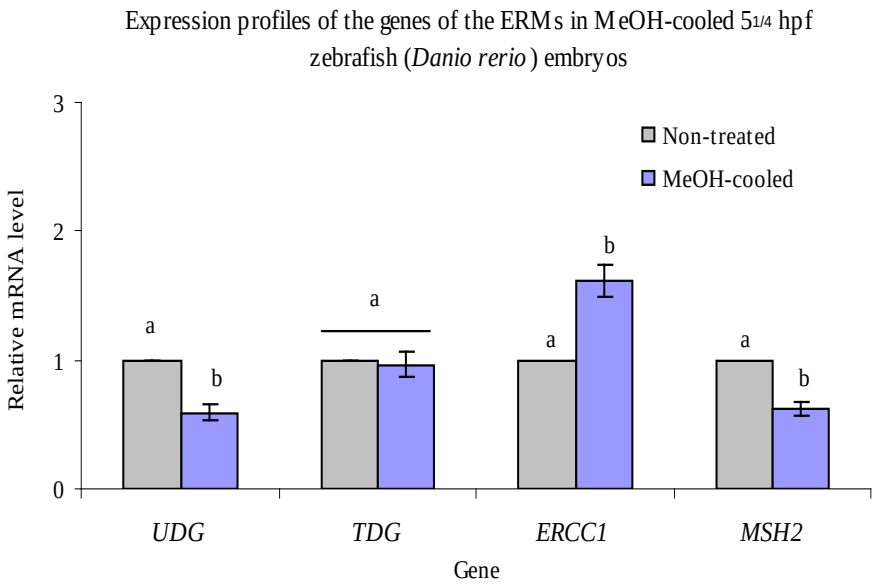

B

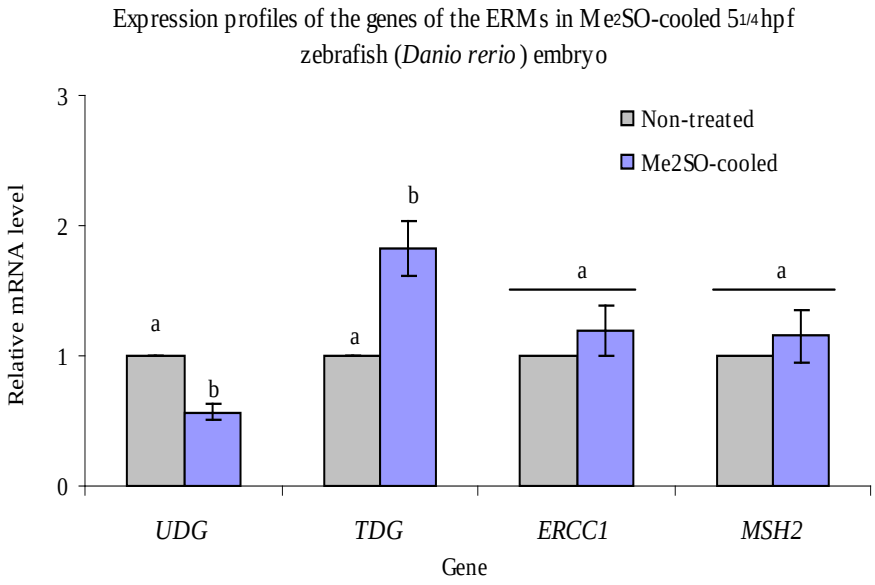

Figure 6.8: Expression levels of the genes selected from the ERMs were affected by cooling and warming. **(A)** Graphical presentation of the expression profiles of the genes of the ERMs in MeOH-cooled embryos (B) Graphical presentation of the expression profiles of the genes of the ERMs in Me_2SO-cooled embryos. Values shown are mean +/- SEM of *ACTB* and *EF1 alpha*-normalised expression levels of the genes obtained from three independent experiments and presented as relative to those in the corresponding non-treated embryos. Different letter indicates statistically significant ($p>0.05$) difference among the groups being compared.

6.4 Discussion

6.4.1. Cooling with MeOH resulted in the occurrence of SSBs rather than DSBs in the genome of 5¼ hpf zebrafish (*Danio rerio*) embryos

For the reasons described in chapter 4 and 5, the investigation of activation of DDR proteins in embryos cooled to -35C using MeOH as CPA was carried out on total proteins extracted immediately following warming. As discussed in chapter 3, in the event of DSBs in the genome of 5¼ hpf zebrafish (*Danio rerio*) embryos, the protein p38 is down-regulated and the protein p150 is deactivated probably to facilitate cell cycle arrest, whereas, the proteins p22, p31, p34, p62, and p100 are activated probably to facilitate cell cycle arrest as well as the repair of the damage. The patterns of down-regulation, deactivation and activation of DDR proteins characteristic of the occurrence of DSBs in the genome of 5¼ hpf zebrafish (*Danio rerio*) embryos was maintained in the DSB^+ embryos in this part of the study (compare DSB^- and DSB^+ lane in Figure 6.5), which confirmed the sensitivity of the antibody for the S*/T*Q motif. However, none of the DDR proteins activated in the DSB^+ 5¼ hpf embryos were activated in 5¼ hpf embryos cooled to -35°C using MeOH as the CPA. Nevertheless, the p150 protein was found deactivated in the embryos cooled to -35°C using MeOH as the CPA. Similarly, the p38 protein was also hyper-activated in the embryos cooled with MeOH as the CPA. The pattern of deactivation of the p150 protein and hyper-activation of the p38 protein observed in the embryos cooled with MeOH is consistent with the patterns of the expression of DDR proteins observed in SSB^+ 5 ¼ hpf zebrafish (*Danio rerio*) embryos. Recall from section 3.5.3 in chapter 3 that in the event of SSBs in the genome of 5¼ hpf embryos, the protein p150 is deactivated and the protein p38 is hyper-activated. Therefore, the findings indicate that cooling of 5¼ hpf zebrafish (*Danio rerio*) to -35C using MeOH as the CPA resulted in the occurrence of SSBs rather than DSBs in the genome.

However, SSBs are not lethal for biological objects. In a cell capable of initiating an efficient DDR, SSBs are readily repaired (Grafstrom et al., 1984; O'connell et al., 2010). But increased number of SSBs may overwhelm the repair mechanisms leading to the damage being left un-repaired, in which case, SSBs would lead to the formation of DSBs in the genome of newly replicated progeny cells by way of stalled replication fork (Helleday, 2003; Saleh-Gohari et al., 2005). Nevertheless, in the follow up experiment, it

was found that the expression of the proteins p150 and p38 returned to the base line level represented by the expression levels of the proteins in the non-treated embryos (Figure 6.6). This indicates that the SSBs observed in the embryos cooled to -35°C using MeOH as the CPA, were repaired when the embryos were provided with a recovery time. The finding, therefore, rules out the possibility of the occurrence of SSB-mediated DSBs in the genome of the progeny cells generated in the MeOH-cooled embryos. However, as discussed in chapter 1, most of the DNA repair mechanisms in eukaryotes are error prone (Dinant et al., 2008; Cox et al., 2012) and various mutations are introduced into the genome during the repair process. Therefore, the findings add to the possibility of the occurrence of various forms of sequence alteration secondary to damage repair in the genome of 5¼ hpf embryos cooled to -35˚C using MeOH as the CPA.

6.4.2. Cooling with Me_2SO did not result in the occurrence of DSBs or SSBs in the genome of 5¼ hpf zebrafish (*Danio rerio*) embryos

As in the case of MeOH-cooled embryos, none of the DDR proteins, activated in the event of DSBs in the genome of 5¼ hpf zebrafish (*Danio rerio*) embryos (Figure 6.7 A and B), was activated in the embryos cooled to -35°C using Me_2SO as the CPA (Figure 6.7 A and D). Moreover, the p38 protein and the p150 protein which are down-regulated and deactivated, respectively, in the event of DSBs in the genome of 5¼ hpf zebrafish (*Danio rerio*) embryos (Figure 6.7 A and B) were maintained at the base line levels in 5¼ hpf embryos cooled to 35°C using Me_2SO as the CPA (Figure 6.7 A and D). The findings indicate that cooling of 5¼ hpf zebrafish (*Danio rerio*) embryos to -35˚C using Me_2SO as the CPA did not result in the occurrence of DSBs in the genome. As it was established in chapter 3, in the event of SSBs in the genome of 5¼ hpf zebrafish (*Danio rerio*) embryos, the p150 protein is deactivated and the p38 protein is hyper-activated (Figure 6.8 C). Therefore, the finding of this part of the study also indicate that Me_2SO-mediated cooling of 5¼ hpf zebrafish embryos did not result in the occurrence of SSBs in the genome either. However, as in the case of the findings of MeOH-mediated cooling, the findings of this section of the study could not rule out the possibility of the occurrence of DNA damage other than strand breaks. Hence, the possibility of the occurrence of various forms of sequence alteration in the genome of 5¼ hpf zebrafish (*Danio rerio*) embryos cooled to -35˚C using both MeOH and Me2SO as CPAs was investigated by analysing the genes of the ERMs.

6.4.3 Expression of the genes of the ERMs were affected in 5¼ hpf zebrafish embryos cooled to -35˚C

In the previous part of the study (presented in chapter 5), it was observed that treatment with 2M MeOH led to reduced expression of the gene *UDG* from the *UDG*-dependant BER, the gene *TDG* from the *TDG*-dependant BER, the gene *ERCC1* from the NER, and the gene *MSH2* from the MMR mechanisms, whereas, treatment with 1.5M Me_2SO led to reduced expression of the latter three genes in 5¼ hpf zebrafish *(Danio rerio)* embryos (Figure 5.5 and 5.6). It was hypothesised that the gene suppression observed following CPA treatment was due to DNA methylation by the CPAs as both MeOH and Me_2SO are known to have methylating properties. This part of the study found that the gene *UDG* from the *UDG*-dependant BER and the gene *MSH2* from the MMR mechanisms were depressed in the embryos cooled to -35˚C using 2M MeOH as the CPA (Figure 6.8 A), whereas, the gene *UDG* from the *UDG*-dependant BER was depressed in the embryos cooled to -35˚C using 1.5M Me_2SO as the CPA (Figure 6.8 B). The findings add to the hypothesis regarding DNA methylation by the CPA. However, as mentioned in the previous chapter, the hypothesised DNA methylation by the CPAs needs to be further investigated, which is beyond the scope of the current study. Nevertheless, the genes chosen for the current study play key roles in the individual ERMs, therefore, suppression of the genes, as observed, indicates that the activity of the corresponding repair mechanisms were also impaired, in which case the embryos in question were more susceptible to the type of damage repaired by the particular repair mechanism.

This part of the study also found that the gene *ERCC1* from the NER and the gene *TDG* from the *TDG*-dependant were up-regulated in MeOH-cooled (Figure 6.8 A) and Me_2SO-cooled embryos (Figure 6.8 B), respectively. As discussed in chapter 1, the gene *ERCC1* and the gene *TDG* play significant roles in the NER and the BER mechanisms, respectively. As discussed in chapter 1, The NER mechanism is responsible for repairing large and bulky DNA lesions that distort the double helix, whereas, the *TDG*-dependant BER mechanism is responsible for removing misincoroprated thymine base from the DNA. The findings, therefore, indicate that the occurrence of the helix distorting lesions was increased in the embryos cooled to -35°C using MeOH as the CPA and the occurrence of misincroporated thymine was increased in the embryos cooled to -35°C using Me_2SO as the CPA. Although the up-regulation of the genes *ERCC1* and *TDG* and thereby, the NER and TDG-dependant BER mechanisms suggests that the damages in

question were repaired in the embryos cooled to -35°C, the possibility of the maintenance of such damages in the genome can not be ruled out as increased occurrence of damages often overwhelm the repair mechanism resulting in the damage being left un-repaired.

6.5 Summary

This is the first study to report cooling of 5¼ hpf zebrafish (*Danio rerio*) embryos to subzero temperature as low as -35°C. In this study, a number of parameters of an established cooling protocol were optimised to cool 5¼ hpf zebrafish (*Danio rerio*) embryos. In this study, it was found that rapid warming at a rate of ~425C/min and serial dilution of CPA solution in five steps were optimum conditions for cooling 5¼ hpf zebrafish (*Danio rerio*) embryos. This study is also the first to investigate the effects of cooling to -35°C and subsequent warming on the genome of 5¼ hpf zebrafish (*Danio rerio*) embryos. The study found that cooling and warming using 2M MeOH and 1.5M Me_2SO as CPAs did not result in the occurrence of DSBs in the genome 5¼ hpf zebrafish (*Danio rerio*) embryos. However, it was found that MeOH-mediated cooling and warming resulted in the occurrence of SSBs in genome of the embryos but the SSBs were efficiently repaired when the teleost embryos were provided with a recovery time. This part of the study also found that cooling and warming process involved in slow ccoling cryopreservation have the potential to cause various forms of sequence alteration in the genome of biological objects as evidenced by the suppression of the genes of the ERMs in 5¼ hpf zebrafish (*Danio rerio*) embryos cooled to -35°C. However, the findings of this part of the study failed to agree with the studies that implicated cooling and warming with increased DNA fragmentation.

This work is being prepared for publication

CHAPTER 7: CONCLUSIONS

7.1 Reiteration of the aims and objectives

In recent years, a large number of studies have linked cryopreservation with compromised genetic integrity of biological objects in question. It has been shown that cryopreservation caused increased occurrence of mutations (Kopeika et al, 2005), increased DNA fragmentation (Baumber et al., 2003; Peris et al., 2004; Perez et al., 2008) and the event of apoptosis (Duru et al., 2001; Martin et al., 2004; Ortega-Ferrusola, 2008). However, the effects of cryopreservation on the genome of biological objects are not well established. As discussed in chapter 1 in detail, some of the evidence linking cryopreservation to increased DNA fragmentation and the event of apoptosis is inconclusive (Martin et al., 2004; Ortega-Ferrusola, 2008; Thompson et al., 2009). Moreover, the techniques employed in most of the studies to investigate DNA fragmentation and apoptosis in cryopreserved biological objects have been under severe scrutiny for their reliability (Collins et al., 2008) (discussed in chapter 1). In these settings the current study set out to investigate the effects of cryopreservation on the genome of biological objects in the context of the occurrence of DSBs, SSBs, and various forms of sequence alteration.

Identifying the apparent limitations of the conventional methods, such as Comet assay and TUNEL assay, to detect DNA damage in the form of DSBs and SSBs (discussed in chapter 1), the current study hypothesised that the ideal way to characterise the nature of the putative DNA damage resulting from cryopreservation was to monitor the DDR from the cryopreserved biological objects. A DDR, as discussed in chapter 1, is a complex network of surveillance mechanisms consisting of the cell cycle checkpoints and the DNA repair mechanisms that leads to repair of the damage or initiation of apoptosis (Dinant et al., 2008). Eukaryotic cells respond differently to different types of DNA damage and therefore, the current study set out to investigate different types of DDR in cryopreserved biological objects, and thereby, characterise the nature of the putative DNA damage. However, cryopreservation is a multi-parametric method involving CPA treatment, chilling, cooling and warming; and the evidence linking cryopreservation to various forms of DNA damage suggests that any or all of the cryopreservation parameters may contribute to the putative DNA damage (Rajaei et al., 2005; Rajaei et al., 2006;

Scandalios, 1993; Tsang et al, 1991; Prasad, 1996; Wood and Youle, 1995). Thus, the present study aimed to investigate different types of DDR in biological objects treated with different parameters of cryopreservation.

The current study argued that the investigation of the nature of cryopreservation-induced DNA damage in a biological object capable of initiating a DDR would give valuable insight into the underlying mechanism of damage. To that end, zebrafish (*Danio rerio*) embryos were identified as the ideal test material for the current study. The organism is known to have all the key components of the eukaryotic DDR (Misun et al., 2007). Since different types of cells respond differently to DNA damage, the study further argued that it would be ideal to employ the embryos at a developmental stage in which all the cells are at the same stage and are not committed to specific cell type. To that effect, the study employed 5¼ hpf zebrafish (*Danio rerio*) embryos, in which the cells are not committed and the organism is also known to have a competent DDR (Ikegami et al., 1997).

In eukaryotes, DDR in the event of DSBs is facilitated by ATM and that in the event of SSBs is facilitated by ATR. Therefore, the present study intended to investigate the occurrences of DSBs and SSBs in the genome of 5 ¼ hpf zebrafish (*Danio rerio*) treated with different cryopreservation parameters by way of investigating the activation of ATM and ATR, respectively. However, a direct detection of ATM or ATR using Western blot was deemed not ideal in the context of the current study for the reasons discussed in chapter 1, and therefore, the study employed an antibody against the phosphorylated substrate motif (S*/T*Q) of the kinases to that effect. It was hypothesised that the antibody against the substrate motif would allow a simultaneous detection of most of the downstream substrates of the kinases. Although ATM and ATR share a large number of substrate proteins, there exist substrate proteins which are specifically activated by the individual kinases (Abraham et al., 2001, Yang et al., Yang et al, 2004) (discussed in chapter 1 and 3 in detail). The current study validated the specificity of the kinases for their respective substrates in zebrafish (*Danio rerio*) embryos, and then utilised the specific activation pattern of the substrate proteins to investigate the activation of ATM and that of ATR, and thereby, the occurrences of DSBs and SSBs in the genome of the embryos treated with different cryopreservation parameters.

In eukaryotes, DNA lesions other than strand breaks are usually repaired by the ERMs (discussed in chapter 1 in detail). The present study investigated the occurrence of various

forms of sequence alteration in the genome of the embryos treated with different cryopreservation parameters by way of investigating the individual ERMs at the gene level using qRT PCR.

7.2 Review of the main findings

7.2.1 Optimisation, development and validation of techniques and methods used in the investigation of the effects of different cryopreservation parameters on the genome of 5¼ hpf zebrafish (*Danio rerio*) embryos

The objective of this part of the study was to optimise, develop, and validate the technique and methods to be used in the investigation of the effects of different cryopreservation parameters on the genome of 5¼ hpf zebrafish (*Danio rerio)* embryos. The experimental works began with the optimisation of a number of parameters of Western blot that contribute to successful detection of the protein of interest. During the course of the optimisation work for Western blot, it was observed that the biotin-streptavidin detection system used in the study generated two very intense protein bands of approximately 75 kDa and 150 kDa. The bands were identified to be the result of non-specific binding of the streptavidin-Qdot molecule to endogenous biotin or biotinylated proteins. In this part of the study, a novel method based on pre-hybridisation of the biotinylated secondary antibody and the streptavidin-Qdot molecule was developed that efficiently eliminated non-specific binding inherent to biotin-streptavidin/avidin detection system. The optimised Western blot protocol together with the newly developed method were then utilised to validate the use of the antibody against the S*/T*Q motif to distinguish between the activation of ATM and ATR in 5¼ hpf zebrafish (*Danio rerio*) embryos. The embryos were treated with a known DSB-inducing drug camptothecin and a known SSB-inducing chemical H_2O_2, respectively, and proteins from both groups of embryos were probed with the S*/T*Q antibody. The study found that treatment of the embryos with DSB-inducer and SSB-inducer resulted in different patterns of substrate protein activation and deactivation in the embryos. However, the substrate proteins detected in the embryos treated with DSB-inducer and SSB-inducer were not thoroughly identical to the commonly known substrates of ATM and ATR. The findings indicate that although ATM-mediated DDR in the event of DSBs and ATR-mediated DDR in the event of SSBs are conserved in zebrafish (*Danio rerio*) embryos, the activation of

downstream substrates by ATM and ATR in terms of the proteins involved is not thoroughly conserved in the teleost embryos. However, the patterns of the activation of substrate proteins in the event of DSBs and SSBs in 5¼ hpf zebrafish (*Danio rerio*) were distinctively different to facilitate the investigation of the event of DSBs and SSBs in the genome of the embryos treated with different cryopreservation parameters.

This part of study then investigated the expression of the genes selected from the individual ERMs, namely, the BER, the NER and the MMR mechanism in 5¼ hpf zebrafish (*Danio rerio*) embryos. It was found that the genes were expressed in the embryos, and therefore, the expression profiles of the genes could be analyse to investigate the occurrence of various forms of sequence alteration in the genome of the embryos treated with the cryopreservation parameters. Analysis of gene expression profile using qRT-PCR requires normalisation of the expression value of the gene of interest against the expression value of a stably expressed reference gene. To that end, this part of the study validated the stability of expression of the HKGs *ACTB* an *EF1 alpha* in the embryos treated with different cryopreservation parameters. It was found that the expression of profiles the genes in the embryos were not significantly affected by the cryopreservation parameters, and therefore, the HKGs could be utilised as reference genes in the investigation of the expression profiles of the genes from the ERMs.

7.2.2 Investigation of the effects of chilling on the genome of 5¼ hpf zebrafish (*Danio rerio*) embryos

This part of the study utilised the assays developed for DSB-affected DDR proteins and SSB-affected DDR proteins, and the expression profiles of the genes of the ERMs to investigate the effects of short-term chilling on the genome of 5¼ hpf zebrafish (*Danio rerio*) embryos. The study hypothesised that the effects of short term chilling at 0˚C would give an insight into the chilling effects sustained by biological objects during controlled slow cooling cryopreservation. The experimental work began with the investigation of the effects of short-term chilling on the survival of 5¼ hpf zebrafish (*Danio rerio*) embryos. It was found that short term chilling as used in the current study had no effect on the survival of the embryos. The study then investigated the occurrences of DSBs and SSBs in the genome of the embryos chilled for different time points by analysing the DDR proteins detected in the embryos by S*/T*Q antibody against the

DDR proteins detected in the camptothecin-treated and H_2O_2-treated embryos. The occurrence of various sequence alteration in the genome of the embryos chilled for different time periods were investigated by analysing the expression profiles of the genes selected from the ERMs. An up-regulation of a gene from a particular pathway was regarded as an indication of the increased occurrence of the type of sequence alteration repaired by the pathway. The study found that chilling treatment did not induce any DSBs or SSBs in the genome of the embryos. However, it was found that the chilling treatment increased the expression the gene *MSH2*, indicating that MMR pathway was up-regulated in such embryos. The finding suggests that the chilling treatment increased the occurrence mismatched bases in the genome of 5¼ hpf zebrafish (*Danio rerio*) embryos

.

7.2.3 Investigation of the effects of MeOH and Me_2SO on the genome of 5¼ hpf zebrafish (*Danio rerio*) embryos

In this part of the study, the effects of two CPAs, namely MeOH and Me_2SO, on the genome of 5¼ hpf zebrafish (*Danio rerio*) embryos were investigated. The experimental works began with assessing the effects of the CPAs on the survival of the embryos. It was found that neither MeOH treatment nor Me_2SO treatment had any effect on the survival of the embryos in terms of the hatching rates. The study then moved on to investigate the occurrences of DSBs and SSBs in the genome of the embryos following CPA treatment. To that end, the phosphorylated proteins detected by S*/T*Q antibody in the embryos treated with different concentrations of MeOH and Me_2SO were analysed against the phosphorylated proteins detected in the camptothecin-treated and H_2O_2-treated embryos. The findings of this part of the study indicated that none of the CPAs at concentrations used caused the occurrence of DSBs or SSBs in the genome of 5¼ hpf zebrafish (*Danio rerio*) embryos. The study then investigated the expression profiles of the genes selected from the ERMs as indicators of the occurrence of various forms of sequence alteration in the genome of the MeOH-treated and Me_2SO-treated embryos. The expression levels of the gene *TDG*, the gene *ERCC1* and the gene *MSH2* were decreased in the embryos treated 1, 2 and 3M MeOH, whereas, the expression level of the gene *UDG* was decreased in the embryos treated with 1M and 2M MeOH but significantly increased in the embryos treated with 3M MeOH. Similar results were obtained following treatment with Me_2SO.

7.2.4 Investigation of the effects of cooling and warming on the genome of 5¼ hpf zebrafish (*Danio rerio*) embryos

Experimental works in this part of the study were carried out in two stages. In the first stage, an existing protocol for cooling pre-hatched zebrafish (*Danio rerio*) embryos to -25˚C was optimised to cool 5¼ hpf embryos to -35˚C. In the second stage, the effects of cooling to -35˚C and subsequent warming on the genome of 5¼ hpf zebrafish embryos in terms of the event of DSBs, SSBs, and the occurrence of various forms of sequence alteration were investigated.

The optimisation of the cooling protocol began with adapting the existing protocol to cool 5¼ hpf embryos. It was found that the existing protocol resulted in significantly reduced survival of 5¼ hpf embryos. Two parameters of the cooling protocol, namely, thawing rate and CPA removal step, were then empirically optimised by cooling the embryos to -10˚C. It was found that a relatively faster thawing rate of ~425C/min and a 5 step removal of the CPA solution significantly improved the survival of 5¼ hpf embryos cooled to -10˚C. The optimised cooling protocol was then utilised to cool 5¼ hpf embryos to the lowest temperature possible with a reasonable survival rate that would yield sufficient number of embryos to carry out the experimental work in the subsequent parts of the study. Two CPAs, namely, MeOH and Me_2SO at 2M and 1.5M, respectively, were used as CPA to cool the embryos. The concentrations of the CPAs used in this part of the study were shown to be optimum for blastomere cells from 5¼ hpf zebrafish (*Danio rerio*) embryos (Lin et al., 2009). The optimised cooling protocol resulted in successful cooling of 5¼ hpf embryos to subzero temperature as low as -40˚C. However, the survival rate of the embryos cooled to -40˚C was very low to allow subsequent experimental works, whereas, the survival rate of the embryos cooled to -35˚C was reasonably sufficient to allow manipulation in the subsequent experiments. Therefore, in the subsequent experiments, the investigation of the effects of cooling and warming on the genome was carried out on the embryos cooled to -35˚C.

To investigate the effects of cooling to -35˚C and subsequent warming on the genome of 5¼ hpf zebrafish (*Danio rerio*) embryos in the context of the occurrences of DSBs and SSBs, the patterns of phosphorylated proteins detected in such embryos by S*/T*Q antibody was compared against the patterns of phosphorylated proteins in camptothecin-treated and H_2O_2-treated embryos. It was found that cooling the embryos to -35˚C using

MeOH as CPA did not induce DSBs but induced SSBs in the genome. However, in a follow up experiment investigating the SSB-activated DDR proteins in the embryos cooled to -35˚C, warmed and provided with 30 minutes recovery time, it was found that SSB-affected DDR proteins returned to the base line levels. The finding indicated that the observed SSBs in the embryos cooled to -35˚C were repaired when provided with an appropriate recovery time. It was also found that cooling to -35˚C using 1.5 M Me_2SO as CPA did not induce either DSBs or SSBs in the genome of 5¼ hpf zebrafish (*Danio rerio*) embryos.

The study then analysed the expression profiles of the genes selected from the ERMs as indicators of the occurrence of various forms of sequence alteration in the genome of 5¼ hpf embryos cooled to -35C and warmed subsequently. It was found that in the embryos cooled to -35˚C using MeOH as CPA, the expression of the gene *ERCC1* was significantly increased, whereas, that of the genes *UDG* and *MSH2* was significantly decreased. The genes *ERCC1*, *UDG* and *MSH2* are representatives of the NER, the BER, and the MMR mechanisms, respectively. Therefore, the findings indicate that in the embryos cooled using MeOH as CPA, the NER mechanism was up-regulated suggesting that the occurrence of helix distorting single stranded lesion was increased in the embryos. The findings also indicate that the embryos were susceptible to increased occurrence of misincorporation of uracil and other mismatched bases in the DNA as the gene *UDG* in the BER is responsible for removing misincorporated uracil from DNA and the gene *MSH2* in the MMR is responsible for detecting mismatched bases in the DNA. Conversely, in the embryos cooled using Me_2SO as CPA, the expression of the gene *TDG* from the *TDG*-dependant BER was significantly increased. Since the gene *TDG* is responsible for encoding protein that remove misincroporated thymine from DNA, the finding indicated that the occurrence of misincorporated thymine was increased in 5 ¼ hpf embryos cooled to -35˚Cusing Me_2SO as CPA.

7.3 Conclusions

The present study embarked on to investigate how biological objects respond to different cryopreservation parameters, and thereby, characterise the nature of the putative DNA damage in the context of the occurrences of DSBs, SSBs, and the occurrence of various

forms of sequence alteration in the genome. To that end, the study was successful to achieve its goal. The study monitored the responses from 5¼ hpf zebrafish (*Danio rerio*) embryos to the occurrences of DSBs and SSBs in the genome and then compared such responses to the responses of the embryos to different cryopreservation parameters. The study also analysed the genome maintenance mechanisms, the ERMs, with a view to investigate the effects of different cryopreservation parameters in terms of the occurrence of various forms of sequence alteration in the genome. The overall finding of the study indicated that the cryopreservation parameters did not induce DSBs but induced SSBs in the genome, which were readily repaired. However, the findings of the present study indicated that the cryopreserved biological objects may be susceptible increased occurrence of various sequence alterations in the genome.

The present study made original contributions into a number of areas, which may be of interest to the scientific community. The original contributions made by the current study are outlined as follows:

a) Development of a novel method that eliminated non-specific binding inherent to biotin-streptavidin/avidin detection system

The experimental work in this study led to the development of a novel method that efficiently eliminated non-specific binding resulting from biotin-streptavidin/avidin detection system commonly used in Western blot, ELISA, IHC and ICC. In biotin-streptavidin/avidin detection system, the secondary antibody is biotinylated and the reporter molecule is coupled to a streptavidin or avidin molecule. In an immunological technique such as Western blot, the primary antibody bound to the antigen of interest is probed with the secondary antibody raised against the IgG molecule of the species in which the primary antibody was raised. The complex of the primary antibody and the secondary antibody is then identified or localised via streptavidin molecule coupled to a reporter molecule. However, the streptavidin molecule coupled to the reporter molecule binds to any endogenous biotin or biotinylated proteins resulting in non-specific bands in Western blot or false positive signals in other immunological techniques. The method developed in this study is based on pre-hybridisation of the biotinylated secondary antibody and the streptavidin/avidin-coupled reporter molecule. Pre-hybridisation facilitates binding four molecules of biotinylated secondary antibody to four biotin-binding sites in the

streptavidin/avidin molecule resulting in a complex in which the streptavidin or avidin molecule does not have any free biotin binding sites. Consequently, when the complex is used to detect or localised the primary antibody bound to the antigen of interest, the streptavidin or avidin molecule coupled to the reporter molecule can not bind to endogenous biotin or biotinylated proteins; and the only reactive sites remained in the complex are the four secondary antibody bound to the streptavidin or avidin molecule. As a result, any signal generated from such a complex would be due to the affinity of the secondary antibody for the primary antibody. The method was successfully applied in all Western blot experiments carried out in the present study. However, the method is not limited to Western blot only; it can be applied to any immunological technique that employs biotin-streptavidin/avidin as detection system, where it would eliminate the non-specific binding without the need for a costly second blocking step for endogenous biotin or biotinylated proteins.

1) Development of zebrafish (*Danio rerio*) protein based assays for DNA DSBs and SSBs

This is the first study to develop Western blot based assays for native zebrafish proteins affected in the event of DSBs and SSBs in the genome. The study utilised an antibody against the common substrate motif of DSB-activated kinase ATM and SSB-activated kinase ATR to detect the downstream substrate proteins activated in 5¼ hpf embryos treated with DSB inducing drug camptothecin and SSB inducing chemical H_2O_2, respectively. It was found that a total of five proteins of apparent molecular weight of 22 kDa, 31 kDa, 34 kDa, 62 kDa and 100 kDa were phosphorylated in the embryos in response to camptothecin-induced DSBs. It was also found that two proteins of apparent molecular weight of 38 kDa and 150 kDa were hypophosphorylated and dephosphorylated, respectively, in camptothecin-treated embryos. The 150 kDa protein was found dephosphorylated in H_2O_2 -treated embryos too. However, it was of great interest to notice that the 38 kDa protein, which was hypophosphorylated in camptothecin-treated embryos, was hyperphosphorylated in H_2O_2-treated embryos. The 38 kDa protein appeared to be a novel protein as there is no mention of such a protein in any published literature. Similarly, the 150 kDa proteins together with the 22 kDa, 31 kDa and 100 kDa proteins also have not been reported before. To that end, the current study is the first

to report these proteins and further research needs to be undertaken to identify these proteins. Eukaryotic DDR is mediated by a concerted action of the cell cycle check points and the DNA repair mechanisms. Cell cycle checkpoints arrest cell cycle via down-regulation or deactivation of key proteins that promote cell cycle so that the damage could be repaired by the DNA repair mechanism. To that effect, the current study has managed to capture the whole or a large portion of the DDR in 5¼ hpf zebrafish (*Danio rerio*) embryos in a single Western blot. The findings of this part of the study added to the notion about the status of zebrafish as an ideal model organism for studying key eukaryotic metabolic pathways. The findings will also be of great interest to researchers investigating eukaryotic DDR in the context of various human neoplastic diseases.

2) Utilisation of the ERMs as indicators of the occurrence of various forms of sequence alteration in the genome

The ERMs are responsible maintaining the genomic integrity by correcting the lesser forms of DNA lesions that do not result in strand breaks. The individual ERMs are responsible for correcting specific forms of DNA lesions. Therefore, the activity of a particular ERM would serve as an indication of the extent of the occurrence of the form of DNA lesion repaired by the pathway. The present study is the first to utilise the expression levels of a number of key genes from the individual ERMs as indicators of the occurrence of sequence alteration in the genome of 5¼ hpf zebrafish (*Danio rerio*) embryos treated with different cryopreservation parameters.

3) Investigation of DDR in chilled embryos

Chilling temperature has been shown to impart oxidative stress on biological objects (Tsang et al., 1991; Fujita 1999) and apoptosis. The effects of chilling temperature on 5 ¼ hpf zebrafish embryos in terms of survival and gene expression had been investigated in the past. This is the first study to investigate the effects of chilling temperature on 5¼ hpf zebrafish (*Danio rerio*) embryos in the context of the occurrence of DSBs, SSBs and various forms of sequence alteration. It was found that short term chilling did not induce DSBs or SSBs but increased the occurrence of

mismatched DNA bases in the genome of 5¼ hpf zebrafish (*Danio rerio*) embryos. The findings of the study would be of great significance to the scientific community interested in chilled storage of biological objects for research and transplantation purposes.

4) Investigation of DDR in CPA-treated embryos

CPA treatment has been linked with increased DNA fragmentation and decreased cell survival (Rajaei et al., 2005). This is the first study to investigate the occurrence of DSBs, SSBs and various sequence alterations in the genome of biological objects treated with CPAs. Effects of CPAs on 5¼ hpf zebrafish embryos in terms of embryo survival had been studied in the past (Lin et al., 2009) but this is the first study to investigate the effects of CPA on 5¼ hpf zebrafish embryos in the context of various forms of DNA damage. It was found that MeOH and Me_2SO did not induce DSBs or SSBs but up-regulated the *UDG*-dependant BER mechanisms, indicating increased occurrence of uracil misincorporation in the genome of the embryos. It was of great significance to observe that both of the CPAs down-regulated the gene from the *TDG*-dependant BER, the gene ERCC1 from the NER and the gene MSH2 from the MMR mechanisms. The down-regulation of the gene was suggestive of gene silencing via the epigenetic event, DNA methylation; and the present study is the first to report such event. However, further investigation needs to be carried out to identify the underlying cause of gene suppression following CPA treatment. The finding of the study, nonetheless, would provide valuable information to the scientific community interested in cryopreservation of biological objects as well as epigenetic event of DNA methylation.

5) Optimisation of a protocol to cool 5¼ hpf zebrafish (*Danio rerio*) embryos to -35˚C

Pre-hatched zebrafish embryos had been cooled to subzero temperature, as low as -25˚C in the past (Zhang et al., 1993). This is the first study to report cooling of 5¼ hpf zebrafish (*Danio rerio*) embryos to subzero temperature as low as -35˚C. The finding of this study would be of great significance to researchers interested in

cryopreservation of zebrafish (*Danio rerio*) embryos. This is also the first study to investigate the occurrence of DSBs, SSBs, and various sequence alteration in the genome of 5¼ hpf zebrafish (*Danio rerio*) embryos cooled to -35˚C. The study found that cooling to -35˚C using MeOH as CPA and subsequent warming did not induce DSBs but induced SSBs in the genome of the embryos; and the SSBs were repaired when the embryos were provided with a recovery time. Cooling of the embryos to -35˚C using MeOH as CPA also up-regulated the NER mechanism, indicating an increased occurrence of helix distorting single stranded DNA lesions. On the other hand, cooling to -35C using Me_2SO as CPA did not result in the occurrence of DSBs or SSBs in the genome of 5¼ hpf zebrafish (*Danio rerio*) embryos. However, in Me_2SO-cooled embryos, the *TDG*-dependant BER mechanism was up-regulated indicating an increased occurrence of misincoporated thymine in the genome. The finding of this part of the study would significantly enhance the current knowledge of the effects of cryopreservation on the genome of biological objects.

7.4 Future work

The findings of the present study raised a number of questions regarding the DDR in zebrafish (*Danio rerio*) embryos and the effects of different cryopreservation parameters on the genome. Further investigation in the following areas would significantly enhance the understanding of the DDR in zebrafish (*Danio rerio*) embryos as well as the effects of different cryopreservation parameters on the genome.

7.4.1 Identification of the DDR proteins detected in 5¼ hpf zebrafish (*Danio rerio*) embryos

Some of the downstream substrates of ATM and ATR kinases, the 38 kDa and the 150 kDa proteins in particular, as detected in the present study have not been reported previously. The 38 kDa protein was down-regulated in the event of DSBs but up-regulated in the event of SSBs, whereas, the 150 kDa protein was deactivated in the event of both DSBs and SSBs. The expression patterns of the proteins indicated that these proteins play essential roles in cell cycle checkpoints. However, there is no mention of such proteins in any published literature. Therefore, a thorough investigation needs to be carried out to determine the identity of these proteins. To that effect, a technique known

as matrix-assisted laser desorption ionisation-mass spectrometry-peptide mass fingerprinting (MALDI-MS-PMF) could be utilised. In this technique, the protein of interest is purified using 2-D gel electrophoresis, enzymatically or chemically cleaved and analysed by mass spectrometry. The peptide fingerprint obtained thus is then compared to virtual fingerprints of peptide sequences stored in databases (Gevaert and Vandekerckhove, 2000). If MALDI-MS-PMF analysis does not result in identification of the proteins, *de novo* sequencing of the proteins could be undertaken using a technique known as electrospray ionisation-tandem mass spectrometry (ESI-tandem MS) (Jensen et al., 199). Identification of the proteins will significantly enhance our understanding of zebrafish (*Danio rerio*) DDR.

7.4.2 Investigation of DNA methylation by CPAs

The present study found that both of the CPAs, namely, MeOH and Me_2SO, down-regulated the expression of some of the genes of the ERMs. The pattern of down-regulation of the genes was suggestive of gene silencing via DNA methylation and both of the CPAs are known to have methylating properties. The findings of the present study, therefore, called for further research into the investigation of the effects of the CPAs in the context of DNA methylation. There are a number of techniques available for studying DNA methylation, most of which are based on selective de-amination of cytosine to uracil via sodium bisulfite. Methylation specific PCR (MSP) is one such technique. In this technique, cytosines in DNA samples are converted to uracils by sodium bisulfite treatment, while cytosines that are methylated (5-methylcytosines) are resistant to this modification and remain cytosines. Bisulfite-modified DNA is then amplified using methylation-specific primers that can distinguish methylated DNA from unmethylated DNA. Because the distinction is part of the PCR amplification, extraordinary sensitivity can be achieved while maintaining specificity. Results are obtained immediately following PCR amplification and gel electrophoresis without the need for further analysis (Herman et al., 1996). MSP could be utilised to investigate the extent of global DNA methylation in the CPA-treated embryos, the finding of which would provide important insights in the effects of the CPAs on the genome.

7.4.3 Investigation of the occurrence of mutation

Down-regulation of the ERMs in the embryos treated with different cryopreservation parameters as observed in the present study indicated that the embryos were susceptible to increased occurrence of the lesions repaired by the particular ERMs. Therefore, further research need to be undertaken to investigate if the putative sequence alterations in the genome amount to mutation being introduced into the genome. There are a large number of techniques available for investigating global mutation in the genome. Among the techniques, denaturing gradient gel electrophoresis (DGGE) is the most commonly used to that effect. DGGE could be utilised to investigate the occurrence of global mutation in the genome of the embryos treated the CPAs. High resolution melting (HRM) analysis is yet another powerful technique to investigate mutation in the genome. However, the technique requires prior knowledge of the mutated gene to be analysed. Nevertheless, the technique could be utilised to investigate the occurrence of mutation in a mutation-prone gene such as *p53* in the embryos treated with the CPAs. The p53 gene is extremely susceptible to mutation as evident by the fact that it is mutated in 45-50% of all human cancers (Greenblatt et al., 1994). HRM analysis of the p53 gene would serve as an indication of the occurrence of global mutation in the genome of the embryos treated the CPAs. The study also found that MeOH-mediated cooling resulted in the occurrence of SSBs in the genome of the embryos, and the SSBs were repaired when the embryos were provided with a recovery time. Since, most of the eukaryotic repair mechanisms are error prone (as discussed in chapter 1), the occurrence of global mutation should be investigated in the cooled embryos too.

7.5 Closing words

The main aim of this research was to characterise the effects of different cryopreservation parameters on biological objects in the context of DSBs, SSBs and other lesser forms of single stranded DNA lesions. The exploratory work in this research has led to characterisation of the DSB-initiated DDR and SSB-initiated DDR in zebrafish (*Danio rerio*) embryos. The research has also exemplified the utilisation the ERMs as indications of various sequence alterations in the genome. This work has enlightened a number of areas for further investigation, which would greatly redefine the current dogma of the effects of cryopreservation on the genome of a biological object.

REFERENCES

Abcam Plc. (2012) 'Western Blotting: A Beginner's Guide' (online). Available at www.abcam.com/ps/pdf/protocols/WB-beginer.pdf. [Accessed on 02/2012]

Abraham, R. (*2001*). 'Cell cycle checkpoint signaling through the ATM and ATR kinases'. *Genes Dev. 15, 2177–2196.*

Alban, A. M. (2003) 'Cryopreservation of bovine oocytes: current status and recent developments'. *Reprod Nutr Dev,* 43**,** 325-330.

Ananthaswamy, H. and Eisenstark, A. (1977). 'Repair of hydrogen peroxide-induced single-strand breaks in Escherichia coli deoxyribonucleic acid'. *Journal of bacteriology*, 130**,** 187-191.

Ataian, Y. and Krebs, J. E. (2006). 'Five repair pathways in one context: chromatin modification during DNA repair' *Biochemistry and cell biology,* 84**,** 490-494.

Auclair, Y., Rouget, R., Affar, E. B. and Drobetsky, E. A. (2008). 'ATR kinase is required for global genomic nucleotide excision repair exclusively during S phase in human cells'. *Proceedings of the National Academy of Sciences*, 105**,** 17896-17901.

Balajee, A., and Geard, C (2006) 'Is Ataxia Telangiectasia a Result of Impaired Cordination between DNA Repair and Cell Cycle Checkpoint Regulators?' In Balajee, A. (ed) *DNA Repair and Human Disease*, Springer Science: New York

Balasubramanian, S., and Rho, G.J (2006) 'Effect of chilling on the development of in vitro produced bovine embryos at various cleavage stages'. *Journal of Assisted Reproduction and Genetics,* 23**,** 55-61.

Ball, B. A., Vo, A. T., and Baumber, J. (2001) 'Reactive oxygen species generation by equine spermatozoa'. *Am J Vet Res,* 62:5508–5515.

Barbazuk, W. B., Korf, I., Kadavi, C., Heyen, J., Tate, S., Wun, E., Bedell, J. A., Mcpherson, J. D. and Johnson, S. L. (2000). 'The Syntenic Relationship of the Zebrafish and Human Genomes'. *Genome Research,* 10**,** 1351-1358.

Baumber, J., Ball, B. A., Linfor, J. J. & Meyers, S. A. 2003. Reactive Oxygen Species and Cryopreservation Promote DNA Fragmentation in Equine Spermatozoa. *J Androl,* 24**,** 621-628.

Beckwith, L. G., Moore, J. L., Tsao-Wu, G.S., Harshbarger, J. C., and Cheng, K. C. (2000) 'Ethylnitrosourea induces neoplasia in zebrafish (*Danio rerio*)'. *Lab Invest* 80*:*379*–385*

Bender, C. M., Zingg, J. M. and Jones, P. A. (1998). 'DNA Methylation as a Target for Drug Design'. *Pharmaceutical Research,* 15**,** 175-187.

Best, B. (2012) 'Viability, Cryoprotectant Toxicity and Chilling Injury in Cryonics', (online). Available at www.benbest.com/cryonics/viable/html [accessed on 02/12/2012]

Bird, A. (2002). 'DNA methylation patterns and epigenetic memory'. *Genes & Development,* 16**,** 6-21.

Blackledge, N. P. and Klose, R. (2011). 'CpG island chromatin: A platform for gene regulation'. *Epigenetics,* 6**,** 147-152.

Blanpain, C., Mohrin, M., Sotiropoulou, P. A. and Passegue, E. (2011) 'DNA-Damage Response in Tissue-Specific and Cancer Stem Cells'. *Cell Stem Cell,* 8**,** 16-29.

Boenisch, T. (2009) 'Antibodies' in Kumar, L. G and Rudbeck, L. *Immunohistochemical Staining Methods.* 5th edition (online). Available at http://www.dako.com/08002_ihc_staining_methods_5ed.pdf

Chanoux, R. A., Yin, B., Urtishak, K.A., Asare, A., Bassing, C. H., and Brown, E. J. (2009) 'ATR and H2AX cooperate in maintaining genome stability under replication stress'. *J. Biol. Chem*. 284:5994–6003.

Chen, B. P. C., Uematsu, N., Kobayashi, J (2007) 'Ataxia telangiectasia mutated (ATM) is essential for DNA-PKcs phosphorylations at the Thr-2609 cluster upon DNA double strand break' *Journal of Biological Chemistry*, vol. 282, no. 9, 6582–6587.

Chen, G., liu, H., Wang, X. and Li, Z. (2010). ,In vitro methylation by methanol: Proteomic screening and prevalence investigation'. *Analytica Chimica Acta,* 661**,** 67-75.

Choi, M. R., Park, J., Park, T., Jung, K. H., Chai, J. C., Chung, M. K., Lee, Y. S. and Chai, Y. G. (2012). 'Genome-scale DNA methylation pattern profiling of human bone marrow mesenchymal stem cells in long-term culture'. *Experimental & Molecular Medicine,* 44**,** 503-512.

Collins, A. R., Oscoz, A. A., Brunborg, G., Gaivo, I., Giovannelli, L., Kruszewski, M., Smith, C. C. Ttina, R. (2008). 'The comet assay: topical issues'. *Mutagenesis,* 23**,** 143-151.

Cooke, M. S., Evans, M. D., Dizdaroglu, M. & Lunec, J. (2003). 'Oxidative DNA damage: mechanisms, mutation, and disease'. *The FASEB Journal,* 17**,** 1195-1214.

Cooper, M. G and Hausman, R. E. (2009) 'The Cell: A Molecular Approach' 5th Edition, ASM Press/Sinauer, Washington, D.C.

Corbett Research (2006) 'High Resolution Melt Assay Design and Analysis' *CorProtocol™ 6000-1-Sept06*

Cox M. M., Doudna, J. A., and O'Donnell, M. (2012) *Molecular Biology: Principles and Practice,* W. H. Freeman and Company: New York.

Das, P. M. and Singal, R. (2004). ,DNA Methylation and Cancer'. *Journal of Clinical Oncology,* 22**,** 4632-4642.

De Gruijl, F. R., Van Kranen, H. J. and Mullenders, L. H. F. (2001). 'UV-induced DNA damage, repair, mutations and oncogenic pathways in skin cancer'. *Journal of Photochemistry and Photobiology B: Biology,* 63**,** 19-27.

Demott, M. S., Zigman, S. anhd Bambara, R. A. (1998). ’Replication Protein A Stimulates Long Patch DNA Base Excision Repair’. *Journal of Biological Chemistry*, 273**,** 27492-27498.

Derheimer, F. A. and Kastan, M. B. (2010). Multiple roles of ATM in monitoring and maintaining DNA integrity. *FEBS letters,* 584**,** 3675-3681.

Desai, K., Spikings, E. and Zhang, T. (2011). ‘Effect of chilling on sox2, sox3 and sox19a gene expression in zebrafish (*Danio rerio*) embryos’. *Cryobiology*, 63**,** 96-103.

Dinant, C., Houtsmuller, B., Vermeulen, W. (2008) ‘Chromatin structure and DNA damage repair’. *Epigenetics & Chromatin*, 1:9

Drobnis, E. Z., Crowe, L. M., Berger, T., Anchordoguy, T. J., Overstreet, J. W. and Crowe, J. H. (1993) 'Cold shock damage is due to lipid phase transitions in cell membranes: A demonstration using sperm as a model', *Journal of Experimental Zoology*, 265(4), 432-437.

Du, Y., Zhang, L., Xu, F., Huang, B., Zhang, G. and Li, L. (2013). ‘Validation of housekeeping genes as internal controls for studying gene expression during Pacific oyster (Crassostrea gigas) development by quantitative real-time PCR’. *Fish & Shellfish Immunology,* 34**,** 939-945.

Duru, N. K., Morshedi, M. S., Schuffner, A. & Oehninger, S. (2001) ‘Cryopreservation-Thawing of fractionated human spermatozoa is associated with membrane phosphatidylserine externalization and not DNA fragmentation’. *J Androl,* 22**,** 646-651.

Education Portal, (2013). ‘What is DNA?’ *Structure, Lesson & Quiz* (Online). Available at http://education-portal.com/academy/lesson/what-is-dna---structure-lesson-quiz.html [Accessed on 02/03/2013]

Eells, J. T., Henry, M. M., Lewandowski, M. F., Seme, M. T., and Murray, T. G. (2000) ‘Development and characterisation of a rodent model of methanol-induced retinal and optic nerve toxicity’ , *Neurotoxicology,* 21 (3): 321-330.

Elmore S. (2007) 'Apoptosis: a review of programmed cell death'. *Toxicol Pathol* 35(4):495-516,

Fernandez-Capetillo, O. and Murga, M. (2008). 'Why cells respond differently to DNA damage: A chromatin perspective,. *Cell Cycle,* 7**,** 980-983.
Fleck, O., Nielsen, O (2004) 'DNA Repair'. *Journal of Cell Science* 117, 515-517.

Flynn, R. L., Zou, L. (2011) 'ATR: a master conductor of cellular responses to DNA replication stresse'. *Trends Biochem Sci*. 2011; 36:133–140

Fortini, P., Pascucci, B., Belisario, F. and Dogliotti, E. (2000). 'DNA polymerase β is required for efficient DNA strand break repair induced by methyl methanesulfonate but not by hydrogen peroxide'. *Nucleic Acids Research,* 28**,** 3040-3046.

Fujita, J. (1999) 'Cold shock response in mammalian cells', *J Mol Microbiol Biotechnol,* 1(2):243-255

Gentle, A., Anastasopoulos, F and McBrien, N. A. (2001) 'High-resolution semi-quantitative real-time PCR without the use of a standard curve', *Biotechniques,* 31(3):502, 504-6, 508.

Gevaert, K. and Vandekerckhove, J. (2000). 'Protein identification methods in proteomics'. *Electrophoresis,* 21**,** 1145-1154.

Grabarz, A., Barascu, A., Guirouilh-Barbat, J., Lopez, B. S. (2012) 'Initiation of DNA double strand break repair: signaling and single-stranded resection dictate the choice between homologous recombination, non-homologous end-joining and alternative end-joining'. *American Journal of Cancer Res*. 2 (3): 249–268.

Gracia-Kaeufer, M., Hafner, C., Gartisar, S., Keiter, S. H., and Hollert, H. (2009) 'Evaluation of genotoxicity od sediment samples using zebrafish embryos and comet assay' (online). Avaliable at http://www.hydrotox.de/pdf/SETAC%20DanTox%20Comet%2012-05-2012.pdf [Accessed on 02/12/2012].

Grafstrom, R. C., Fornace, A. and Harris, C. C. (1984). 'Repair of DNA Damage Caused by Formaldehyde in Human Cells'. *Cancer Research,* 44**,** 4323-4327

Greenblatt, M. S., Bennet, W. P., Holstein, M., and Harris, C.C. (1994) 'Mutations in the p53 tumour suppressor gene: clues to cancer etiology and molecular pathogenesis'. *Cancer Res* 54: 4855-4878

Gregory, C. D. and Milner, A. E. (1994). 'Regulation of cell survival in burkitt lymphoma: Implications from studies of apoptosis following cold-shock treatment'. *International Journal of Cancer,* 57**,** 419-426.

Grudzenski, S., Raths, A., Conrad, S., Rübe, C. E. and Löbrich, M. (2010). 'Inducible response required for repair of low-dose radiation damage in human fibroblasts'. *Proceedings of the National Academy of Sciences*.

Gudmundsdottir, K., Witt, E., Ashworth, E. (2006) *Roles of the BRCA1 and BRCA2 Breast Cancer Susceptibility Proteins in DNA Repair* In In Balajee, A. (ed) DNA Repair and Human Disease, Springer Science: New York

Hays, L. M., Crowe, J. H., Wolkers, W. and Rudenko, S. (2001). 'Factors Affecting Leakage of Trapped Solutes from Phospholipid Vesicles during Thermotropic Phase Transitions'. *Cryobiology,* 42**,** 88-102.

Helleday, T. (2003). 'Pathways for mitotic homologous recombination in mammalian cells'. *Mutation Research/Fundamental and Molecular Mechanisms of Mutagenesis,* 532**,** 103-115.

Herman, J. G., Graff, J. R., Myöhänen, S., Nelkin, B. D. and Baylin, S. B. (1996). 'Methylation-specific PCR: a novel PCR assay for methylation status of CpG islands'. *Proceedings of the National Academy of Sciences,* 93**,** 9821-9826.

Hagedorn, M., Mccarthy, M., Carter, V. L. and Meyers, S. A. (2012). 'Oxidative Stress in Zebrafish (*Danio rerio*) Sperm'. *PLoS ONE,* 7**,** e39397.

Haramis, A. P., Hurlstone, A., Van der Velden, Y. (2006) 'Adenomatous polyposis coli-deficient zebrafish are susceptible to digestive tract neoplasia'. *EMBO Rep,* 7*:*444*–449*

Hill, A. J., Teraoka, H., Heideman, W., and Peterson, R. (2005) 'Zebrafish as a Model Vertebrate for Investigating Chemical Toxicity' *Biological Sciences,* 86 (1): 6-9

Ho, R. and Kimmel, C. (1993) 'Commitment of cell fate in the early zebrafish embryo'. *Science*, 261**,** 109-111.

Ikegami R, Rivera-Bennetts AK, Brooker DL, Yager TD (1997) 'Effect of inhibitors of DNA replication on early zebrafish embryos: evidence for coordinate activation of multiple intrinsic cell-cycle checkpoints at the mid-blastula transition'. *Zygote*. (2):153-75.

Iwatani, M., Ikegami, K., Kremenska, Y., Hattori, N., Tanaka, S., YAGI, S. and Shiota, K. (2006). 'Dimethyl sulfoxide has an impact on epigenetic profile in mouse embryoid body'. *Stem Cells,* 24**,** 2549-2556.

Jain, M., Nijhawan, A., Tyagi, A. K. and Khurana, J. P. (2006). 'Validation of housekeeping genes as internal control for studying gene expression in rice by quantitative real-time PCR'. *Biochemical and Biophysical Research Communications,* 345**,** 646-651.

Jensen, E. C. (2012). 'The Basics of Western Blotting'. *The Anatomical Record: Advances in Integrative Anatomy and Evolutionary Biology,* 295**,** 369-371.

Jensen, O., Wilm, M., Shevchenko, A. and Mann, M. (1999). ,Sample Preparation Methods for Mass Spectrometric Peptide Mapping Directly from 2-DE Gels'. *In:* Link, A. (ed.) *2-D Proteome Analysis Protocols.* Humana Press.

Kastan, M. B. and Lim, D. S. (2000). 'The many substrates and functions of ATM'. *Nat Rev Mol Cell Biol,* 1**,** 179-186.

Kapa Biosystem (2013). 'Introduction to High Resolution Melt Analysis', (Online). Available at http://www.kapabiosystems.com/public/pdfs/kapa-hrm-fast-pcr-kits/Introduction_to_High_Resolution_Melt_Analysis_Guide.pdf [Accessed on 08/2012]

Kent, M. L., Bishop-Stewart, j. k., Matthews, J. L., Spitsbergen, J. M. (2002) 'Pseudocapilliaria tomentosa, a nematode pathogen, and associated neoplasms of zebrafish (*Danio rerio*) kept in research colonies', *Comp Med,* 52: 354-358

Kim, S.T., Lim, D.S., Canman, C. E., Kastan, M. B. (1999) 'Substrate specificities and identification of putative substrates of ATM kinase family members'. *J. Biol. Chem.* 274:37538-37543.

Komrakova, M. and Holtz, W. (2009). 'Factors responsible for successful chilled storage of unfertilized rainbow trout (Oncorhynchus mykiss) eggs'. *Aquaculture,* 286**,** 156-163.

Kong, Y., Cui, H., Ramkumar, C. and Zhang, H. (2011). 'Regulation of Senescence in Cancer and Aging'. *Journal of Aging Research,* 2011.

Kopeika, J., Zhang, T., Rawson, D. M., Holt., D.W. (2003) 'Detrimental effects of cryopreservation of loach (Misgurnus fossilis) sperm on subsequent embryo development are reversed by incubating fertilised eggs in caffeine'. *Cryobiology. 46, 43-52*

Kopeika, J., Zhang, T., Rawson, D. M., Elgar, G (2005) 'Effect of cryopreservation on mitochondrial DNA zebrafish (*Danio rerio*) blastomere cells'. *Mutar Res., 570, 49-61*

Kosmehl, T., Hallare, A. V., Reifferscheid, G., Manz, W., Braunbeck, T. and Hollert, H. (2006). 'A novel contact assay for testing genotoxicity of chemicals and whole sediments in zebrafish embryos'. *Environmental Toxicology And Chemistry / SETAC,* 25**,** 2097-2106.

Kunkel, T. A. (2004). 'DNA Replication Fidelity'. *Journal of Biological Chemistry,* 279**,** 16895-16898.

Kyrylkova, K., Kyryachenko, S., Leid, M. and Kioussi, C. (2012). 'Detection of Apoptosis by TUNEL Assay'. *In:* Kioussi, C. (ed.) *Odontogenesis.* Humana Press.

Lattman, E. E. (1994) 'Small angle scattering studies of protein folding', *Current Opinion in Structural Biology,* 4(1), 87-92.

Lawen, A. (2003). 'Apoptosis—an introduction'. *BioEssays*, 25**,** 888-896

Lempiainen, H. and Halazonetis, T. D. (2009). 'Emerging common themes in regulation of PIKKs and PI3Ks'. *The EMBO journal,* 28**,** 3067-3073.

Li, Z., Musich, P. R., Serrano, M. A., Dong, Z., and Zou, Y. (2011) 'XPA-Mediated Regulation of Global Nucleotide Excision Repair by ATR is p53-Dependant and Occurs Primarilly in S-Phase.' *Plos ONE* 6 (12): e28326

Lin, C., Spikings, E., Zhang, T. and Rawson, D. (2009a) 'Housekeeping genes for cryopreservation studies on zebrafish embryos and blastomeres', *Theriogenology*, 71(7), 1147-1155.

Lin, C., Spikings, E., Zhang, T. and Rawson, D. M. (2009b) 'Effect of chilling and cryopreservation on expression of Pax genes in zebrafish (Danio rerio) embryos and blastomeres', *Cryobiology*, 59(1), 42-47.

Lindahl, T. (1993) 'Instability and decay of the primary structure of DNA'. *Nature*, 362 (6422), 709-715.

Linfor, J and Meyers, A. (2002) 'Detection of DNA Damage in Response to Cooling Injury in Equine Spermatozoa Using Single-Cell Gel Electrophoresis'. *Journal of Andrology, 23:107–113* .

Link, V., Shevchenko, A., Heisenberg, C. P (2006) Proteomics of early zebrafish embryos'. *Bmc developmental biology*, 6**,** 1.

Liu, S., Shiotani, B., Lahiri, M., Maréchal, A., Tse, A., Leung, Charles Chung Y., Glover, J. N. M., Yang, Xiaohong H. and Zou, L. (2011). 'ATR Autophosphorylation as a Molecular Switch for Checkpoint Activation'. *Molecular Cell*, 43**,** 192-202.

Martin, G., Sabido, O., Durand, P., Levy, R (2004) 'Cryopreservation Induces an Apoptosis-1 Like Mechanism in Bull Sperm'. *Biology of Reproduction 10., 1095*

Matthews, J. L. (2004) 'Common diseases of laboratory zebrafish', *Methods Cell Biol*, 77: 617-643

Mazur, P. (1977) 'The role of intracellular freezing in the death of cells cooled at supraoptimal rates', *Cryobiology*, 14(3), 251-72.

Mazur, P. (2004) ‘Priciples of Cryobiology’' In Fuller, B. J., Lane, N. and Benson, E. E., eds., *Life in the Frozen State*, London: CRC Press, 415-435.

Mello Filho, A., Hoffmann, M. and Meneghini, R. (1984). ‘Cell killing and DNA damage by hydrogen peroxide are mediated by intracellular iron’. *Biochemical Journal*, 218**,** 273.

Millipore Corporation (2012) ‘Protein Blotting Handbook’, 6th Edition, (online). Available at www.milipore.com/techpublications/tech1/tp001en00. [Accessed on 02/2012]

Minard, B. J. and Cawley, L. P. (1978). ‘Use of horseradish peroxidase to block nonspecific enzyme uptake in immunoperoxidase microscopy’. *Journal of Histochemistry & Cytochemistry*, 26**,** 685-7.

Misun, H., Cha, Y., Luigi, M. and Bo, L. (2007) ‘Zebrafish as a Model System to Screen Radiation Modifiers’. *Current Genomics*, 8: 360-369.

Mizigireuv, I. V., Majorova, I. G., Gorodinskaya, V. M., Khudoley, V. V., and Revskoy, S. Y. (2004) ‘Carcinogenic effect of *N*-nitrosodimethylamine on diploid and triploid zebrafish (Danio rerio)’. *Toxicol Pathol*, 32: 514-518

Moore, C. (2009) ‘Introduction to Western Blotting’ (online). Available at www.abdserotec.com/westernblot [Accessed on 11/2012]

Morris JP, Berghmans S, Zahrieh D, Neuberg DS, Kanki JP (2003) ‘Zebrafish sperm cryopreservation with N,N-dimethylacetimide’. *Biotechniques* 35: 956–958.

Mordes, D. A. and Cortez, D. (2008) ‘Activation of ATR and related PIKKs’. *Cell Cycle*, 7, 2809-2812.

Muldrew, K., Acker, J. P., Elliot. J. A. W., McGann, L. (2004) 'The Water to Ice Transition: Implication for Living Cells’ In Fuller, B. J., Lane, N. and Benson, E. E., eds., *Life in the Frozen State*, London: CRC Press, 415-435.

Muslimović, A., Nyström, S., Gao, Y. and Hammarsten, O. (2009). ’Numerical Analysis of Etoposide Induced DNA Breaks’. *PLoS ONE,* 4**,** e5859.

Negritto, M. C. (2010) ‘Repairing Double-Strand DNA Breaks’. Nature Education 3(9):26

O'connell, D., Cox, L., hyland, W., Mcmahon, S., Graham, B., Gans, T. and Currell, F. (2010). ‘Interactions of cold atmospheric pressure plasma jets with plasmid DNA’. *In:* Plasma Science, Abstracts IEEE International Conference on, 20-24. 1-1.

Ortega-Ferrusola, C., Sotillo-Galan, Y., Varela-Fernandez, E., Gallardo-Bolanos, J. M., Muriel, A., Gonzalez-Fernandez, L., Tapia, J. A. & Pena, F. J. 2008. Detection of "Apoptosis-Like" Changes During the Cryopreservation Process in Equine Sperm. *J Androl,* 29**,** 213-221.

Ozkavukcu, S. and Erdemli, E. (2002). ‘Cryopreservation: basic knowledge and biophysical effects’. *J Ankara Medical School,* 24**,** 187-196.

Palmer, S., Wiegand, A. P., Maldarelli, F., Bazmi, H., Mican, J. M., Polis, M., Dewar, R. L., Planta, A., Liu, S., Metcalf, J. A., Mellors, J. W. and Coffin, J. M. (2003). ‘New Real-Time Reverse Transcriptase-Initiated PCR Assay with Single-Copy Sensitivity for Human Immunodeficiency Virus Type 1 RNA in Plasma.’ *Journal of Clinical Microbiology,* 41**,** 4531-4536.

Perez-Cerezales, S., Martinez-Paramo, S., Herraez, M (2008) ‘Sperm chromatin fragmentation and oxidization during short and long-term storage of sex reversed rainbow trout (*Oncorhynchus mykiss*) males’. *Cybium 2008, 32(2) suppl.: 221.*

Peris, S., Morrier, A., Dufour, M., Bailey, J (2004) ‘Cryopreservation of Ram Semen Facilitates Sperm DNA Damage: Relationship Between Sperm Andrological Parameters and the Sperm Chromatin Structure Assay’. *Journal of Andrology. 25, 224-233*

Pfaffl, M. W. (2004). ‘Quantification strategies in real-time PCR’. *AZ of quantitative PCR,* 1**,** 89-113.

Pollard, J. W., and Leibo, S. P. (1994) 'Chilling Sensitivity of Mammalian Embryos', *Theriogenology,* 41: 101-106

Pop, C. and Salvesen, G. S. (2009). 'Human Caspases: Activation, Specificity, and Regulation'. *Journal of Biological Chemistry,* 284**,** 21777-21781.

Prasad, T. K. (1996) 'Mechanisms of chilling-induced oxidative stress injury and tolerance in developing maize seedlings: changes in antioxidant system, oxidation of proteins and lipids, and protease activities', *The Plant Journal,* 10(6), 1017-1026.

Prokhortchouk E., and Hendrich B. (2002). 'Methyl-CpG binding proteins and cancer: Are MeCpGs more important than MBDs'? *Oncogene 21*:5394-5399

Purves, W. K., Orians, G. H., Heller, H. C., and Sadava, D (1997) 'Life: The Science of Biology, ***5th Edition Volume 1,*** W. H. Freeman & Company.

Rajaei, F., Karja, N.W.K., Agung, B., Wongsrikeao, P., Taniguchi, M., Murakami, M., Sambuu, R., Nii, M., Oti, T. (2005) 'Analysis of DNA fragmentation of porcine embryos exposed to cryoprotectants.' *Reproduction in domestic animals. 40. 429-432*

Robertson, K. D. and Jones, P. (2000). 'DNA methylation: past, present and future directions'. *Carcinogenesis,* 21**,** 461-467.

Rochette, P. J. and Brash, D. E. (2010). 'Human Telomeres Are Hypersensitive to UV-Induced DNA Damage and Refractory to Repair'. *PLoS Genet,* 6**,** e1000926.

Rodier, F. and Campisi, J. (2011) 'Four faces of cellular senescence'. *The Journal of Cell Biology,* 192**,** 547-556.

Rojas, E., Mussali, P., Tovar, E. and Valverde, M. (2009). '[DNA-AP sites generation by Etoposide in whole blood cells'. *BMC Cancer,* 9**,** 398.

Rundell, M. S., Wagner, E. D. and Plewa, M. J. (2003) 'The comet assay: Genotoxic damage or nuclear fragmentation?' *Environmental and Molecular Mutagenesis,* 42**,** 61-67.

Sabehat A, Lurie S, and Weiss D. (1998**). '**Expression of small heat -shock proteins at low temperatures'. *Plant Physiology***,** 117**,**651–*658.*

Saleh-Gohari , N., Bryant, H. E., Schultz, N., Parker, K. M., Cassel, T. N. And Helleday, T. (2005) 'Spontaneous Homologous Recombination Is Induced by Collapsed Replication Forks That Are Caused by Endogenous DNA Single-Strand Breaks'. *Molecular and Cellular Biology*, 25**,** 7158-7169.

Santoriello, C., Deflorian, G., Pezzimenti, F., Kawakami, K., Lanfrancone, L., D'adda Di Fagagna, F. and Mione, M. (2009). 'Expression of H-RASV12 in a zebrafish model of Costello syndrome causes cellular senescence in adult proliferating cells'. *Disease Models & Mechanisms*, 2**,** 56-67.

Scandalios, J. G. (1993) 'Oxygen Stress and Superoxide Dismutases', *Plant Physiol*, 101(1), 7-12.

Schraufstatter, I. U., Hinshaw, D. B., Hyslop, P. A., Spragg, R. G. and Cochrane, C. G. (1986). 'Oxidant injury of cells. DNA strand-breaks activate polyadenosine diphosphate-ribose polymerase and lead to depletion of nicotinamide adenine dinucleotide'. *Journal of Clinical Investigation*, 77**,** 1312.

Schneider, U and Mazur, P. (1984). 'Osmotic consequences of cryoprotectant permeability and its relation to the survival of frozen-thawed embryos', *Theriogenology*, 21(1), 68-79.

Shell, S. M., Li, Z., Shkriabai, N. (2009) 'Checkpoint kinase ATR promotes nucleotide excision repair of UV-induced DNA damage via physical interaction withxeroderma pigmentosum group A' *Journal of Biological Chemistry*, vol. 284, no. 36, 24213–24222

Shepard, J. L., Amatruda, J. F., Finkelstein, D. (2007) 'A mutation in separase causes genome instability and increased susceptibility to epithelial cancer'. *Genes Dev*, 21:55–*5*9

Singal, R., Ferris, R., Little, J. A., Wang, S. Z. and Ginder, G. D. (1997). 'Methylation of the minimal promoter of an embryonic globin gene silences transcription in primary erythroid cells'. *Proceedings of the National Academy of Sciences,* 94**,** 13724-13729.

Singal, R. and Ginder, G. D. (1999). 'DNA Methylation'. *Blood,* 93**,** 4059-4070.

Singal, R., Van Wert, J. and Bashambu, M. (2001). 'Cytosine Methylation Represses Glutathione S-Transferase P1 (GSTP1) Gene Expression in Human Prostate Cancer Cells'. *Cancer Research,* 61**,** 4820-4826.

Siu, W. Y., Lau, A., Arooz, T., Chow, J. P. H., Ho, H. T. B. and Poon, R. Y. C. (2004). 'Topoisomerase poisons differentially activate DNA damage checkpoints through ataxia-telangiectasia mutated–dependent and –independent mechanisms'. *Molecular Cancer Therapeutics,* 3**,** 621-632.

Smolowitz, R., Hanley, J., Richmond, H. (2002) 'A three year retrospective study of abdominal tumours in zebrafish maintained in an aquatic laboratory animal facility', *Biol Bull*, 203: 265-266

So, S., Davis, A. J. and Chen, D. J. (2009). 'Autophosphorylation at serine 1981 stabilizes ATM at DNA damage sites'. *The Journal of Cell Biology,* 187**,** 977-990.

Spitsbergen, J. M., Tsai, H. W., and Reddy, A. (2000), 'Neoplasia in zebrafish (*Danio rerio*) treated with 7,12-dimethylbenz[a]anthracene by two exposure routes at different developmental stages'. *Toxicol Pathol,* 28*:*705*–15*

Stokes, M. P., Rush, J., Macneill, J., Ren, J. M., Sprott, K., Nardone, J., Yang, V., Beausoleil, S. A., Gygi, S. P., Livingstone, M., Zhang, H., Polakiewicz, R. D. and Comb, M. J. (2007). 'Profiling of UV-induced ATM/ATR signaling pathways'. *Proceedings of the National Academy of Sciences,* 104**,** 19855-19860.

Sussman, R. (2007). 'DNA repair capacity of zebrafish'. *Proceedings of the National Academy of Sciences,* 104**,** 13379-13383.

Tate, P. H. and Bird, A. P. (1993). 'Effects of DNA methylation on DNA-binding proteins and gene expression'. *Current Opinion in Genetics & Development,* 3**,** 226-231.

Thaler, R., Spitzer, S., Karlic, H., Klaushofer, K. and Varga, F. (2012). 'DMSO is a strong inducer of DNA hydroxymethylation in pre-osteoblastic MC3T3-E1 cells'. *Epigenetics,* 7**,** 635-651.

Thermo Scientific (2013) 'Choosing a secondary antibody: A guide to fragment specificity' *Tech Tip 59* (online). Available at www.therno.com/pierce. [Accessed on 04/2013]

Thomson, L.K., Fleming, S.D., Aitken, R.J., De lulis, G.N., Zieshang, J.A, and Clark, A.M. (2009) 'Cryopreservation-induced human sperm DNA damage is predominantly mediated by oxidative stress rather than apoptosis', *Human Reproduction,* Vol.24: 2061-2070.

Tibbetts R.S. and Abraham R.T (2000)' 'PI3K-related kinases: Roles in cell-cycle regulation and DNA damage responses' in Gutkind J.S *ed. Signaling networks and cell cycle control: The molecular basis of cancer and other diseases,* Humana Press, Totowa, NJ, *pp 267–301.*

Tibbetts R.S., Brumbaugh K.M., Williams J.M., Sarkaria J.N., Cliby W.A., Shieh S.Y., Taya Y., Prives C., Abraham R.T.*(*1999*)* 'A role for ATR in the DNA damage-induced phosphorylation of p53'. *Genes & Dev. 13:152–157.*

Tsang, E. W., Bowler, C., Hérouart, D., Van Camp, W., Villarroel, R., Genetello, C., Van Montagu, M. and Inzé, D. (1991) 'Differential regulation of superoxide dismutases in plants exposed to environmental stress', *The Plant Cell Online,* 3(8), 783-92.

Uto, K., Inoue, D., Shimuta, K., Nakajo, N. and Sagata, N. 2004. Chk1, but not Chk2, inhibits Cdc25 phosphatases by a novel common mechanism. *EMBO J,* 23**,** 3386-3396.

Ukaji N, Kuwabara C, Takezawa D, Arakawa K, Yoshida S, Fujikawa S. (1999**).** **'**Accumulation of small heat shock protein homologs in the endoplasmic reticulum of cortical parenchyma cells in mulberry in association with seasonal cold acclimation'. *Plant Physiology*,120**,**481–***489.***

Valen, G. (2003). 'The basic biology of apoptosis and its implications for cardiac function and viability'. *Ann Thorac Surg*, 75**,** S656-660.

Van Der Mynsbrugge, J., Visur, M., Olsbye, U., Beato, P., Bjørgen, M., Van Speybroeck, V. and Svelle, S. (2012). 'Methylation of benzene by methanol: Single-site kinetics over H-ZSM-5 and H-beta zeolite catalysts'. *Journal of Catalysis*, 292**,** 201-212.

Wan, Q., Whang, I., Choi, C. Y., Lee, J.-S. and Lee, J. (2011). 'Validation of housekeeping genes as internal controls for studying biomarkers of endocrine-disrupting chemicals in disk abalone by real-time PCR'. *Comparative Biochemistry and Physiology Part C: Toxicology & Pharmacology*, 153**,** 259-268.

Wang, S., Gong, Z., Chen, R., Liu, Y., Li, A., Li, G. and Zhou, J. (2009). 'JWA regulates XRCC1 and functions as a novel base excision repair protein in oxidative-stress-induced DNA single-strand breaks'. *Nucleic Acids Research*, 37**,** 1936-1950.

Westerfield M. (2000). 'The zebrafish book. *A guide for the laboratory use of zebrafish (Danio rerio)*' 4th ed. Eugene, Univ. of Oregon Press

Wood, K. and Youle, R. (1995) 'The role of free radicals and p53 in neuron apoptosis in vivo', *The Journal of Neuroscience*, 15(8), 5851-5857.

Wood J.L, Chen J (2007) 'DNA damage sensing and signaling' In: Wei Q, Li L, and Chen DJ, (eds). *DNA Repair, Genetic Instability, and Cancer*. World Scientific Publishing. pp 1–22.

Wu, Q. and Vasquez, K. M. (2008). 'Human MLH1 Protein Participates in Genomic Damage Checkpoint Signaling in Response to DNA Interstrand Crosslinks, while MSH2 Functions in DNA Repair'. *PLoS Genet*, 4**,** e1000189.

Yajima, H., Lee, K. J., Zhang, S., Kobayashi, J., and Chen, B. P. C. (2009) 'DNA double-strand break formation upon UV-induced replication stress activates ATM and DNA-PKcs kinases' *Journal of Molecular Biology*, vol. 385, no. 3, 800–810.

Yang, J., Yu, Y., Hamrick, E., Penelope J (2003) 'ATM, ATR and DNA-PK: initiators of the cellular genotoxic stress responses'. *Carcinogenesis 24, 1571-1580*

Yang, J., Xu, Z., Huang, Y., Hamrick, E., Penelope J., Yu, Y (2004) 'ATM and AT: Sensing DNA damage'. *World Journal of Gastroenterology, 10, 155-160*

Yildiz, C., Ottaviani, P., Law, N., Ayearst, R., Liu, L. & Mckerlie, C. 2007. Effects of cryopreservation on sperm quality, nuclear DNA integrity, in vitro fertilization, and in vitro embryo development in the mouse. *Reproduction,* 133**,** 585-595.

Yokochi, T. and Robertson, K. D. (2004). 'Dimethyl sulfoxide stimulates the catalytic activity of de novo DNA methyltransferase 3a (Dnmt3a) in vitro'. *Bioorganic Chemistry*, 32**,** 234-243.

Yu, B., Qin, Z., Wijewickrama, G. T., Edirisinghe, P., Bolton, J. L. and Thatcher, G. R. J. (2009). 'Comparative Methods for Analysis of Protein Covalent Modification by Electrophilic Quinoids Formed from Xenobiotics'. *Bioconjugate Chemistry,* 20**,** 728-741.

Zhao, H. and Piwnica-Worms, H. (2001) *Mol.Cell. Biol.* 21, 4129–4139.

Zeng, Z., Richardson, J., Verduzco, D., Mitchell, D. L. and Patton, E. E. (2009). 'Zebrafish have a competent p53-dependent nucleotide excision repair pathway to resolve ultraviolet B–induced DNA damage in the skin'. *Zebrafish,* 6**,** 405-415.

Zhao, H., Rybak, P., Dobrucki, J., Traganos, F. and Darzynkiewicz, Z. (2012). 'Relationship of DNA damage signaling to DNA replication following treatment with DNA topoisomerase inhibitors camptothecin/topotecan, mitoxantrone, or etoposide'. *Cytometry Part A,* 81A**,** 45-51.

Zhang, T. and Rawson, D. M. (1995) 'Studies on Chilling Sensitivity of Zebrafish (*Brachydanio rerio*) Embryos', *Cryobiology,* 32(3), 239-246.

Zhang, T. (2004) 'Cryopresrvation of Gametes and Embryos of Aquatic Species' In Fuller, B. J., Lane, N. and Benson, E. E., eds., *Life in the Frozen State*, London: CRC Press, 415-435.

Zou, L. and Elledge, S. J. (2003) ‘Sensing DNA damage through ATRIP recognition of RPA-ssDNA complexes’ Science, vol. 300, no. 5625, 1542–1548.

Zuco, V., Benedetti, V. and Zunino, F. (2010). ‘ATM- and ATR-mediated response to DNA damage induced by a novel camptothecin, ST1968’. *Cancer Letters,* 292**,** 186-196.

APPENDIX A

The chemicals used in the experimental works for the study

Chemicals	Source	Product No.
Agarose	Bioline	BIO-41025
ATX Ponceau S	Sigma-Adrich	9189
Biotaq DNA polyymerase	Bioloine	BIO-21040
dNTP mix	Bioline	BIO-39053
Dimethylsulfoxide	Sigma-Adrich	D4540
Ethanol	Fisher Scientific	E/0500DF/08
Ethidium bromide	Sigma-Adrich	E1510
EZNA gel extraction kit	Omega Bio-tek	A112907W
Gel loading buffer	Sigma-Adrich	G2526
HyperLadder V	Bioline	Bio-33031
MagicMark XP Westtern protein standard	Invitrogen	LC5602
Methanol	Fisher Scientific	M/4000/17
Phosphatase inhibitor cocktail 3	Sigma-Adrich	P0044
Precision nanoscript RT kit	Primer Design	RT-nanoscript
Proterase	Sigma-Adrich	P6911-1G
Protease inhibitor cocktail	Sigma-Adrich	P8340
Protogel	Fisher Scientific	ELR-210-010P
Quantipro BCA Assay kit	Sigma-Adrich	QPBCA
Resolving buffer	Fisher Scientific	ELR-210-060A
RNAqueous-Micro kit	Invitrogen	AM1931
Sample buffer, Laemmli 2 x concentrate	Sigma-Adrich	S3401
SDS solution 10%	Fisher Scientific	BPE2436-1
Sea salt	ZM Ltd	N/A
SensiMix SYBR No-ROX kit	Bioline	QT650-05
Stacking buffer	Fisher Scientific	ELR-210-070U
TEMED	Fisher Scientific	T/P190/04
Tris buffered saline	Sigma-Adrich	T5912
WesternDot 625 Goat Anti-rabbit kit	Invitrogen	W10142

APPENDIX B

B.1 Optimisation of de-yolking

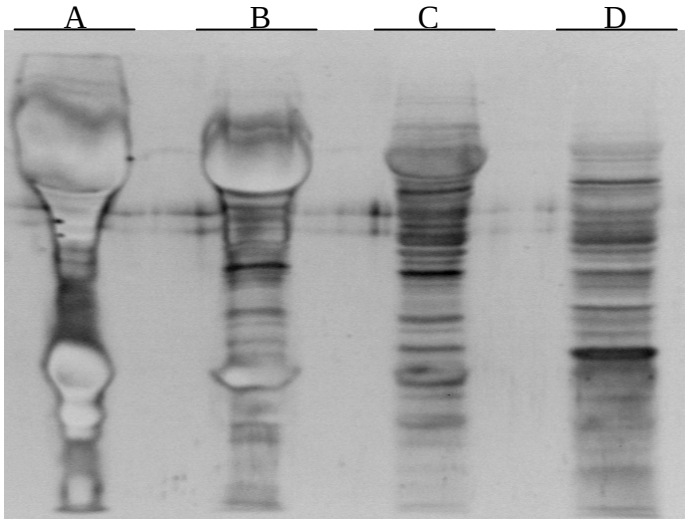

Figure B.1: Showing effects of de-yolking on protein resolution. Total proteins were extracted from the intact embryos (A) and the embryos de-yolked once (B), twice (C) and thrice (D), separated by SDS-PAGE, blotted onto PVDF membrane and stained with Sypro Ruby.

B.2 Determination of number of embryos for protein extraction

To determine the number of embryos for protein extraction, the loading volume per well, the recommended sample and loading buffer ratio and the suggested range of total protein to be probed were taken into consideration. The capacity of each well in the mini-gel system used in this study is 44 µl. However, it is ideal not to use the full capacity of a well to avoid spillage into adjacent wells. In the case of this study, a load volume of 20 µl appeared appropriate. Accounting for the recommended sample and loading ratio of 1:1, it was apparent that the maximum volume of the sample that could be loaded per well was 10 µl. The suggested range of total protein to be probed in a mini-gel is 40-80 µg. However, it was decided that 40 µg of total proteins would be used as a guideline in establishing the number of embryos. Therefore, the absolute minimum concentration of total protein required for the experiment was 40 µg /10 µl, or, 4 µg/ µl, or, 4 mg/ml. In this experiment, the number of embryos from which ≥ 4 mg/ml of total proteins can be extracted was investigated.

Groups of 20, 40, 60, 80, 100, 120, 140, 160, 180, 200embryos were de-chorinated and de-yolked. Total proteins from the de-chorinated and de-yolked embryos were extracted and quantified. Concentrations of total proteins obtained from each group of embryos were plotted against the number of embryos in the respective groups to determine the number of embryos that would yield sufficiently concentrated protein as required by the study.

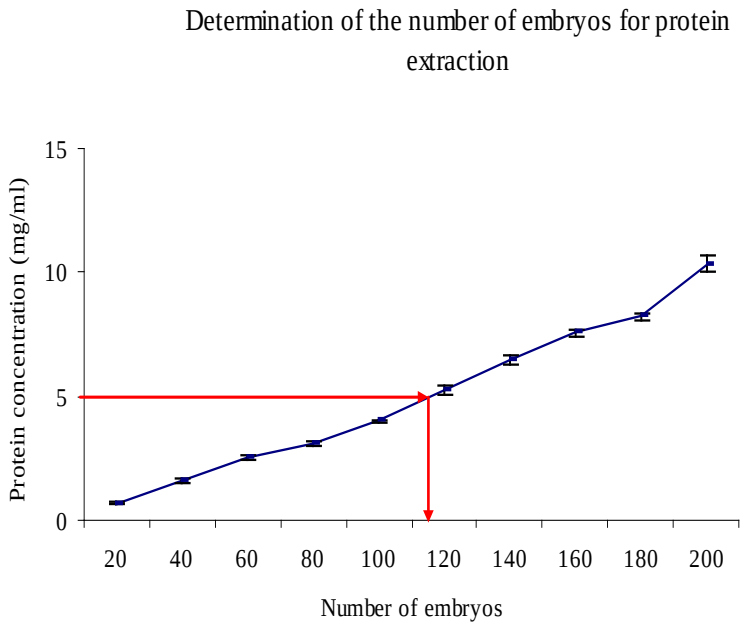

Figure B.2: Showing mean concentrations of protein against groups of different number of embryos

B.3 Effects of MeOH on protein transfer (Gel image)

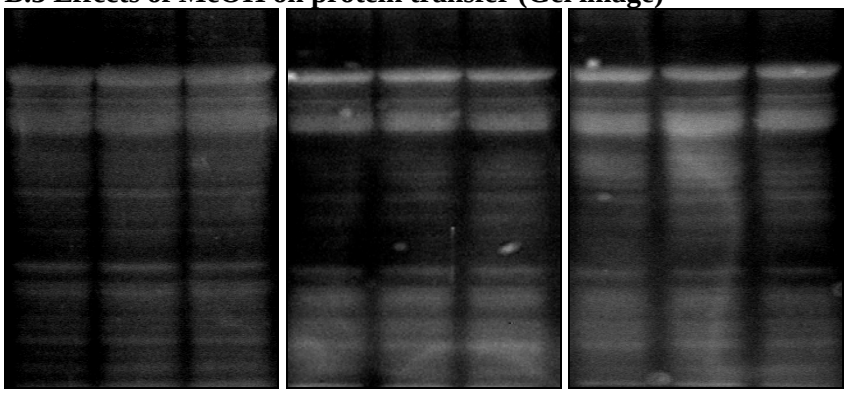

B.4 Effects of blotting duration on protein transfer (Gel image)